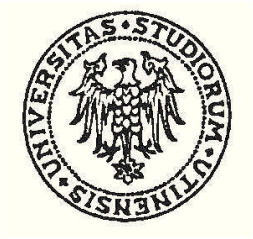

UNIVERSITÀ DEGLI STUDI DI UDINE

Dottorato di Ricerca in Scienze e Biotecnologie Agrarie
Ciclo XXVI
Coordinatore: prof. Mauro Spanghero

TESI DI DOTTORATO DI RICERCA

Stolbur phytoplasma and its interactions with the phloem tissue

DOTTORANDO
Dott.ssa Federica De Marco

SUPERVISORE
Dott.ssa Rita Musetti
Dott.ssa Simonetta Santi

ANNO ACCADEMICO 2013/2014

CONTENTS

ABSTRACT

The phloem is the plant vascular tissue that permits the translocation of photoassimilates and other compounds from source to sink organs. Phloem is even the site where phytopathogenic bacteria called phytoplasmas live and spread.

Phytoplasmas are plant pathogens that are responsible for relevant diseases on several plant species. These bacteria belong to the class *Mollicutes*, which distinguishes microorganisms that lack a rigid cell wall. Phytoplasmas are surrounded by a triple-layered unit membrane and they are pleomorphic in shape. They are characterized by having a minimal genome, lacking genes considered to be essential for cell metabolism (e.g., ATP synthases, enzymes involved in sugar uptake and use). Therefore, phytoplasmas strongly depend on their host for their nutrition.

Infections caused by phytoplasmas provoke from weak to severe symptoms on the host plants. Thus phytoplasmas can cause losses in terms of quality and quantity of crop production. Phloem-sucking insects as leafhoppers, psyllids and planthoppers are the transmission vectors of these phytopathogenic bacteria.

Although the interactions between phytoplasmas and their hosts, and plant responses to infection have been investigated in several works, biochemical and molecular aspects of the diseases are not completely understood. Moreover, as there are not curative methods for plants affected by these prokaryotes, a first important step for the management of these diseases is to increase the knowledge about plant defense reactions to phytoplasma infection.

Symptoms shown by phytoplasma-infected plants suggest that the pathogen is responsible for disturbance of hormone balance and impairment of phloem functions.

In the present work, research focused on the '*Candidatus* Phytoplasma solani', whose infection affects several economically important crops as grapevine (*Vitis vinifera* L.) and tomato (*Solanum lycopersicum* L.). The disease associated to '*Ca*. P. solani' is named Stolbur, and it is present in Europe and in the Mediterranean Basin. If occurring on grapevines it is also called Bois noir. *Hyalesthes obsoletus* Signoret (Hemiptera: Cixiidae) is one of the most active vectors of '*Ca*. P. solani'.

'*Ca*. P. solani' belongs to the 16SrXII group and it provokes symptoms as yellowing and discoloration of leaves, lack or incomplete lignification of shoots and shriveling of fruits. The general decline caused by the infection can even lead to the host death. However, an interesting phenomenon, frequently reported in grapevine as well as in other pluriannual crops, is called "recovery" and it is a spontaneous remission of symptoms in previously symptomatic plants.

In order to have a better understanding of the interactions between '*Ca*. P. solani' and its hosts, different experiments were set up using healthy and symptomatic plants of grapevine and

tomato. Moreover, recovered grapevines were employed to explore this interesting phenomenon.

Histological observations were performed using light, confocal and transmission electron microscopy and they have been associated to gene expression analyses and localization of mRNAs through *in situ* hybridization technique. Leaf and roots samples from healthy, symptomatic and recovered plants were collected and processed depending on the planned experiments.

Leaf samples were used to check the presence of the pathogen by Real Time PCR. In most cases, molecular diagnosis confirmed the presence of the phytoplasmas in symptomatic plants, while no pathogen was detectable in leaves collected from healthy and recovered plants.

Microscopy investigations on grapevine and tomato infected leaves allowed to detect phytoplasmas in the sieve elements of the phloem and to observe tissue modifications caused by the infection. In general, cell wall thickenings and large amounts of callose at sieve plates were observed in infected samples. These ultrastructural observations were consistent with the increase in the transcript level of some genes coding for callose synthases in diseased grapevine plants. Even in tomato leaves, callose synthases expression has been investigated founding two genes that showed a transcript level higher in symptomatic plants than in healthy individuals. Moreover, in grapevine leaves, genes coding for sucrose synthases were found to be upregulated, indicating a potential coordination of the two classes of enzymes in the synthesis of new callose.

Regarding leaf samples from recovered grapevines ultrastructural observations and gene expression analyses suggested that the spontaneous remission of symptoms is accompanied by a fully restoration of the source function of mature leaves.

Tomato leaf tissues were checked for gene expression of structural proteins as Phloem Protein 2 and Sieve Element Occlusion protein, showing a decrease of transcript level in infected plants. These results were consistent with *in situ* hybridization experiments performed on the same genes.

Furthermore, diagnosis on root samples was developed using Real Time PCR based on TaqMan® probes chemistry. Results demonstrated the difficulties to detect phytoplasmas in root samples, and this is maybe due to the low and uneven distribution of the pathogen in the root apparatus.

In conclusion, the present work demonstrated that phytoplasmas cause severe changes in phloem functions of their hosts, establishing impairments in source-sink plant balance. Further investigations on plant-pathogen interactions could lead to acquire more information relevant in the control of disease spreading and development.

INTRODUCTION

1. Phytoplasmas

Phytoplasmas are a group of pathogenic bacteria that colonize plants and are responsible of several diseases affecting hundreds of plant species including economically important crops (McCoy *et al.*, 1989). Phytoplasma-associated diseases cause severe losses in terms of quality and production (Bertaccini, 2007; Lee *et al.*, 2000).
Phytoplasmas are transmitted in nature by insect vectors, in particular phloem feeders, which permit the dispersal of those pathogens in different host plants (Hogenhout *et al.*, 2008).
Symptoms of phytoplasma diseases were observed since ancient times in China, where poinsettia (*Euphorbia pulcherrima* Willd.) flowers emerged in a delicate green color instead of the typical red or yellow (Strauss, 2009). This feature was considered pretty and valuable for this ornamental plant, but normally phytoplasmas have negative effects on plants because they provoke severe alteration of the plant habit and metabolism (Christensen *et al.*, 2005).

Phytoplasma discovery

The first disease then associated to phytoplasmas has been described in 1926 by Kunkel, who reported an infectious chlorosis on the China asters (*Callistephus chinensis* L.). The disease was named aster yellow. Since the pathogen was transmitted by insects and not cultivable *in vitro*, aster yellows were supposed to be caused by viruses. For more than 40 years scientists had examined the disease looking for a virus and finally, only in 1967, Doi and colleagues used electron microscopy to discover bacteria without rigid cell walls that resembled mycoplasmas (infectious agent of animals and humans causing several diseases) in plant tissues. They termed those microbes mycoplasma-like organisms (MLOs). In plants, phytoplasmas have been observed in phloem sieve elements where they find excellent conditions for the spread in the host (McCoy *et al.*, 1989). Phytoplasmas infect several species worldwide: for example it has been reported that aster yellows disease can occur in at least 350 mono- and dicotyledonous, both cultivated and wild plants (Hollingsworth *et al.*, 2008).
In 1992, the Phytoplasma Working Team, during the 9th Congress of the International Organization of Mycoplasmology (IOM), named 'phytoplasmas' the MLOs found in plant tissues (Firrao *et al.*, 2004). According to their lack of a firm cell wall, phytoplasmas belong to the class of *Mollicutes* and they are grouped in the provisional genus '*Candidatus* (*Ca.*) Phytoplasma' (Firrao *et al.*, 2004).

Researches on phytoplasmas proceed slowly compared to the other bacteria affecting plants, because of the inability to culture these microorganisms in cell-free media. Recently, Contaldo *et al.*, (2012) described a protocol for phytoplasma *in vitro* culture using specific commercial media, but the method awaits further confirmation.

Phytoplasma morphology

Phytoplasma cells lack a rigid cell wall and are surrounded by a triple-layered unit membrane (Doi *et al.*, 1967). Phytoplasmas are pleomorphic in shape, non-helical and they have rounded to filamentous form when observed by transmission electron microscope (Figure 1). Phytoplasmas have a mean diameter of 0.2-0.8 µm (Kube *et al.*, 2012) and contain a genome of about 530 - 1350 kilobases. Genomes can be organized in circular chromosomes, as in '*Ca*. P. asteris' and '*Ca*. P. australiense', or linear chromosomes as in '*Ca*. P. mali', '*Ca*. P. pyri' and '*Ca*. P. prunorum' (Oshima *et al.*, 2004; Bai *et al*., 2006; Tran-Nguyen *et al*., 2008; Kube *et al.*, 2008). The average number of genes founded in phytoplasma genomes is 700 (Christensen *et al.*, 2005). Phytoplasma genomes often contain extrachromosomal elements, which have been found in several phytoplasma strains (Tran-Nguyen and Gibb, 2006). The genetic material of the extrachromosomal elements can be integrated into chromosomes and it has a role in the vector transmissibility (Nishigawa *et al.*, 2002). Phytoplasma genomes contain a low G+C content in their DNA (23.0–29.5 mol%) (Kollar and Seemüller, 1989; Sears *et al.*, 1989).

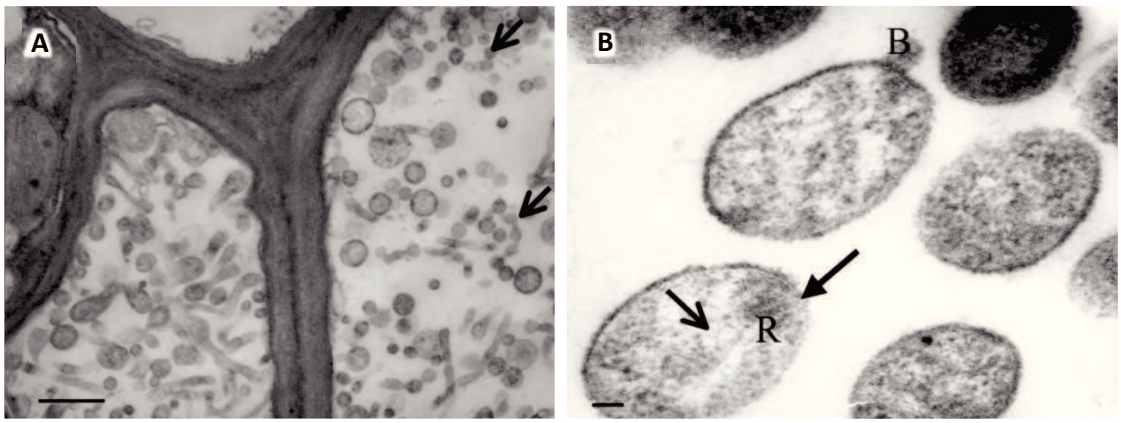

Figure 1. Transmission electron micrographs of phloem tissue of *Catharanthus roseus* L. leaf infected with Apple Proliferation (A) and European Stone Fruit Yellow (B) phytoplasmas. A. Phytoplasmas in sieve elements. They are numerous and pleomorphic in shape, some are organized into short chains (arrows). Bar=1 µm. B. High magnification of ESFY phytoplasma cells. The three layered membrane (closed arrow), ribosomes (R) and nucleic acid (arrow) are visible. Letter B indicates the development of a probable budding process. Bar=0.1 µm. (Musetti and Favali, 2003).

Phytoplasma classification and genomics

As stated above phytoplasmas belong to the class of *Mollicutes* and they are grouped in the provisional genus '*Candidatus* Phytoplasma' (Firrao *et al.*, 2004). Phytoplasma genus is a member of the order *Acholeplasmatales* and it is closely related to the genus *Acholeplasma*, with which phytoplasmas share the usage of UGA as a stop codon (Lim and Sears, 1992; Toth *et al.*, 1994; Razin *et al.*, 1998).

To date, thirty-four phytoplasma strains had been identified on the basis of 16S rDNA sequences and their phylogenetic tree is shown in Figure 2 (Kube *et al.*, 2012).

Four complete phytoplasma genomes have been sequenced. The first two genomes belong to '*Ca*. P. asteris' genus and they are the onion yellows phytoplasma strain OY-M subgroup 16SrI-B, and the aster yellows witches'-broom phytoplasma strain AY-WB subgroup 16SrI-A (Oshima *et al.*, 2004; Bai *et al*., 2006). Moreover, in 2008 '*Ca*. P. australiense' and '*Ca*. P. mali' have also been sequenced (Tran-Nguyen *et al*., 2008; Kube *et al.*, 2008). Phytoplasma genomes sequencing took years because of the difficulties in obtaining suitable DNA. Phytoplasma DNA occurs in small amounts in infected plants and thus enrichment and purification procedures are necessary. Also genome assembling was time-consuming for the presence of AT-rich regions in the sequences (Kube *et al.*, 2008; Fleischmann *et al.*, 1995).

The sequencing of four genomes allowed the identification of genes possessed by phytoplasmas. It was possible to discover that phytoplasmas lack several genes that other bacteria, as *E. coli*, need for metabolism. In particular, phytoplasmas have no genes coding for phosphotransferases (*PTS*), a class of enzymes that are usually used by bacteria for sugars import and phosphorylation (Oshima *et al.*, 2004).

In addition, genes for *de novo* synthesis of amino acids, fatty acids, nucleotides and genes involved in the tricarboxylic acid cycle and oxidative phosphorylation were not found (Oshima *et al.*, 2004; Christensen *et al.*, 2005).

However, as regards sugars import, phytoplasma genomes showed the presence of an ABC (ATP Binding Cassette) maltose transporter that allows the microorganisms to import maltose, trehalose, sucrose and palatinose, while they lack enzymes required to metabolize these sugars. Thus, it has been supposed that phytoplasmas may use phosphorylated hexoses present in the plant cells as a source of carbon (Christensen *et al.*, 2005).

Other genes found in the sequenced genomes code for enzymes and proteins involved in the bacterial replication fork, in the transcription (RNA polymerases subunits) and translation (rRNA operons and translation factors) processes (Kube *et al.*, 2012). A wide diversity of membrane proteins was also found and a sec-dependent secretion pathway was well described. Secreted proteins as TENGU and SAP11 found in '*Ca.* P. asteris' are supposed to be "effector proteins", involved in the interaction of phytoplasmas with their hosts (Bai *et al.*, 2009).

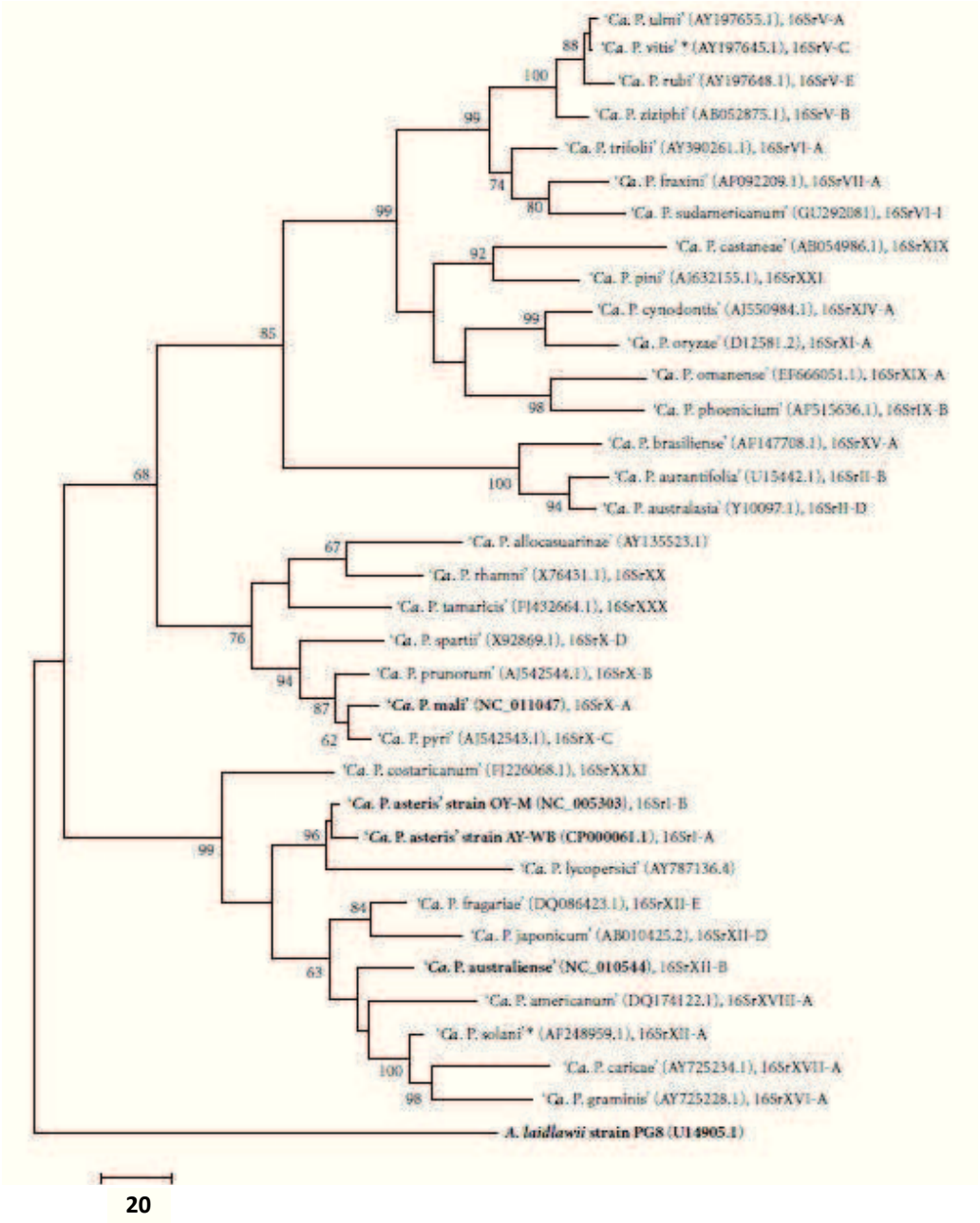

Figure 2. Phylogenetic tree constructed on 16S rDNA sequences of 34 phytoplasmas strains ('*Ca.* Phytoplasma' species) employing *Acholeplasma laidlawii* as outgroup. The completely sequenced strains are in bold while asterisks indicate strains which were not yet formally described. (Kube *et al.*, 2012)

Recently, Saccardo *et al.*, (2012) were able to obtain the draft of four phytoplasma genomes by second-generation sequencing technique, developing an ad hoc multiple-step assembly method. The sequencing of four phytoplasma strains belonging to the 16SrIII group permitted to observe

that they do not differ significantly concerning genes of their potential basic metabolism from the genomes of other previously sequenced phytoplasmas. Conversely, they are distinct from strains of other species, as well as among each other, in genes encoding functions probably related to interactions with the host.

Phytoplasma life cycle

Phytoplasmas have a peculiar life cycle that requires replication in plants and insects, two hosts belonging to different kingdoms. In plants phytoplasmas are found mainly in sieve elements, while in insects they occur in gut, haemolymph, salivary gland and other organs (Weintraub and Beanland, 2006).

Phytoplasmas are transmitted by insects confined to three main taxonomic groups: leafhoppers (Auchenorrhyncha: Cicadellidae), planthoppers (Auchenorrhyncha: Fulgoromorpha), and psyllids (Sternorrhyncha: Psyllidae) (Dickinson and Hodgetts, 2013).

Some phytoplasmas are transmitted by one or few vectors while others can be found in multiple vectors (for example, phytoplasma causing aster yellows is transmitted by at least 24 vectors) (Seemüller *et al.*, 2002; Lee *et al.*, 2003).

More in detail (Figure 3), insects acquire phytoplasmas from the plant phloem while sucking phloem sap. Ingested phytoplasmas move through the stylet's food canal and intestine and so they enter the hemolymphatic circulatory system (Christensen *et al.*, 2005). Phytoplasmas multiply in the secretory salivary gland cells and move along with the saliva. After a period of time called latency period during which phytoplasmas spread into the insect and reach an infectious level, new plants can be infected during feeding and salivation of the insect. The latency period is variable and can last a few days to three weeks (Webb *et al.*, 1999; Carraro *et al.*, 2001).

Several studies investigated the phytoplasma-insect relationship and showed opposite conclusions. In most cases insect hosts may benefit from their association with phytoplasma (Nault, 1990; Purcell and Nault, 1991), as for example, the aster leafhoppers, *Macrosteles quadrilineatus* Forbes, that when exposed to aster yellows phytoplasma live longer than non-exposed leafhoppers (Beanland *et al.*, 2000). Conversely, in 2005 Bressan and colleagues highlighted a reduced fitness of *Scaphoideus titanus* Ball leafhopper exposed to Flavescence dorée phytoplasmas.

Phytoplasmas are also occasionally transmitted in nature by dodder species. This system is often used in experimental studies to transmit phytoplasmas from plants grown in the fields to plants that can be easily maintained in greenhouses as *Catharanthus roseus* L. (Bertaccini, 2007). Also known as the Madagascar periwinkle, this plant is very susceptible to infections by phytoplasmas, although the reasons are not still understood. For this feature *C. roseus* is commonly used as an experimental host and for phytoplasma collection maintenance (Seemüller *et al.*, 1998; Favali *et al.*, 2004).

Depending on the plant host phytoplasma titre is variable, and in particular very low levels are found in trees plants and grapevines. *C. roseus* instead tends to show a high concentration of the pathogen (Berges *et al.*, 2000).

Experimentally, it is also possible to transmit the majority of phytoplasmas by grafting or insect transmission. However some phytoplasmas are very host-specific, thus it is necessary to maintain the pathogen on the original host.

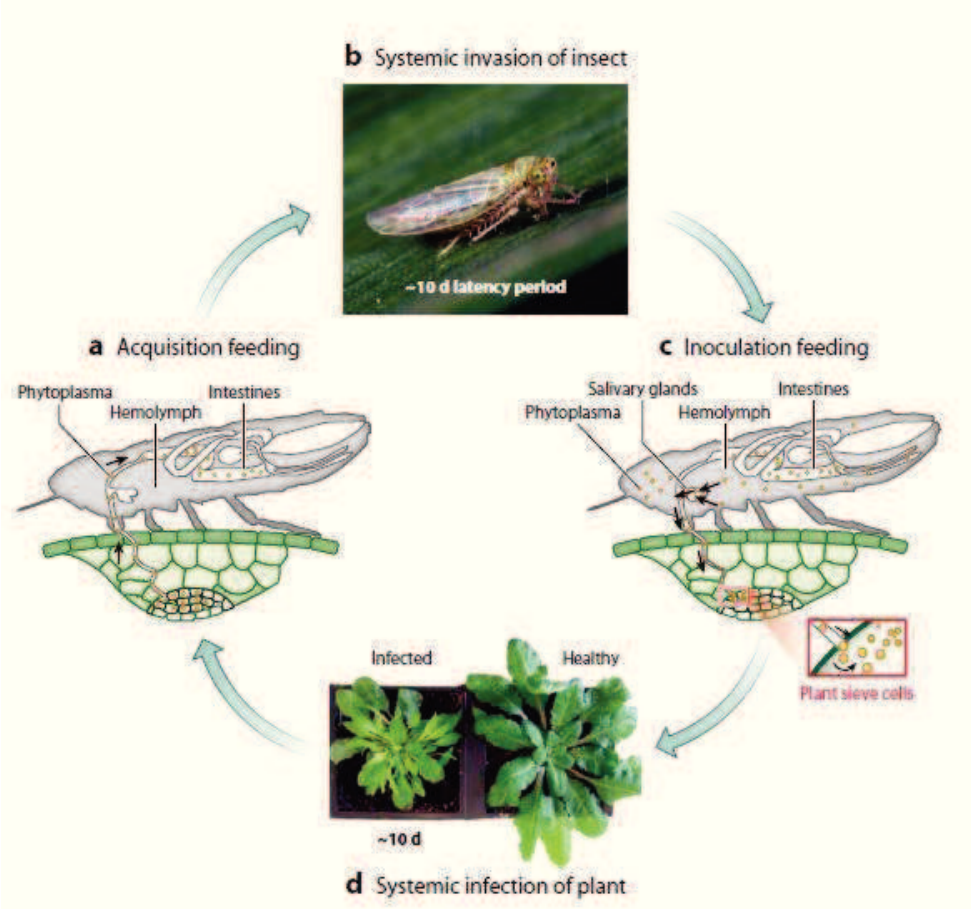

Figure 3. Schematic representation of phytoplasma life cycle. (a) Leafhopper acquires the phytoplasmas feeding on an infected plant. (b) Phytoplasmas spread in the insect. (c) Insect transmits phytoplasmas while feeding on a new plant. (d) Infected plant shows symptoms of the disease. (Sugio *et al.*, 2011)

Phytoplasma interactions with host plants

Symptoms of phytoplasma-induced diseases depend on phytoplasma strain, host and environmental factors. Typical symptoms consist of alteration of plant organs and often include yellow or red discoloration of leaves, floral virescence (development of green pigmentation in petals), phyllody (development of floral organs into leaf-like structures), reduced fruit size, witches' broom (abnormal proliferation of shoots), lack or incomplete lignification of shoots, stunting, general decline and even the death of the plant (Dickinson and Hodgetts, 2013) (Figure 4).

Figure 4. Typical symptoms caused by different strains of phytoplasma on *Catharanthus roseus*. a. Healthy plant. b. Presence of deformed petals. c. Floral virescence. d-f. Various stages of phyllody. Pictures from Dickinson and Hodgetts, 2013.

Macroscopic symptoms that are visible on infected plants reflect the modifications that phytoplasmas cause on plant metabolism and hormonal regulation.

Alteration in phloem functions is a typical symptom found in phytoplasma infected plants and it is characterized by callose deposits at sieve plates, aggregation of phloem protein filaments, necrosis of sieve elements and collapse of the cells (Lee *et al.*, 2000) (Figure 5).

Callose synthesis and transition of phloem proteins into aggregate state are non-specific responses of plants to the phytoplasma attack used to control the spread of the pathogen. These mechanisms are Ca^{2+}-dependent (Knoublach *et al.*, 2001) as it was observed in apple trees

infected by apple proliferation phytoplasma where a decrease in cytosolic Ca^{2+} occurred in the phloem (Musetti *et al.*, 2008).

Recently, Musetti e*t al.*, (2013a) investigated the role of Ca^{2+} in the pathosystem *Vicia faba* L./'*Ca*. P. vitis'. Experiments suggested that phytoplasma infection leads to Ca^{2+} influx in sieve tubes, inducing sieve plate occlusions by callose deposition or protein plugging. Moreover Ca^{2+} influx seemed to be involved in cell wall thickenings of sieve elements.

Disturbance of sugars metabolism and impaired photosynthesis have been described in several phytoplasma-plant systems. In particular, levels of soluble carbohydrates and starch are accumulated in source leaves and reduced in roots and sink leaves of periwinkle, tobacco and coconut palms (Lepka *et al.*, 1999; Maust *et al.*, 2003). Observations of starch accumulation in chloroplasts and disorganizations of thylakoids have been reported by Musetti in 2006.

The decrease of the photosynthetic process has also been related to the inhibition of chlorophyll biosynthesis and the reduction of stomatal conductance (Tan and Whitlov, 2001; Matteoni and Sinclair, 1983).

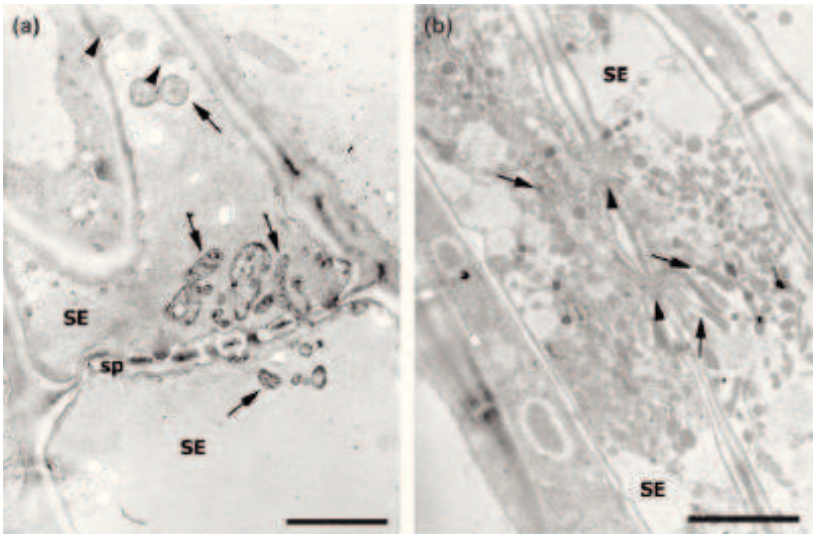

Figure 5. Transmission electron micrographs from Christensen *et al.*, (2005). Longitudinal sections through the phloem of periwinkle (*Catharanthus roseus*) infected with Green Valley X phytoplasmas. (a). A sieve plate with phytoplasmas (arrows) sorrounding the sieve pores (headarrows: mythocondria). Bar=2 µm. (b). Two sieve elements with lateral sieve pores (headarrows) and numerous phytoplasma (arrows). Bar=2 µm.

Another effect of phytoplasma presence is the increase of the total amount of proteins in infected plants. For example, in maize plants affected by maize bush stunt phytoplasma Junqueira and colleagues (2004) reported an increase of proteins in infected plants, among which those related to the defense mechanisms as peroxidases, chitinases and β-1,3-glucanases.

Moreover, several studies reported an alteration on the content of secondary metabolites in infected plants.
Phytoplasma-infected *C. roseus* shows an accumulation of metabolites involved in the synthesis of phenylpropanoids or terpenoid indole alkaloids in leaves (Choi *et al.*, 2004; Favali *et al.*, 2004).
Phytoplasmas interact with plant and insect hosts through the production of effector proteins (Bai *et al.*, 2009). The effectors are compounds secreted by the pathogen that share sequence, functional, or structural features with host proteins and thus can interfere with plant or insect cell processes (Desveaux *et al.*, 2006).
Sequencing of the four genomes allowed to identify several potential phytoplasma effectors. In particular, 56 proteins were found in AY-WB genome and named "secreted AY-WB proteins" (SAPs) (Bai *et al.*, 2009), while 45 were identified in OY genome. Effectors have been found also in other genomes of phytoplasmas belonging to group I (Bai *et al.*, 2009). Most characterized effectors are proteins SAP11 (9 kDa) of AY-WB and TENGU (<5 kDa) of OY phytoplasmas (Bai *et al.*, 2009; Hoshi *et al.*, 2009). Noteworthy, SAP11 contains a nuclear localization signal (NLS), which has the function to target the protein inside nucleus. Nuclei are not present in phloem sieve cells, thus indicating that probably this effector targets cells of other tissues (probably meristems) (Bai *et al.*, 2009).

Economic impact of phytoplasma-associated diseases

Phytoplasmas have been found associated with several diseases of plants worldwide and they can affect both economically important crops and weeds (Dickinson and Hodgetts, 2013).
Economic relevant diseases caused by phytoplasmas affect hundreds of plant species among fruit plants (i.e., apple, pear, plum, apricot, cherry, citrus, grapevine), crops (i.e., rice, potato, tomato, sugarcane, cotton), forest trees (i.e., elm, poplar, ash, pine) and ornamental plants. The economic losses caused by phytoplasmas could be relevant: as an example, losses due to the disease associated to '*Ca*. Phytoplasma mali' in apple orchards is estimated in 100 million €/year lost in Germany and Italy (Strauss, 2009).
Phytoplasma diseases are widespread in numerous countries and the more affected regions are the center-East Europe, the Mediterranean basin, America and Oceania (Martelli, 1993).
In Friuli Venezia Giulia region (north-eastern Italy) several phytoplasma-associated diseases have been reported. In particular apple proliferation and grapevine yellows are widespread in the area (Martini *et al.*, 2008; Bellomo *et al.*, 2007).

Seasonal distribution

A seasonal distribution of the phytoplasmas has been reported in different plant hosts. A well characterized example of colonization behavior of phytoplasmas is described in apple proliferation disease. '*Ca*. P. mali' infects apple trees and the variation in symptom expression is

related to the presence/absence of the pathogen in the above ground part of trees (Seemuller *et al.*, 1984). In particular, during winter the pathogen is almost always not present in the above ground part of the plants and this is related to the degeneration of the sieve tubes in the previous year's phloem. The next spring the aerial part of the tree can be recolonized by the phytoplasmas from the roots, where they persist the whole year (Schaper and Seemüller, 1984; Seemüller *et al.*, 1984).

Regarding phytoplasma-infected grapevine, studying five different cultivars located in Italy, Terlizzi and Credi (2007) showed that the concentration of stolbur phytoplasma was highest in summer, while the number of infected samples strongly decreased in winter season. These results are similar to the seasonal distribution of phytoplasmas described for "Australian grapevine yellows" disease (Constable *et al.*, 2003).

Spatial distribution inside the host plants

Phytoplasmas colonize most organs of infected plants, as leaves, flowers and roots. Phytoplasmas have been also found in seeds, even if seed transmission is not believed to be possible because of the lack of a direct phloem connection to the seed (Cordova *et al.*, 2003). Several studies on phytoplasmas distribution inside the hosts have been conducted, showing in some cases, contrasting results. For example, Siddique and colleagues in 1998 reported the presence of phytoplasmas mostly in sink organs as roots and immature leaves, while in *Euphorbia pulcherrima* infected by branch-inducing phytoplasma, the pathogen was mainly found in source leaves (Christensen *et al.*, 2004).

An investigation conducted on the translocation of onion yellows phytoplasmas infecting plants of *Chrysanthemum coronarium* showed that the movement of the pathogen cannot be explained merely with the movement of photoassimilates in the phloem (Wei *et al.*, 2004).

Because it has been shown that phytoplasmas are able to adhere to cell membranes of host cells (Lefol *et al.*, 1993) it has been hypothesized that they might grow along the cell membrane of sieve elements (Christensen *et al.*, 2005). The distribution of phytoplasmas in the plant organs can vary also depending on the stage development of the host.

Phytoplasmas are able to move freely through sieve pores and are transported along with the assimilate flow from leaves to sink tissues as immature leaves and roots (Wei *et al.*, 2004). In some cases phytoplasmas have been reported also in source leaves (Christensen et al., 2004; Kaminska *et al.*, 2003).

The lack of genes coding for flagella or other elements involved in cell motility renders unlikely an active movement of phytoplasmas. It has been supposed that phytoplasmas might adhere to host cells (Lefol *et al.*, 1993), like other *Mollicutes* (Berg *et al.*, 2001; Razin, 1999), and thus move along sieve elements against the assimilate flow.

It has been reported that movement of '*C*a. P. mali' through sieve elements seems to be actin-based (Boonrod *et al.*, 2012). Moreover, host plasma-membrane adherence is considered an

important factor in pathogenesis (Seemüller *et al*., 2013) and the endoplasmic reticulum (ER) might be involved in the complex interactions occurring between phytoplasmas and sieve element endomembrane network.

Recently Buxa *et al.*, (2013) described a relevant reorganization of sieve element endomembrane system in tomato plants infected with '*Ca*. P. solani'. In particular, TEM observations revealed membrane junctions or overlays between phytoplasmas and sieve element plasma membrane and a re-organization of ER network in infected areas. In addition, experiments based on immunogold labeling localized actin on the phytoplasmas membrane surface giving new details to explain the movement mechanism of the pathogen.

2. Phloem: the phytoplasma habitat

Being phytoplasmas phloem-restricted pathogens it is noteworthy to give special attention to the structure and function of this tissue.
During evolution, the increase in dimensions and complexity of plants led to the development of two distinct systems, the phloem and the xylem, that permit the translocation of nutrients and photoassimilates in the whole plant (Schulz, 1998).
Phloem translocates the products of photosynthesis from mature leaves (source organs) to organs where photosynthates are metabolized or stored, such as roots, immature fruits and seeds, flowers and not developed leaves (sink organs).

Phloem structure

Phloem tissue consists of several different specialized cells (Figure 6). Sieve elements (SE) are arranged longitudinally to create sieves tubes. Each module is associated with one or a few companion cells (CC). A meristematic mother cell generates both sieve element and associated companion cells (Esau, 1969; Behnke and Sjolund, 1990). In particular, the precursor cell divides longitudinally in two cells of different dimensions (Behnke and Sjolund, 1990).
One of the two cells develops in a sieve element going through a process that results in the loss of the nucleus, ribosomes, Golgi bodies, tonoplast and to the reduction in the number of mitochondria (Esau 1969; Behnke and Sjolund, 1990). Organelles that finally remain are endoplasmic reticulum, plastids, some mitochondria and the plasma membrane. The other daughter cell generated from the precursor one develops in one or more companion cells, which are metabolically active and are responsible for processes as protein biosynthesis that are reduced or loss in sieve elements. Moreover, CCs are rich in mitochondria and provide energy to SEs in the form of ATP. Finally, CCs permit the translocation of photoassimilates between parenchyma cells and SEs (Taiz and Zeiger, 1998).
Companion cells are connected with parenchyma cells and sieve elements by highly specialized plasmodesmata that are responsible for permanent and selective exchange of micro- and macromolecules (Ruiz-Medrano *et al.*, 2001).
Sieve elements are connected together through plasmodesmata that are transformed into large pores up to 1 µm to form the sieve plate, through which compounds are translocated (Evert, 1990).

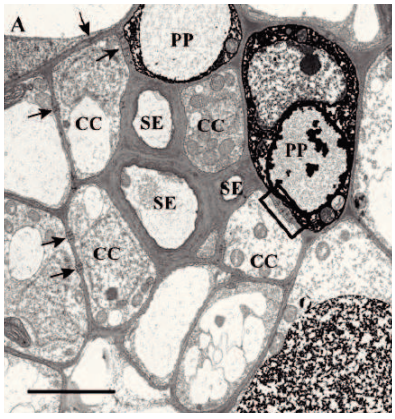

Figure 6. Transmission electron micrograph of phloem tissue. Transversal section of *Liquidambar styraciflua* leaf. Companion cells (CC), sieve elements (SE) and phloem parenchyma cells (PP) are visible. Arrows indicate plasmodesmata. Bar=3 µm (Turgeon and Medville, 2004).

The study of phloem tissue by means of transmission electron microscopy has permitted to identify protein bodies typical of sieve elements. These structures have been named phloem proteins, or P-proteins and historically were defined as "proteinaceous material in the phloem that is sufficiently characteristic when observed with the electron microscope to warrant a special term" (Cronshaw, 1975). In mature SEs, P-proteins have been found to be amorphous, crystalline, filamentous, tubular and fibrillar (Cronshaw and Sabnis, 1990; Evert, 1990).

P-proteins have been observed in all dicotyledonous and most monocotyledonous plants (Eleftheriou, 1990; Evert, 1990).

The best known phloem proteins are PP1 and PP2 found in pumpkin. PP1 (96 kDa) has been described as a protein that forms filaments, while PP2 (25 kDa) is a dimeric lectin (carbohydrate binding protein) that binds covalently to PP1 (Botswick *et al.*, 1992; Golecki *et al.*, 1999). In *Fabaceae* it has been observed a particular class of phloem proteins that has been called forisomes. These proteins are able to undergo a conformational change associated with a dramatic volume increase (Knoblauch *et al.*, 2001; Peters *et al.*, 2006). Forisomes consist of subunits of Sieve Element Occlusion (SEO) proteins (Pélissier *et al*., 2008). These proteins were firstly identified in *Fabaceae*, but *in silico* studies revealed that genes potentially coding for SEOs are widely present in many Dicots (Ruping *et al.*, 2010).

The function of phloem proteins is still unclear, but it has been hypothesized that they have a role in the maintaining of turgor pressure in the sieve cell after injury, and that they are involved in pathogen and pest defense (Read and Northcote, 1983). It has been reported that the insertion of a microcapillary tip into sieve elements caused a rapid disintegration of crystalloid protein bodies, which were restored after some minutes. Moreover, the same response was obtained as a consequence of a change in the osmotic potential of the phloem tissue. Turgor changes are thought to be responsible of Ca^{2+} influx in the sieve elements which is directly

involved in the structural modifications of these crystalloid proteins (Knoblauch *et al.*, 2001; Arsanto, 1986).

Recent biochemical and cytological studies demonstrated the presence of a cytoskeleton in sieve elements and its involvement in several mechanisms. Cytoskeleton is suggested to have a role in intracellular signaling cascades and for example, in controlling cold-shock-induced Ca^{2+} influx into sieve elements which leads to forisome dispersion and sieve plate occlusion in *Vicia faba* (Hafke *et al.*, 2013).

Sugars translocation in the phloem

Numerous classes of compounds are transported over long distances in the plant through phloem tissue. Besides carbohydrates produced in mesophyll cells, phloem sap is rich in amino acids, minerals, phytohormones, secondary metabolites and RNAs (e.g., Ziegler 1975; Zimmermann and Ziegler 1975; Lohaus *et al.*, 1995; Hayashi *et al.*, 2000; Murray and Christeller, 1995; Christeller *et al.*, 1998; Hartmann, 1999; Dannenhoffer *et al.*, 2001; Ruiz-Medrano *et al.*, 2001).

Already in 1930, Ernst Münch hypothesized that phloem flux was generated thanks to the gradient of osmotic pressure that occurs between source and sink organs. Phloem loading and unloading are processes that involve several steps and result in the development of the gradient between organs.

Among the sugars synthesized in plants, sucrose is the mainly form of carbon found in phloem sap. In some species poly- and oligosaccharides of the raffinose family (RFO) are found in the phloem (Rennie and Turgeon, 2009). RFOs seem to be involved in the polymer trapping mechanisms which was proposed by Turgeon in 1996, according to which small sugars as sucrose when moving to sieve elements are polymerized to raffinose and other complex oligosaccharides and in this way they cannot move back but only proceed along the flux.

In a limited number of species, belonging to *Ranunculaceae* and *Papaveraceae* families, hexoses transport has been reported, highlighting the differences among species (van Bel and Hess, 2008).

Recently, Lemoine *et al.*, (2013) published an update review on source-to-sink sugar transport. As shown in Figure 7, phloem loading and unloading can follow apoplastic or symplastic pathway.

Symplastic pathway of phloem loading involves plasmodesmata and the polymer trapping mechanism (Rennie and Turgeon, 2009).

In the apoplastic mechanisms sucrose transporters are responsible of the sucrose loading from apoplast to companion cells and act exploiting the proton gradient established by H^+/ATPases located in the same cells (dark green circle in the enlargement of CC/PP contact area, Figure 7) (Lalonde *et al.*, 1999). Sucrose enters the apoplast from phloem parenchyma cells through

facilitators of the recently characterized SWEET family (pale green circle in the enlargement of CC/PP contact area, Figure 7) (Chen *et al.*, 2012).

Numerous sucrose transporters have been characterized in several plant species, and have been indicated as SUTs (SUcrose Transporters) or SUCs (SUcrose Carriers) (Lemoine *et al.*, 2000).

Gene expression of sucrose transporters has been reported in sink organs and it was tissue- and development phase-specific (Lalonde *et al.*, 1999).

In particular *Arabidopsis* transporter SUC2, was found in phloem tissue and proposed as a marker of companion cells (Imlau *et al*., 1999; Ivashikina *et al.*, 2003; Deeken *et al.*, 2008). Knock-out mutants of SUC2 of *Arabidopsis* (Gottwald *et al.*, 2000) and SUT1 of maize (Slewinski *et al.*, 2010) displayed a carbohydrate accumulation in leaves and an impaired growth and poor development of sink organs.

In grapevine three sucrose transporters have been identified: *VvSUC11*, *VvSUC12* and *VvSUC27* (Davies *et al.*, 1999; Afoufa-Bastien *et al.*, 2010), and different functions were highlighted. *VvSUC11* and *VvSUC12* mRNAs were revealed more in seeds than other organs, while *VvSUC27* was highly expressed in grapevine vegetative organs and lowly in berries.

The discovery of the SWEET transporters family has finally explained how sucrose is released from mesophyll cells or phloem parenchyma cells into the apoplast before enter CC/SE complex. For example, SWEET11 and 12 in *Arabidopsis* and SWEET11 and 14 in rice facilitate sucrose efflux without energy consumption (Chen *et al.*, 2012). It has been hypothesized that this release is due to the concentration gradient between mesophyll/parenchyma cells and apoplast. Moreover, a transcriptional induction of SWEET11 and 14 in rice was reported upon infection with *Xanthomonas oryzae* pv. *oryzae* (Chen *et al.*, 2010).

SWEET family consists of at least 17 members in *Arabidopsis* and 21 in rice and they are subdivided in four clades on the basis of phylogenetic analyses. SWEET transporters supply different carbohydrates to a variety of tissues. For example, AtSWEET1 and AtSWEET8 have been found to be involved in glucose efflux.

SWEET transporters are predicted to be small proteins which form a pore from seven transmembrane helices (Chen *et al.*, 2010).

As sucrose loading mechanism, also the unloading process can occur symplastically or apoplastically, depending on plant species and involved organs. Switches between the apoplastic and symplastic pathways can also due to different developmental stages or as a response to the environment (Roitsch, 1999; Godt and Roitsch, 2006). Symplastic pathway seems to be more relevant in developing sink organs or storing organs, while apoplastic pathway have been detected in specific sink organs as apical meristems (Patrick, 1990).

Apoplastic unloading involves sucrose transporters that act as sucrose/H^+ antiporters (Walker *et al.*, 1995). An important role has been also pointed out for cell wall invertases (pale blue circle, Figure 7) (Eschrich, 1989). These enzymes hydrolyze sucrose in hexoses as glucose and fructose

that will be translocated in sink cells by monosaccharide transporters (Ehness and Roitsch, 1997).

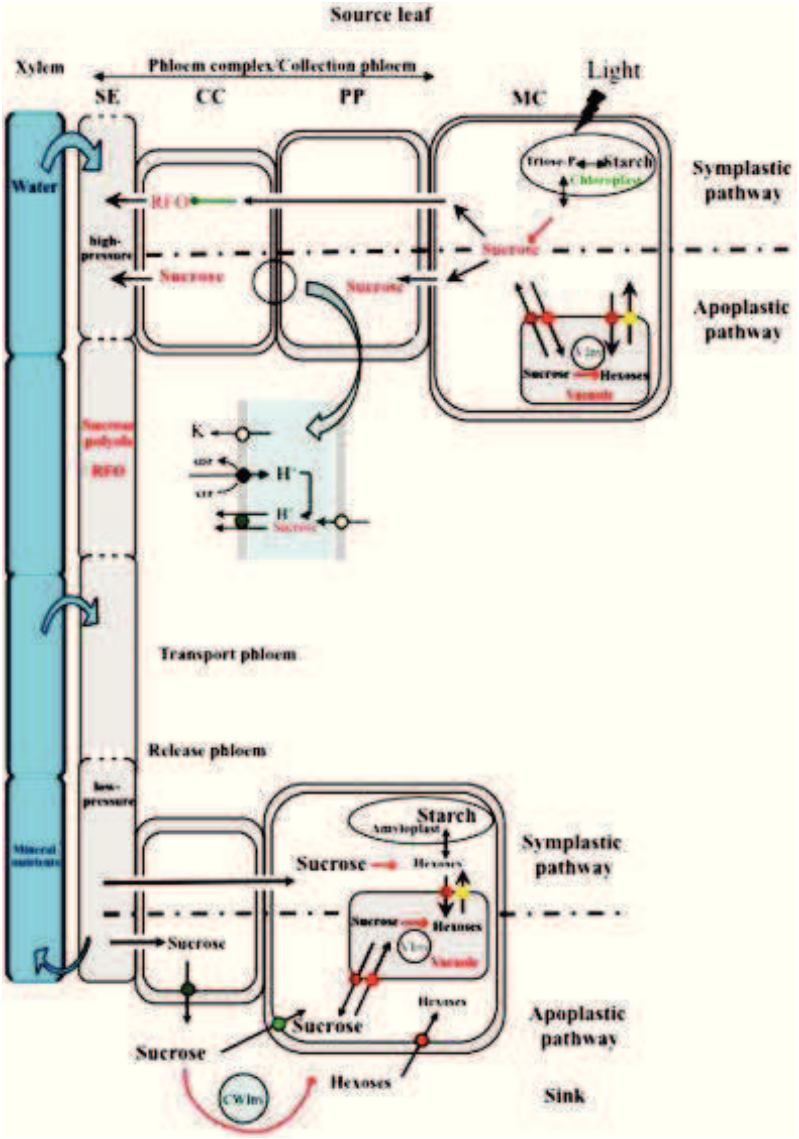

Figure 7. Schematic representation of sugar transport from Lemoine *et al.*, 2013. Sucrose is synthesized in mesophyll cells and enters the phloem through symplastic or apoplastic pathways. The major players of the apoplastic mechanism are shown in the enlargement of the area between phloem parenchyma cells and companion cells. SWEET transporter is shown as a pale green circle, and sucrose transporter as a dark green circle. The unloading apoplastic pathway involves the activity of a cell wall invertase (pale blue circle).

3. '*Candidatus* Phytoplasma solani'

'*Candidatus* Phytoplasma solani' is associated with diseases known as stolbur or big bud, that affect wild and cultivated plants, as species belonging to *Solanaceae* (tomato, tobacco, eggplant) (Cousin *et al.*, 1989; Panjan, 1950; Suhov and Vovk, 1949), grapevine (Maixner *et al.*, 1995), *C. roseus* (Jarausch *et al.*, 2001), celery (Carraro *et al.*, 2008), corn (Duduk and Bertaccini, 2006), blackberry (Bobev *et al.*, 2013). Grapevine stolbur disease is also known as Bois noir, Legno nero or Vergilbungskrankheit (Maixner, 1994; Sforza *et al.*, 1998; Alma *et al.*, 2002).

Based on *16S rRNA* gene sequence identity and biological properties, '*Candidatus* Phytoplasma solani' ('*Ca*. P. solani') belongs to 16SrXII group. This group includes several species as '*Ca. P.* australiense', '*Ca*. P. japonicum', and '*Ca*. P. fragariae'.

Typical symptoms of stolbur disease are flower malformations (Figure 8, A-D) that are very visible on infected tomato plants (Pracros *et al.*, 2006). They also include virescence, phyllody and malformations of the stamens and carpels that can lead to plant sterility (Cousin and Abadie, 1982).

As regards stolbur-diseased grapevines symptoms vary depending on the cultivar and environmental conditions. Manifestation of the disease can be systemic or localized to some branches. More evident symptoms on leaves are the discoloration and the downward folding of the lamina, processes that make the leaf more fragile (Figure 8, E-G). Moreover, plants show an irregular lignification of shoots, floral abortion and shriveling of the grapes (Terlizzi and Credi, 2007; Albertazzi *et al.*, 2009; Romanazzi *et al.*, 2009b).

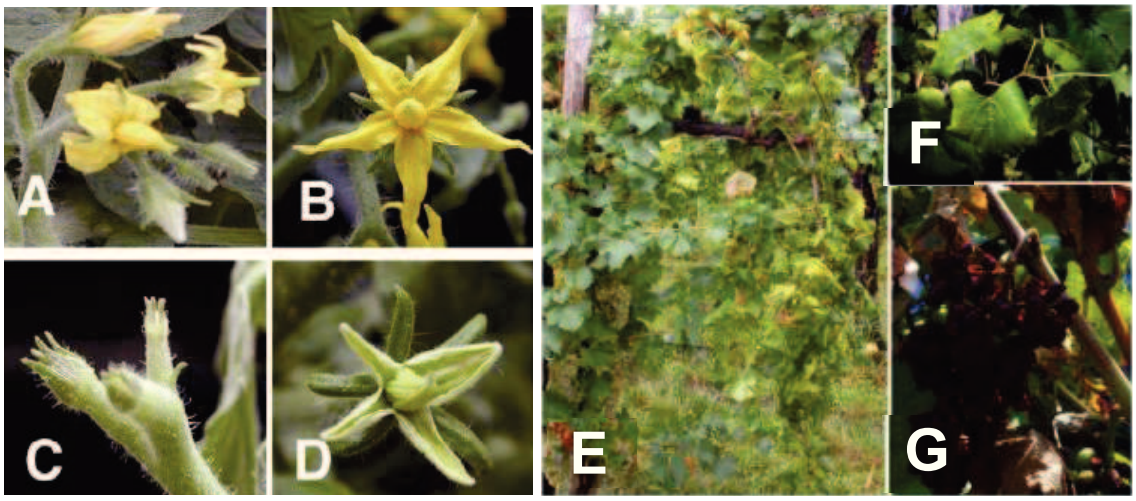

Figure 8. Symptoms on tomato and grapevine plants infected by '*Ca.* Phytoplasma solani'. A and B. Mature flowers of healthy tomato. C and D. Abnormal floral development in infected tomato plants. Notice overdeveloped petioles (C) and green petals (D) (Pracros *et al.*, 2006). E-G. Infected grapevine plant and details on yellowing and curling on leaves and a shriveled grape (Hren *et al.*, 2009a).

Investigations conducted at molecular level showed a clear alteration in the expression profiles of several genes of plants infected by '*Ca*. P. solani' (Lepka *et al.*, 1999; Hren *et al*., 2009a; Albertazzi *et al.*, 2009). In particular, genes that are modulated by the infection are involved in primary and secondary metabolism of the host. Many metabolic pathways are influenced by the presence of the pathogen, such as anabolic and catabolic processes of carbohydrates, photosynthesis mechanisms, systems of defense, signaling and regulation.

It has been hypothesized that phytoplasmas modulate the activity of enzymes involved in the carbohydrate metabolism in order to fulfill their energetic requests. Sucrose can enter the pathogen cells through ABC transporters, whose genes have been identified in the genomes of sequenced phytoplasmas. Moreover in '*Ca.* P. solani' genome, sequences coding for enzymes involved in the glycolytic pathway have been found, but it has been supposed that the microorganism uses hexoses present in the plant cells for its nourishment (Lepka *et al.*, 1999; Hren *et al.*, 2009a; Albertazzi *et al.*, 2009).

This hypothesis is supported by the upregulation of vacuolar invertases, sucrose synthases (SUSs) and alpha amylase genes which code for enzymes involved in hexose production from sucrose and starch (Albertazzi *et al.*, 2009; Hren *et al.*, 2009a,b).

4. The phenomenon of 'Recovery'

Several plant species infected by phytoplasmas may show a decrease in the symptom expression up to a complete remission from the disease. This spontaneous disappearance of symptoms is called recovery and it has been reported in several woody species as apples, apricots and grapevine (Osler *et al.*, 2000; Osler *et al.*, 1993; Musetti *et al.*, 2004).

This process is not clearly understood yet, as well as its physiological basis. It has been hypothesized that the remission of symptoms is associated with a lower phytoplasma titre and with a different distribution inside the plant. Studies conducted on apples affected by '*Ca.* P. mali' reported that in infected trees phytoplasmas were detectable in the whole plant, while in recovered trees the presence of the pathogen was limited to the roots (Caudwell *et al.*, 1961; Musetti *et al.*, 2004; Carraro et al., 2004; Musetti *et al.*, 2008). Also in the case of grapevines, both infected by Bois Noir and Flavescence Dorée, recovery has been reported (Osler *et al.*, 1993). The phenomenon is associated with the disappearance of the phytoplasmas from the crown (Osler *et al.*, 1993).

In Friuli Venezia Giulia (Italy) recovery is a relevant phenomenon, in fact it can occur in 50% of phytoplasma-infected grapevines after the first year of infection and in 70% after two years (Bellomo *et al.*, 2007).

At cytological and molecular level numerous are the modifications that have been detected in recovered plants (not only in grapevines but also in apple and apricot trees). These modifications lead to the increase in the activity of particular compounds or plant secondary metabolites linked to the induction of systemic acquired resistance (SAR) (Weintraub and Jones, 2010; Osler *et al.*, 2000).

Studies conducted on several species (apple, apricot and grapevine) reported an increase in the quantity of hydrogen peroxide (H_2O_2) in phloem tissues (Musetti *et al.*, 2004; Musetti *et al.*, 2005; Musetti *et al.*, 2007). Hydrogen peroxide is a reactive oxygen species with antimicrobial and signaling functions. The over-accumulation of this compound is due to a significant decrease in the activity of two enzymes that are involved in H_2O_2 scavenging (catalase, CAT and ascorbate peroxidase, APX). The presence of H_2O_2 was detectable in phloem cells of recovered grapevines by TEM investigations using a co-precipitation with cerium (Musetti *et al.*, 2007).

Another aspect that seems to be involved in recovery phenomenon is the deposition of callose in the sieve elements. In phloem tissues of recovered apple trees abnormal callose accumulations have been reported by ultrastructural investigations. These results were consistent with an up-regulation in the expression of some callose synthase coding genes in respect to healthy and infected samples (Musetti *et al.*, 2010).

It has been reported that callose deposition is a process regulated by the increase of Ca^{2+} concentration inside sieve elements (Musetti *et al.*, 2007; Musetti *et al.*, 2010). Similarly, the

Ca^{2+} acts as a signal for the conformational change of proteins typical of the phloem tissues (Phloem proteins or PP). These proteins are normally present in the lumen of sieve elements in a fibrillar-dispersed state. In recovered trees, a switch to aggregate state of these proteins has been found, that appears to be responsible of the occlusion of sieve pores. This process is associated with the increase of gene expression of *MdPP2,* which codes for a phloem specific lectin (Musetti *et al.*, 2010) (Figure 9). These findings support the hypothesis that recovered plants are able to develop resistance mechanisms depending on Ca^{2+} signal activity (Musetti *et al.*, 2010, 2013b). Recently, the activation of Jasmonate (JA)-related defense mechanism, via JA gene up-regulation, has also been demonstrated in apple trees recovered from AP disease (Patui *et al.*, 2013; Musetti *et al.*, 2013b).

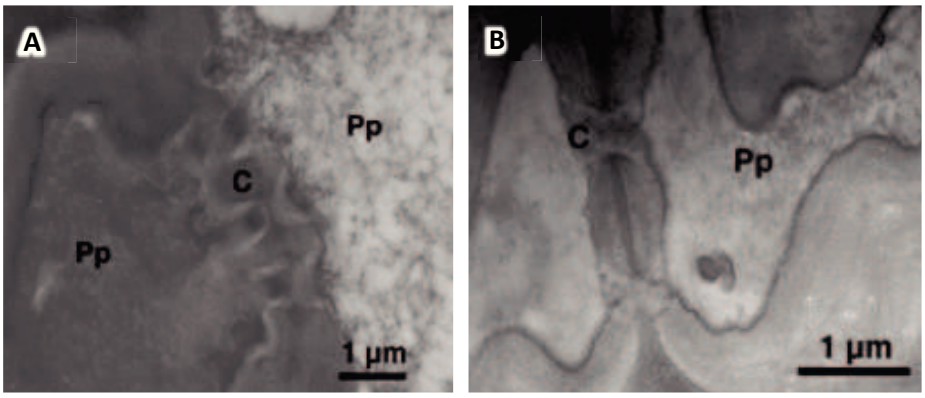

Figure 9. Transmission electron micrographs of phloem tissue of apple leaf from recovered apple plants. A and B. Accumulations of phloem proteins (Pp) are filling the cell lumen, and callose deposits are present around sieve pores (C) (Musetti *et al.*, 2010).

5. Phytoplasma diagnosis

As most attempts of *in vitro* cultivation of phytoplasmas have failed, the diagnosis of these pathogens relies on microscopic and molecular techniques.

Fluorescence microscopy is used to detect phytoplasmas in organs using DAPI (4',6-diamino-2-phenylindole), a molecule that binds specifically to DNA filaments rich in A-T bases. This method is very sensitive but it is not phytoplasma specific. Electron microscopy is also used to detect phytoplasmas and the diagnosis is reliable, but the method needs a qualified operator and a long procedure for the preparation of the sample (Christensen *et al.*, 2004).

Molecular diagnosis has developed several methods. Polymerase chain reaction (PCR) is used to detect the presence of specific DNA or RNA sequences of phytoplasmas in vegetal samples. In particular nucleic acids are extracted from a sample and are used as PCR template. Using universal or species-specific primers it is possible to amplify and detect phytoplasma nucleic acids. Primers used in PCR are mostly designed on 16S-23S regions of ribosomal RNA (Martini *et al.*, 2007). Where phytoplasmas are present at low titres, a nested PCR approach is often required. PCR or nested-PCR may be followed by a RFLP (Restriction Fragment Length Polymorphisms) analysis that allows to have more information on the pathogen and assign it to a specific group (Weintraub and Jones, 2010).

Recently, Real Time PCR systems have been proposed in phytoplasmas' diagnosis in order to increase the speed and sensitivity of detection. Based on fluorescent detection methods Real Time PCR does not need post-PCR manipulation such as electrophoresis and it is suitable for phytoplasma detection because even small quantities of DNA are detectable. SYBR Green binding dye and TaqMan® probes are the common used chemistries in microorganisms revelation. Especially using TaqMan® probes it is possible to achieve high specificity in the detection (Weintraub and Jones, 2010).

Because phytoplasma titres are affected by seasonal variation and environmental factors, PCR and Real Time PCR results should be associated to symptoms observations, ultrastructural investigations and studies on insect vectors. In this way it is possible to correlate a specific phytoplasma to a disease (Dickinson and Hodgetts, 2013).

PURPOSES

'*Ca*. Phytoplasma solani', the phytoplasma associated with grapevine Bois noir, causes relevant losses in viticulture in Europe and in the Mediterranean Basin. Bois noir disease adversely influences the quality and the quantity of the production. Although several studies have been conducted on the interactions occurring between phytoplasmas and grapevine, molecular mechanisms involved in the disease process are not still completely understood (Garau *et al.*, 2007; Landi and Romanazzi, 2011).
Recently, microarray analyses and gene expression investigations on grapevine permitted to discover plant genes that are modulated by phytoplasma infection (Albertazzi *et al*., 2009; Hren *et al.*, 2009a).

In this study, integrated approaches have been used to gain new insights in the plant-phytoplasma interactions. In particular, morpho-physiological changes of phloem tissue related to the impaired balance between source and sink organs provoked by the presence of phytoplasmas, were considered. Experiments were performed on two pathosystems, grapevine and tomato plants both infected by '*Ca*. Phytoplasma solani'. Grapevine samples were used to investigate the disease in a woody pluriannual plant, while tomato was used as a model herbaceous plant, easier to grow and to use for the set-up of the experiments. In this way it was possible to acquire information on two different hosts infected by the same pathogen.
An interesting phenomenon that occurs in grapevine and other pluriannual species infected by phytoplasmas is the recovery, a spontaneous remission of symptoms (Osler *et al.*, 2000; Osler *et al.*, 1993). Samples collected from recovered grapevine were also employed in experiments in order to gain insight in this relevant mechanism.
The combination of microscopy and ultramicroscopy techniques was used to have both global and detailed knowledge about morphological changes in infected leaf and root tissues. As the main morphological change in infected plants is the impairment of the phloem mass flow due to callose and/or protein deposition at the sieve plate, expression analyses were conducted on plant genes coding for proteins involved in sucrose metabolism and translocation (i.e., callose synthases, sucrose synthases, SWEETs) and genes coding for structural proteins of the phloem (i.e., SEOs, P-proteins). For some genes, like SEO, it was also interesting to confirm their localization at phloem level, by *in situ* hybridization experiments. Investigations on genes gave complementary informations to those obtained by microscopic analyses, allowing us to have new details about the plant response to the infection, mainly at phloem level.

As phytoplasmas systemically spread in the host plants, and diagnosis in the root apparatus of the woody plants is difficult, a specific protocol to detect phytoplasmas in grapevine roots was set up. Being able to perform diagnosis about phytoplasma presence in roots would mean to have information about the phytosanitary status of the plant all over the year.

MATERIALS AND METHODS

1. Sample collection

Grapevine leaf and root collection

Grapevine samples were collected from *Vitis vinifera* L. plants, cv. Chardonnay. Plants were grown in an experimental field located in Lucinico (Gorizia) in North-Eastern Italy. Plants were regularly treated with fungicides and their phytosanitary status has been monitored for several years.

Since the early of 2000s some plants have begun to show typical symptoms of Bois noir infection ('*Candidatus* Phytoplasma solani', subgroup 16 SrXII-A) as leaf blade yellowing and curling, irregular lignification of canes and internode shortenings. In the following years, many of the symptomatic plants recovered from disease symptoms.

Monitoring the plants year by year allowed us to obtain an accurate map of healthy, symptomatic and recovered plants. Plants were intended recovered if they did not show any symptoms for at least three consecutive years.

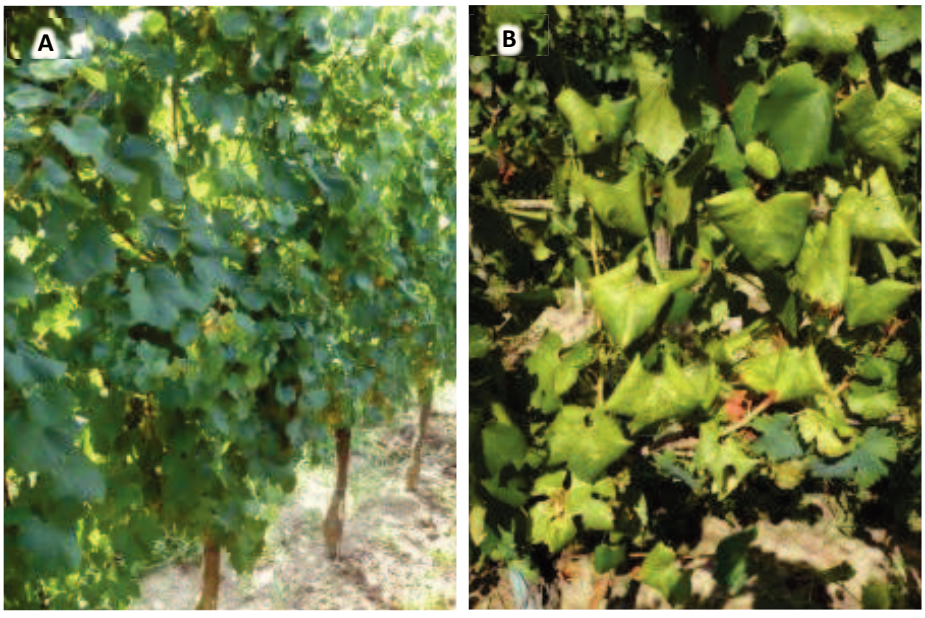

Figure 10. Grapevines in the experimental field. A. Healthy individuals showing vigorous and luxuriant habit. B. Infected plants showing typical Bois noir symptoms as leaf curling, yellowing of the intervein and irregular lignification of the canes.

The sample collection was carried out in late summer when typical stolbur symptoms were present and easy to distinguish. Fully expanded, not damaged leaves were sampled from healthy (never symptomatic since planting), symptomatic and recovered grapevines. At least four leaves were sampled from each plant (Figure 10, A and B).

Figure 11. Example of grapevine roots collected from the soil.

As concerns roots, samples were collected in October, after grape harvest. Approximately two grams of hairy roots were taken from the soil (Figure 11).
Once collected, samples intended for RNA extraction and gene expression analyses were stored at -80°C, while samples that would be employed for microscopy observations and *in situ* hybridization experiments, have been immediately processed for fixation and embedding.

Tomato leaf and root collection

Tomato plants (*Solanum lycopersicum* L., cv. Micro-tom) were grown from seed and maintained in greenhouse (Department of Agricultural and Environmental Sciences, Udine, Italy) at 27°C during the day and 20°C during the night (Figure 12.A). A group of plants was infected with '*Candidatus* Phytoplasma solani', subgroup 16 SrXII-A, type V9 (Pacifico *et al.*, 2009), by grafting using scions from greenhouse-maintained infected tomato plants as source of inoculum. Another group was not grafted and used as uninfected healthy control. The stolbur phytoplasma V9 had been first isolated from naturally infected tomato plants, grown in field, and graft-transmitted to Micro-tom.
Leaves from healthy and infected plants were collected for ultrastructural investigations, gene expression analyses and *in situ* hybridization experiments. At least three leaves from three plants were collected when symptoms on grafted plants were evident (i.e., small, yellowing and curling leaves, witches' brooms), approximately three months after grafting (Figure 12.B). From the same plants roots were also collected for TEM observations and diagnosis experiments.

Figure 12. Tomato plants grown in the greenhouse. A. Healthy plant with regular growth. B. Stolbur infected plant with leaf discoloration and witches' broom.

Arabidopsis stems collection

Arabidopsis (*Arabidopsis thaliana* L. Heynh, cv. Columbia 0) plants were grown in soil in the greenhouse (Institut Jean-Pierre Bourgin, INRA-Centre of Versailles, France) with long-day conditions (16-h-light/8-h-dark cycle). Floral stems for *in situ* hybridization experiments were harvested after complete flowering, as shown in Figure 13. Stems were cut 10 cm long from the basis and sliced in smaller pieces of 0.5 mm.

Figure 13. Schematic representation of *Arabidopsis* plant. Dashed lines indicate the sampled portion.

2. Light microscopy

Light microscopy investigations have been performed on grapevine and tomato leaves to have a global comprehension of the structure of vascular bundles. Observations were conducted on paraffin embedded samples collected from grapevine and tomato healthy plants. An Axio Zoom.V16 stereo zoom microscope (Carl Zeiss GmbH, Munchen, Germany) was used in the experiments. Samples sections were obtained from paraffin embedded segments of leaf vein cut with a rotary microtome (Leica, Bensheim, Germany) into 8-µm thick slices. Paraffin embedding procedure is described in "8. *In Situ* Hybridization experiments - Samples preparation" section.
Light microscopy investigations have been performed at the Institut Jean-Pierre Bourgin (INRA, Centre of Versailles, France).

3. Confocal microscopy

Grapevine and tomato leaf samples from healthy and infected plants were observed at confocal laser scanning microscope (CLSM, Leica TCS SP2, Leica Microsystems, Germany) after staining with carmine green solution. 8-µm thick slices were cut from paraffin embedded vein segments, mounted on slides and immersed in staining solution for 20 minutes after paraffin removal by ten minutes in histoclear (Agar Scientific, Stanstead, UK).
Confocal microscopy investigations have been performed at the Institut Jean-Pierre Bourgin (INRA, Centre of Versailles, France).

4. Transmission Electron Microscopy

Transmission electron microscopy (TEM) was used to observe the ultrastructural organization of cells in grapevine and tomato samples. More in detail, leaf samples of healthy, infected and recovered grapevine plants and healthy and infected tomatoes were observed, focusing on phloem tissue.
Samples were prepared following the procedure described by Ehlers *et al.*, (2000). This method allows a gentle preparation of samples preventing tissue degradation.
Leaf tissues containing the vein were sliced in approximately 6 mm in length and 2 mm in width segments. Pieces were immersed for two hours at room temperature in buffer containing 10 mM NaOH-2-(*N*-morpholino) ethanesulfonic acid, 2 mM $CaCl_2$, 1 mM $MgCl_2$, 0.5 mM KCl, and 200 mM mannitol, pH 5.7 (van der Schoot and van Bel, 1989). Thus, the solution was replaced with a fixation buffer consisting of 3% paraformaldehyde and 4% glutaraldehyde in 50 mM sodiumcacodylate buffer plus 2 mM $CaCl_2$, pH 7.2. This buffer was replaced every 30 minutes for 6 total hours. After this incubation, samples were immersed in 50 mM sodiumcacodylate buffer

containing 2 mM $CaCl_2$ (pH 7.2) for 1 hour at 4°C and postfixed overnight with 2% (w/v) OsO_4 in the same buffer at 4°C. After a dehydration step through a graded ethanol series and propylene oxide, samples were embedded in Epon/Araldite epoxy resin (Electron Microscopy Sciences, Fort Washington, PA, USA).

The different samples were cut in several ultrathin sections (60-70 nm thick). They were collected on copper grids and stained with uranyl acetate and lead citrate. Sections were observed under a Philips CM 10 (Eindhoven, The Netherlands) transmission electron microscopy operating at 80 kV.

5. Ribonucleic acids extraction and cDNA synthesis

Grapevine RNA extraction

Ribonucleic acids from approximately 2 grams of leaf or root samples were extracted grinding the sample in liquid nitrogen using mortars and pestles. Leaf samples were enriched in midribs to increase the phloem tissue portion of the sample.

Leaf and root samples were collected from at least three plant for each different group (healthy, symptomatic and recovered plants).

The RNeasy® Plant Mini Kit (Qiagen GmbH, Hilden, Germany) was used to extract nucleic acids. Grapevine tissues contain phenolic compounds, which often compromise the quality and efficiency of the RNA extraction (Newbury and Possingham, 1977; Gehrig *et al.*, 2000). In order to achieve better results, some modifications were introduced in the protocol of RNeasy® Plant Mini Kit (MacKenzie *et al.*, 1997).

Grapevine leaf samples were processed as follows, introducing a modification to the RLT Buffer Lysis provided by RNeasy® Plant Mini Kit. The modification consisted in adding 25mg/mL of Polyvinylpyrrolidone 40 (PVP, Sigma-Aldrich S.r.l, Milan, Italy) to the RLT Buffer Lysis. After the homogenization of the grinded sample in the RLT modified buffer an incubation of 5 minutes at room temperature (RT) with 1/10 volume of Sodium Lauryl Sarcosinate 20% v/v (Sigma-Aldrich S.r.l, Milan, Italy) has occurred. The following step was an incubation for 10 minutes at 70° C and centrifugation (5 minutes at 3000g) to recover the supernatant for further steps.

As concerns RNA extraction from root samples the protocol was modified with the addition of 1 volume of chloroform isoamyl alcohol (24:1) in the adapted RLT buffer (with PVP), before a centrifugation at 14000g at 4°C for 15 minutes.

Thus, the obtained supernatants were collected and transferred to a QIAshredder column (supplied by the Qiagen Kit). Then extraction was performed according to the manufacturer's instructions. Briefly, the lysate was purified and adsorbed by the column filter and after a series of washing steps eluted in 30-50 μL of RNase free water.

Tomato RNA extraction

RNA extraction from tomato leaves was performed using the RNeasy® Plant Mini Kit, following the manufacturer's instructions without modifications. On the other hand, the modified protocol described for grapevine was used to extract RNA from tomato roots. The amount of starting material was approximately 2 grams of leaves or roots.

RNA quantification

Nucleic acids were quantified using a NanoDrop ND-1000 UV-visible spectrophotometer (Thermo Fisher Scientific, Inc., Waltham, MA, USA). Adsorbance ratios of A^{260}:A^{280} and A^{260}:A^{230} were studied in order to check RNA quality. These two indexes should range between 1.8 and 2.0. An A^{260}:A^{230} index lower than 1.8 may indicate a problem with the sample or with the extraction procedure, in particular it reveals the presence of polysaccharide, while an A^{260}:A^{280} index lower than 1.8 denotes a contamination by proteins and polyphenols. RNA samples were stocked at -80°C.

cDNA synthesis

Extracted RNAs were used to obtain complementary DNA (cDNA), which is the template of polymerase chain reactions (PCRs). PCR allows the amplification of the genes of interest (Mullis *et al.*, 1986).

RNAs from grapevine and tomato leaves were reverse-transcribed with QuantiTect® Reverse Transcription Kit (Qiagen GmbH, Hilden, Germany) with random hexamers following manufacturer's instructions. Briefly, an incubation of 2 minutes at 42°C in gDNA Wipeout Buffer occurred in order to eliminate genomic DNA. The entire genomic DNA elimination reaction was then incubated for 30 minutes at 42°C in a mix containing 20X Reverse-transcription master mix, 5X Quantiscript RT Buffer, 20X RT Primer Mix in a total volume of 20 µL. The reaction mixture was incubated for 3 minutes at 95°C to inactivate Quantiscript Reverse Transcriptase. cDNAs were stocked at -20°C.

High Capacity cDNA Reverse Transcription Kit was used to obtain cDNA from grapevine and tomato roots RNA samples. Briefly, RNA was mixed with 10X RT Buffer, 25X dNTP Mix (100 mM), 10X RT Random Primers, MultiScribe™ Reverse Transcriptase, RNase Inhibitor in a total volume of 20 µL. The mix was incubated at 25°C for 10 minutes, 37°C for 120 minutes and finally at 85°C for 5 minutes. cDNAs were stocked at -20°C.

6. Real Time PCR analyses

Gene expression analyses

cDNAs obtained from leaf samples were used to conduct gene expression analyses and phytoplasma detection using the Real Time polymerase chain reaction technique (Bustin, 2005).
The Real Time PCR is an evolution of the classical PCR and it permits to reveal the presence of a gene and its expression level while the amplification reaction is carried on. The revelation is possible since the instrument is able to detect the fluorescence of a marker that binds to the double helix of the amplicon.
During the extension step Taq polymerase enzyme produces the second strand of the DNA and the dye can be incorporated. The detected signal is proportional to the amplicon concentration.
The amplification curve has a characteristic profile (Figure 14), where it is possible to distinguish a first phase when fluorescence remains at background levels, and increases in fluorescence are not detectable. This phase is followed by an exponential one in which all the mixture components are not limiting and the amount of PCR product approximately doubles in each cycle. Finally, reaction components are consumed and the reaction enters a linear trend, called "*plateau* phase"(Bio-Rad Laboratories, 2006).
Moreover, in a Real Time PCR amplification graph it is possible to identify a threshold line, which interpolates all the amplification curves in their exponential phase. The cycle in which the threshold line intersects the amplification curve is called Quantification cycle (Cq). There is a linear correlation between the Cq value and the PCR product and it is possible to calculate the amount of template present at the beginning of the reaction (Bustin, 2005).
After the amplification cycles, it is possible to obtain a dissociation curve which permits to obtain a "melting temperature" for each amplicon. Temperature is raised from 60°C to 95°C degrees and fluorescence is revealed at regular time intervals during all the increase. This melting temperature derived from the dissociation curve indicates the temperature in which 50% of the amplicons are associated and 50% are dissociated. This temperature depends on length and basis composition of the amplicons.

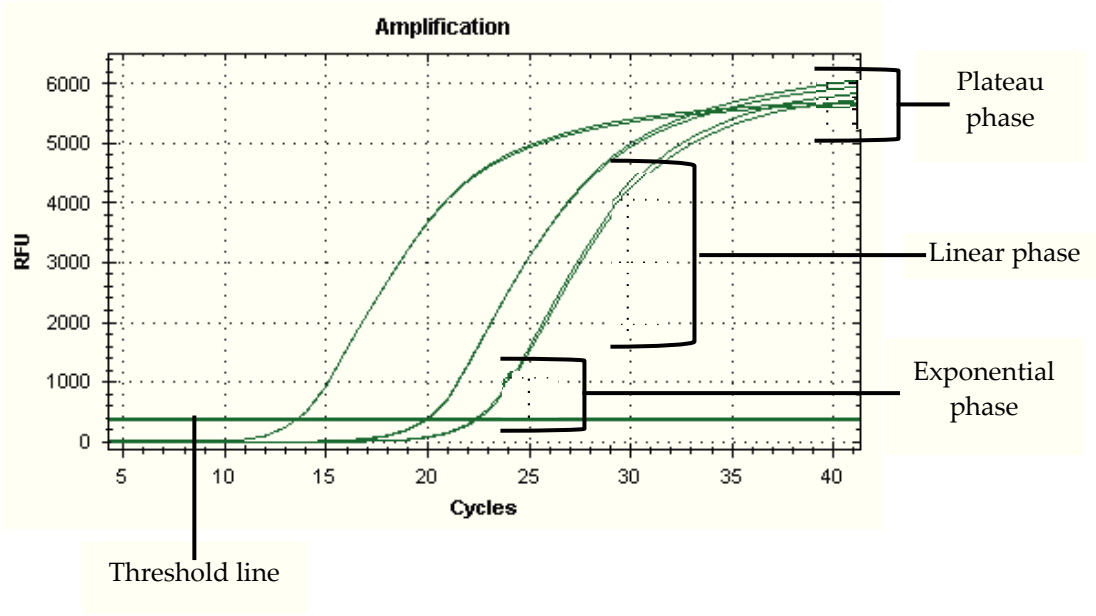

Figure 14. Schematic representation of a Real Time PCR amplification curve.

Different dyes and amplification kits are commercially available. Sso Fast™ Eva Green® Supermix (Bio-Rad Laboratories Co., Hercules, CA, USA) was used for the analysis of some grapevine genes (callose synthases) and diagnosis on grapevine and tomato leaves. Real Master Mix SYBR ROX (5 Prime, Eppendorf, Hamburg, Germany) was used for grapevine sucrose synthases genes. Finally, expression levels of tomato genes were checked with MESA FAST qPCR kit for SYBR® Assay (Eurogentec, Seraing, Belgium). Real Time PCRs using MESA FAST qPCR kit were performed at the Institut Jean-Pierre Bourgin, INRA, Centre of Versailles.

Reaction mixtures and amplification cycles for the three different kits are shown in Table 1. Real Time PCR experiments were performed on a CFX96 Real Time PCR Detection System (Bio-Rad Laboratories Co., Hercules, CA, USA).

Sso Fast™ Eva Green® Supermix				
Component	Volume (µL)	Phase	Conditions	Cycles
Eva Green Supermix	5	Initial denaturation	3 min at 95°C	1
Primer Forward (10 µM)	0.3-0.5	Denaturation	5 sec at 95°	40
Primer Reverse (10 µM)	0.3-0.5	Annealing-Extension	10 sec at 60°C	
RNase-free water	Variable	Plate reading		
cDNA (2.5 ng/µL)	4	Melting curve	65°C to 95°C, increment 0.5°C, plate reading every 5s	1
Total volume	10			

Real Master mix SYBR ROX				
Component	Volume (µL)	Phase	Conditions	Cycles
RealMasterMix SYBR ROX 2.5X with SYBR GREEN	9	Initial denaturation	5 min at 95°C	1
Primer Forward (10 µM)	0.6-1	Denaturation	15 sec at 94°	40
Primer Reverse (10 µM)	0.6-1	Annealing	20 sec at 58°C	
RNase-free water	Variable	Extension	30 sec at 68°C	
cDNA (2.5 ng/µL)	4	Plate reading		
Total volume	20	Melting curve	65°C to 95°C, increment 0.5C, plate reading every 5 sec	1

MESA FAST qPCR kit				
Component	Volume (µL)	Phase	Conditions	Cycles
MESA FAST mix	5	Initial denaturation	5 min at 95°C	1
Primer Forward (10 µM)	0.15	Denaturation	10 sec at 95°	40
Primer Reverse (10 µM)	0.15	Annealing-Extension	20 sec at 55-60°C	
RNase-free water	2.2	Plate reading		
cDNA (2.5 ng/µL)	2.5	Melting curve	65°C to 95°C, increment 0.5C, plate reading every 5 sec	1
Total volume	10			

Table 1. Real Time PCR mixtures and conditions.

Gene sequences

Grapevine and tomato sequences used in the experiments were retrieved from literature and from blasting analysis with other species, using NCBI database (*National Center for Biotechnology Information,* http://www.ncbi.nlm.nih.gov/).

Blast (Basic Local Alignment Search Tool) analysis permits the research of homologous gene sequences in different species (Altschul, 1990).

Grapevine gene sequences were also checked in the Grape 12X Genome database of the Grape Genome Browser (http://www.genoscope.cns.fr/externe/GenomeBrowser/Vitis/).

Primers used in PCRs were designed using Primer3 software (http://bioinfo.ut.ee/primer3-0.4.0/primer3/) (Untergrasser *et al.*, 2012; Koressaar and Remm, 2007).

Primers were designed taking into account the length of the amplicon, which was imposed approximately 100 base pairs and the melting temperature which ranged between 55 and 60°C. Then they were evaluated using the BLASTN algorithm (Altschul *et al.*, 1997) to check their specificity.

Standard curves of three different dilutions of pooled cDNA were used to calculate PCR efficiency for each primer pair as described by Pfaffl (2001). Amplification efficiency was determined from the slope of the curve.

The equation used for the efficiency value calculation was $E= 10^{[-1/slope]}$ ($\%E=10^{[-1/slope]}-1$), when the logarithm of the initial template concentration is plotted on the *x* axis and the Cq is plotted on the *y* axis. The theoretical efficiency value of 100% indicates that the amount of product doubles with each sample (Bustin *et al.*, 2009).

Genes and primers sequences for expression analysis are reported in Table 2 (E= Primer efficiency).

Grapevine					
Gene	Primer forward 5'-3'	Primer reverse 5'-3'	nM	E	NCBI acces. no.
VvUBQ-L40	CCAAGATCCAGGACAAGGAA	GAAGCCTCAGAACCAGATGC	300	2.05	XM_002273532.1
VvCAS1	GCCTTGCGCTTTTTCATCTA	CTTCGCCTTCCAACAGAGAG	300	2.01	XM_002271612.2
VvCAS2	TTCACCCCAGTTGCATTTCT	CCGATCCTTCCTATGACCAC	300	2.05	XM_002283262.2
VvCAS5	GCATGGTTCCCATTTGTCTC	TCATCACAGCCTCACTCTGC	300	1.96	XM_002274301.1
VvCAS7	GCTGGGAAGGGCTTATGAGT	GGCCTCTACTGAATGCCTGA	300	2.01	XM_002279310.2
VvCAS10	GATGCTGGGATGGGTATGAT	CCTGCAAGGATGATGGAGAT	300	2.03	XM_002275082.2
VvCAS11	GCTGAACAGAGCTGGGAAAC	CGCCGTACTGGAAAAAGAAG	300	1.97	XM_002263721.2
VvSUS2	GGCTGGGGTTTATGGTTTCT	ATTTTGCCAGATCACGGAAC	300	2.06	XM_002271860.1
VvSUS4	GCTGGCTCAATCAGTTCCTC	CCAAGCCTCAAACAATGACA	500	2.01	XM_002275119.1
VvSUS5	GCAGGGATGATTCAGACCAT	CTTGCTTGTGTTCCGTGTTC	300	2.07	XM_002266984.2
VvSUS6	TATGGCTTCTGGAGGCAGTT	CCTTCGCCAATTTTCTGAAT	500	2.02	XM_002270825.1

Tomato					
Gene	Primer forward 5'-3'	Primer reverse 5'-3'	nM	E	NCBI acces. no.
SlUPL3	AGCGCTGATCCCTCATTGCAT	GCTGTTTACAAATTCCTCCGAGG	200	1.90	XM_004230989.1
SlCAS2	GTTGACGATGTGGAGGAACA	AACCTTTTTCCGCAATTCCT	200	2.07	XM_004229311.1
SlCAS3	TGTTCGGAGAGCTGGATTCT	AAACCAAGCCAGAAAAGCAA	200	1.97	XM_004228545.1
SlCAS7	GGGACTTGGAATTTGGGATT	CTCTGATACGAATGGGAACCA	200	2.06	XM_004243161.1
SlCAS8	TGTAAACGACCTGGGGAATC	CAGTTCTGTGGGTGACCTTG	200	1.96	XM_004244335.1
SlCAS9	CTTGGTTCCCCTTCATTTCA	TGTTTGGATTGTTTCCAGCA	200	1.97	XM_004228544.1
SlCAS10	TTTGGCATCTCAAGTTCCATC	ATTTGGTCACCCCATCTTCA	200	1.95	XM_004236267.1
SlCAS11	TTCATTTTTCGTGGGCTCTT	AAACTGGTGCAAACCTCGTC	200	2.07	XM_004232827.1
SlCAS12	CTGTCTTGGTTGCCTGGTTT	CTGGAATATCCGCAGACCTC	200	1.97	XM_004243304.1
SlPp2	TGAAGGTGGGAACTGGAAGA	CTGGGCTTAACGCCAAATC	150	1.99	XM_004233183.1
SlSEO	AGGAGTTGGGTCGCGTCTA	GGAAAAGCTGTTTATTGATTCTTCA	150	2.09	XM_004239105.1
SlSWEET1	CAAATGGCAAGTCTCACCAA	TTTATTTGAGCAGGCAGCAA	150	1.99	XM_004237674.1

Table 2. List of primers and accession number sequences used in Real Time PCRs.

Real Time PCR results were analyzed as described by Muller *et al.*, (2002), calculating a mean normalized expression (MNE) for each gene of interest. The mean expression level was normalized to the level of a selected reference gene. Reference or "housekeeping" gene should not be regulated or influenced by the experimental procedure (Radonić *et al.*, 2004).

For both grapevine and tomato, several potential reference genes were retrieved from literature and checked on samples in order to identify the most stable one. The geNorm software (Vandesompele *et al.*, 2002) was used to compare different genes and find a stable one. In Table 3 checked genes and primers used are listed for both species. *SlUBI* and *SlACT* primers were retrieved from Løvdal and Lillo, (2009).

Grapevine			
Gene	Primer forward 5'-3'	Primer reverse 5'-3'	NCBI accession no.
VvUBQ-L40	CCAAGATCCAGGACAAGGAA	GAAGCCTCAGAACCAGATGC	XM_002273532.1
VvACT	TTTTGTTCTGCTCACGCATC	GTAGCCCTCTTCGGACGTAA	XM_002282480.2
Vv60srp	CCTCCGATGTCTCTCTCCAG	TTCAATGTCGGCACCTCATA	XM_002270599.1
VvCF	CTATATGCTCGCTGCTGACG	AAGCCAGGCAGAGACAACTC	XM_002274299.1
Tomato			
Gene	Primer forward 5'-3'	Primer reverse 5'-3'	NCBI accession no.
SlUPL3	AGCGCTGATCCCTCATTGCAT	GCTGTTTACAAATTCCTCCGAGG	XM_004230989.1
SlUBI	GGACGGACGTACTCTAGCTGAT	AGCTTTCGACCTCAAGGGTA	XM_004244105.1
SlACT	GAAATAGCATAAGATGGCAGACG	ATACCCACCATCACACCAGTAT	XM_004236699.1

Table 3. List of primers and accession no. sequences used for gene reference selection.

Real Time PCR analyses – TaqMan® probe chemistry

Real Time PCR technique can be also based on fluorescent probes. In particular, TaqMan® probes were introduced by Holland *et al.*, in 1991 in order to perform an assay with high specificity and high signal-to-noise ratio. TaqMan® probes are gene-specific and are used in the reaction in addition to the sequence-specific primers.

Taqman® probes possess a fluorophore called reporter at the 5'-end of the oligonucleotide and a quencher at the 3'-end. At the beginning of the reaction the fluorescence of the reporter is masked by the quencher molecule. During the annealing and extension step of the PCR reaction, the probe hybridizes to the target sequence and Taq polymerase activity separates the reporter from the quencher. In this way, fluorescence is emitted and the signal is proportional to the amount of the amplicon in the reaction (Bio-Rad Laboratories, 2006). Several combinations of reporter-quencher are commercially available.

For their high specificity TaqMan® probes were used in diagnosis experiments on grapevine roots, as it will be described in the "7. Phytoplasma detection" section. Real Time PCR experiments were performed on a CFX96 instrument (Bio-Rad Laboratories Co., Hercules, CA, USA).

7. Phytoplasma detection

Phytoplasma detection on grapevine leaves

Phytoplasma detection was carried out on grapevine and tomato RNA leaves by means of Real Time PCR.

Reactions were set up with Sso Fast™ EvaGreen® Supermix (Bio-Rad Laboratories Co., Hercules, CA, USA) using the specific primers designed on the *16S rRNA* gene of '*Ca*. P. solani' (accession no. AF248959) 16Sstol(RT)F2 and 16Sstol(RT)R3 (Martini *et al.*, unpublished results; Santi *et al.*, 2013).

Real Time PCR analyses were performed in a CFX96 Real Time PCR Detection System (Bio-Rad Laboratories Co., Hercules, CA, USA), imposing the following standard thermal profile: 98°C for 2 minutes, followed by 45 cycles for 5 seconds at 98°C and 5 seconds at 60°C. A melting curve analysis of the products was performed from 65 to 95°C to check primer specificity. In Table 4 are reported the used primers.

Gene	Primer forward	Primer reverse
16S rRNA	5'-AGGGTAGCTAAAGCGTAAGC-3'	5'-CATCAACCCTACCTTAGACG-3

Table 4. List of primers used for phytoplasma detection.

Phytoplasma detection on tomato leaves

Phytoplasma presence in tomato leaves samples was checked by means of Real Time PCR. Experiments were set up as described above for grapevine using the specific primers designed on the *16S rRNA*.

Phytoplasma detection on grapevine roots

cDNAs obtained from grapevine root samples were used to develop an efficient method for phytoplasma detection in the root tissues.

High Capacity cDNA Reverse Transcription Kit (Applied Biosystems, Life Technologies, Darmstadt, Germany) was used to obtain cDNAs from RNAs samples.

To check RNA integrity and cDNA synthesis, a Real Time PCR was performed using specific primers for plant *18S rRNA* (Osman *et al*., 2007). Amplification parameters consisted of: 95°C for 10 minutes, 32 cycles of 95°C for 15 seconds, 60°C for 1 minutes and 95°C for 15 seconds, and finally 60°C for 1 minute. Water controls were included in the assay.

cDNA was at first used to perform a Real Time PCR (Margaria *et al*., 2009), using primers 210F-280R and a TaqMan® probe designed on the BNp *16S rRNA* (Table 5). The probe (Eurogentec, Seraing, Belgium) was labeled with FAM-6 (6-carboxyfluorescein) at the 5'-end as reporter and with TAMRA (tetramethylrhodamine) at the 3'-end as quencher.
A two-step protocol consisting in a PCR followed by a Real time nested PCR was performed.
The first PCR reaction was carried out following the protocol reported in Margaria *et al*. (2009) using primers based on the *16S rRNA* (190F-660R, Table 5). A 1:30 dilution of the first amplicon (*16S rRNA* PCR) was used as template in Real Time nested-PCR. The reaction was prepared in 25 μL total volume as follows: 2X Taqman Fast Universal PCR Master mix (Applied Biosystems, Life Technologies, Darmstadt, Germany), 200 nM probe, and 300 nM each primer. Amplification consisted of 10 minutes at 95°C and 45 cycles of 15 seconds at 95°C and 1 minute at 60°C. Positive control (BN infected periwinkle) and water were included in each assay.
Real Time PCRs for phytoplasma detection on grapevine roots have been performed at the CNR Institute, Torino, Italy.

BNp RT-PCR	190F – Primer forward	5'-GAGATAAGAAGGCATCTTCTTA-3'
	660R – Primer reverse	5'-AACAGTTTTTATAGCATCACAA-3'
Real Time nested-PCR	210F – Primer forward	5'-CTTCTTATTTTTAAAAGACCTAGCAATAGG-3'
	280R – Primer reverse	5'-GTCTTGGTAGGCCATTACCC-3'
	BN-P – TaqMan® Probe	5'-TTAGGGAAGAGCTTGCGTCA-3'

Table 5. List of primers used in phytoplasma detection on roots.

Phytoplasma detection on tomato roots

The protocol developed to detect phytoplasmas in grapevine roots was applied also to RNA samples obtained from tomato roots. Conditions and reagents used were the same described for grapevine.

8. *In situ* hybridization experiments

In situ hybridization analysis

In situ hybridization is an invaluable tool for the examination of gene expression on histological tissue sections. The principle of the technique is using a labelled nucleic acid probe, which can hybridize to a complementary sequence of mRNA. In this way it is possible to identify cell types expressing the gene of interest (Wilcox, 1993).

Tissue samples used in *in situ* experiments have to be processed in order to preserve anatomical structure and nucleic acids. In general, samples are fixed in buffers containing aldehydes and embedded in a matrix (i.e., wax, paraffin). 5-10 µm slices are obtained from blocks and mounted on slides.

In situ hybridization can be performed using different types of probes as complementary RNA (riboprobes), DNA sequences, or oligonucleotides. Riboprobes are RNA sequences which can be obtained using a transcription vector system starting from cDNA sequences as template or directly through *in vitro* transcription using a modified cDNA sequence recognizable by a T7 polymerase.

The transcription vector system was employed to obtain ubiquitin riboprobes for grapevine leaf samples. The method is described below.

The cDNA insert was obtained through a PCR using the Platinum® Taq DNA Polymerase (Invitrogen, Life Technologies Co., Carlsbad, CA, USA) with the following reaction mix: 1X PCR Buffer, 0.5 mM dNTPs, 1.5 mM $MgCl_2$, 1 µM each primer, 1 unit of Platinum® Taq DNA Polymerase, 50 ng cDNA template in a total volume of 50 µL. The cycle parameters were: 94° C for 2 minutes, 30 cycles of 94° C for 30 seconds, 55° C for 30 seconds and 72° C for 30 seconds. The PCR product was checked on a 2% agarose gel and purified with Wizard® SV Gel and PCR Clean-Up System using the manufacturer's instructions (Promega, Madison, WI, USA). After quantification with a NanoDrop ND-1000 UV-visible spectrophotometer (Thermo Fisher Scientific, Inc., Waltham, MA, USA) the cDNA product was subcloned in a pCR®II vector included in the "TA Cloning® Kit Dual Promoter (pCR®II)" (Invitrogen, Life Technologies Co., Carlsbad, CA, USA). The ligation reaction was performed using 10X Ligation Buffer, 25 ng/µL linearized pCR®II, 4 units/µL T4 DNA Ligase in a total volume of 10 µL. The amount of purified PCR product needed was estimated using the formula: X= (N° bp PCR product* 50 ng pCR®II Vector)/ (size in bp of the pCR®II vector: ~3900). The reaction was performed overnight at 14°C.

The day after incubation, competent *E. coli* One Shot® cells (Invitrogen, Life Technologies Co., Carlsbad, CA, USA) were transformed using a heat shock procedure. Ligation reaction was mixed with competent cells vials and incubated on ice for 30 minutes before keeping them 30 seconds at 42° C and again stored in ice. Following the manufacturer's instructions 250 µL of S.O.C. medium was added and vials were shacked horizontally at 37° C for 1 hour.

100 µL of each transformation were spread on LB agar plates containing ampicillin (100 µg/mL), X-Gal (40 µL/plate of 40 mg/mL X-Gal), and IPTG (40 µL/plate of 100 mM IPTG). Plates were incubated overnight at 37°C.

After an incubation at 4°C for 2 hours to allow proper color development, white colonies were picked and plated in new LB agar plates overnight at 37°C. A "colony PCR" followed by an agarose gel run was performed to check the insertion and choose colonies. Colonies with a good insertion were grown overnight in a shaker in LB medium added with ampicillin.

Thus, plasmids were purified with Wizard® Plus SV Miniprep DNA Purification System (Promega, Madison, WI, USA), linearized with BAM HI and ECO RV restriction enzymes (Fermentas, Vilnius, Lithuania) following the procedure shown in Table 6 and finally the obtained cDNA fragments were purified using Wizard® SV Gel and PCR Clean-Up System (Promega, Madison, WI, USA).

Component	Volume (µL)
Buffer 10X	2
Plasmid	15
Enzyme (BAM HI or ECO RV)	0.5
RNase-free water	2.5
Total volume	20

Table 6. Linearization reaction.

Approximately one microgram of purified DNA was used as template for the production of a RNA probe labeled with Digoxigenin molecules. DIG RNA Labeling Kit (Sp6/T7) (Roche Diagnostic GmbH, Mannheim, Germany) was used following the manufacturer's instructions.

The other probes tested in *in situ* experiments on grapevine, tomato and *Arabidopsis* were obtained directly through *in vitro* transcription. In detail, for each gene of interest the reverse primer used to obtain the cDNA was modified at the 5'-end with a 23-nucleotides tail (TGTAATACGACTCACTATAGGGC), which was recognizable by the T7 polymerase of Riboprobe system T7 kit (Promega, Madison, WI, USA). Briefly, a PCR was performed using Phusion® High-Fidelity DNA Polymerase (Thermo Fisher Scientific, Inc., Waltham, MA, USA) as described in Table 7 and the obtain cDNA was purified using NucleoSpin® PCR Clean Up and Gel Extraction Kit (Clontech Laboratories, Palo Alto, CA, USA). Then cDNA was used as the template for T7 Riboprobe system to obtain a Digoxigenin-labeled RNA probe. Reaction mix (indicated in Table 8) was incubated at 1 hour at 37°C followed by a DNase treatment for 15 minutes.

Component	Volume (µL)	Phase	Conditions	Cycles
Buffer Phusion® High-Fidelity DNA Polymerase	10	Initial denaturation	3 min at 98°C	1
dNTP's (10 mM)	1	Denaturation	10 sec at 98°C	40
Primer Forward (10 µM)	1	Annealing	30 sec at 55-60°C	
Primer Reverse (10 µM)	1	Extension	45 sec at 72°C	
Taq Polymerase	0.5	Final extension	15 min at 72°C	1
RNase-free water	31.5			
cDNA (2.5 ng/µL)	5			
Total volume	50			

Table 7. PCR reaction and conditions.

Component	Volume (µL)
Buffer 10X	2
ATP	1.5
GTP	1.5
CTP	1.5
UTP	1
DIG-UTP	1
RNasin	1
T7 RNA polymerase	2
RNase-free water	3.5
PCR product	5
Total volume	20

Table 8. *In vitro* transcription reaction.

RNA probes have been precipitated with 20 µL of ammonium acetate 10 M and 240 µL of 100% ethanol overnight at -20°C. After a centrifugation for 30 minutes at 4°C (15000g) pellet was resuspended in 20 µL RNase-free water plus 20 µL of deionized formamide. Before resuspension, probes longer than 500 base pairs (probes used to detect *Arabidopsis SWEET11* and *SWEET12* genes) underwent a hydrolysis reaction in carbonate buffer (Na_2CO_3 120 mM, $NaHCO_3$ 80 mM, pH 10.2) for 45 minutes at 60°C.

Further *in situ* hybridization steps are reported in *Appendix* chapter. Briefly, slides were rehydrated through an ethanol series, treated with Proteinase K to increase target accessibility and incubated with acetic anhydride to reduce nonspecific hybridization. Then, samples were immersed in prehybridization buffer (a mixture containing all components of the hybridization mixture except for RNA probe) for two hours and in the hybridization buffer (containing RNA probe) overnight. A series of washing steps permitted to remove nonspecific hybridization

before the RNA-RNA hybrids detection. The revelation of RNA-RNA signal was performed using an antibody against DIG conjugated with alkaline phosphatase, and adding the enzyme substrate NBT/BCIP (nitroblue tetrazolium/5-bromo-4-chloro-3-indolyl-phosphate).
Except from ISH experiments on grapevine ubiquitin gene, which was performed at the Department of Agricultural and Environmental Sciences in Udine, all *in situ* hybridizations were performed at the Institut Jean-Pierre Bourgin, INRA, Centre of Versailles.

Samples preparation

Samples used for *in situ* hybridization analysis were fixed in formaldehyde buffer and embedded in paraffin.
Grapevine samples were collected in the experimental field at the end of August. Main veins were cut in fixation buffer containing 45% of ethanol 100%, 5% acetic acid, 5% formalin (40% in volume of formaldehyde) and 45% DMDC-treated water. Sample pieces were approximately 6 mm long and 3 mm wide and contained midribs and part of the leaf blade. They were immediately put in vials containing the fixation buffer and vacuum was applied three times for 1 min and then released to facilitate fixative penetration into tissues. To prevent samples degradation the cutting step was conducted in ice and samples were kept overnight at 4°C. The day after buffer was removed and replaced with an ethanol series: 50% EtOH for 1 hour, 50% EtOH for 1 hour, 70% EtOH for 1 hour, 70% EtOH for 3 hours, 96% EtOH for 1 hour, 100% Etoh for 1 hour, 100% EtOH overnight. The third day samples underwent to the following embedding steps: 100% EtOH : 100% Rothi Histol (Carl Roth GmbH, Karlsruhe, Germany) for 2 hours, 100% Rothi Histol for 2 hours, 100% Rothi Histol for 2 hours. All the steps were performed on a shaking platform.
Samples were then transferred into histological plastic cassettes and kept in Paraplast Plus melted paraffin (Mc Cormick Scientific, St. Louis, MO, USA) at 60°C for 2 hours. Paraffin was replaced with new one and samples were kept overnight at 60°C. After another replacement of paraffin for two hours, samples were embedded in Paraplast plus using HistoStar™ Embedding Workstation (Thermo Fisher Scientific, Inc., Waltham, MA, USA).
Tomato leaves and *Arabidopsis* floral stems were cut as described for grapevine samples and fixed in 4% paraformaldehyde in PBS (Phosphate Saline Buffer). After a night in fixation buffer samples were transferred twice in 1X PBS buffer for 30 minutes, in an ethanol series (30%, 40%, 50%, 60%, 70%, 96%) for one hour each and overnight in 0.1 % eosin. Thus, samples were transferred in an ethanol-histoclear (Agar Scientific, Stanstead, UK) series (2:1, 1:1, 1:2) and to 100% histoclear for one hour each. All the steps were performed on a shaking platform. Finally they were put in histological plastic cassettes in histoclear-Paraplast Plus melted paraffin at 60°C for 1 hour and in pure paraffin overnight. After another day in melted paraffin at 60°C, samples were embedded in Paraplast Plus and block were kept at 4°C.

The different samples were sectioned into 8 µm-thick slices on a rotary microtome (Leica, Bensheim, Germany), laid on Probe On Plus Microscope slides (Fisherbrand, Thermo Fisher Scientific, Inc., Waltham, MA, USA) and incubated at 42°C overnight before *in situ* hybridization experiments.

RESULTS

1. Structural observations

Light microscopy observations

Paraffin-embedded samples were used to perform histological observations of grapevine and tomato leaves. Transversal sections of the leaves' main veins allowed the localization and the comparison of the different tissues in healthy and stolbur-infected samples. Figure 15 shows sections of grapevine samples (Figure 15, A and B) and tomato samples (Figure 15, C and D).

In the grapevine, from the outer layer it was possible to identify epidermis, some layers of collenchyma cells, parenchyma cells and vascular bundles (Figure 15.A). In the leaf blade, palisade parenchyma was detectable directly under the upper (adaxial) epidermis and spongy mesophyll was recognizable by the characteristic cells surrounded by large inter-cellular spaces.

More in detail, phloem (Figure 15.B, blue arrows) and xylem (Figure 15.B, yellow arrows), situated in the inner part of the vein, were grouped in several collateral bundles. The phloem tissue was located toward the outer (abaxial) margin of the leaf while xylem vessels showed large and hollow tubular structures.

As in the grapevine, in the tomato samples it was possible to distinguish different tissues. Epidermis layer, collenchyma cells, parenchyma cells and a bicollateral vascular bundle were present in transversal sections of the main vein. In particular, the vascular bundle was located in the middle of the vein with the xylem on the centre and the phloem distributed on both the adaxial and abaxial side of the bundle, as described by Hayward in 1938 (Figure 15, C and D).

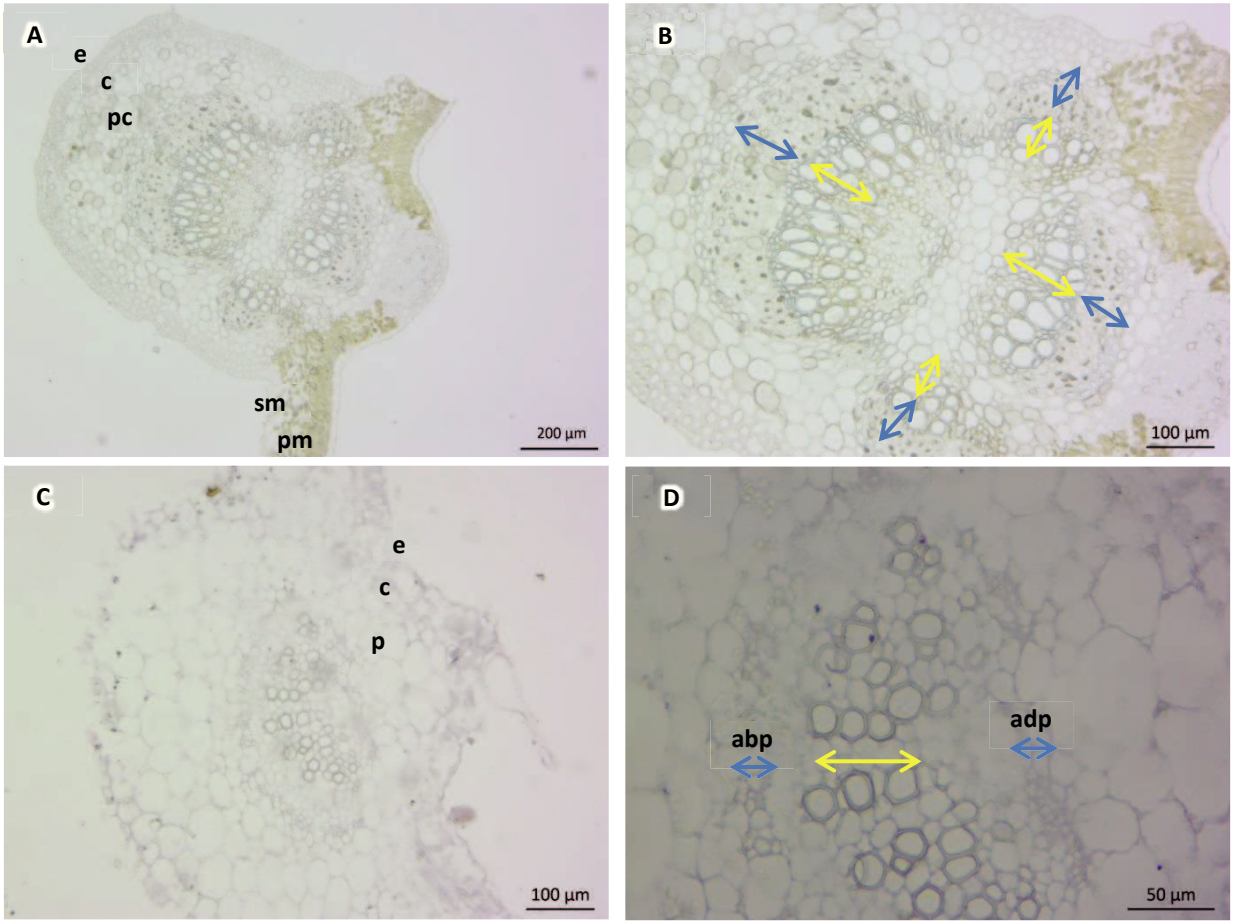

Figure 15. Light microscopy images of grapevine and tomato samples. A and B. Global overview and details of a transversal section of grapevine leaf main vein. C and D. Global overview and details of a transversal section of tomato leaf main vein. (e, epidermis; c, collenchyma cells; pc, parenchyma cells; sm, spongy mesophyll; pm, palisade mesophyll; abp, abaxial phloem; adp, adaxial phloem).

Confocal laser scanning microscopy (CLSM) observations

A confocal laser scanning microscope (CLSM) was used to observe grapevine and tomato leaf samples previously stained with carmine green. The presence of lignin was indicated in the images by the color blue, while cellulose was traced in pink.

In Figure 16 the structure of a grapevine main vein was visible. Phloem and xylem tissues were easily recognizable; in particular it was possible to detect several vascular bundles. As expected, lignin was present especially in the walls of xylem vessels of grapevine veins.

In addition, samples of asymptomatic (healthy and recovered plants) and diseased plants were compared. Cells of asymptomatic samples were characterized by a regular distribution and

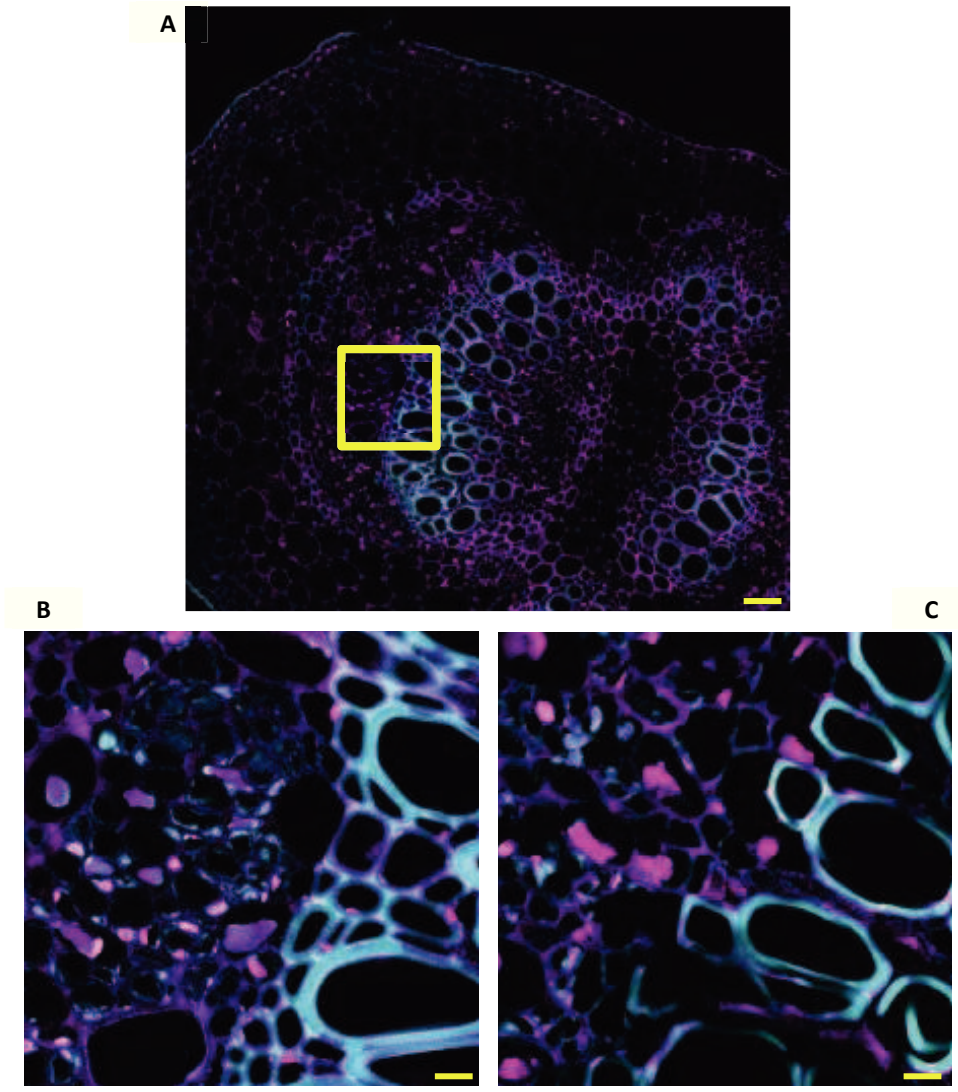

Figure 16. Grapevine leaf section observed at CLSM. The presence of cellulose is indicated by pink color and lignin in blue. A. Global overview of a main vein leaf section. Bar=50 µm. B and C. Details of phloem and xylem tissues in healthy (B) and infected (C) samples. Bar=240 µm.

organization and cell walls were preserved. On the contrary, phloem tissue of infected plants often looked disorganized. The cell walls appeared thicker than the walls of the healthy control samples and a different distribution of the signal from the diverse cell wall components was visible.

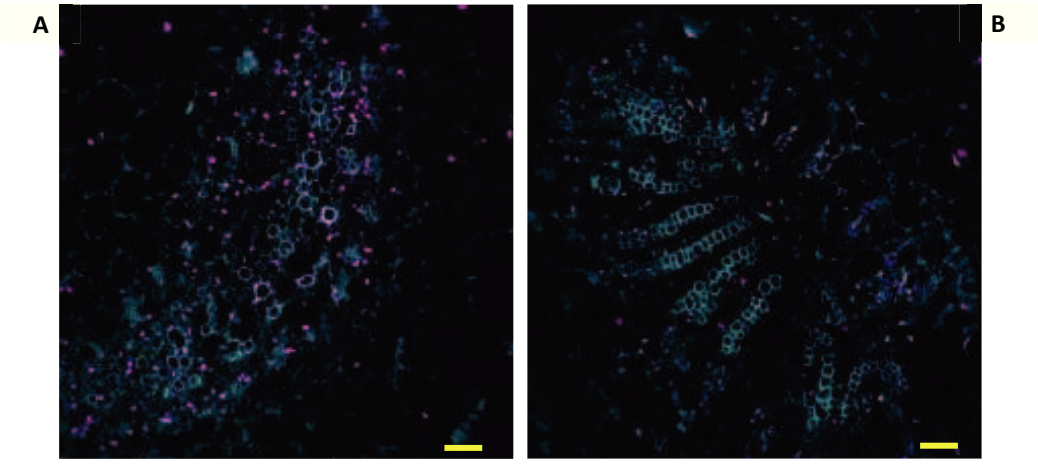

Figure 17. Tomato leaf section observed at CLSM. The presence of cellulose is indicated by pink color and lignin in blue. Details of phloem and xylem tissues in asymptomatic (A) and infected (B) samples. Bar=50 µm.

In tomato samples CLSM permitted to observe vascular tissues and in particular the different organization of xylem vessels in healthy and infected plants. The lignin signal was very evident in cell walls of xylem vessels, showing an arrangement similar to strings in infected samples which was not present in healthy ones (Figure 17).

Transmission electron microscopy observations

Ultrastructural observations of grapevine leaf tissues

Grapevine leaf samples were investigated by means of transmission electron microscopy (TEM) to closely observe the structure of the inner tissues and to improve knowledge about the effects caused by the phytoplasmas at cytological level.

Leaves of healthy, infected and recovered grapevines were resin-embedded, cut in ultrathin sections and observed.

Healthy tissues were conserved and phytoplasmas were not present in the sieve elements of these plants (Figure 18, A and B). The cellular morphology and organelles structure were well preserved (Figure 18.A) and regular organization of sieve elements and companion cells was observed. Phloem proteins, when visible in the cells, were found uniformly dispersed in sieve elements' lumen. Moreover, in several sieve elements callose depositions were detected surrounding sieve pores without occluding their lumen (Figure 18.B).

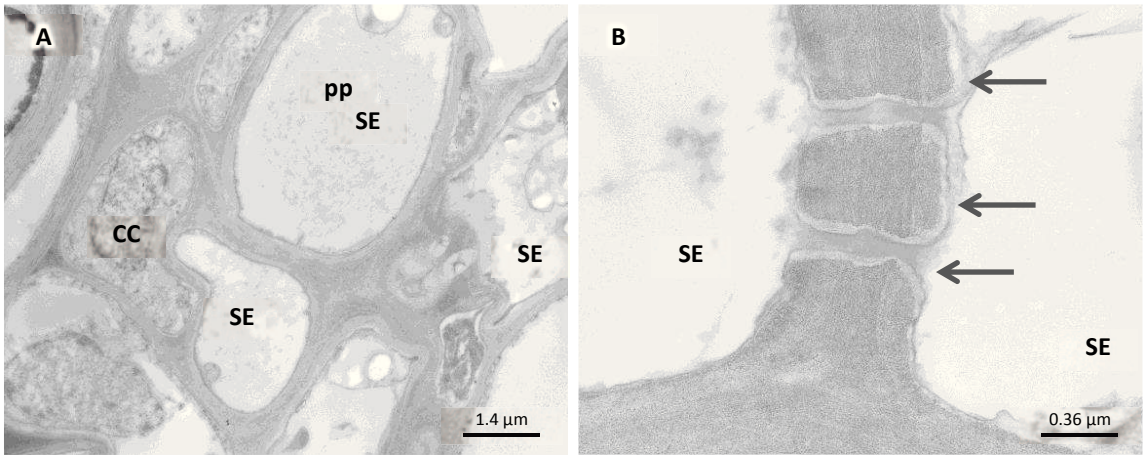

Figure 18. TEM micrographs from ultrathin sections of healthy grapevine leaf. A. Phloem tissue ultrastructure is well preserved and Phloem protein (pp) is uniformly dispersed in the lumen of the sieve elements (SE). (CC, companion cells). B. Thin callose deposits surround sieve pores (arrows).

In stolbur-infected plants, phytoplasmas were visible in the phloem of the leaves and severe ultrastructural modifications had occurred (Figure 19.A). As shown in Figure 19.B, C and F phloem tissue is completely disorganized and many sieve tubes appeared collapsed or necrotized. In several samples the phloem was disrupted and thus it was not easy to evidence the presence of the pathogen. P-protein filaments are organized in dense plugs (Figure 19.C) and sieve plates often presented an evident thickening and deformation of cell walls. Large deposits of callose occluded sieve pores (Figure 19, D and E). Plasmalemma detachment from cell walls and consequent cytoplasm condensation are well shown in Figure 19.F.

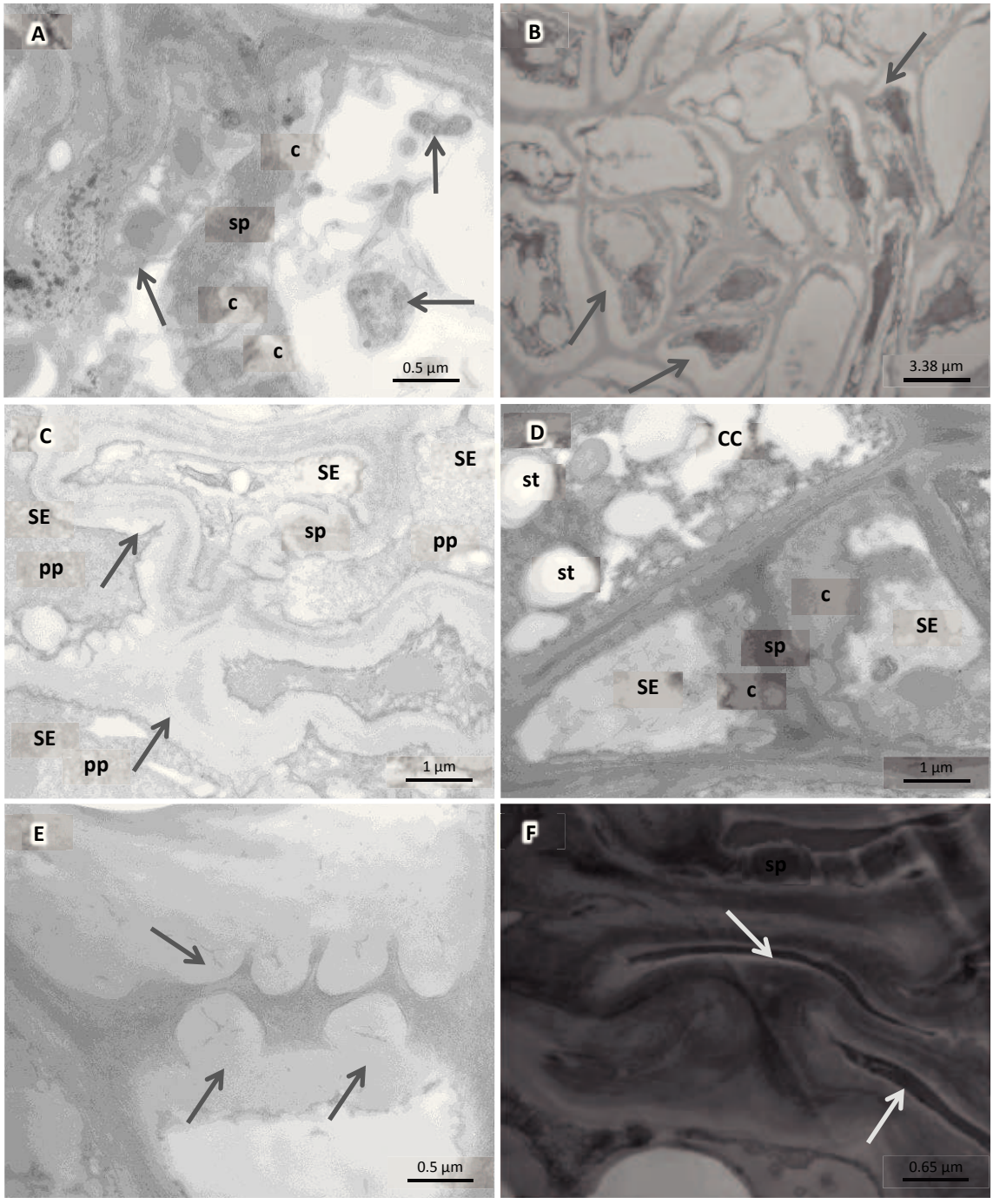

Figure 19. TEM micrographs from ultrathin sections of stolbur-infected grapevine leaf tissues. A. Phytoplasmas are present in the lumen of sieve elements (arrows). Callose accumulations are visible at the sieve plate (sp). B. Plasmalemma detachment occurs in phloem parenchyma and companion cells (arrows). Some cells are necrotized (n). C. Cell walls thickenings (arrows) and dense plugs of P-proteins are shown (sp, sieve plate). D and E. Sieve plates are occluded by big accumulations of callose (arrows); starch is present in companion cells (st). F. Tissue disorganization and collapsed cells (arrows) are shown. (c, callose; CC, companion cell; n, necrotized cell; pp, phloem protein; SE, sieve element; sp, sieve plate).

Leaf tissues from recovered plants were also observed. Phytoplasmas were not detected in the sieve elements (Figure 20, A and B). Tissues did not show ultrastructural modifications and the cells' organization was fairly well preserved. Callose depositions were present in the sieve tubes, in particular around the sieve pores (Figure 20.A). In addition, phloem proteins were found as aggregated clumps or as filaments at the sieve plates in correspondence of the sieve pores (Figure 20, A and B).

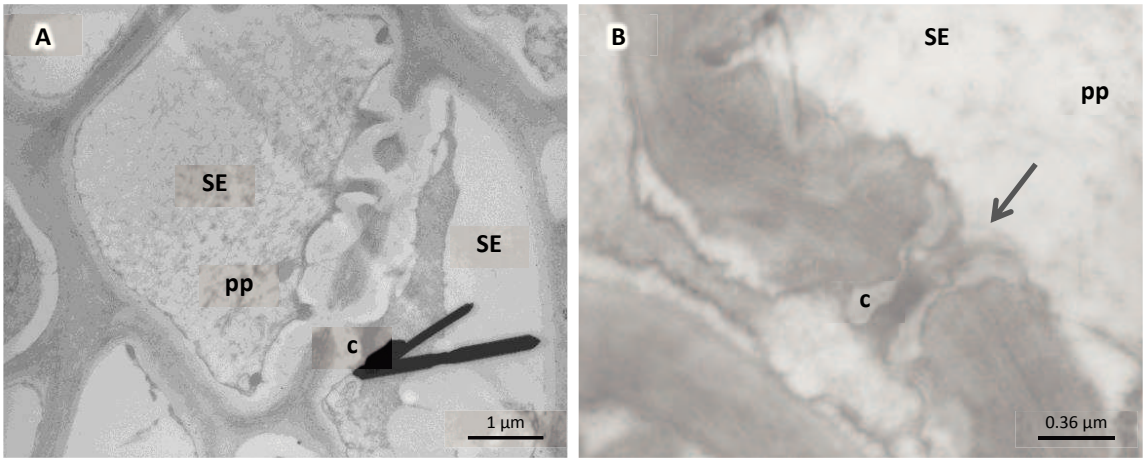

Figure 20. TEM micrographs from ultrathin sections of recovered grapevine leaf tissues. A. P-protein (pp) is visible in condensed form in sieve elements (SE). Callose collars (c) are present around sieve pores. B. P-protein (pp) filaments seems to pass through sieve pores (arrow), which are surrounded by thin callose layers (c).

Ultrastructural observations of grapevine root tissues

Transmission electron microscopy was used to observe transversal sections of grapevine roots. Root tissues from healthy grapevines were resin embedded and observed. As shown in Figure 21, phytoplasmas were not present in sieve elements. Sieve elements cells showed a well-preserved structure and thin layers of callose were present on sieve plates (Figure 21, A and B). Phloem protein filaments were present in uniformly dispersed state (Figure 21 A).

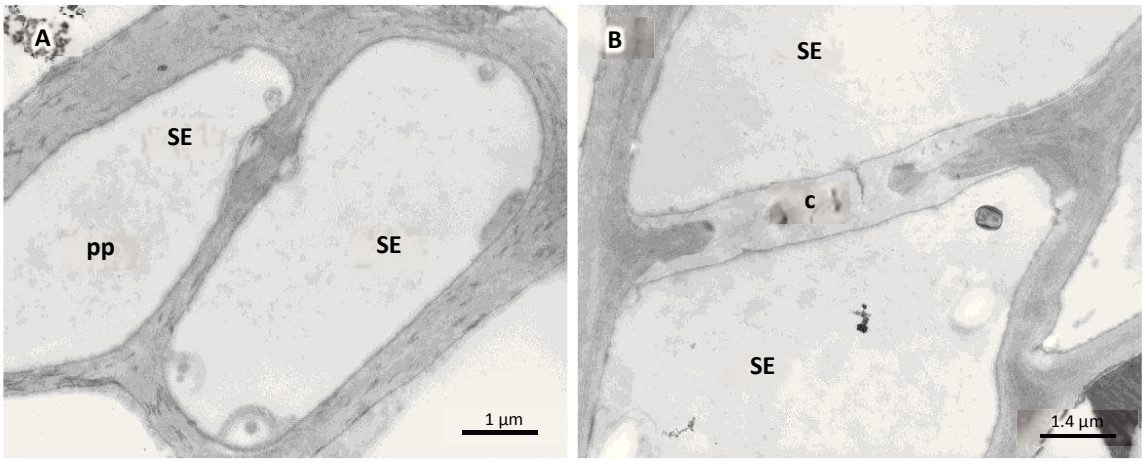

Figure 21. TEM micrographs from ultrathin sections of healthy grapevine root tissues. A and B. Cells are well preserved and phytoplasmas are not present in sieve elements. A. P-proteins are uniformly dispersed in sieve element lumen (pp) B. Thin callose collars (c) are present around sieve pores.

Root samples collected from symptomatic plants showed a general disorganization of the tissues with cell necrosis, cell wall thickenings (Figure 22.A), and accumulation of callose (Figure 22, A and B). Several starch bodies were present and vacuolar phenolic compounds were densely organized in phloem parenchyma cells (Figure 22, C and D).

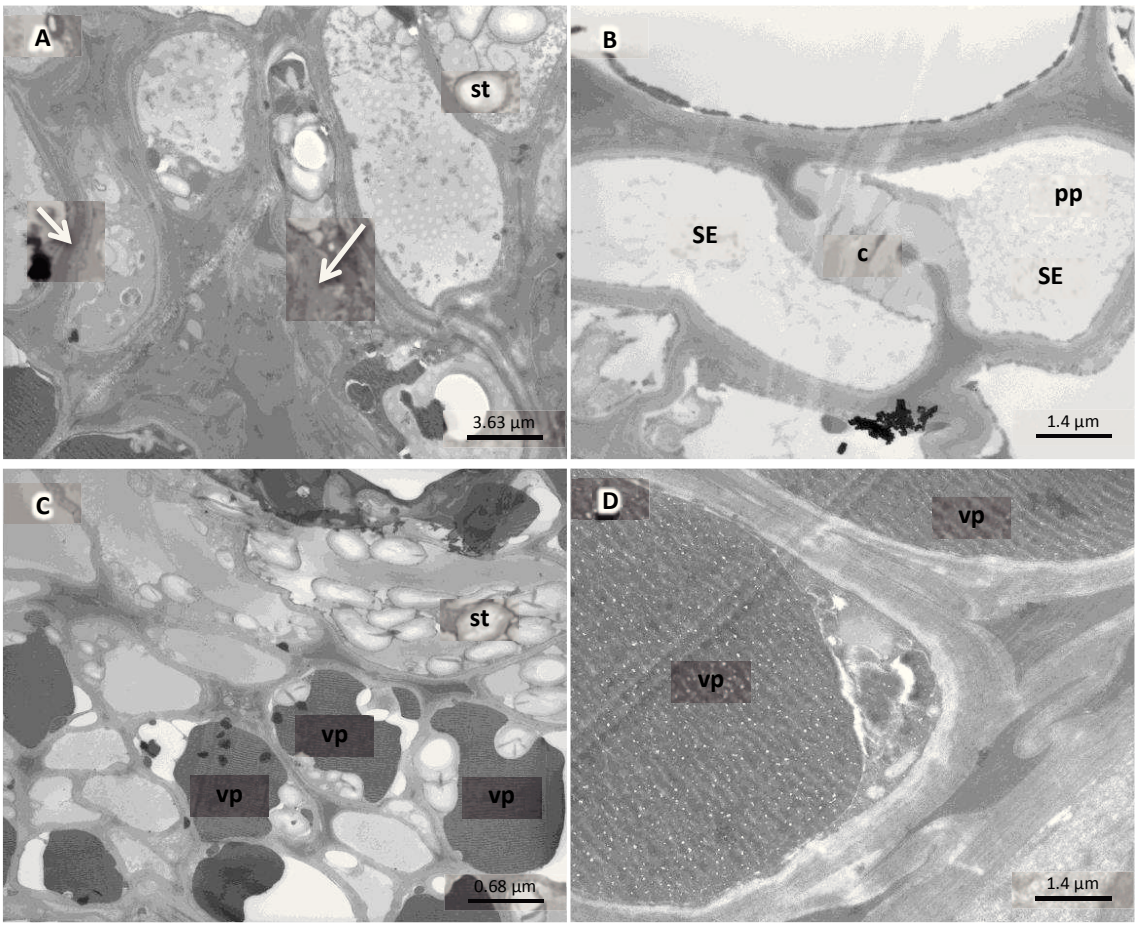

Figure 22. TEM micrographs from ultrathin sections of diseased grapevine root tissues. A. Cell organization is lacking and cell walls appear thick (arrows). B. Callose collars (c) are present around sieve pores and phloem proteins (pp) are present in sieve elements. C and D. In phloem parenchyma cells vacuolar phenolics are organized in dense bodies. (SE, Sieve element; st, starch).

Samples of roots from recovered plants showed P-protein in aggregated state, cell wall thickenings. Pleomorphic bodies, similar to phytoplasmas were sporadically detected only in few samples (Figure 23).

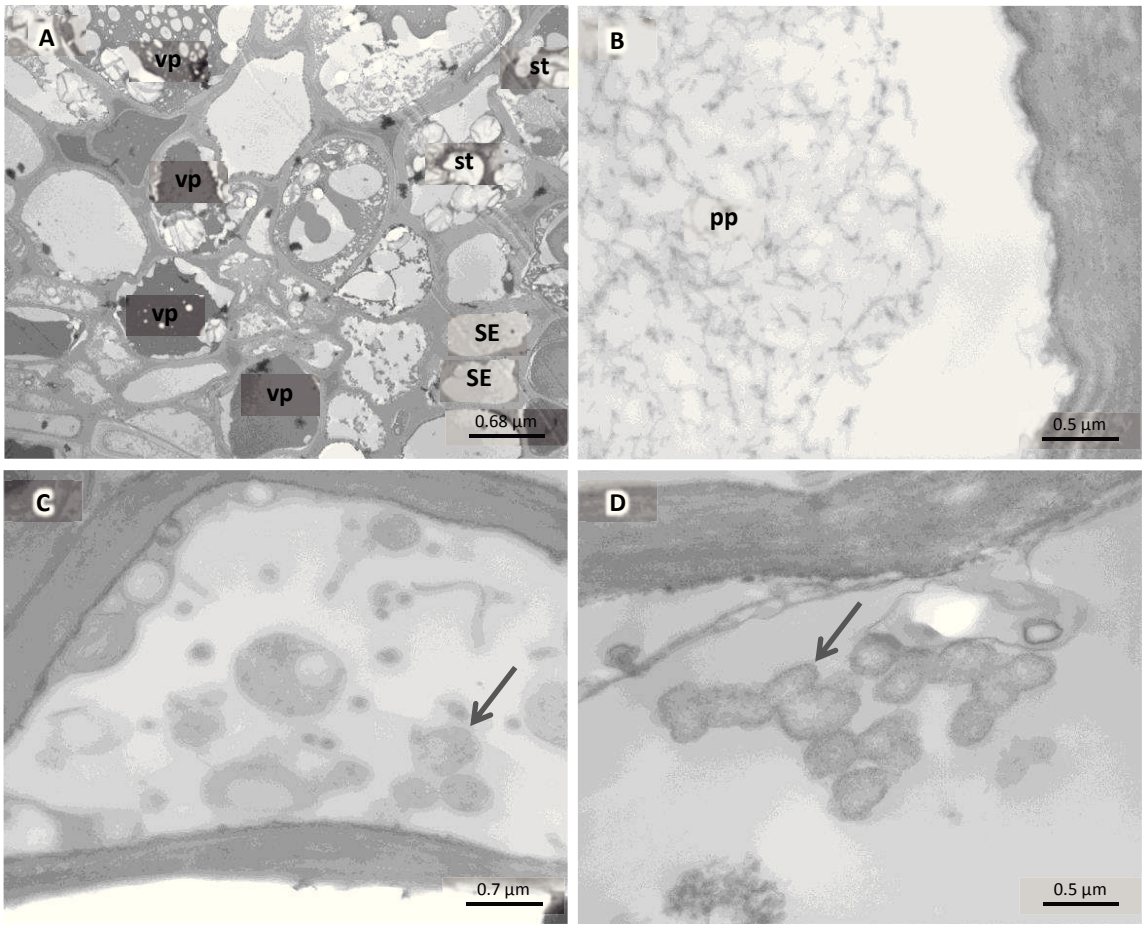

Figure 23. TEM micrographs from ultrathin sections of recovered grapevine root tissues. A. Low magnification of root tissues from recovered grapevine. Sieve elements (SE) appeared empty. In parenchyma cells vacuolar phenolic compounds (vp) and starch are visible. B. Phloem proteins aggregations are present in sieve elements. C and D. Pleomorphic bodies, resembling phytoplasmas, are detectable in the phloem (arrows).

Ultrastructural observations of tomato leaf tissues

TEM was used to observe and compare phloem tissue of healthy and stolbur-infected tomato leaves. Healthy samples showed well preserved tissue structure, without ultrastructural modifications. Cell organization was preserved and no phytoplasmas were detected in the sieve tubes. Filaments of phloem proteins were observed in the lumen of most sieve elements in uniformly dispersed state (Figure 24).

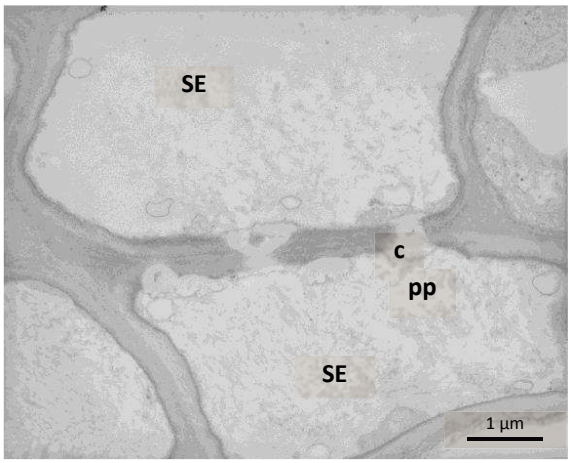

Figure 24. TEM micrograph of healthy tomato leaf tissue. Sieve element (SE) structure is preserved and phloem protein (pp) is found uniformly dispersed in the cell lumen (c, callose).

TEM images from infected samples showed numerous sieve elements filled with phytoplasmas (Figure 25). The pleomorphic shape of phytoplasmas was well evident, thus filamentous and roundish forms could be detected. Together with phytoplasma cells, phloem protein in the aggregate state was often visible in the sieve element lumen (Figure 25.A).

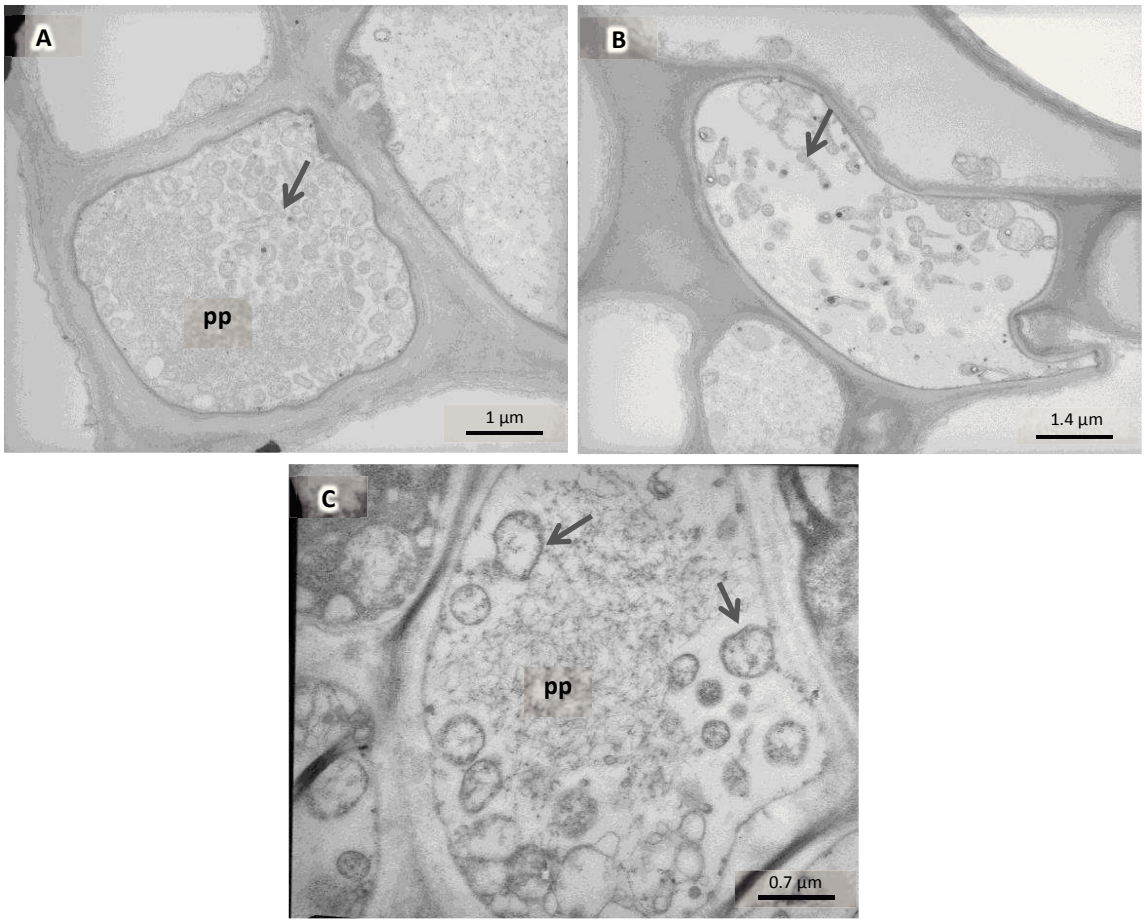

Figure 25. TEM micrographs of stolbur-infected tomato leaf tissue. A, B and C. Phytoplasmas (arrows) in the lumen of sieve elements; in A and C phloem protein (pp) filaments are organized in dense clumps.

Ultrastructural observations of tomato root tissues

Root tissues from healthy tomato plants were well preserved at ultrastructural level. No phytoplasmas were detectable and cells showed regular shapes (Figure 26).

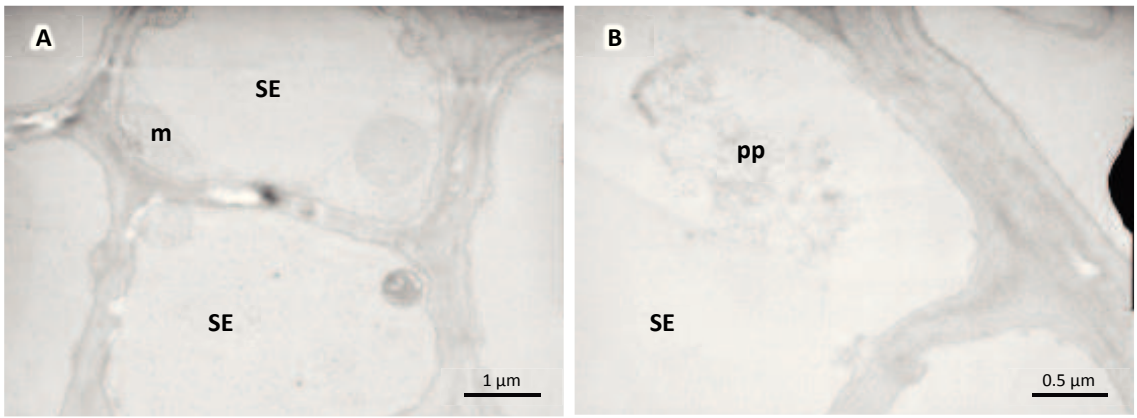

Figure 26. TEM micrographs of healthy tomato root tissue. A and B. Cells structure is well preserved. (SE, sieve element; m, mitochondria; pp, phloem protein).

In the stolbur-infected roots, cell wall thickenings were the most relevant ultrastructural modification. Cell organelles were well structured and phytoplasmas were rare to detect in sieve elements, due to their irregular distribution in the phloem. Callose deposits were detectable at the sieve plates (Figure 27).

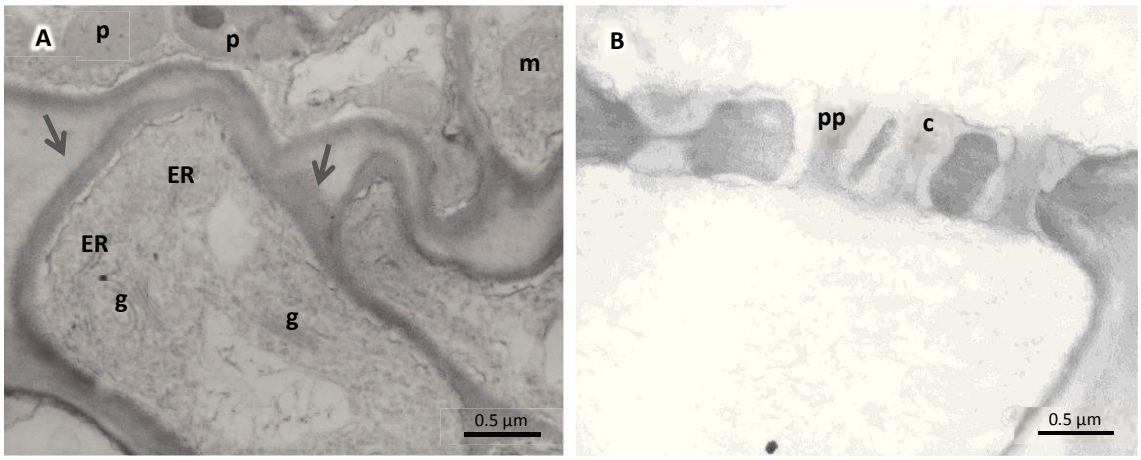

Figure 27. TEM micrographs of diseased tomato root tissue. A and B. Cells structure is characterized by cell wall thickenings (arrows) and deposits of callose (c) at the sieve plates. Phloem protein filaments are present passing through the sieve plate pores. (p, plastid; m, mitochondria; ER, endoplasmic reticulum; g, Golgi bodies).

2. Phytoplasma molecular detection

Phytoplasma detection in grapevine and tomato leaves

Real Time RT-PCR technique was performed to detect phytoplasmas in grapevine and tomato leaves.

The primers used were designed to amplify a region of *16S rRNA* gene specific to '*Ca.* Phytoplasma solani'.

Concerning the grapevine, stolbur *16S rRNA* transcripts were found in symptomatic samples, while no amplicons were detected in asymptomatic healthy or recovered samples. In particular, Cq (Quantification Cycle) values of symptomatic plants ranged between 23.5 and 25.0 when using 10 ng of total RNA and 400 nM of each primer.

Similarly, molecular diagnosis was performed on tomato leaves collected from healthy and symptomatic plants, using *16S rRNA* primers. The presence of phytoplasmas was detected in symptomatic samples at an average Cq value of 17.75±0.67 (Mean ± Standard error of the mean).

Phytoplasmas detection in grapevine roots

Although diagnostic protocols are well developed to check phytoplasmas presence in grapevine leaves, at present no reliable methods are available to detect these bacteria in grapevine root tissues. For this reason, new methods to investigate phytoplasma presence in root samples were set up and tested.

Root RNA quality was controlled performing a Real Time PCR using specific primers for plant *18S rRNA* gene (Osman *et al.*, 2007). As shown in Table 8, Cq values of *18S rRNA* amplicons ranged between 9.98 and 15.75 confirming the effectiveness of RNA extraction and amplification method.

Direct Real Time PCR experiments were assessed to amplify a portion of the stolbur *16S rRNA* gene using a couple of primers and a TaqMan® probe as reported in Margaria *et al*., (2009). This protocol failed in all root samples checked, including symptomatic samples. Cq values were much higher compared to the positive control (BNp +) and for some samples it was not even possible to obtain any amplification curve (Table 9).

An attempt to obtain better results was made by introducing a nested step in the protocol. A first PCR using external primers was followed by a Real Time PCR with inner primers and the TaqMan® probe.

In this case it was possible to detect stolbur phytoplasma in two out of four symptomatic plants and three out of five recovered ones. No amplification was obtained from healthy samples and water control.

Sample code			Plant 18S rRNA	BNp 16S rRNA	
Row	Plant	Phytopatological status	Real Time PCR (Cq)	Real Time PCR (Cq)	Real Time nested-PCR (Cq)
10	155	H	13.55	35.88	Undetermined
10	166	H	14.03	38.75	38.43
8	182	H	14.44	Undetermined	Undetermined
10	171	H	14.83	36.20	Undetermined
10	180	H	15.75	Undetermined	Undetermined
10	123	R	14.51	Undetermined	38.25
10	127	R	13.92	36.76	11.7
10	147	R	12.62	37.38	25.39
11	43	R	15.04	Undetermined	38.61
11	71	R	13.56	36.30	17.71
10	133	D	13.22	Undetermined	36.45
10	144	D	14.47	38.14	16.22
10	59	D	12.24	38.26	20.33
10	63	D	9.98	36.90	37.17
BNp +			8.55	15.14	2.10
Water			Undetermined	Undetermined	37.20

Table 9. Results of Real Time PCR for plant 18S rRNA and BNp detection (Cq, quantification cycle).

Phytoplasmas detection in tomato roots

The Real Time nested-PCR technique was used also on tomato roots samples. The protocol used was the same one applied to grapevine samples. As shown in Table 10, six plants were checked for the presence of the phytoplasma. It was possible to detect an amplicon for two plants which showed symptoms on leaves at approximately 10 and 26 Cq. Not symptomatic plants showed Cq values higher than 30, which were not considered relevant for detection, due to nonspecific amplification. One slightly symptomatic plant showed a Cq of 31.95.

Plant	Symptoms observations	Real Time nested-PCR on roots sample (Cq)
1	Plant without symptoms	32.32
2	Plant without symptoms	42.23
3	Plant without symptoms	34.49
4	Slightly symptomatic plant	31.95
5	Symptomatic plant	10.04
6	Symptomatic plant	26.11
C+		11.28

Table 10. Results of Real Time nested-PCR for stolbur detection.

3. Gene expression analysis

Grapevine reference gene selection

For grapevine gene expression analyses, reference genes were selected in order to normalize the target genes' expression. Ubiquitin-60S ribosomal protein L40-like (UBQ-L40, accession number XM_002273532.1) was found to be expressed stably in grapevine leaf tissues. The stability of this gene was compared with the stability of genes coding for actin (accession number XM_002282480.2), ubiquitin conjugating factor (accession number XM_002274299.1) and 60S ribosomal protein L18 (accession number XM_002270599.1). According to the geNorm program, the stability value of UBQ-L40 was 0.45, thus making UBQ-L40 acceptable as a reference gene (Vandesompele *et al.*, 2002).

Gene expression analyses of grapevine leaf samples

Real Time RT-PCR technique was used to define the transcriptional profiles of some genes involved in sugar metabolism. Analyses were conducted on at least three fully expanded grapevine leaves enriched in midribs. Leaves were sampled from at least three different healthy, infected and recovered plants. Primers were designed to amplify genes coding for callose synthases and sucrose synthases.

Callose synthase gene expression analyses

Seven genes encoding for callose synthases were identified by the Grape Genome Browser in the Grape 12X Genome Browser, and six of them were detected in the leaf tissue (Figure 28). The expression levels were compared in infected, recovered and healthy grapevine leaf tissues.

The genes showed different levels of expression and among them *VvCAS1* (accession number XM_002271612.2) was the most expressed. The *VvCAS8-like* gene (accession number XM_002267920.2) was almost undetectable and thus it is not shown in the figure.

VvCAS2 (accession number XM_002283262.2) and *VvCAS7* (accession number XM_002279310.2) were the only up-regulated genes in the presence of the phytoplasma. In particular *VvCAS2* expression level was 9.9 MNE (Mean Normalized Expression) units in the infected samples and 3.8 and 4.0 MNE units respectively for the healthy and recovered plants. For *VvCAS7* the expression levels were 5.5, 1.2 and 1.0 MNE units respectively for infected, healthy and recovered plants. The significant ($P<0.05$) up-regulation of *VvCAS2* and *VvCAS7* was confirmed by an ANOVA Tukey-Kramer Multiple Comparisons Test.

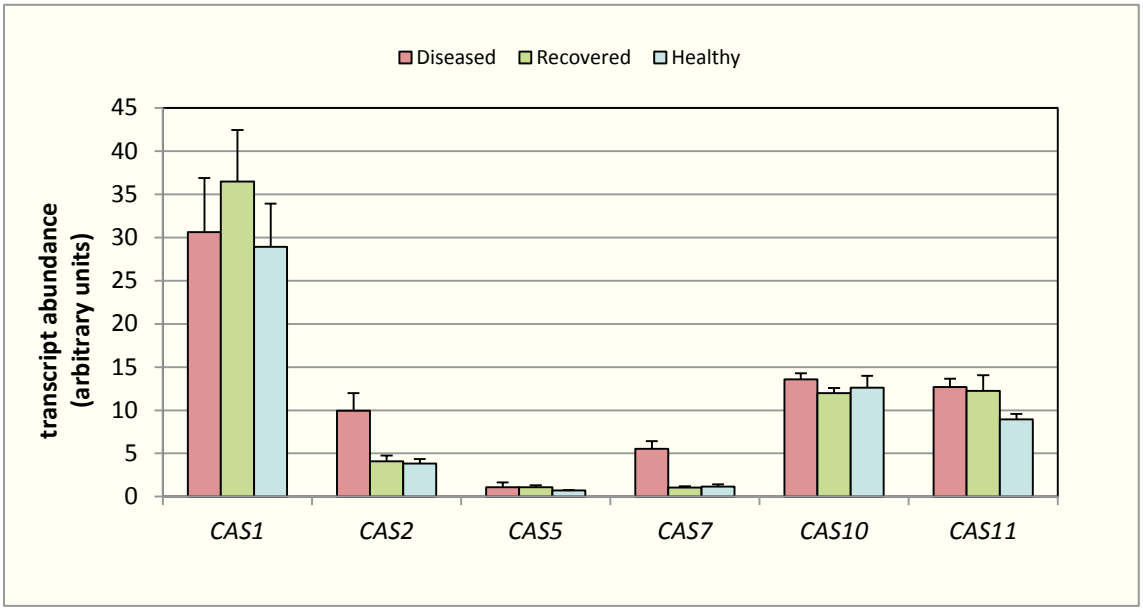

Figure 28. Gene expression analyses of *Vitis vinifera* callose synthase genes. Transcript levels for each plant group and standard error bars are shown. Mean expression values are normalized to ubiquitin L-40 (expression level = 100).

Sucrose synthase gene expression analysis

Five genes encoding for sucrose synthases were retrieved from the Grape Genome Browser and their expression levels were studied in grapevine leaf tissues, by comparing healthy, diseased and recovered samples.

One of the five identified genes, whose accession number is XM_002271494, showed a very low transcription level and thus it was not considered further in the study.

As shown in Figure 29 the different sucrose synthase isoforms were expressed at different levels in the grapevine leaf. However, they all showed a significant ($P<0.05$) up-regulation of the expression level in the infected samples compared to the healthy and recovered ones. In particular, *VvSUS4* and *VvSUS2* were the two most expressed genes. *VvSUS4* (accession number XM_002275119.1) was induced in infected leaves with an expression level of 60.8 MNE units compared to 6.6 and 7.9 MNE units of healthy and recovered samples. *VvSUS2* (accession number XM_002271860.1) was induced 4.7-fold in infected plants compared to healthy plants and 5.2-fold to recovered ones. *VvSUS5* (accession number XM_002266984.2) and *VvSUS6* (accession number XM_002270825.1) transcription levels were very low in healthy and recovered plants while the amount of transcripts in diseased samples was approximately 3.7 and 9.1 MNE units.

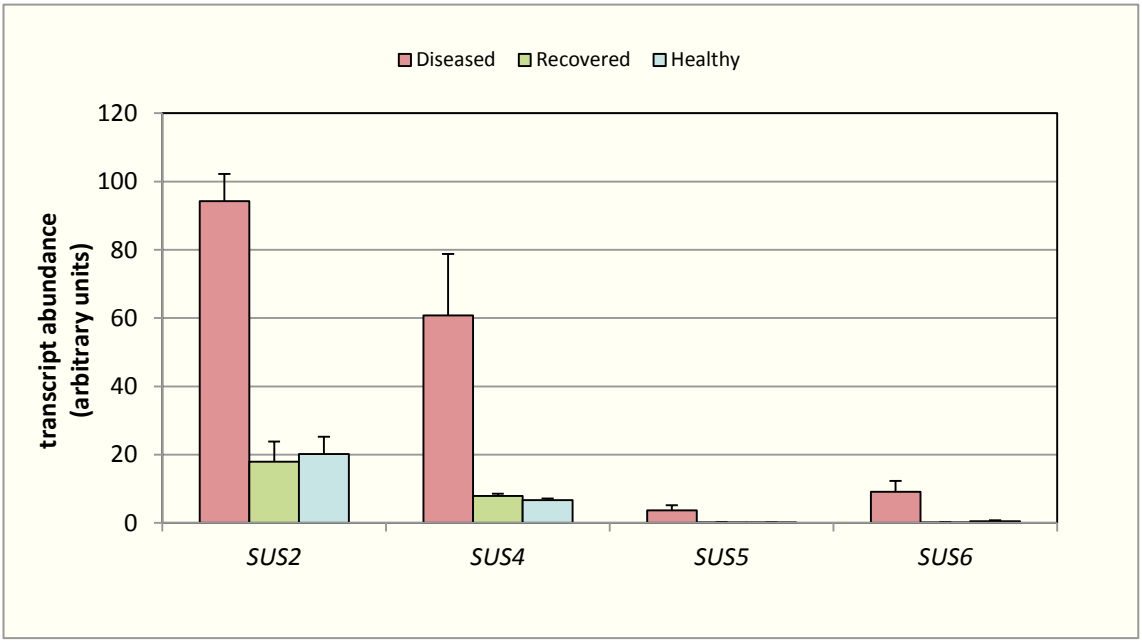

Figure 29. Gene expression analyses of *Vitis vinifera* sucrose synthase genes. Transcript levels for each plant group and standard error bars are shown. Mean expression values are normalized to ubiquitin L-40 (expression level = 100).

Tomato reference gene selection

Tomato gene expression levels were normalized to Ubiquitin-protein ligase UPL3-like (UPL3-like, accession number XM_004230989.1). Ubiquitin-protein ligase UPL3-like was found to be the more stably expressed gene in tomato leaf tissues. The stability of this gene was compared with the stability of genes coding for polyubiquitin-like protein (accession number XM_004244105.1) and actin-97-like (accession number XM_004236699.1). According to the geNorm program, the stability value of UPL3-like was 0.55, thus making UPL3-like acceptable as a reference gene (Vandesompele *et al.*, 2002).

Gene expression analyses of tomato leaf samples

Real Time PCR technique was used to analyze the expression level of some tomato genes encoding for callose synthases and proteins peculiar to the phloem.

Callose synthase gene expression analyses

The expression level of eight isoforms coding for callose synthases was checked (Figure 30). *SlCAS10* (accession number XM_004236267.1) resulted as the most expressed gene in healthy and diseased samples. Differences between healthy and diseased samples were not statistically significant, but it was interesting to note that *SlCAS7* (accession number XM_004243161.1), which is an ortholog of the *Arabidopsis CalS*7 responsible for callose deposition in the phloem (Xie *et al.*, 2011), was more expressed in D leaf tissues compared to H plants. Similarly, it was possible to observe an up-regulation in infected samples for *SlCAS8* gene (accession number XM_004244335.1). The other genes showed an expression level that had not been modulated by the infection.

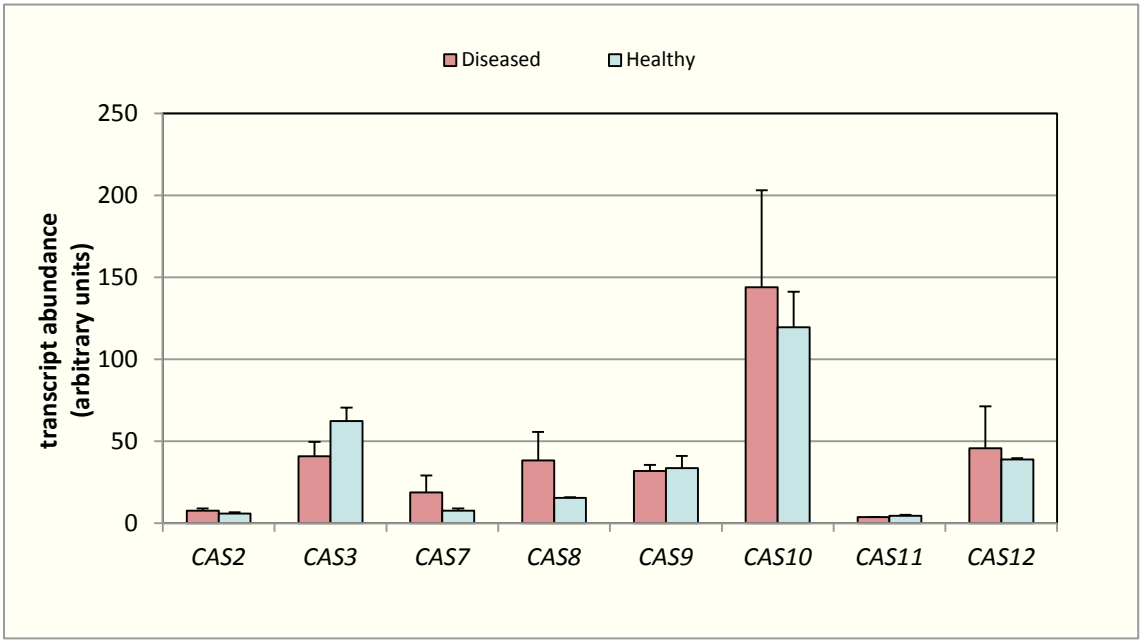

Figure 30. Gene expression analyses of *Solanum lycopersicum* genes coding for callose synthases. Transcript levels for each plant group and standard error bars are shown. Mean expression values are normalized to ubiquitin protein ligase (expression level = 100).

Expression analyses for genes coding for phloem proteins

A gene coding for a phloem protein (Pp2, accession number XM_004233183.1) and a sieve element occlusion protein (SEO, accession number XM_004239105.1) were investigated. Pp2 gene showed a similar level of expression in both samples (Figure 31), with a slight decrease in diseased ones compared to healthy plants (94 and 142 MNE units, respectively).

Concerning the gene encoding the SEO protein, a significant decrease of expression level in diseased samples was observed. The amount of transcripts was approximately 200 MNE units for healthy samples while diseased samples showed a level of 30 MNE units.

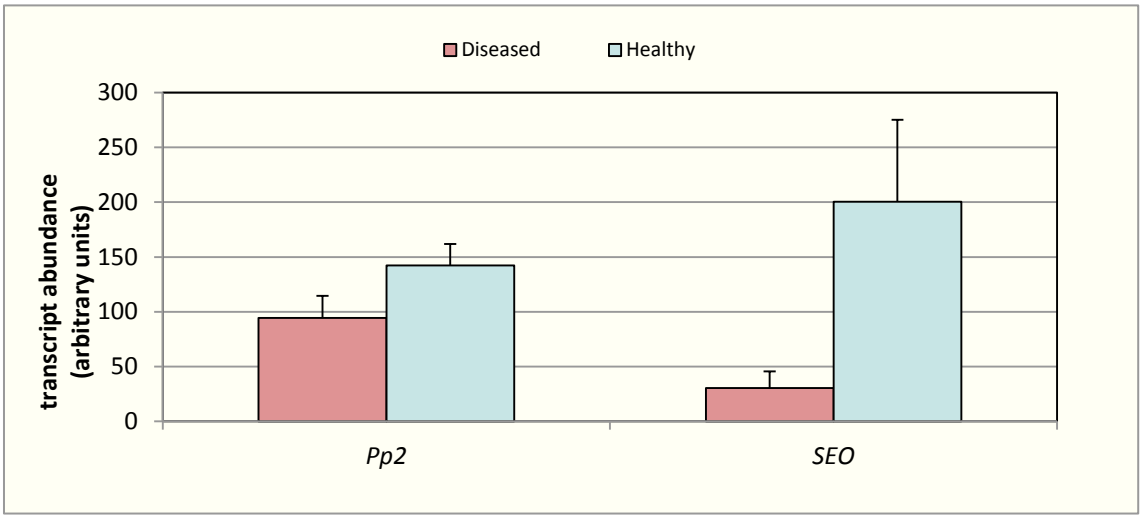

Figure 31. Gene expression analysis of *Solanum lycopersicum* phloem protein (Pp2) and Sieve element occlusion (SEO) protein genes. Transcript levels for each plant group and standard error bars are shown. Mean expression values are normalized to ubiquitin protein ligase.

SWEET transporter gene expression analyses

Finally, a gene coding for a glucose transporter was analyzed. SWEET1 coding gene sequence (accession number XM_004237674.1) was identified in NCBI database by sequence homology with SWEET1 gene of *Arabidopsis thaliana*.

The gene expression profile showed an important decrease of transcript in diseased samples compared to healthy ones. In particular, the amount of transcripts in infected leaves was approximately 8.5 MNE units while it was 133 MNE units in non-symptomatic samples (Figure 32).

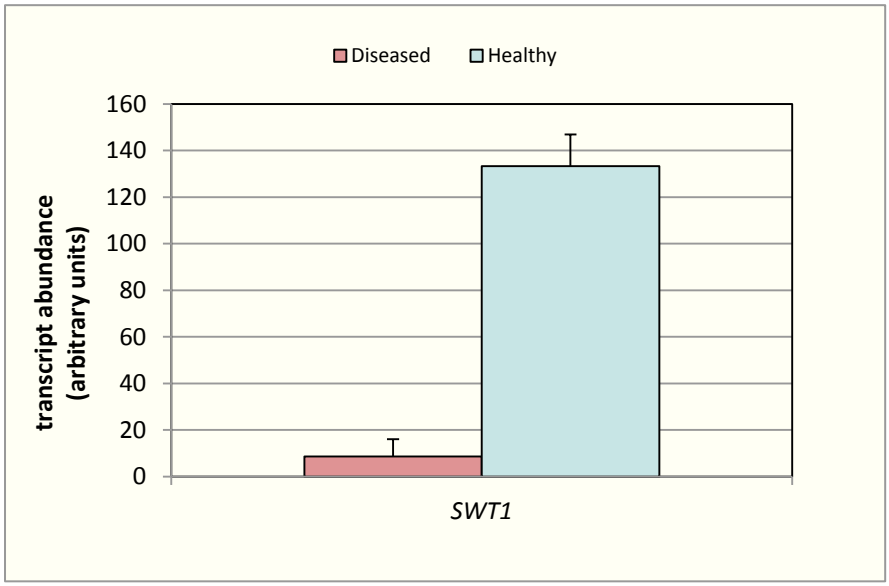

Figure 32. Gene expression analysis of *Solanum lycopersicum* glucose transporter SWEET1. Transcript levels for each plant group and standard error bars are shown. Mean expression values are normalized to ubiquitin protein ligase.

4. *In situ* hybridization experiments

In situ hybridization experiments on *Arabidopsis* floral stems

In situ hybridization technique was set up on the model plant *Arabidopsis thaliana*. In particular experiments were conducted on *Arabidopsis* floral stems to localize transcripts coding for two sucrose transporters: *SWEET11* (Tair accession number: At3g48740) and *SWEET12* (Tair accession number: At5g23660). Floral stems of wild type plants (cv. Columbia 0) were transversally cut into 5 mm-long pieces and embedded in paraffin.

Two probes of respectively 870 and 858 base pairs were obtained to detect *SWEET11* and *SWEET12*. Before using them in the incubation step, the probes underwent an alkaline hydrolysis in order to shorten their length and allow their diffusion into the tissues.

As shown in Figure 33, tissue organization was maintained and it was possible to observe several vascular bundles, surrounding the central pith tissue (Handakumbura and Hazen, 2012). In the detailed image (Figure 21.B) it is possible to localize phloem and xylem tissues. Moreover, in negative control slides no signal was detectable (Figure 33).

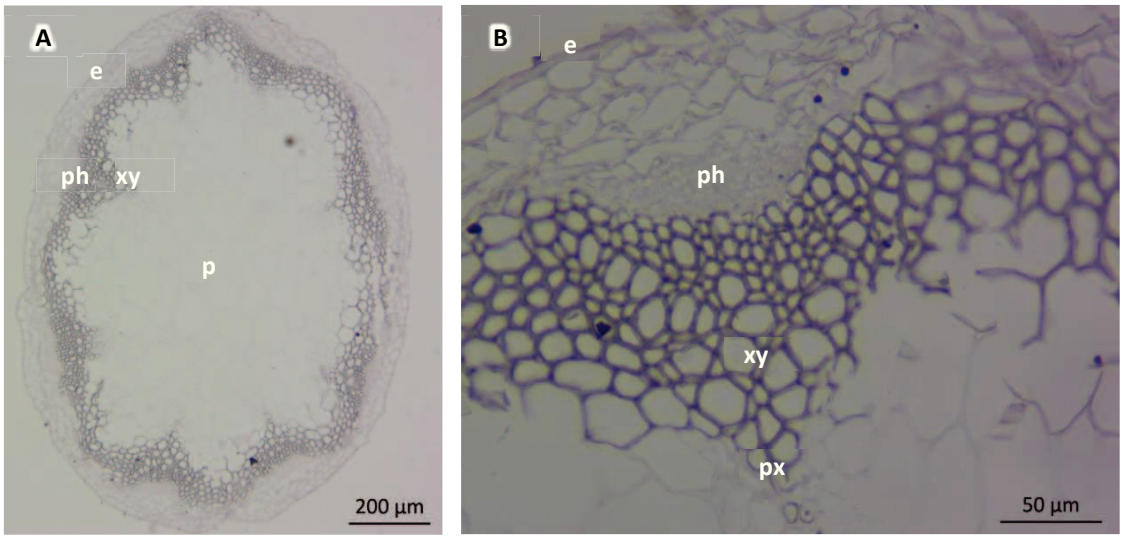

Figure 33. Light microscopy images of *Arabidopsis thaliana* floral stem. A and B. Global overview and details of transversal section of floral stem. (e, epidermis; ph, phloem; xy, xylem; px, protoxylem; p, pith).

Slides incubated with *SWEET11* probe showed an accumulation of transcripts in each vascular bundle as it is possible to observe in Figure 34. Precipitates were observed in some cells of the phloem tissue and in protoxylem cells.

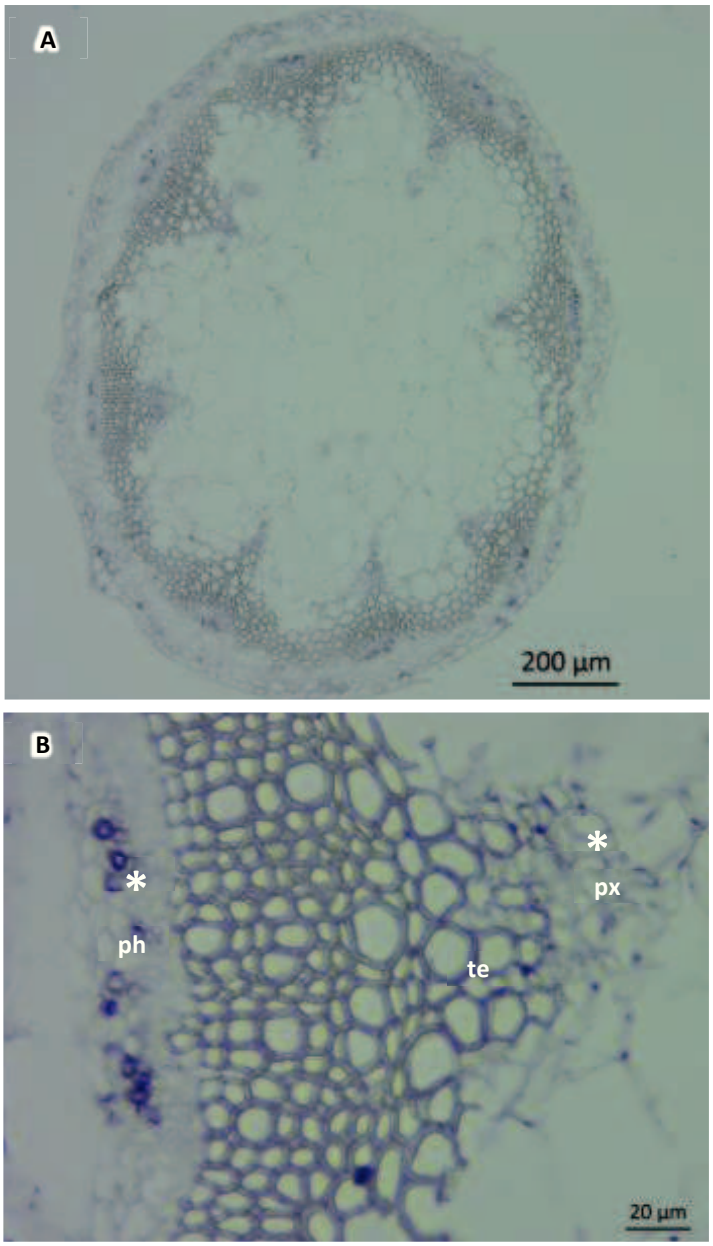

Figure 34. *In situ* hybridization analysis of *SWEET11* gene in *Arabidopsis thaliana* floral stem. A. Global overview of a transversal section hybridized with an antisense probe for *SWEET11*. Signal is present as blue-violet staining in phloem tissue and protoxylem cells of each vascular bundle. B. Details of a vascular bundle. The presence of precipitates is indicated by an asterisk. (ph, phloem; te, tracheid elements; px, protoxylem).

As regarding *SWEET12* gene, hybridization experiments showed similar results to *SWEET11*. As shown in Figure 35 a signal was detectable in the vascular bundles of the stem. In particular, blue-violet spots were present in some phloem and protoxylem cells.

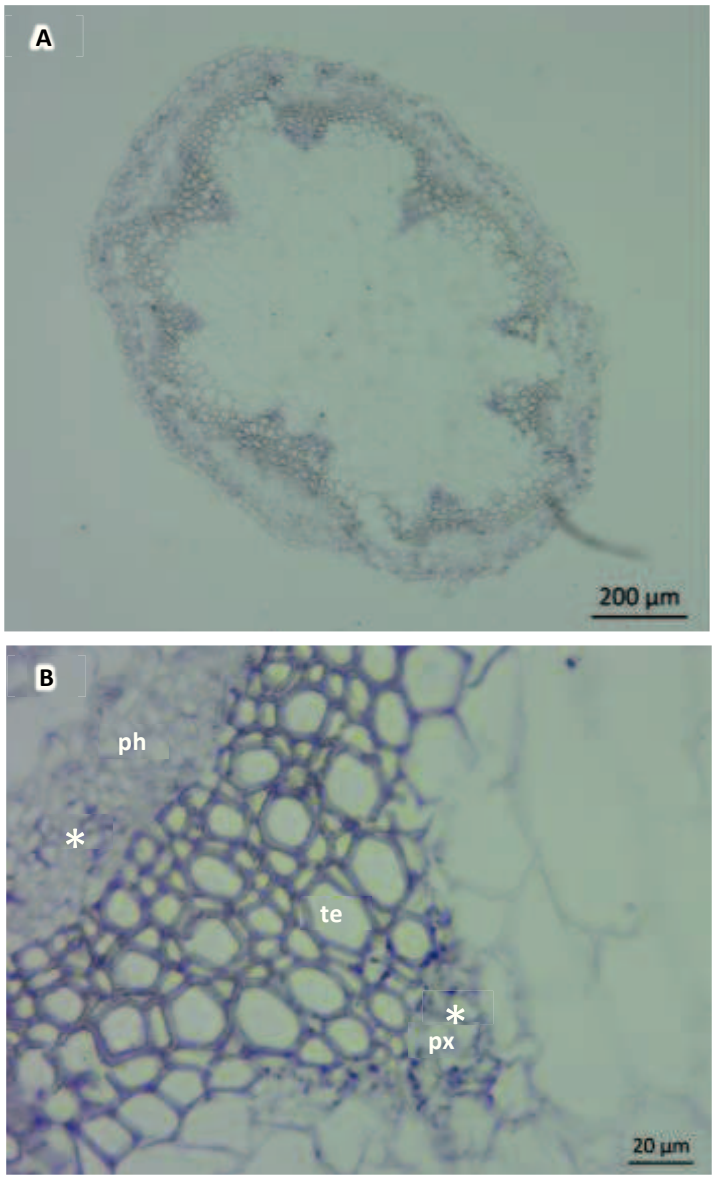

Figure 35. *In situ* hybridization analysis of *SWEET12* gene in *Arabidopsis thaliana* floral stem. A. Global overview of a transversal section hybridized with an antisense probe for *SWEET12*. Signal is present as blue-violet staining in phloem tissue and protoxylem cells of each vascular bundle. B. Details of a vascular bundle. The presence of precipitates is indicated by an asterisk. (ph, phloem; te, tracheid elements; px, protoxylem).

In situ hybridization experiments on grapevine leaves

The *in situ* hybridization technique was performed to localize several grapevine genes.

To set up the experimental plan, at first, the localization of the reference gene Ubiquitin-60S ribosomal protein L40-like gene (accession number XM_002273532.1) was studied. A couple of primers amplifying a 190 base pairs region was used to obtain two RNA probes. The first one was complementary to the RNA sequence of the gene (antisense probe), while the other one exactly reproduced the gene sequence (sense probe). This second probe was used to have a negative control in the experiment.

Eight-micron-thick sections from paraffin embedded leaf samples were hybridized with digoxygenin-labeled probes. Detecting reaction produces a blue-violet precipitate. As shown in Figure 36.A no signal was detectable when using sense probe. This result confirmed that there was no background signal in the experiment.

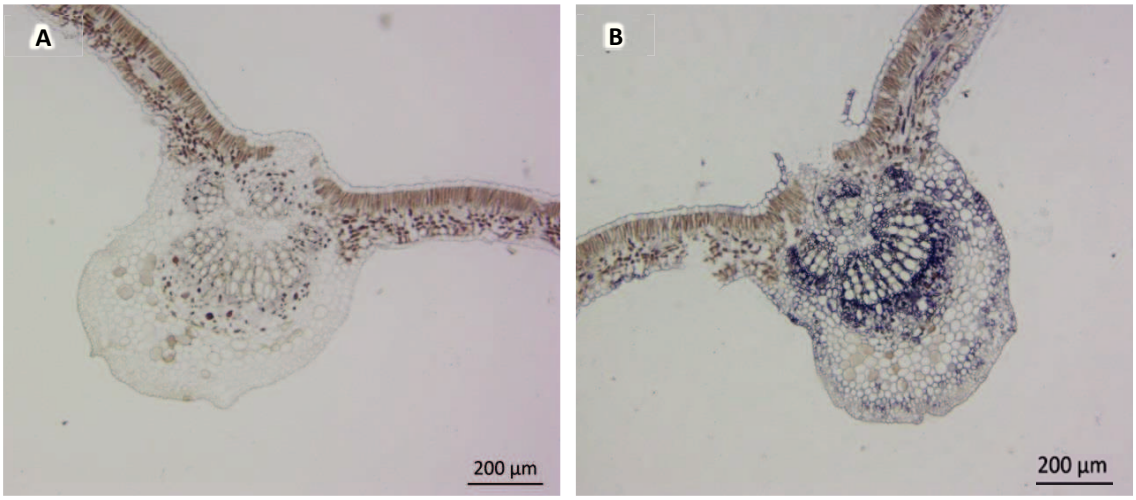

Figure 36. *In situ* hybridization analysis of ubiquitin gene in grapevine leaf. A. Transversal section of main vein hybridized with a sense probe for UBQ L-40. No signal is detectable. B. Transversal section of main vein hybridized with an antisense probe for UBQ L-40. Signal is visible in violet-blue coloration.

On the contrary, samples hybridized with an antisense probe showed a detectable precipitate in most of the tissues. In particular a strong signal was found in phloem cells and parenchyma cells among xylem vessels. Moreover, signal was detectable in collenchyma cells and epidermis (Figure 36.B).

Another gene which has been investigated in grapevine was a sucrose transporter (*VvSUC27*, accession number AF021810.1). Experiments were conducted on transversal sections of leaf main vein from healthy and infected samples.

Slides incubated without the antisense probe were observed as negative controls.

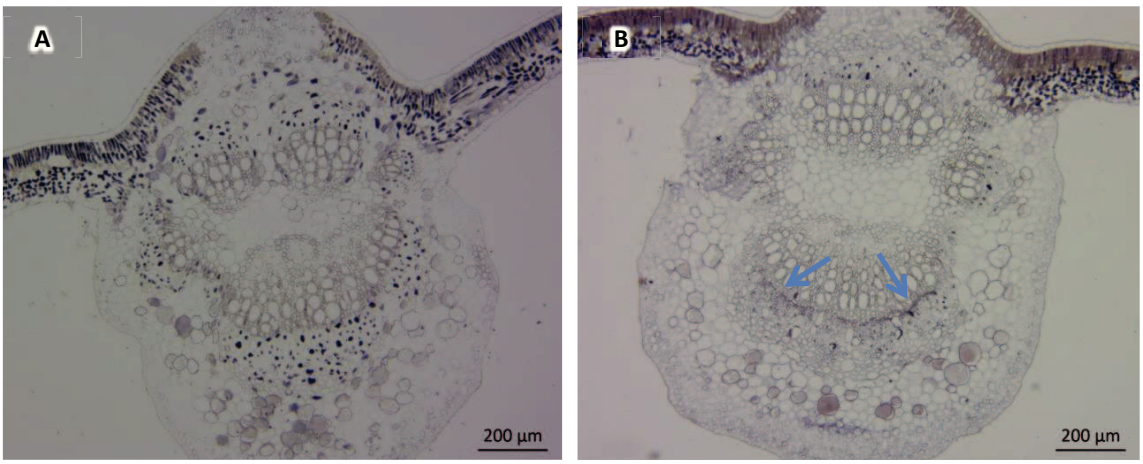

Figure 37. *In situ* hybridization analysis of a sucrose transporter gene in healthy grapevine leaf A. Transversal section of main vein hybridized without any probe. Nonspecific signal is present as large violet-blue spots. B. Transversal section of main vein hybridized with an antisense probe for SUC27. Signal is seen in violet-blue coloration (arrows).

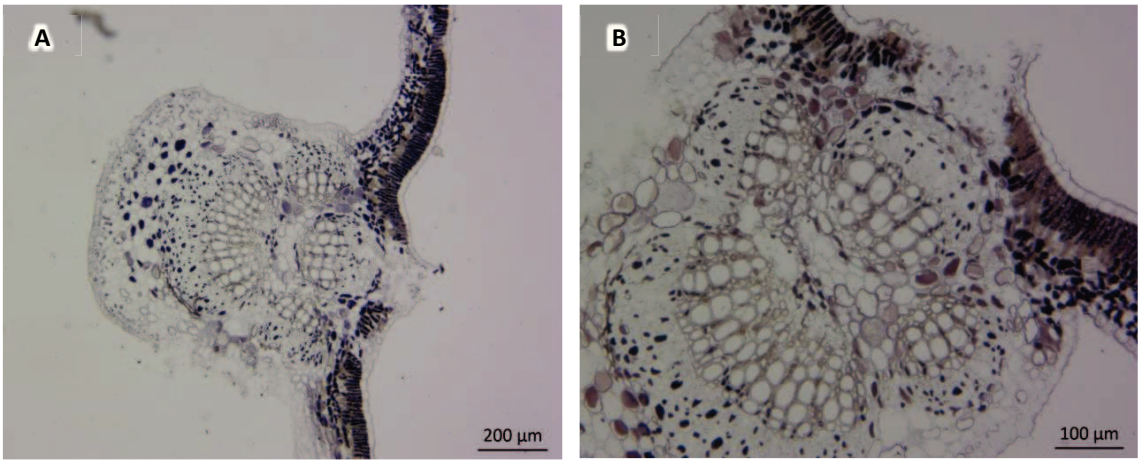

Figure 38. *In situ* hybridization analysis of a sucrose transporter gene in diseased grapevine leaf. A. Transversal section of main vein hybridized without any probe. Nonspecific signal is present as large violet-blue spots. B. Transversal section of main vein hybridized with an antisense probe for SUC27. Nonspecific signal is present as large violet-blue spots.

As shown in Figure 37.A no clear signal was detectable in sections incubated without probe. Big violet spots were present, mainly due to nonspecific precipitations. In healthy sample, on the other hand, coloration was present in the phloem cells near xylem tissue (Figure 37.B).
As regards infected samples, sections incubated without probe (Figure 38.A), and even sections incubated with *SUC27* probe (Figure 38.B) presented only large nonspecific spots.

In situ hybridization experiments on tomato leaves

Tomato genes, investigated by Real Time PCR, were also investigated by using the *in situ* hybridization technique to study their localization in tomato leaf tissues.

The investigated genes coded for a glucose transporter (SWEET1, accession number XM_004237674.1), a sieve element occlusion protein (SEO, accession number XM_004239105.1), and a phloem protein (PP2, accession number XM_004233183.1).

Experiments were conducted on transversal sections of the main vein of tomato leaves collected from healthy and infected plants. In order to have a negative control sections of healthy and infected samples were incubated without a detecting probe.

As shown in Figure 39 no signal was detected in negative control slides for healthy (Figure 39.A) and infected (Figure 39.B) samples.

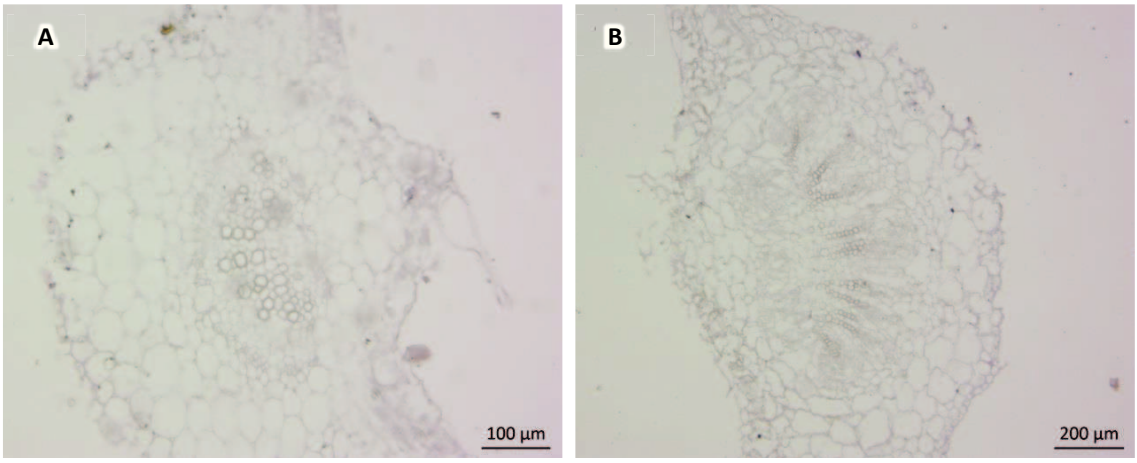

Figure 39. *In situ* hybridization analysis of tomato samples without any probe. A. Transversal section of a healthy plant. No signal is detectable. B. Transversal section of an infected plant. No signal is detectable.

Probe constructed to detect SEO gene gave precipitates in phloem cells of healthy leaf sections as shown in Figure 40, A and C. Samples from symptomatic leaves showed no signal in phloem tissue (Figure 40, B and D).

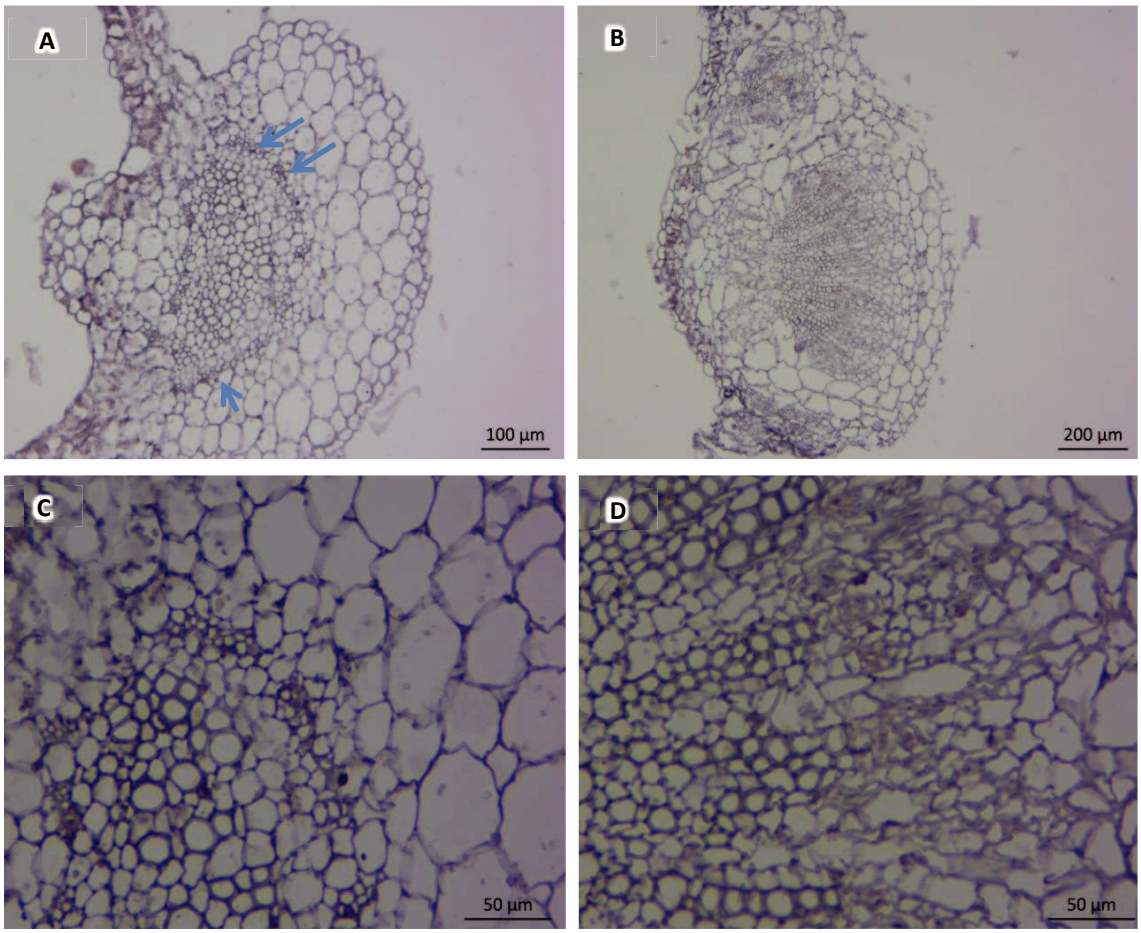

Figure 40. *In situ* hybridization analysis of a sieve element occlusion coding gene in healthy and diseased tomato leaf. A and C. Global overview and details of healthy sample: transversal section of main vein hybridized with antisense probe for SEO. Signal is present as large violet-blue spots in phloem cells (arrows). B and D. Global overview and details of diseased sample: transversal section of main vein hybridized with an antisense probe for SEO. No signal is detectable.

For phloem protein (PP2) some slight spots were detectable in correspondence of phloem tissue of healthy samples (Figure 41, A and C), while no clear signal was observed in infected sections (Figure 41, B and D).

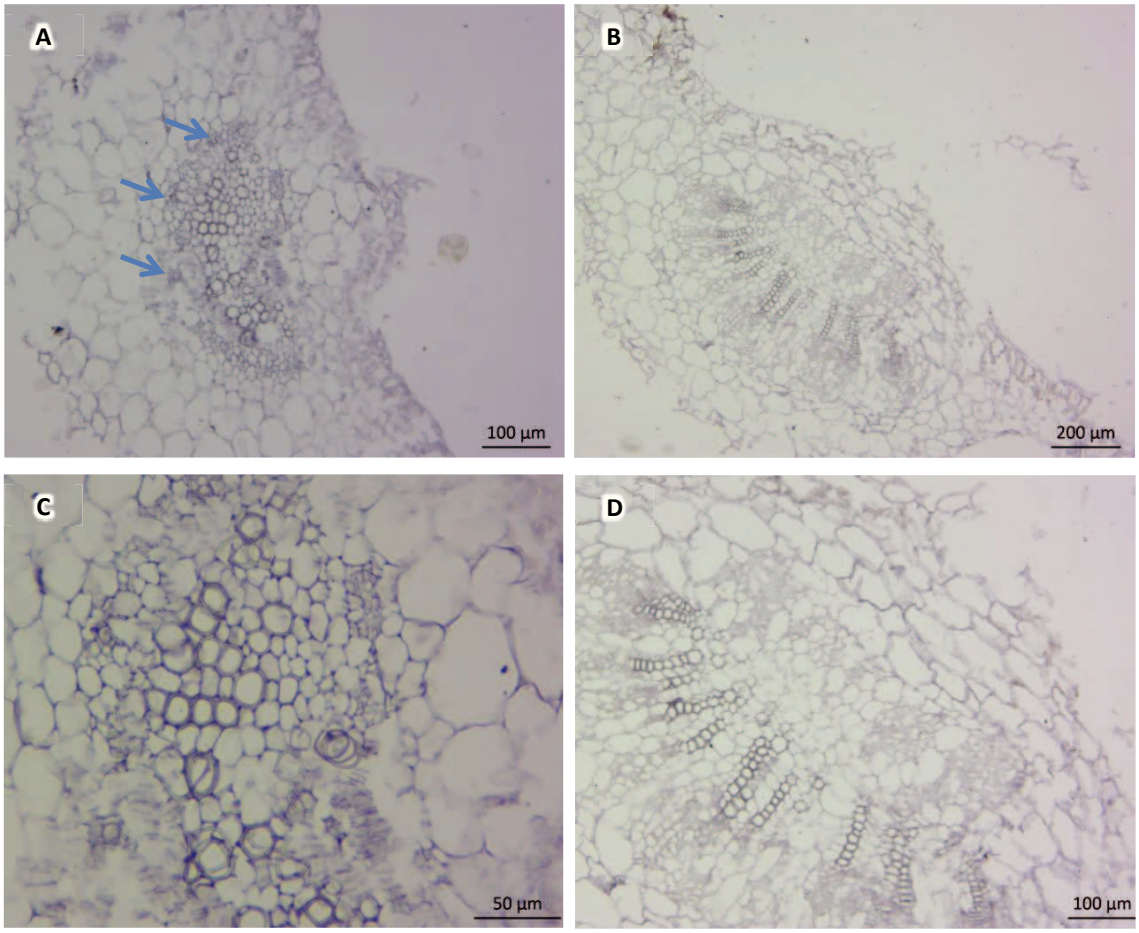

Figure 41. *In situ* hybridization analysis of a phloem protein coding gene in healthy and diseased tomato leaf. A and C. Global overview and details of healthy sample: transversal section of main vein hybridized with antisense probe for PP2. Signal is present as large violet-blue spots in phloem cells (arrows). B and D. Global overview and details of diseased sample: transversal section of main vein hybridized with an antisense probe for PP2. No clear signal is detectable.

A probe detecting SWEET1 transcripts was used and results are shown in Figure 42. In healthy samples it was possible to detect a slight signal in correspondence of phloem cells (Figure 42, A and C), while for infected samples no signal appeared (Figure 42, B and D).

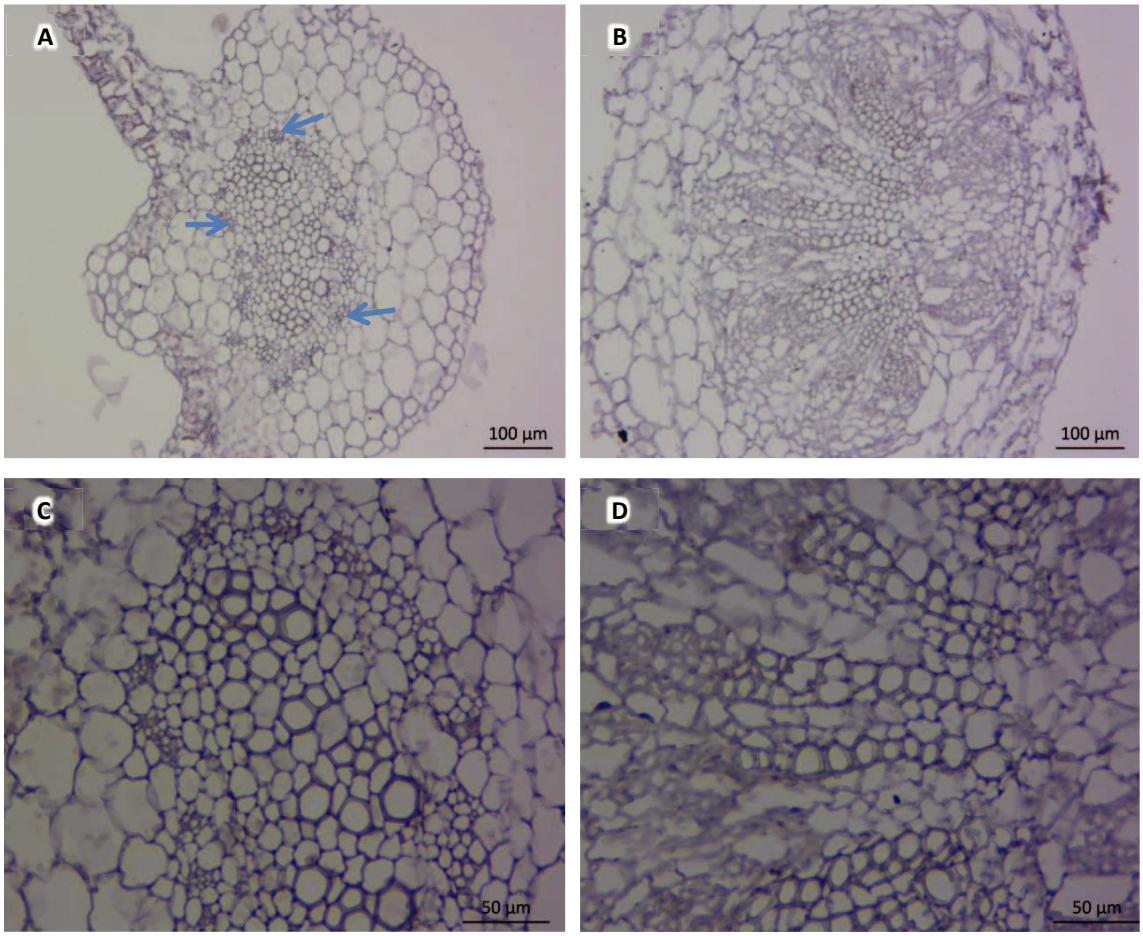

Figure 42. *In situ* hybridization analysis of a glucose transporter gene in healthy and diseased tomato leaf. A and C. Global overview and details of healthy sample: transversal section of main vein hybridized with antisense probe for SWEET1. Signal is present as large violet-blue spots in phloem cells (arrows). B and D. Global overview and details of diseased sample: transversal section of main vein hybridized with an antisense probe for SWEET1. No signal is detectable.

DISCUSSION

The phloem is the plant vascular tissue that is responsible for the translocation of photoassimilates and other compounds from source to sink organs. The phloem is a preferred destination for plant pathogens since it is a pathway for pathogen movement, and an important transmission route for photoassimilates that are used as nutrients by the microorganisms.
Compromised phloem functionality may have disastrous consequences for plant health and development.
Phytoplasmas are phloem-restricted pathogens associated with economically relevant diseases on several plant species. Phytoplasma-associated diseases are not curable, thus, studying and understanding the interactions existing between the host and the pathogen and the mechanisms at the basis of plant response to infection are essential for phytoplasma control and disease management.
Different integrated approaches have been used to gain insights on these subjects, using grapevines grown in an experimental field and tomato plants grown in greenhouse, both infected by '*Ca*. P. solani'.
Among the methods chosen for the investigations, *in situ* hybridization technique (ISH) was applied to stolbur-infected grapevine and tomato samples. Because of the difficulties that might occur setting up the method on these plants, especially on woody species, ISH was set up and performed firstly on the model plant *Arabidopsis thaliana*.
Transversal sections of *Arabidopsis* stems were employed to localize mRNAs of genes coding for *SWEET11* and *SWEET12*. These genes belong to SWEET family which codes for transporters involved in the release of sucrose or glucose from phloem parenchyma cells to the apoplast. They have been found to be expressed in phloem cells. Moreover, inhibition of these transporters reduces leaf assimilate exudation and induces sugar accumulation in leaves (Chen *et al.*, 2012).
Arabidopsis stems showed several vascular bundles with phloem in the outer layer and xylem tissue in the inner side. Observations allowed to detect *SWEET11* and *SWEET12* signal in phloem cells and even in protoxylem cells. These results confirm a possible involvement of SWEET transporters in apoplastic loading mechanisms of the phloem and suggest an involvement of the protein also in xylem tissue before complete differentiation of cells in xylem vessels.

Grapevine-'*Ca*. P. solani' interaction

Microscopy techniques, including Light Microscopy (LM), Confocal Laser Scanning Microscopy (CLSM) and Transmission Electron Microscopy (TEM), were used to obtain a wide-ranging comprehension about the leaf structure and about the ultrastructural modifications occurring during the infection as well as when recovery has been established. Particular attention has been paid about the organization of the cells forming the vascular tissues.

LM observations were useful to identify xylem and phloem and to highlight the structural characteristic of grapevine leaf tissues. Grapevine main veins showed several vascular bundles formed by phloem, which is located outside, and xylem that is situated in the internal side.

CLSM and histological dyes were used to compare sections of leaves from asymptomatic (healthy and recovered) and symptomatic grapevines. Carmine green staining permitted the identification of lignin and cellulose in the tissues. In asymptomatic plants lignin was present mostly in xylem vessels of vascular bundles and phloem cells showed a regular organization. In symptomatic samples it was possible to observe a different organization of the cell wall components, in particular of phloem and parenchyma cells among xylem vessels. These observations suggest a possible disturbance not only of phloem cells but also of surrounding tissues when the phytoplasma infection is severe. Further investigations could lead to confirm if the disease provokes alteration of the xylem and other tissues not directly involved in the life and spread of the pathogen. Recently, it has been reported that phytoplasmas, by the secretion of effector proteins, are able to lead alterations of plant growth pattern in different plant tissues and meristems, also far from the infection site (Bai *et al.*, 2009; Sugio *et al.*, 2011; Wei *et al.*, 2013).

Ultrastructural observations permitted to compare tissues of healthy, infected and recovered plants, thus allowing the detection of phytoplasmas in host sieve elements and the identification of structural changes occurring in the phloem according to the different plant phytosanitary status.

Phloem disorganization and phloem parenchyma cell necrosis are the main ultrastructural traits of infected samples. Moreover, callose accumulation is another ultrastructural characteristic of sieve elements of the diseased plants. Large amounts of callose were present at sieve plates of infected grapevines plants, occluding sieve pores. The callose accumulations could be responsible for sieve elements occlusion and the subsequent mass flow disturbance, which may be directly associated with the macroscopic symptoms of the disease. These results are comparable with investigations performed on *Vicia faba* L./ '*Ca*. P. vitis' pathosystem, as described by Musetti *et al.*, (2013a).

Through the combined use of ultrastructural and gene expression analyses of leaf tissues, for the first time we have also investigated and reported modifications occurring in the sieve elements of plants "recovered" from the Bois noir disease.

Interestingly, the ultrastructural characteristics found in the sieve elements of recovered plants

were not different from those observed in the healthy plants, apart from callose. Callose depositions in sieve elements of the recovered plants appeared thicker than those observed in the healthy grapevines and, only in some sporadic cases, they occluded the pores of the sieve plates. It seems that these ultrastructural characteristics are compatible with the correct physiology of recovered plants that are asymptomatic and look identical to healthy plants. It has been demonstrated that callose deposition in the phloem is not only associated with responses to wounding or to pathogen spread but also that it takes part in the normal processes of phloem maturation in intact plants, influencing the length of the sieve-plate pores and determining the flow properties (Barratt *et al.*, 2011; Xie *et al*., 2011).

Ultrastructural observations about callose deposition in grapevine were in accordance with the results obtained from the gene expression analyses, demonstrating that at least two different isoforms of callose synthase genes (*VvCAS7* and *VvCAS2*) are triggered in grapevine during phytoplasma infection and that they return to a lower level (not different from the healthy plants) during the "recovery" phase.

It is interesting to note that *VvCAS7* is ortholog of the *Arabidopsis CalS7*, that is responsible for callose deposition in the phloem (Xie *et al.*, 2011), the site of phytoplasma infection.

Moreover, *VvCAS2* has found to be induced in whole leaf tissues of grapevine, as already reported by Hren *et al.*, (2009a). It is noteworthy to report that the same gene is not upregulated when only phloem cells are analyzed, as observed by Santi *et al*., (2013).

This result underlines the different roles of the several isoforms of the same enzyme and the necessity to check them in order to understand which are rightly involved in a specific plant-pathogen interaction.

The anomalous deposition of callose in the infected phloem tissue and the altered modulation of two callose synthase genes were only a part of the large modifications observed for sucrose metabolism and transport in the leaf. Accumulations of soluble carbohydrates and starch in source leaves, complemented by a decrease of sugar levels in sink organs, have been reported for periwinkle, tobacco, and coconut palm infected by phytoplasmas (Lepka *et al.*, 1999; Maust *et al.*, 2003). Thus, in healthy, diseased and recovered grapevine leaf tissues, genes coding for sucrose synthases were also analyzed. Four genes were expressed in leaves and, although the expression level among the genes was different, they all showed a significant induction in infected plants compared to healthy and recovered samples.

It has been demonstrated that, analogously to other obligate biotrophs that need to acquire most nutrients from the host plant, the stolbur phytoplasma induces the establishment of a carbohydrate sink in the phloem of the leaf, thus altering the normal pattern of sugar partitioning of a source leaf (Santi *et al.*, 2013). In fact, in laser-microdissected phloem tissue of stolbur-infected leaves, a dramatic decrease of expression of *SUC27*, the grapevine transporter mediating sucrose apoplastic loading into the phloem, has been reported together with a huge up-regulation of a SUS gene (*VvSUS4*; Santi *et al.*, 2013). A co-regulation of both sucrose

transport and cleavage would be advantageous for the pathogen as both responses are crucial to access hexoses, which could be the only usable carbon source (Christensen *et al.*, 2005).

Sucrose synthases are enzymes that cleave sucrose producing fructose and both uridine diphosphate-glucose (UDPG) and adenosine diphosphate-glucose (ADPG) (Amor *et al.*, 1995; Geigenberger *et al.*, 1993). UDPG is used by callose synthases as a glucose donor for the production of callose (Amor *et al.*, 1995). It has been proposed that callose synthesis is performed by a callose synthase complex, having a hydrophilic loop interacting with different proteins, among which sucrose synthases (Verma and Hong, 2001).

The upregulation of callose synthases and sucrose synthases in infected grapevine plants confirmed the pivotal role of callose in plant–pathogen interactions.

Recently, the expression profiles of genes coding for sucrose transporters have been characterized by Santi *et al.*, (2013) in grapevine analyzing only cells from phloem tissue. Using laser microdissection microscopy it was possible to study the transcript levels of sucrose transporters in phloem cells of grapevine leaves infected by stolbur. In particular, among three examined sucrose transporters (Vv*SUC11, VvSUC12, VvSUC27*) only *VvSUC27* was significantly expressed in phloem cells and this resulted strongly down-regulated in phytoplasma infected samples. *VvSUC27* was proposed by Afoufa-Bastien *et al.*, (2010) as being involved in phloem loading and sugar retrieval during long-distance transport. The reduction of *VvSUC27* transcripts in infected phloem cells compared to healthy ones suggested a reduced phloem loading. This result associated with the increase in sugars concentrations supports the hypothesis that the presence of the pathogen induces an establishment of a carbohydrate sink in the source leaf. This phenomenon has often been observed during infection by other obligate biotrophs that achieve nutrients from host cells (Hayes *et al.*, 2010).

In situ hybridization was performed to confirm the involvement of *VvSUC27* in grapevine/phytoplasma interactions. In particular a riboprobe was obtained to detect mRNAs of *VvSUC27* in grapevine samples.

In healthy grapevine samples coloration was detectable in phloem cells close to xylem tissue, while there was no specific signal in infected samples, reinforcing results obtained by Santi *et al*., (2013).

As regards phloem proteins, TEM observations revealed a conformation change in recovered plants, where they formed aggregations and clamps in the sieve element lumen and at the sieve plates. Phloem protein plugs may represent the sieve tube's first line of defense against the loss of assimilates due to wounding or pathogens or pests. Besides defensive plugging and sieve cell differentiation, recent studies have demonstrated that phloem proteins are able to interact with RNA molecules, are involved in the long-distance trafficking of macromolecules and thus they may play a role in long-distance signaling in response to infection by plant pathogens (Golecki *et al.*, 1999). Furthermore, phloem proteins might be involved in defense reaction by participating in the trafficking, synthesis, modulation or amplification of systemic signals. Phloem protein

aggregation in the phloem might play important roles in the recovery of grapevines from phytoplasma disease, similarly to what demonstrated for apple trees (Musetti *et al.*, 2010).

Tomato-'*Ca*. P. solani' interaction

Observed at LM, tomato leaves showed an arrangement of vascular tissue different from grapevine. In fact, a central vascular bundle is present with xylem tissue surrounded by phloem cells. This organization was described by Hayward in 1938 and it occurs in several species belonging to *Solanaceae* family as potato (Hayward, 1938) and tobacco (Avery, 1933).

As already reported for grapevine, CLSM permitted to highlight differences between sections from healthy and symptomatic plants. In particular, in infected samples the lignin signal showed a peculiar arrangement of xylem vessels in strings.

TEM observations revealed that, unlike what was observed in the grapevine, leaf tissues from stolbur-infected tomato did not show necrosis. Otherwise, the callose accumulation at the sieve plates is a common ultrastructural characteristic of grapevine- and tomato-phytoplasma interactions. This common trait was confirmed by gene expression analyses, showing also in tomato, the over expression of different callose synthase isoforms, among which *SlCAS7*, which is ortholog of both *VvCAS7* and *AtCAL7* (Xie *et al.*, 2011).

Another ultrastructural modification observed in the phloem of infected tomato leaves was the presence of phloem proteins organized in dense clumps in sieve element lumen, often associated with phytoplasmas.

The function of phloem proteins remains not clear, but it has been hypothesized that they play a role in the maintaining of turgor pressure in the sieve cell after injury, and thus that they are engaged in plant response to pathogens (Read and Northcote, 1983). For example in cucurbits, phloem proteins PP1 and PP2 appear to be involved in occlusion of sieve tubes and wound surface by gelling (Alosi *et al.*, 1988). Moreover, sieve element occlusion (SEO) proteins have been found in *Fabaceae* to undergo a conformational change associated with a dramatic volume increase in response to different stresses (Knoblauch *et al.*, 2001, Peters *et al.*, 2006).

In order to check if phloem proteins are involved in this aspect of the plant-pathogen interaction, genes coding for a phloem protein (PP2, XM_004233183.1) and a sieve element occlusion protein (SEO, XM_004239105.1) were analyzed. Phloem protein gene showed a slight decrease of transcript in diseased samples compared to healthy ones. The transcript level of SEO gene was found approximately six times lower in infected plant. The expressions of the same genes were checked also using *in situ* hybridization technique. Observations confirmed the results of Real Time PCRs. The signal for both transcripts appeared more evident in sections from healthy tomatoes than in those from the infected ones, even if PP2 transcript signal was weaker.

These results suggest that the involvement of phloem proteins in the interactions with pathogens is not related to the new synthesis of the proteins but only to a conformation change. Moreover, these results are consistent with those obtained by Musetti *et al.*, (2010)

investigating apple proliferation disease. In fact, leaves of infected apple plants showed a transcription level of phloem protein genes lower or at least equal to healthy samples (Musetti *et al.*, 2010).

Sugar translocation in the phloem is the result of the involvement of several enzymes and transporters. As already stated, a new class of transporters has been recently characterized in *Arabidopsis thaliana* and called SWEETs (Chen *et al.*, 2010). It has been reported that biotrophic bacteria (*Pseudomonas syringae* pv. *tomato*) or fungi (*Golovinomyces cichoracearum* and *Botrytis cinerea*) induce mRNA levels of different SWEET genes (Chen *et al.*, 2010).

On the basis of this information a SWEET gene of tomato (SWT1, XM_004237674.1) was analyzed. Real Time PCR and *in situ* hybridization techniques showed that the checked gene was down-regulated in infected samples. This result seems to be in contrast with the observations reported by Chen *et al.*, (2010), but it is necessary to underline that several SWEET transporters are present in tomato, thus it will be necessary to check all the different isoforms to understand if they are really affected by phytoplasma infection.

Phytoplasma detection

Phytoplasma detection in grapevines and tomato plants has been a significant section of the work. Real Time RT-PCR technique and TEM was used on leaf samples. Amplification of a specific region of *16S rRNA* permitted to detect '*Ca*. P. solani' in symptomatic plants, and this fact was confirmed by microscopic observations.

Different protocols were checked in order to detect phytoplasmas also in root tissues. In several species phytoplasmas have been found in roots (Bertaccini and Duduk, 2009) and thus a method based on TaqMan® probes was performed to gain insights about grapevine and tomato plants. TEM ultrastructural observations of root tissues were moreover performed. Although the sensitivity and specificity of the molecular method, not every sample that previously resulted infected on leaves was showing the presence of the phytoplasmas in roots. This occurred in both grapevine and tomato plants. Also TEM detection resulted difficult at root level. The difficulty to detect phytoplasmas in roots in a reliable way it is probable due to the uneven distribution and low titer of the pathogen and, about molecular method, to problems involved in RNAs extraction from root samples. Especially for tomato, further investigations taking into account a larger number of samples will be useful to confirm the validity of the protocol.

The set-up of a method for phytoplasma diagnosis in roots allowed us to hypothesize the distribution of the phytoplasmas in recovered grapevines. Stolbur was not detected in leaves of recovered grapevines and this is in accordance with results obtained on apple trees affected by apple proliferation disease (Carraro *et al.*, 2004; Musetti *et al.*, 2010). As stated above, detection of phytoplasmas in root samples was very difficult, so it remains unclear if the pathogens move from the aerial part to the above ground part to overwinter, as in apple trees (Carraro *et al*.,

2004). Further investigations could be necessary to confirm if recovered grapevines phytoplasmas are still present in the root apparatus of recovered grapevines.

The present work demonstrated how phytoplasma infection severely affects phloem tissue and leads to relevant changes in plant development and physiology. Several genes and enzymes involved in sucrose transport and metabolism are modulated by the presence of the pathogen, while plants that are able to recovered from disease seem to restore all the correct phloem functions. The use of different techniques and the comparison of two pathosystems permitted to have a major comprehension of plant-phytoplasma interactions.
Further investigations should be directed to the understanding of the mechanisms that lead to gene modulation and how the plant balances the recruitment of energy for defense response (e.g., callose deposits).

REFERENCES

Afoufa-Bastien D, Medici A, Jeauffre J, Coutos-Thévenot P, Lemoine R, Atanassova R, Laloi M (2010). The *Vitis vinifera* sugar transporter gene family: phylogenetic overview and macroarray expression profiling. *BMC Plant Biology,* 10: 245.

Albertazzi G, Milc J, Caffagni A, Francia E, Roncaglia E, Ferrari F, Tagliafico E, Stefani E, Pecchioni N (2009). Gene expression in grapevine cultivars in response to Bois Noir phytoplasma infection. *Plant Science,* 176: 792–804.

Alma A, Soldi G, Tedeschi R, Marzachì C (2002). Role of *Hyalesthes obsoletus* Signoret (Homoptera: Cixiidae) in the transmission of grapevine Bois noir in Italy. In: Proceedings of the Second Italian Meeting on Phytoplasma Diseases (Barba M, ed.). *Istituto Sperimentale per la Patologia Vegetale*, Roma, pp. 57–58.

Alosi MC, Melroy DL, Park RB (1988). The regulation of gelation of phloem exudate from *Cucurbita* fruit by dilution, glutathione, and glutathione reductase. *Plant Physiology* 86: 1089–1094.

Altschul SF, Madden TL, Schäffer AA, Zhang J, Zhang Z, Miller W, Lipman DJ (1997). Gapped BLAST and PSI-BLAST: a new generation of protein database search programs. *Nucleic Acids Research,* 25: 3389-3402.

Altschul SF, Gish W, Miller W, Myers EW, Lipman DJ (1990). Basic local alignment search tool. *Journal of Molecular Biology,* 215: 403-410.

Amor Y, Haigler CH, Johnson S, Wainscott M, Delmer DP (1995). A membrane-associated form of sucrose synthase and its potential role in synthesis of cellulose and callose in plants. *Proceedings of the National Academy of Sciences of the United States of America,* 92: 9353–9357.

Arsanto JP (1986). $Ca2^{+}$ binding sites and phosphatase activities in sieve element reticulum and P-protein of chick-pea phloem: a cytochemical and X-ray microanalysis survey. *Protoplasma*, 132: 160–171

Avery GS (1933). Structure and development of the tobacco leaf. *American Journal of Botany,* 20: 565-592.

Bai X, Correa VR, Toruño TY, Ammar ED, Kamoun S, Hogenhout SA (2009). AY-WB phytoplasma secretes a protein that targets plant cell nuclei. *Molecular Plant-Microbe Interactions,* 22: 18–30.

Bai X, Zhang J, Ewing A, Miller SA, Jancso Radek A, Shevchenko DV, Tsukerman K, Walunas T, Lapidus A, Campbell JW, Hogenhout SA (2006). Living with genome instability: the adaptation of phytoplasmas to diverse environments of their insect and plant hosts. *Journal of Bacteriology,* 188: 3682–3696.

Barratt DH, Kölling K, Graf A, Pike M, Calder G, Findlay K, Zeeman SC, Smith AM (2011). Callose synthase GSL7 is necessary for normal phloem transport and inflorescence growth in Arabidopsis. *Plant physiology*, 155: 328-341.

Beanland L, Hoy CW, Miller SA, Nault LR (2000). Influence of aster yellows phytoplasma on the fitness of aster leafhopper (Homoptera: Cicadellidae). *Annals of the Entomological Society of America,* 93: 271-276.

Behnke HD, Sjolund RD (1990). Sieve Elements. Comparative structure, induction and development. *Springer-Verlag*, Berlin.

Bellomo C, Carraro L, Ermacora P, Pavan F, Osler R, Frausin C, Governatori G (2007). Recovery phenomena in grapevines affected by grapevine yellows in Friuli Venezia Giulia. *Bulletin of Insectology,* 60: 235-236.

Berg, M, Melcher U, Fletcher J (2001). Characterization of *Spiroplasma citri* adhesion related protein SARP1, which contains a domain of a novel family designated sarpin. *Gene,* 275: 57–64.

Berges R, Rott M, Seemüller E (2000). Range of phytoplasma concentrations in various plant hosts as determined by competitive polymerase chain reaction. *Phytopathology,* 90: 1145–1152.

Bertaccini A, Duduk B (2009). Phytoplasma and phytoplasma diseases: a review of recent research. *Phytopathologia Mediterranea*, 48: 355-378.

Bertaccini A (2007). Phytoplasmas: diversity, taxonomy, and epidemiology. *Frontiers in Bioscience,* 12: 673-689.

Bio-Rad Laboratories (2006). Real-Time PCR Applications Guide. *Bulletin,* 5279.

Bressan A, Girolami V, Boudon-Padieu E (2005). Reduced fitness of the leafhopper vector *Scaphoideus titanus* exposed to Flavescence dorée phytoplasma. *Entomologia Experimentalis et Applicata* 115: 283-290.

Bobev SG, De Jonghe K, Maes M (2013). First Report of *Candidatus* Phytoplasma solani on Blackberry (*Rubus fruticosus*) in Bulgaria. *Disease Notes,* 97: 282.

Boonrod K, Munteanu B, Jarausch B, Jarausch W, Krczal G (2012). An immunodominant membrane protein (Imp) of '*Candidatus* Phytoplasma mali' binds to plant actin. *Molecular Plant-Microbe Interactions,* 25: 889–895.

Botswick DE, Dannenhoffer JM, Skaggs MI, Lister RM, Larkins BA, Thompson GA (1992). Pumpkin phloem lectin genes are specifically expressed in companion cells. *Plant Cell,* 4: 1539-1548.

Bustin SA, Benes V, Garson JA, Hellemans J, Huggett J, Kubista M, Mueller R, Nolan T, Pfaffl MW, Shipley GL, Vandesompele J, Wittwer CT (2009). The MIQE guidelines: minimum information for publication of quantitative real-time PCR experiments. *Clinical chemistry,* 55: 611-622.

Bustin SA (2005). Real-Time PCR. In: Encyclopedia of Diagnostic Genomics and Proteomics (Fuchs J and Podda M, eds.). *Marcel Dekker Inc,* New York, pp. 1117-1125.

Buxa SV, Polizzotto R, De Marco F, Loschi A, Kogel KH, van Bel AJE, Musetti R (2013). Re-arrangement of sieve element endomembrane network in tomato leaves infected by Stolbur phytoplasma. *New Perspectives in Phytoplasma Disease Management COST Action FA 0807,* pp. 78-79.

Carraro L, Ferrini F, Martini M, Ermacora P, Loi N (2008). A serious epidemic of stolbur on celery. *Journal of Plant Pathology,* 90: 131-13.

Carraro L, Ermacora P, Loi N, Osler R (2004). The recovery phenomenon in apple proliferation infected apple trees. *Journal of Plant Pathology,* 86: 141–146.

Carraro L, Loi N, Ermacora P (2001). Transmission characteristics of the European stone fruit yellows phytoplasma and its vector *Cacopsylla pruni*. *European Journal of Plant Pathology,* 107: 695–700.

Caudwell A (1961). Les phenomenes de retablissement chez la Flavescence doree de la vigne. *Annuelles Epiphyt,* 12: 347–354.

Chen LQ, Qu XQ, Hou BH, Sosso D, Osorio S, Fernie AR, Frommer WB (2012). Sucrose efflux mediated by SWEET proteins as a key step for phloem transport. *Science,* 335: 207-211.

Chen LQ, Hou BH, Lalonde S, Takanaga H, Hartung ML, Qu XQ, Guo WJ, Kim JG, Underwood W, Chaudhuri B, Chermak D, Antony G, White FF, Somerville SC, Mudgett MB, Frommer WB (2010). Sugar transporters for intercellular exchange and nutrition of pathogens. *Nature,* 468: 527-532.

Choi YH, Tapias EC, Kim HK, Lefeber AW, Erkelens C, Verhoeven JT, Brzin J, Zel J, Verpoorte R (2004). Metabolic discrimination of *Catharanthus roseus* leaves infected by phytoplasma using 1H-NMR spectroscopy and multivariate data analysis. *Plant physiology,* 135: 2398-2410.

Christeller JT, Farley PC, Ramsay RJ, Laing WA (1998). Purification, characterization and cloning of an aspartic protease inhibitor from squash phloem exudate. *European Journal of Biochemistry,* 254: 160–167.

Christensen NM, Axelsen KB, Nicolaisen M, Schulz A (2005). Phytoplasmas and their interactions with hosts. *TRENDS in Plant Science,* 10: 526-535.

Christensen NM, Nicolaisen M, Hansen M, Schulz A (2004). Distribution of phytoplasmas in infected plants as revealed by real-time PCR and bioimaging. *Molecular Plant–Microbe Interactions,* 17: 1175–1184.

Constable FE, Gibb KS, Symons RH (2003). Seasonal distribution of phytoplasmas in Australian grapevines. *Plant Pathology,* 52: 267–276.

Contaldo N, Bertaccini A, Paltrinieri S, Windsor HM, Windsor GD (2012). Axenic culture of plant pathogenic phytoplasmas. *Phytopathologia Mediterranea*, 51: 607-617.

Cordova I, Jones P, Harrison NA, Oropeza C (2003). *In situ* PCR detection of phytoplasma DNA in embryos from coconut palms with lethal yellowing disease. *Molecular Plant Pathology,* 4: 99-108.

Cousin MT, Dafalla G, Demazeau E, Theveu E, Grosclaude J (1989). *In situ* detection of MLOs for solanaceae stolbur and faba bean phyllody by indirect immunofluorescence. *Journal of Phytopathology,* 124: 71–79.

Cousin MT, Abadie M (1982). Action des mycoplasmes sur l'anthère. Etude en microscopies photonique et électronique. *Revue de Cytologie et de Biologie Vegetales - Le Botaniste,* 5: 41-57.

Cronshaw J (1975). P-proteins. In: Phloem Transport (Aronoff S, Dainty J, Gorham PR, Srivastava LM, Swanson CM, eds.). *Plenum*, New York, pp. 79-115.

Cronshaw J, Sabnis D (1990). Phloem proteins. In: Sieve Elements: comparative structure, induction and development (Behnke HD, Sjolund RD, eds.). *Springer-Verlag*, Berlin, pp. 257-283.

Dannenhoffer JM, Suhr SC, Thompson GA (2001). Phloem-specific expression of the pumpkin fruit trypsin inhibitor. *Planta,* 212: 155–162.

Deeken R, Ache P, Kajahn I, Klinkenberg J, Bringmann G, Hedrich R (2008). Identification of *Arabidopsis thaliana* phloem RNAs provides a search criterion for phloem-based transcripts hidden in complex datasets of microarray experiments. *The Plant Journal,* 55: 746–759.

Desveaux D, Singer AU, Dangl JL (2006). Type III effector proteins: Doppelgangers of bacterial virulence. *Current Opinion in Plant Biology,* 9: 376-382.

Davies C, Wolf T, Robinson SP (1999). Three putative sucrose transporters are differentially expressed in grapevine tissues. *Plant Science,* 147: 93-100.

Dickinson M, Hodgetts J (2013). Phytoplasma. Methods and protocols. *Springer, Humana press*.

Doi YM, Teranaka M, Yora K, Asuyama H (1967). Mycoplasma or PLT-group-like microorganisms found in the phloem elements of plants infected with mulberry dwarf, potato witches' broom, aster yellows, or paulownia witches' broom. *Annals of the Phytopathological Society of Japan,* 33: 259-266.

Duduk B, Bertaccini A (2006). Corn with symptoms of reddening: new host of stolbur phytoplasma. *Plant Disease,* 90: 1313-1319.

Ehlers K, Knoblauch M, van Bel AJE. (2000) Ultrastructural features of well-preserved and injured sieve elements: minute clamps keep the phloem transport conduits free for mass flow. *Protoplasma,* 214: 80-92.

Ehness R, Roitsch T (1997). Co-ordinated induction of mRNAs for extracellular invertase and a glucose transporter in *Chenopodium rubrum* by cytokinins. *The Plant Journal,* 11**:** 539–548.

Eleftheriou EP (1990). Monocotyledons. In: Sieve Elements: Comparative Structure, Induction and Development (Behnke HD, Sjolund RD, eds.). *Springer-Verlag*, Berlin, pp. 139–156.

Esau K (1969). The Phloem. In: Encyclopedia of Plant Anatomy, Vol. 5. *Bornträger*, Berlin.

Eschrich W (1989). Phloem unloading of photoassimilates. In: Transport of photoassimilates (Baker DA, Milburn JA, eds.). *Longman Scientific & Technical*, New York, pp: 206-263.

Evert RF (1990). Dicotyledons. In: Sieve Elements: Comparative Structure, Induction and Development (Behnke HD, Sjolund RD, eds.). *Springer-Verlag*, Berlin, pp. 103–137.

Favali MA, Musetti R, Benvenuti S, Bianchi A, Pressacco L (2004). *Catharanthus roseu*s L. plants and explants infected with phytoplasmas: alkaloid production and structural observations. *Protoplasma,* 223: 45-51.

Firrao G et al. (2004). '*Candidatus* Phytoplasma', a taxon for the wall-less, non-helical prokaryotes that colonize plant phloem and insects. *International Journal of Systematic and Evolutionary Microbiology,* 54: 1243–1255.

Fleischmann RD, Adams MD, White O, Clayton RA, Kirkness EF, Kerlavage AR, Bult CJ, Tomb JF, Dougherty BA, Merrick JM, et al. (1995). Whole-genome random sequencing and assembly of *Haemophilus influenzae* Rd. *Science,* 269: 496-512.

Garau R, Sechi A, Prota VA, Moro G (2007). Productive parameters in Chardonnay and Vermentino grapevines infected with "bois noir" and recovered in Sardinia. *Bulletin of Insectology,* 60: 233-234.

Gehrig HH, Winter K, Cushman J, Borland A, Taybi T (2000). An improved RNA isolation method for succulent plant species rich in polyphenols and polysaccharides. *Plant Molecular Biology Reporter,* 18: 369-376.

Geigenberger P, Langenberger S, Wilke I, Heineke D, Heldt HW, Stitt M (1993). Sucrose is metabolised by sucrose synthase and glycolysis within the phloem complex of *Ricinus communis* L. seedlings. *Planta,* 190: 446-453.

Godt D, RoitschT (2006). The developmental and organ specific expression of sucrose cleaving enzymes in sugar beet suggests a transition between apoplasmic and symplasmic phloem unloading in the tap roots. *Plant Physiology and Biochemistry,* 44: 656–665.

Golecki B, Schultz A, Thompson GA (1999). Translocation of structural P proteins in the phloem. *Plant Cell,* 11: 127-140.

Gottwald JR, Krysan PJ, Young JC, Evert RF, Sussman MR (2000). Genetic evidence for the *in planta* role of phloem-specific plasma membrane sucrose transporters. *Proceedings of the National Academy of Sciences of the United States of America,* 97: 13979-13984.

Hafke JB, Ehlers K, Föller J, Höll SR, Becker S, van Bel AJE. Involvement of the sieve element cytoskeleton in electrical responses to cold shocks. *Plant physiology*, 162: 707-719.

Handakumbura PP, Hazen SP (2012). Transcriptional regulation of grass secondary cell wall biosynthesis: playing catch-up with *Arabidopsis thaliana*. *Frontiers in Plant Science*, 3: 74.

Hartmann T (1999). Chemical ecology of pyrrolizidine alkaloids. *Planta,* 207: 483–495.

Hayashi H, Fukuda A, Suzui N, Fujimaki S (2000). Proteins in the sieve tube-companion cell complexes: their detection, localization and possible functions. *Australian Journal of Plant Physiology,* 27: 489–496.

Hayes A, Feechan A, Dry IB (2010). Involvement of abscisic acid in the coordinated regulation of a stress-inducible hexose transporter (VvHT5) and a cell wall invertase in grapevine in response to biotrophic fungal infection. *Plant Physiology*, 153: 211–221.

Hayward HE (1938). The structure of economic plants. *Macmillan,* New York.

Hogenhout SA, Oshima K, Ammar ED, Kakizawa S, Kingdom HN, Namba S (2008). Phytoplasmas: bacteria that manipulate plants and insects. *Molecular Plant Pathology,* 9: 403-423.

Holland PM, Abramson RD, Watson R, Gelfand DH (1991). "Detection of specific polymerase chain reaction product by utilizing the 5'-->3' exonuclease activity of *Thermus aquaticus* DNA polymerase". *Proceedings of the National Academy of Sciences of the United States of America,* 88: 7276–7280.

Hollingsworth CR, Atkinson LM, Samac DA, Larsen JE, Motteberg CD, Abrahamson MD, Glogoza P, MacRae IV (2008). Region and field level distributions of aster yellows phytoplasma in small grain crops. *Plant Disease,* 92: 623-630.

Hoshi A, Oshima K, Kakizawa S, Ishii Y, Ozeki J, Hashimoto M, Komatsu K, Kagiwada S, Yamaji Y , Namba S (2009). A unique virulence factor for proliferation and dwarfism in plants identified from a phytopathogenic bacterium. *Proceedings of the National Academy of Sciences of the United States of America,* 106: 6416-6421.

Hren M, Nikolic P, Rotter A, Blejec A, Terrier N, Ravnikar M, Dermastia M, Gruden K (2009a). 'Bois Noir' phytoplasma induces significant reprogramming of the leaf transcriptome in the field grown grapevine. *BMC Genomics,* 10: 460.

Hren M, Ravnikar M, Brzin J, Ermacora P, Carraro L, Bianco PA, Casati P, Borgo M, Angelini E, Rotter A, Gruden K (2009b). Induced expression of sucrose synthase and alcohol dehydrogenase I genes in phytoplasma-infected grapevine plants grown in the field. *Plant Pathology,* 58: 170-180.

Imlau A, Truernit E, Sauer N (1999). Cell-to-cell and long distance trafficking of the green fluorescent protein in the phloem and symplastic unloading of the protein into sink tissues. *The Plant Cell,* 11: 309–322.

Ivashikina N, Deeken R, Ache P, Kranz E, Pommerrenig B, Sauer N, Hedrich R (2003). Isolation of AtSUC2 promoter-GFP-marked companion cells for patch-clamp studies and expression profiling. *The Plant Journal,* 36: 931–945.

Jarausch W, Jarausch-Wehrheim B, Danet JL, Broquaire JM, Dosba F, Saillard C, Garnier M (2001). Detection and identification of European stone fruit yellows and other phytoplasmas in wild plants in the surroundings of apricot chlorotic leaf roll-affected orchards in southern France. *European Journal of Plant Pathology,* 107: 209-217.

Junqueira A, Bedendo I, Pascholati S (2004). Biochemical changes in corn plants infected by the maize
bushy stunt phytoplasma. *Physiological and Molecular Plant Pathology* 65: 181–185.

Kaminska M, Sliwa H, Malinowski, Skrzypczak Cz (2003). The association of aster yellows phytoplasma with rose dieback disease in Poland. *Journal of Phytopathology,* 151: 469-476.

Knoblauch M, Peters WS, Ehlers K, Van Bel AJE (2001). Reversible calcium regulated stopcocks in legume sieve tubes. *Plant Cell,* 13: 1221–1230.
Kollar A, Seemüller E (1989). Base composition of the DNA of mycoplasmalike organisms associated with various plant diseases. *Journal of Phytopathology,* 127: 177–186.

Koressaar T, Remm M (2007). Enhancements and modifications of primer design program Primer3. *Bioinformatics*, 23: 1289-91.

Kube M, Mitrovic J, Duduk B, Rabus R, Seemüller E (2012). Current view on phytoplasma genomes and encoded metabolism. *The Scientific World Journal,* 2012: 185942.

Kube M, Schneider B, Kuhl H, Dandekar T, Heitmann K, Migdoll AM, Reinhardt R, Seemüller E (2008). The linear chromosome of the plant-pathogenic mycoplasma *'Candidatus* Phytoplasma mali'. *BMC Genomics,* 9: 306.

Kunkel LO (1926). Studies on aster yellows. *American Journal of Botany,* 23: 646-705.

Lalonde S, Boles E, Hellmann H, Barker L, Patrick JW, Frommer WB, Warda JM (1999). The dual function of sugar carriers: transport and sugar sensing. *The Plant Cell,* 11: 707–726.

Landi L, Romanazzi G (2011). Seasonal variation of defense-related gene expression in leaves from Bois noir affected and recovered grapevines. *Journal of Agricultural and Food Chemistry,* 59: 6628-6637.

Lee IM, Martini M, Bottner KD, Dane RA, Black MC, Troxclair N (2003). Ecological implications from a molecular analysis of phytoplasmas involved in an aster yellows epidemic in various crops in Texas. *Phytopathology,* 93: 1368–1377.

Lee IM, Davis RE, Dawn EGR (2000). Phytoplasma: Phytopathogenic *Mollicutes*. *Annual Review of Microbiology,* 54: 221-255.

Lefol C, Caudwell A, Lherminier J, Larrue J (1993). Attachment of the Flavescence doree pathogen (MLO) to leafhopper vectors and other insects. *Annals of Applied Biology,* 123: 611–622.

Lemoine R, La Camera S, Atanassova R, Dédaldéchamp F, Allario T, Pourtau N, Bonnemain JL, Laloi M, Coutos-Thévenot P, Maurousset L, Faucher M, Girousse C, Lemonnier P, Parrilla J, Durand M (2013). Source-to-sink transport of sugar and regulation by environmental factors. *Frontiers in Plant Science,* 24: 272.

Lemoine R (2000). Sucrose transporters in plants: update on function and structure. *Biochimica et Biophysica Acta,* 1465: 246-262.

Lepka P, Stitt M, Moll E, Seemüller E (1999). Effect of phytoplasmal infection on concentration and translocation of carbohydrates and amino acids in periwinkle and tobacco. *Physiological and Molecular Plant Pathology,* 55: 59–68.

Lim PO, Sears BB (1992). Evolutionary relationships of a plant-pathogenic mycoplasmalike organism and *Acholeplasma laidlawii* deduced from two ribosomal protein gene sequences. *Journal of Bacteriology,* 174: 2606-2611.

Lohaus G, Winter H, Riens B, Heldt HW (1995). Further studies of the phloem loading process in leaves of barley and spinach. The comparison of metabolite concentrations in the apoplastic compartment with those in the cytosolic compartment and in the sieve tubes. *Botanica Acta,* 108: 270–275.

Løvdal T, Lillo C (2009). Reference gene selection for quantitative real-time PCR normalization in tomato subjected to nitrogen, cold, and light stress. *Analytical Biochemistry,* 387: 238-242.

MacKenzie DJ, McLean MA, Mukerji S, Green M (1997). Improved RNA extraction from woody plants for the detection of viral pathogens by reverse transcription-polymerase chain reaction. *Plant Disease,* 81: 222-226.

Maixner M, Ahrens U, Seemüller E (1995). Detection of the German grapevine yellows (Vergilbungskrankheit) MLO in grapevine, alternative hosts and a vector by a specific PCR procedure. *European Journal of Plant Pathology,* 101: 241-250.

Maixner M (1994). Transmission of German grapevine yellows (Vergilbungskrankheit) by the planthopper *Hyalesthes obsoletus* (Auchenorrhyncha: Cixiidae). *Vitis,* 33: 103–104.

Margaria P, Turina M, Palmano S (2009). Detection of Flavescence dorée and Bois noir phytoplasmas, *Grapevine leafroll associated virus-1* and *-3* and *Grapevine virus A* from the same crude extract by reverse transcription-RealTime Taqman assays. *Plant pathology,* 58: 838-845.

Martelli GP (1993). Graft transmissible diseases of grapevines – Handbook for detection and diagnosis. FAO: 103-106.

Martini M, Ermacora P, Falginella L, Loi N, Carraro L (2008). Molecular differentiation of 'C*andidatus* phytoplasma mali' and its spreading in Friuli Venezia Giulia region (north-east Italy). *Acta Horticulturae*, 781: 395-402.

Martini M, Lee IM, Bottner KD, Zhao Y, Botti S, Bertaccini A, Harrison NA, Carraro L, Marcone C, Khan AJ, Osler R (2007). Ribosomal protein gene based phylogeny for finer differentiation and classification of phytoplasmas. *International Journal of Systematic Bacteriology,* 57: 2037-2051.

Matteoni JA, Sinclair WA (1983). Stomatal closure in plants infected with mycoplasma-like organisms. *Phytopathology,* 73: 398–402.

Maust BE, Espadas F, Talavera C, Aguilar M, Santamaría JM, Oropeza C (2003). Changes in carbohydrate metabolism in coconut palms infected with the lethal yellowing phytoplasma. P*hytopathology,* 93: 976–981.

McCoy RE, Caudwell A, Chang CJ, Chen TA, Chiykowski LN, Cousin MT, Dale JL, de Leeuw GTN, Golino DA, Hackett KJ, Kirkpatrick BC, Marwitz R, Petzold H, Sinha RH, Sugiura M, Whitcomb RF, Yang IL, Zhu BM, Seemüller E (1989). Plant diseases associated with mycoplasmalike organisms. In: The Mycoplasmas (Whitcomb RF and Tully JG, eds.). *Academic Press*, New York, pp. 545-560.

Muller PY, Janovjak H, Miserez AR, Dobbie Z (2002). Processing of gene expression data generated by quantitative real time RT-PCR. *Biotechniques*, 32: 1372–1379.

Mullis K, Faloona F, Scharf S, Saiki R, Horn G, Erlich H (1986). Specific enzymatic amplification of DNA *in vitro*: the polymerase chain reaction. *Cold Spring Harbor Symposia on Quantitative Biology*, 51: 263-273.

Münch E (1930). Die Stoffbewegungen in der Pflanze. *Ed. Gustav Fischer*.

Murray C, Christeller JT (1995). Purification of a trypsin inhibitor (PFT1) from pumpkin fruit phloem exudate and isolation of putative trypsin and chymotrypsin inhibitor cDNA clones. *Biological Chemistry,* 276: 281–287.

Musetti R, Buxa SV, De Marco F, Loschi A, Polizzotto R, Kogel KH, van Bel AJE (2013a). Phytoplasma-triggered Ca^{2+} influx is involved in sieve-tube blockage. *Molecular Plant-Microbe Interactions,* 26: 379-386.

Musetti R, Farhan K, De Marco F, Polizzotto R, Paolacci A, Ciaffi M, Ermacora P, Grisan S, Santi S, Osler R (2013b). Differentially-regulated defense genes in *Malus domestica* during phytoplasma infection and recovery. *European Journal of Plant Pathology,* 136: 13-19.

Musetti R, Paolacci A, Ciaffi M, Tanzarella OA, Polizzotto R, Tubaro F, Mizzau M, Ermacora P, Badiani M, Osler R (2010). Phloem cytochemical modification and gene expression following the recovery of apple plants from apple proliferation disease. *Phytopathology,* 100: 390–399.

Musetti R, Tubaro F, Polizzotto R, Ermacora P, Osler R (2008). Il “Recovery” da Apple Proliferation in melo è associato all' aumento della concentrazione dello ione calcio nel floema. *Petria,* 18: 380-383.

Musetti R, Marabottini R, Badiani M, Martini M, Sanità di Toppi L, Borselli S, Borgo M, Osler R (2007). On the role of H_2O_2 in the recovery of grapevine (*Vitis vinifera* cv. Prosecco) from Flavescence dorée disease. *Functional Plant Biology,* 34: 750–758.

Musetti R (2006). Patogeni e piante di interesse agronomico: un approccio morfologico. In: 1956–2006: 50 anni di Microscopia in Italia tra storia, progresso ed evoluzione (Quaglino D, Falcieri E, Catalano M, Diaspro A, Montone A, Mengucci P and Pellicciari C, eds.). *PI.ME Editrice*, Pavia, pp. 325–334.

Musetti R, Sanità di Toppi L, Martini M, Ferrini F, Loschi A, Favali MA, Osler R (2005). Hydrogenperoxide localization and antioxidant status in the recovery of apricot plants from European Stone Fruit Yellows. *European Journal of Plant Pathology,* 112: 53–61.

Musetti R, Sanità di Toppi L, Ermacora P, Favali MA (2004). Recovery in apple trees infected with the apple proliferation phytoplasma: An ultrastructural and biochemical study. *Phytopathology,* 94: 203– 208.

Musetti R, Favali MA (2003). Cytochemical localization of calcium and X-ray microanalysis of *Catharanthus roseus* L. infected with phytoplasmas. *Micron,* 34: 387–393.

Nault LR (1990). Evolution of an insect pest: maize and the corn leafhopper, a case study. *Maydic*a, 35: 165-175.

Newbury HJ, Possingham JV (1977). Factors affecting the extraction of intact ribonucleic acid from plant tissues containing interfering phenolic compounds. *Plant Physiology,* 60: 543-547.

Nishigawa H, Oshima K, Kakizawa S, Jung HY, Kuboyama T, Miyata S, Ugaki M, Namba S (2002). A plasmid from a non-insect-transmissible line of a phytoplasma lacks two open reading frames that exist in the plasmid from the wild-type line. *Gene,* 298: 195–201.

Oshima K, Kakizawa S, Nishigawa H, Jung HY, Wei W, Suzuki S, Arashida R, Nakata D, Miyata S, Ugaki M, Namba S (2004). Reductive evolution suggested from the complete genome sequence of a plant-pathogenic phytoplasma. *Nature Genetics,* 36: 27–29.

Osler R, Loi N, Carraro L, Ermacora P, Refatti E (2000). Recovery in plants affected by phytoplasmas. In: Proceedings of the 5th congress of European Foundation of Plant Pathology. *Società Italiana di Patologia Vegetale*, pp. 589-592.

Osler R, Carraro L, Loi N, Refatti E (1993). Symptom expression and disease occurrence of a yellows disease of grapevine in north-eastern Italy. *Plant Disease,* 77: 496–498.

Osman F, Leutenegger C, Golino D, Rowhani A (2007). Real-time RT-PCR (TaqMan) assays for the detection of Grapevine leafroll associated virus 1–5 and 9. *The Journal of Virological Methods.* 141: 22–29.

Pacifico D, Alma A, Bagnoli B, Foissac X, Pasquini G, Tessitori M, Marzachì C (2009). Characterization of Bois noir isolates by restriction fragment length polymorphism of a Stolbur-specific putative membrane protein gene. *Phytopathology,* 99: 711-715.

Panjan M (1950). Investigations on stolbur of *Solanaceae* and its control. In: Plant Protection. *Beograd*, pp. 49-58.

Patrick JW (1990). Sieve element unloading: cellular pathway, mechanism and control. *Plant Physiology,* 78: 298-308.

Patui S, Bertolini A, Clincon L, Ermacora P, Braidot E, Vianello A, Zancani M (2013). Involvement of plasma membrane peroxidases and oxylipin pathway in the recovery from phytoplasma disease in apple (*Malus domestica*). *Physiologia Plantarum,* 148: 200-213.

Pélissier HC, Peters WS, Collier R, van Bel AJE, Knoblauch M (2008). GFP tagging of Sieve Element Occlusion (SEO) proteins results in green fluorescent forisomes. *Plant Cell Physiology*, 49: 1699-1710.

Peters WS, van Bel AJE, Knoublach M (2006). The geometry of the forisome-sieve element-sieve plate complex in the phloem of *Vicia fava* L. leaflets. *Journal of Experimental Botany*, 57: 3091-3098.

Pfaffl MW (2001). A new mathematical model for relative quantification in real-time RT-PCR. *Nucleic Acid Research,* 29: e45.

Pracros P, Renaudin J, Eveillard S, Mouras A, Hernould M (2006). Tomato flower abnormalities induced by stolbur phytoplasma infection are associated with changes of expression of floral development genes. *Molecular Plant Microbe Interactions,* 19: 62-68.

Purcell AH, Nault LR (1991). Interactions among plant pathogenic prokaryotes, plants and insect vectors. In: Microbial mediation of plant-herbivore interactions (Barbosa P, Krischik VA, Jones CG, eds.). *Wiley*, New York, pp. 383-407.

Radonić A, Thulke S, Mackay IM, Landt O, Siegert W, Nitsche A (2004). Guideline to reference gene selection for quantitative real-time PCR. *Biochemical and Biophysical Research Communications,* 313: 856-862.

Rasmussen SK (1993). A gene coding for a new plant serpin. *Biochimica et Biophysica Acta,* 1172: 151-154.

Razin S (1999). Adherence of pathogenic mycoplasmas to host cells. *Bioscience Reports,* 19: 367-372.

Razin S, Yogev D, Naot Y (1998). Molecular biology and pathogenicity of mycoplasmas. *Microbiology and Molecular Biology Reviews,* 62: 1094–1156.

Read SM, Northcote H (1983). Subunit Structure and Interactions of the Phloem Proteins of *Cucurbita maxima* (Pumpkin). *European Journal of Biochemistry,* 134: 561-569.

Rennie EA, Turgeon R (2009). A comprehensive picture of phloem loading strategies. *Proceedings of the National Academy of Sciences of the United States of America,* 106: 14162–14167.

Roitsch T (1999). Source-sink regulation by sugar and stress. *Current Opinion in Plant Biology,* 2: 198–206.

Romanazzi G, D'Ascenzo D, Murolo S (2009b). Field treatment with resistance inducers for the control of grapevine Bois noir. *Journal of Plant Pathology,* 91: 725–730.

Ruiz-Medrano R, Xoconostle-Cazares B, Lucas WJ (2001). The phloem as a conduit for inter-organ communication. *Current Opinion in Plant Biology,* 4: 202–209.

Rüping B, Ernst AM, Jekat SB, Nordzieke S, Reineke AR, Müller B, Bomberg-Bauer, Prüfer, Noll GA (2010). Molecular and phylogenetic characterization of the sieve element occlusion gene family in *Fabaceae* and non-*Fabaceae* plants. *BMC Plant Biology*, 10:219.

Saccardo F, Martini M, Palmano S, Ermacora P, Scortichini M, Loi N, Firrao G (2012). Genome drafts of four phytoplasma strains of the ribosomal group 16SrIII. *Microbiology*, 158: 2805-2814.

Santi S, Grisan S , Pierasco A, De Marco F, Musetti R (2013). Laser microdissection of grapevine leaf phloem infected by stolbur reveals site-specific gene responses associated to sucrose transport and metabolism. *Plant, Cell and Environment*, 36: 343-355.

Schaper U, Seemüller E (1984). Recolonization of the stem of apple proliferation and pear decline-diseased trees by the causal organisms in spring. *Journal of Plant Disease and Protection,* 91: 608-613.

Schulz A (1998). Phloem. Structure related to function. *Progress in Botany,* 59: 429–475.

Sears BB, Lim PO, Holland N, Kirkpatrick BC, Klomparens KL (1989). Isolation and characterization of DNA from a mycoplasmalike organism. *Molecular Plant-Microbe Interactions,* 2: 175–180.

Seemüller E, Sule S, Kube M, Jelkmann W, Schneider B (2013). The AAA+ ATPases and HflB/FtsH proteases of '*Candidatus* Phytoplasma mali': phylogenetic diversity, membrane topology, and relationship to strain virulence. *Molecular Plant-Microbe Interactions,* 26: 367-376.

Seemüller E. (2002). Mycoplasmas of plant and insects. In: Molecular biology and pathogenicity of mycoplasmas (Razin S and Herrmann R, eds.). *Kluwer Academic,* London, pp. 91–116.

Seemüller E, Marcone C, Lauer U, Ragozzino A, Göschl M (1998). Current status of molecular classification of the phytoplasmas. *Journal of Plant Pathology,* 80: 3-26.

Seemüller E, Kunze L, Schaper U (1984). Colonization behavior of MLO, and symptom expression of proliferation-diseased apple trees and decline-diseased pear trees over a period of several years. Journal of *Plant Disease and Protection,* 91: 525-532.

Sforza R, Clair D, Daire X, Larrue J, Boudon-Padieu E (1998). The role of *Hyalesthes obsoletus* (Hemiptera: Cixiidae) in the occurrence of bois noir of grapevines in France. *Journal of Phytopathology,* 146: 549–556.

Siddique ABM, Guthrie JN, Walsh KB, White DT, Scott PT (1998). Histopathology and within-plant distribution of the phytoplasma associated with Australian papaya dieback. *Plant Disease,* 82: 1112-1120.

Slewinski TL, Garg A, Johal GS, Braun DM (2010). Maize *SUT1* functions in phloem loading. *Plant Signaling and Behavior,* 5: 687-690.

Strauss E (2009). Phytoplasma research begins to bloom. *Science,* 325: 388-390.

Sugio A, MacLean AM, Kingdom HN, Grieve VM, Manimekalai R, Hogenhout SA (2011). Diverse targets of phytoplasma effectors: from plant development to defense against insects. *Annual Review of Phytopathology*, 49: 175-195.

Suhov KS, Vovk AM (1949). Stolbur of solanaceous plants. *U.S.S.R. Academy of Sciences Publishers*, Moscow.

Taiz L, Zeiger E (2002). Plant physiology. *Sinauer Associates,* Sunderland.

Tan PY, Whitlow T (2001). Physiological responses of *Catharanthus roseus* (periwinkle) to ash yellows phytoplasmal infection. *New Physiologist,* 150: 757–769.

Terlizzi F, Credi R (2007). Uneven distribution of stolbur phytoplasma in Italian grapevines as revealed by nested-PCR. *Bulletin of Insectology,* 60: 365-366.

Toth KF, Harrison N, Sears BB (1994). Phylogenetic relationships among members of the class *Mollicutes* deduced from *rps3* gene sequences. *International Journal of Systematic Bacteriolog*y, 44: 119–124.

Tran-Nguyen LT, Kube M, Schneider B, Reinhardt R, Gibb KS (2008). Comparative genome analysis of '*Candidatus* Phytoplasma australiense' (subgroup tuf-Australia I; rp-A) and '*Ca*. Phytoplasma asteris' Strains OY-M and AY-WB. *Journal of Bacteriology,* 190: 3979–3991.

Tran-Nguyen LT, Gibb KS (2006). Extrachromosomal DNA isolated from tomato big bud and *Candidatus* Phytoplasma australiense phytoplasma strains. *Plasmid,* 56: 153–166.

Turgeon R, Medville R (2004). Phloem Loading. A reevaluation of the relationship between plasmodesmatal frequencies and loading strategies. *Plant Physiology,* 136: 3795-3803.

Turgeon R (1996). Phloem loading and plasmodesmata. *Trends in Plant Science,* 1: 418-423.

Untergrasser A, Cutcutache I, Koressaar T, Ye J, Faircloth BC, Remm M, Rozen SG (2012). Primer3-new capabilities and interfaces. *Nucleic Acids Research,* 40: 115.

van Bel AJE, Hess PH (2008). Hexoses as phloem transport sugars: the end of a dogma? *Journal of Experimental Botany,* 59: 261–272.

van der Schoot C, van Bel AJE. (1989). Glass microelectrode measurements of sieve tube membrane potentials in internode discs and petiole strips of tomato (*Solanum lycopersicon* L.). *Protoplasma* 149: 144–154.

Vandesompele J, De Preter K, Pattyn F, Poppe B, Van Roy N, De Paepe A, Speleman F (2002). Accurate normalization of real-time quantitative RT-PCR data by geometric averaging of multiple internal control genes. *Genome Biology,* 3: research0034.

Verma DPS, Hong Z (2001). Plant callose synthase complexes. *Plant Molecular Biology,* 47: 693-701.

Walker NA, Patrick JW, Zhang W, Fieuw S (1995). Mechanism of photosynthate efflux from seed coats of *Phaseolus vulgaris*: a chemiosmotic analysis. *Journal of Experimental Botany,* 46: 539–549.

Webb DR, Bonfiglioli RG, Carraro L, Osler R, Symons RH (1999). Oligonucleotides as hybridization probes to localize phytoplasmas in host plants and insect vectors. *Phytopathology,* 89: 894-901.

Wei W, Davis RE, Nuss DL, Zhao Y (2013). Phytoplasmal infection derails genetically preprogrammed meristem fate and alters plant architecture. *Proceedings of the National Academy of Sciences of the United States of America,* 110: 19149-19154.

Wei W, Kakizawa S, Suzuki S, Jung HY, Nishigawa H, Miyata S, Oshima K, Ugaki M, Hibi T, Namba S (2004). *In planta* dynamic analysis of onion yellows phytoplasma using localized inoculation by insect transmission. *Phytopathology,* 94: 244-250.

Weintraub PG, Jones P (2010). Phytoplasmas. Genomes, plant hosts and vectors. *CABI*, Wallingford.

Weintraub PG, Beanland LA (2006). Insect vectors of phytoplasmas. *Annual Review of Entomology,* 51: 91–111.

Wilcox JN (1993). Fundamental principles of *in situ* hybridization. *The Journal of Histochemistry and Cytochemistry,* 41: 1725-1733.

Xie B, Wang X, Zhu M, Zhang Z, Hong Z (2011). *CalS7* encodes a callose synthase responsible for callose deposition in the phloem. *The Plant Journal,* 65: 1-14.

Ziegler H (1975). Nature of transported substances. In: Encyclopedia of Plant Physiology (Zimmermann MH and Milbutn JA, eds.). *Springer*, Berlin, pp. 59–100.

Zimmermann MH, Ziegler H (1975). List of sugars and sugar alcohols in sieve-tube exudates. In: Encyclopedia of Plant Physiology (Zimmermann MH and Milbutn JA, eds.). *Springer*, Berlin, pp. 480–503.

APPENDIX

Genes' sequences

Grapevine genes

Alignment of callose synthase genes (*VvCAS1*: XM_002271612.2; *VvCAS2*: XM_002283262.2; *VvCAS5*: XM_002274301.1; *VvCAS7*: XM_002279310.2; *VvCAS8l*: XM_002267920.2; *VvCAS10*: XM_002275082.2; *VvCAS11*: XM_002263721.2). Only the final regions of the transcript sequences have been reported. Primers used in Real Time PCRs are highlighted. Alignment was performed using the multiple sequence alignment program Clustal Omega (http://www.ebi.ac.uk/Tools/msa/clustalo/).

```
VvCAS11   ATACTCATGGCAATCACAAGT------TGGTTCCTTTGGTGGAATATTGGCAAAAGCTGA
VvCAS10   GAAGTCATTTTGTTAAGGCGCTTGAAGTGGCTCTGCTCCTAATAGTATACATCGCA---T
VvCAS7    GAAGTCACTTTGTGAAGGGGTTGGAGCTGCTTATGTTGTTGCTTGTATATCAAATC---T
VvCAS8l   GAAGCCACTTTGTGAAAGGATTTGAACTACTACTCCTGTTGATTGTTTATGATTTG---T
VvCAS5    GAAGCCATTTCGTGAAAGGAATGGAGCTGATGATATTGCTTATAGCATATGAGGTT---T
VvCAS2    GTAGTCATTTTGTTAAGGGAATTGAGCTGATGATTCTGCTTCTTGTTTACCAAATT---T
VvCAS1    GCAGTCATTTTGTTAAGGGAATGGAATTGATGATCCTGCTCCTTGTATATCATATC---T
          . *  **    .: .* . .       *.   .   *  *  ::  :*.  :       :

VvCAS11   ACAGAGCTGGGAAACGTGGTGGTATGAGGAACATGATCATCTGAGAACAACTGGCCTTTG
VvCAS10   ATGGGCACACAGGAGGAGGCTCTGTGTCTTTTA-----TTCTGTTAACTCTTAGCAGTTG
VvCAS7    ATGGAGAATCATATCGTAGTTCAAATATCTATT-----TGTTCGTTACTTTCTCCATGTG
VvCAS8l   TTAGGCGGTCATACCAAAGCAGTATGGCTTATG-----TTCTAATCACTTATTCCATCTG
VvCAS5    ATGGGTCAGCAGCTAGTGATCCTGCTACTTATA-----TTCTCTTCACGTGCTCAATGTG
VvCAS2    TTGGACATACTTATAGAAGTGCAGTTGCTTATG-----TCTTGATCACTATATCAATGTG
VvCAS1    TTGGTAGCTCATACAAAGGCACAGTTGCATATA-----TTTTGATCACTATATCGATGTG
          : .*           .:..   :.     ::       :  *    **       .  **

VvCAS11   GGGAAAGTTGTTGGAGATGATCTTAGATATTCGATTCTTCTTTTTCCAGTACGGCGTTGT
VvCAS10   GTTCCTTGTCA-------TATCATGGCTCTTTGCTCCTTATATTTTTAATCCCTCAGGTT
VvCAS7    GTTCCTGGTTG-------CTTCCTGGTTATTTGCTCCTTCTGTTTTCAATCCATCTGGAT
VvCAS8l   GTTCATGTCCA-------TCACGTGGCTGTTTGCACCATTTCTGTTTAATCCTTCTGGAT
VvCAS5    GTTCCTTGTGG-------CTTCTTGGTTGTTTGCTCCTTTTCTTTTTAACCCTTCAGGAT
VvCAS2    GTTCATGGTGG-------GAACCTGGCTTTTTGCTCCCTTCCTCTTCAATCCTTCTGGGT
VvCAS1    GCTCATGGTGG-------GTACATGGCTTTTTGCTCCATTCCTCTTCAATCCATCAGGGT
          *  ..:              :* *.* * ** *.: * *   * *  *. .*  *    *

VvCAS11   TT-ACAGGCTCAAGATTACT-----------------------------ACATATGC---
VvCAS10   TTGAGTGGCAAAAGACTGTGGAGGACTTCGATGATTGGACCAGTTGGCTCCTATATAAAG
VvCAS7    TTGAGTGGCAGAAAACAGTGGATGATTGGACAGATTGGAAGAGGTGGATGGGAAATCGTG
VvCAS8l   TCAACTGGGGCAATATAGTAGATGACTGGAAAGATTGGAACAAGTGGATAAAGCAGCAAG
```

```
VvCAS5    TTGAATGGCAGAAGATAGTGGATGATTGGGATGATTGGTCAAAGTGGATGAACAGCCGAG
VvCAS2    TTGAGTGGCAGAAGATTGTTGATGATTGGACTGATTGGAATAAGTGGGTAAGCAACCGAG
VvCAS1    TTGAGTGGCAGAAGATTGTTGATGACTGGACGGATTGGAATAAGTGGATAAGCAACCGCG
          *  * :**   ** * :.                                        .

VvCAS11   CCGGGATAAATATTCTGCAACACAGCACAT-------------------CTATTATCGGC
VvCAS10   GTGGAGTTGGGGTGAAGGGAGACCATAGCTGGGAATCTTGGTGGGAGGAAGAACAGGCGC
VvCAS7    GTGGTATTGGTATCCAACAAGATAAAAGCTGGGAGTCCTGGTGGGATATAGAACAAGAAC
VvCAS8l   GCGGTATAGGAATTCAGCAGGACAAAAGCTGGGAATCATGGTGGAACGACGAGCAAGCCC
VvCAS5    GGGGTATTGGTGTTCCGGCAAACAAGAGCTGGGAGTCCTGGTGGGAGGAGGAGCAGGAGC
VvCAS2    GGGGAATTGGTGTAACTGCAGAAAAAAGTTGGGAATCATGGTGGGAGGAGGAGCAAGAAC
VvCAS1    GAGGTATTGGTGTATCTGCAGAGAAGAGTTGGGAATCCTGGTGGGAAAAAGAACAGGAGC
            ** .*:.. .*      . * .. *  *                        *  *    *

VvCAS11   TGGTTCAGCTTCTTGTCATTGTGGTTATAGTACTTGTGATAGTTTTATTCCTGAAATTCA
VvCAS10   ATATCCAAACGCTAAGAG------GCCGTATATTGGAAACAATTTTAAGCTTAAGGTTTA
VvCAS7    ACCTGAAAAGCACAAATATCAGGGGGAGAGTGCTGGAGATAATTCTTGCTTTTCGCTTCT
VvCAS8l   ATCTCCGTCATTCAGGATTGATCGCTAGATTGATTGAGATACTTCTTTCTCTTCGGTTTT
VvCAS5    ATCTTCAGTACACTGGATTTCTAGGACGGTTCTGGGAGACTGTTCTTTCTCTGCGCTTCT
VvCAS2    ATCTTCGTCATTCTGGAAAGCGTGGTATCATTGCTGAGATATTGTTATCGTTAAGATTCT
VvCAS1    ATCTCCATCATTCTGGGAAACGTGGCATCATAGCCGAAATATTGTTGGCCTTGCGCTTTT
          :  * ..      :.           .   *    *:.* : *  *     * .. ** :

VvCAS11   CCAATTTGATATTTCTTGATCT-TATCACAAGCCTGTTGGCATTCATCCCCACAGGATGG
VvCAS10   TTATATTTCAATATGGCATTGTATACAAACTCCATCTCACACAAAAAGATACCTCACTTG
VvCAS7    TCATTTATCAATATGGAATTGTTTACCAGCTCGATATAGCACATCGCAGCAAGAGTTTGC
VvCAS8l   TTATTTATCAGTATGGTCTGGTCTATCACCTTGACATCTCACAAGACAACAAAAATTTTC
VvCAS5    TTATCTATCAGTATGGAATTGTTTATCATCTACATGTGGCCAATGGTGATAAAAGCATTG
VvCAS2    TCATCTATCAATATGGGCTTGTTTATCACCTGAACCTCACAAAGAATACCAAAAGTTTTC
VvCAS1    TCATCTACCAGTATGGGCTTGTATATCACTTGAGCATTACCA---AGAGCAAAAGTTTTC
            *: *: .:.*:*    :  * ** .*  :     *   ..   .    .. :   *

VvCAS11   GGCCTTATA----------------------TCTATTGCCGTGTCCATGCAGACAAGAA
VvCAS10   CGATTTATGGGTTCTCCTGGGTTGTGCTGGTTGGCATTGTCATGATATTCAAGTTATTCA
VvCAS7    TGGTATATGGACTGTCATGGATAGTTATGGCAACTGCTCTTCTGGTATTAAAGATGGTAT
VvCAS8l   TGGTCTATGTGCTTTCATGGGTCGTGATTTTTGCAATTTTCCTCTTAGTCCAGGCAGTGA
VvCAS5    TTGTTTATGGTCTTTCATGGCTGGTCATTGCTGCTGTGATTATCATCTTGAAGATTGTGT
VvCAS2    TGGTCTATGGCATATCATGGCTGGTGATCTGTATAATATTGTTTGTGATGAAGACTGTTT
VvCAS1    TGGTTTATGGTATCTCATGGGTGGTGATCTTTGGAATTTTGTTTGTGATGAAGGCTCTCT
               ***.                            .     *     * .**     :

VvCAS11   TCCTATTCAATGAAGCATTCAGCAGGGGGCTCCAG---ATTTCTCGAATTCTAACCGGCA
VvCAS10   GCTTTAGCCCAAAAAAATCCA---GCAACATCCAGCTAGTGATGCGATTTTCACAGGGAG
VvCAS7    CAATGGGTAGACGAAGATTTGGTACCGACTTTCAGCTAATGTTCAGGATCCTCAAAGGAC
VvCAS8l   AATTGGGAAGACAACAGTTCAGTGCTAATTATCACCTCATATTCAGACTATTTAAAGCAT
VvCAS5    CTATGGGTAGGAAGAAGTTCAGTGCAGATTTCCAACTGATGTTCAGGCTTCTGAAGCTGA
VvCAS2    CTGTGGGACGGCGAAAATTCAGTGCCAATTTCCAACTCATGTTCCGGCTAATTAAAGGAT
VvCAS1    CTGTTGGAAGGCGAAGATTCAGTGCAGATTTTCAGCTTGTGTTTCGACTGATAAAGGGTC
             *    .   ..  .*  .     ..  : **    .* :  .*. *    ..

VvCAS11   AGAAAAATATTGACATGTGA----------------------------------------
VvCAS10   -TTTTTTCCTTAGGACTTGTTGCAGCTCTTTGCCTTGTTGTTGCCTTCACCGATCTGTCA
VvCAS7    -TTTTATTCCTTGGCTTCATATCAGTCATGACTGTGTTATTTGTAGTATGTGGCCTTACA
VvCAS8l   -GCCTTTTCTTGGGTGTTCTTGCTACTATAATTTCTCTCTCTGGCATCTGCCAACTATCT
VvCAS5    -TCCTGTTCATTGGGTTCATAGGCACCCTGGTGATACTATTTGTATTCCTGAGTCTCACA
VvCAS2    -TGATCTTCCTGACATTTGTCTCCATTCTGGTCACTCTGATTGCGCTCCCCCATATGACC
```

```
VvCAS1    -TTATCTTCCTCACCTTTTTTGCCGTTTTGATCATTCTAATAGTAGTTCCCCATATGACA
              : : . * .      :

VvCAS11   ------------------------------------------------------------
VvCAS10   ATTGTAGACCTGTTTGCTAGCATCCTTGCATTTATTCCTACTGGATGGATGATTCTATCT
VvCAS7    GTATCTGATTTATTTGCTGCAGTCCTTGCCTTCCTGCCCACAGGGTGGGCCATTCTTCTT
VvCAS81   TTGATGGACTTACTTGTCTGCTGTCTAGCATTTTTGCCCACTGGGTGGGGTTTGATACTG
VvCAS5    GTAGGAGACATCTTTGCCAGCCTACTGGCCTTCATACCAACTGGATGGGCACTTCTTGGG
VvCAS2    TTACAGGACATCATAGTCTGCATTCTTGCGTTCATGCCGACTGGTTGGGGATTACTTCTG
VvCAS1    TTTGGCGACATCTTGGTGTGCTTTCTTGCAATTTTGCCAACTGGATGGGGATTGCTGCTG

VvCAS11   ------------------------------------------------------------
VvCAS10   TTAGCGATCACATGGAAAAGGGTGGTAAGGAGCCTAGGCTTATGGGATTCAGTCCGGGAG
VvCAS7    ATTGCACAAGCATGCAGGCCTATGATTAAGGGTGTAGGATTCTGGGAATCAATAAAGGAG
VvCAS81   ATTGCACAAGCTGTGAGGCCCAAGATACAGGATACTGGATTGTGGGAGTTGACGAGGGTG
VvCAS5    ATATCACAAGCATTGAGGCCAGCAGTGAAGGCCTTAGGAATGTGGGGGTCTGTAAAAGCT
VvCAS2    ATTGCACAAGCCTGCAAGCCTGTTGTTGAGCGAGCTGGGTTCTGGGCATCGGTTCGAACA
VvCAS1    ATCGCACAGGCCTGCAAGCCTTTGGTTGTGAGAGCTGGAATTTGGAAATCAGTCAGGACA

VvCAS11   ------------------------------------------------------------
VvCAS10   TTTGCTAGAATGTATGATGCTGGGATGGGTATGATCATTTTTGCCCCAATAGCAGTGCTA
VvCAS7    CTGGGAAGGGCTTATGAGTACGTAATGGGACTAATAATCTTCTTGCCGATAGTCATATTA
VvCAS81   CTTGCTCAAGCTTATGACTATGGAATGGGTGCAGTTCTTTTTGCACCCATAGCTTGTCTT
VvCAS5    CTAGGACGAGGATACGAATACATGATGGGGCTGTCGATCTTTGCACCAGTGGCTATCCTG
VvCAS2    CTTGCTCGTGGGTATGAGATCATCATGGGCTTGCTTCTATTCACCCCAGTTGCATTTCTG
VvCAS1    CTTGCTCGTAGTTATGAACTATTCATGGGCTTGATTCTATTCATCCCAGTTGCCTTCCTG

VvCAS11   ------------------------------------------------------------
VvCAS10   TCATGGTTCCCATTTATTTCCACCTTCCAGTCTCGTCTTCTCTTTAACCAAGCATTCAGC
VvCAS7    TCATGGTTTCCATTTGTGTCAGAGTTCCAAACCCGCTTGCTCTTCAATCAGGCATTCAGT
VvCAS81   GCCTGGATGCCAATTATAGCAGCCTTCCAAACTCGTTTTCTTTTCAACGAGGCTTTCAAA
VvCAS5    GCATGGTTCCCATTTGTCTCAGAGTTCCAAACCAGGTTGTTATTCAACCAAGCCTTCAGC
VvCAS2    GCATGGTTTCCCTTTGTTTCAGAGTTCCAAACCCGAATGCTATTCAACCAAGCGTTCAGC
VvCAS1    GCTTGGTTCCCATTTGTTTCAGAATTCCAAACAAGAATGCTCTTCAACCAAGCATTCAGC

VvCAS11   ------------------------------------------------------------
VvCAS10   CGTGGACTGGAGATCTCCATCATCCTTGCAGGAAACAAAGCTAATGTCCAGGCCTGATAG
VvCAS7    AGAGGCCTCCAGATTTCCATGATTCTTGCAGGGAGGAAAGACAGGGATTCATCTAATTGA
VvCAS81   AGGCGATTGCAGATTCAACCAATTCTTGCGGGAAAAAAGAAGCAAAGTTAATTTCCTCAG
VvCAS5    AGAGGACTTCAGATCCAACGTATCCTTGCTGGTGGGAAGAAGAACAAATGAAACTAGCAG
VvCAS2    AGAGGCCTGCAGATCTCTCGTATTCTTGGTGGTCATAGGAAGGATCGGTCTTCTCGCAAC
VvCAS1    AGAGGTCTACAGATTTCTCGTATTCTTGGTGGACAGAGAAAGGACAACTCCTCCAACAAC

VvCAS11   ------------------------------------------------------------
VvCAS10   TTTCCTTCCAATTTCCCAGGTTGTGATTGTAAATTTTGAGCTGAAAATTTTATTGTATCA
VvCAS7    GCTTTCCAGCATCTCACATTCATCCTTTT-------------------TTTCTTTTG-AA
VvCAS81   AGTCAGCAGCGATGTATGTACGTAGTACATGTACAGTCAAA-----TCATTCTTATC---
VvCAS5    AGTGAGGCTGTGATGATAGAGCCCAGCAAGAAGAGACAAAA-----AGTGACTGATTAAA
VvCAS2    AAAGAGTAAGGTAAATGAGAGTATGACTA--AGTGTTCATT-----TCGGTTTAATGTTC
VvCAS1    AAAGACTAAATCCATCCCCTTCTCG-CGA--ATTCTCCAAA-----TCTTTCC--TGTAC
```

```
VvCAS11   ------------------------------------------------------------
VvCAS10   TATTCCCCCATATTTAGATTGCTA------CATATATACATATATATGGTTGGAGGAAAA
VvCAS7    G-GATACTCGTATTTATTTTGGAAAACAGAGGATTGCCATAGTTAT-----TCTGTAAGA
VvCAS8l   --GGTCCTCATTTTGAAATTGGCA----TACCTTAAAGCTAATTAATGTATATAAACATC
VvCAS5    G-GAGACACAGAGAGACATTGAAG-CCAAATGACAGAGATGGAGAATGCATACTGTGATA
VvCAS2    G-TATGT----ACTATTATTGTGA---GCTTGTTCATATCTATTACTGTAAGCTGTTGTA
VvCAS1    A-ACTCT----TGCTCATTCCTCA---GATCATATAATCCTAAAAATGTAAACTGTCATA


VvCAS11   ------------------------------------------------------------
VvCAS10   ATTTGGCAGA-GATGAACACATTTTTGCATTGATTTCTCTGT-GACGATCAGAGTGTCCA
VvCAS7    --TCCATCAACACTGATCTCTTTCTTCTTTTTCCTTTTCGTCTGTATTTGTTGTTGCTGC
VvCAS8l   CTATTAATAAAAATAAAATTGAAATTC-------AGAAGTCT------CAA---------
VvCAS5    TATGTGCTCAAATAGGTGTTTTCTCTCTACCTCCTGTTTCTT-CTGCTTCTGCTTGGAAC
VvCAS2    ATTATATGG--ATTGAGATATTGGCAGCATTTT-TGTTGATT-AGAATTGACTGGG-AAG
VvCAS1    GCTACCTCC--TTCAGTGTAAAGGTTCAAACTA-TGATCACT------TCATTGTGGAAA


VvCAS11   ------------------------------------------------------------
VvCAS10   ACTTATTAAAAAATACAGGGTGTTGGCTGAAAA-CCAACAGCGAGAGCTGCTTGTGGGGT
VvCAS7    CATTGTT----------GTATA-----------AGCACAGTAGACTTATTCCAAGAGTA
VvCAS8l   ------------------------------------------------------------
VvCAS5    CCTCCTT----------GTACTGTGTGGGGAAAAAAAACAATACCAGTTGCTTGTCTGTA
VvCAS2    TCCTGCC----------AGCTCTTTTCTGTA--------CATCTTATTAATTTAAGATTA
VvCAS1    CCGTGTT----------CTCTTTCTAATGTCAAAATGCAAATGCCCTTCTATTCCCAGTT


VvCAS11   ------------------------------------------------------------
VvCAS10   ACTGCAATATGCATTATTTGAAATATTTTAGCCAACAAGCTTATGATTAGCCCTTGTTAC
VvCAS7    ATTTCTCTAAC-ACAAAATCTA-AACACTAGTACTCCAAGAAA-----------------
VvCAS8l   ------------------------------------------------------------
VvCAS5    AAGTCACTTAGAGCAGCCAATA-AATGCTTCAGTACCATGTTTTCACTGCGC--------
VvCAS2    TAT-CATCTATGGGTTCTTGCA-AA----------------------------------
VvCAS1    TTTGAATTCATATCTGACTCAA-GATCCAC-----------------------------


VvCAS11   ------------------------------------------------
VvCAS10   ATACATAATTATGAGGTGGTTGTAATTATTATTATAATAGATTTACC
VvCAS7    ------------------------------------------------
VvCAS8l   ------------------------------------------------
VvCAS5    ------------------------------------------------
VvCAS2    ------------------------------------------------
VvCAS1    ------------------------------------------------
```

Alignment of sucrose synthase genes (*VvSUS2*: XM_002271860.1; *VvSUS2b*: XM_002271494.2; *VvSUS4*: XM_002275119.1; *VvSUS5*: XM_002266984.2; *VvSUS6*: XM_002270825.1). Only the final regions of the transcript sequences have been reported. Primers used in Real Time PCRs are highlighted. Alignment was performed using the multiple sequence alignment program Clustal Omega (http://www.ebi.ac.uk/Tools/msa/clustalo/).

```
VvSUS5    GAGCAACAAGATTGCTGATTTCTTTGAGAAGTGCAGGGATGATTCAGACCATTGGAACAA
VvSUS6    AAGCGACAAGATTGCTGACTTTTTTGAGAAGTGCAAAACAGATAGCGAGTATTGGAACAA
VvSUS4    AGCTGAGCTCCTTGCCAACTTCTTTGAGAAATGCAAGGCAGACCCAACTCACTGGGAAAA
VvSUS2b   TGCATTGCGTTTAGCTGACTTCTTTGAACGATGCCAGAAGGATCCTAGCTACTGGGACGA
VvSUS2    TGCTACAACCATGGTGGATTTCTTTGAAAAGTGCAAGGAGGATTCAAGTCACTGGAATAA
           .     .   * *  .* ** *****....***..... **    .   * ***.* .*

VvSUS5    GATCTCCAAAGCAGGTCTACAACGCATAAACGAGTGCTACACATGGAAAATCTATGCAAA
VvSUS6    GATCTCAACAGCGGGTCTGCAGCGTATATACGAATGCTACACATGGAAGATCTATGCGAC
VvSUS4    GATCTCCAAGGCAGGCCTGAAGCGTATTGAAGAGAAGTATACATGGAAAATTTACTCTGA
VvSUS2b   GATCTCTAATGGAGGGCTTAAACGAATCTATGAAAGGTACACATGGAAAATATATACTGA
VvSUS2    AATCTCGGATGCAGGTCTTCAAAGAATCTATGAAAGGTATACATGGAAGATTTATTCTGA
          .***** .. * .** ** .*..* **  * **.:. ** ********.** **  * ..

VvSUS5    CAAGGTGTTGAATATGGGGTGCGTTTTTAGCTTCTGGAGGCAGTTGAACACGGAACACAA
VvSUS6    CAAAGTGCTGAACATGGGCTCGACCTATGGCTTCTGGAGGCAGTTGAACAAGGATCAGAA
VvSUS4    GAGACTGTTGACCCTGGCTGGGGTTTATGGGTTCTGGAAGTATGTCTCCAACCTTGACCG
VvSUS2b   GAGACTACTGACACTGGCTGGGGTCTACGGGTTCTGGAAGCATGTGTCAAAGCTTGAGAG
VvSUS2    AAGGCTAATGACGTTGGCTGGGGTTTATGGTTTCTGGAAGTATGTCTCTAAACTTTCGAG
           *.. *. ***.  ***     .  *: .* *******.* *  * :. *.  :: . ..

VvSUS5    GCAAGCAAAGCAAAAATACATTCACATGTTCTACACTCTCCAATTTAGGAACTTGGTGAA
VvSUS6    GAATGCGAAGAACAGATACCTTCAATTGTTCTACAATCTCCAATTCAGAAAATTGGCGAA
VvSUS4    CCGTGAGACCCGCCGCTACCTTGAAATGTTTTATGCCCTCAAGTACCGCAAGCTGGCTCA
VvSUS2b   GCGAGAGACTCGGAGATATCTGGAAATGTTTTACATTCTCAAGCTCAAGGATCTGGCGAC
VvSUS2    GCGTGAGACCCGACGATACCTTGAGATGTTCTACACTCTTAAGTTCCGTGATCTGGCAAA
           ..:*..*. .. ...** .*  * :**** ** .  ** .*. : .. .*  ***  ..

VvSUS5    GAATATACCCATACCGGCTAGTGAAGTTCAGCCACCAGTGTC------------G--AGG
VvSUS6    GGGTGTGCCCATCCTAAATGAAGAACCGCGAGAGGAACCCCAACAACCAGCAGCA--ACA
VvSUS4    ATCAGTTCCTCTGGCTGTGGAAGAGTAGCTAAAAGGCAGAGGCATTGGCTAGAAGCAAGC
VvSUS2b   TTCCATTCCACTAGCTGTTGATGAACACTGAGGTTTAGGCAAAGGAG--CTGTACGTGTC
VvSUS2    ATCTGTTCCCCTGGCGATCGATGACCAACATTAAGCTGTGAGACACGAACCGGGACTGGC
              .* ** .*    .  ..:**                                  .

VvSUS5    GCCATAACCAAAGTACCCCCT---ACACAGAGGCATGTCACCTATCCCACAAATTAA---
VvSUS6    GCAATAACTAAACCACAACAACCAGCACCAACGGAGGGAGCTAAGCCCCGACCATCAGCA
VvSUS4    TGCAGGTTTTCTGAGCTGTGTGGAATAACTGTCATTGTTTGAG-GCTTGGCCGAAAAGAA
VvSUS2b   TGCTTGGCCCCAGTT---TCT-TTTTCCCTTTTGTTCTATCTT-TTGCTTCCTGTTTGTT
VvSUS2    ACCATAATGGTAGAA---TCT-GAATAAA----GTTATAT--T-TGTGTGAATATGTGTA
            .: .     :        :     ...     :               ..  : :

VvSUS5    ------------------------------------------------------------
VvSUS6    CCAACCACG------GCACCAAAGCCTC----AGCCAGCAGCAAGACGTCCACAATCTGG
VvSUS4    GGCATTTCAATTTTTGCTTTTTGTTATCTGTAATGTTTGAACATGGGATGTTAAGGCTCC
VvSUS2b   GTTAGTATGTATTT-GTATGAAGGACATGGTACCCTATGAG--TAAC-A-AGTTCTCTTC
VvSUS2    AAAATTCCTCTTAT-GGATGCCGTGTATGGGATATATTGAAAATTAT-C-ATCACTCTTG


VvSUS5    ------------------------------------------------------------
VvSUS6    TGTCCAAAGGGTCAATGAAGGTTTAGATCAGAAGCAGCCTGGCTTGCCTACAAGAATTCG
VvSUS4    TGGATTTC-AATTAAAATCTGTTACACCTTTATTGG----------GTAACACTGCTTGC
VvSUS2b   TGAGTTAA-------------------ACATTAGCC----------GTGGCCCGCAAGAA
VvSUS2    TAGTTTTTGGATGATGACGTGTATGGGATATTTGGA----------AAATCATGGATGAC
```

```
VvSUS5    ------------------------------------------------------------
VvSUS6    CGCGTTTTGCCCCTGGCT---TTGGTGGTTCTTCATCATCAACATCTCTCTTTTCCTCAT
VvSUS4    CAAGATTTGGCTCTGTTATCTGTCATATTGGTTAAGAATCAAATTCCAATCTTTCCCCTA
VvSUS2b   G------AA----------AATTTCTACCTCA--------------------------
VvSUS2    G------TGGATATATGAAAACTATTAAATGTT---------------GTGGTTTTATGG

VvSUS5    ------------------------------------------------------------
VvSUS6    CTGGTATCTCCTAATGAAGTTATAATCAATAAAGTGTGTGCATCTGCCAACGATTTATGT
VvSUS4    CTCCAGTTGCTTCAAGAGAGC---ATTACCTTATT---GGGTGTCTTCAATCTTTAATGC
VvSUS2b   ------------------------------------------------------------
VvSUS2    CTGACATGTATTGGAT---AT---ATTCGCAGAAT---TTCTGTTTACATTGGTCTGAAT

VvSUS5    ------------------------------------------------------------
VvSUS6    GTAATAAACTAATTGATGAAGATCATCAAAATTCTTCAATCTGTAAAGGCTGCAATAC--
VvSUS4    CACGACAACCTTTTCTTGAAGCCAATGGAGATGCCTTCATATGGTGAGGTACTAAAGGAC
VvSUS2b   ------------------------------------------------------------
VvSUS2    CTCACCA-------------------------------------------------------

VvSUS5    ------------------------------------------------------------
VvSUS6    AGTAATAAGATGCCTTCTTT--------GGGACAC----------AATCTCATCATAG--
VvSUS4    CCTCCAAGTAGACCCTTTTTCAGTTCCTTGGACACTATATGGGAAACTCTGAGCAGCAGA
VvSUS2b   ------------------------------------------------------------
VvSUS2    ------------------------------------------------------------

VvSUS5    ------------------------------------------------------------
VvSUS6    ------------------------------------------------------------
VvSUS4    ACTAGACTAGACTGTTTCAGGAATGGGGTCAGTAAGAACCAAATAAAATTTTCAACCGTT
VvSUS2b   ------------------------------------------------------------
VvSUS2    ------------------------------------------------------------

VvSUS5    --
VvSUS6    --
VvSUS4    CA
VvSUS2b   --
VvSUS2    --
```

Coding sequence of grapevine sucrose transporter analyzed using *in situ* hybridization technique. Primers used are highlighted in yellow.

>VvSUC27 (NCBI accession no. AF021810.1)

```
AATTCGCGGCCGCGTCGACCTTCCTTCTTCTTTCTCACAAACAACACAGAGGAGAAAATCCATTTAGATTTA
GTGGAAGAAGAGGCATACAGTAAAAAAAAATAATTAGCCTATGGAGTTAGCCAAGCCTTCTTCAGTGTTTGC
TATTCAAGACCACCAATCCTCTTCTCCTCCCACTCCCATATGGAAAACGGTGGTTGTGGCCTCCATCGCCGC
CGGGATTCAGTTCGGATGGGCGTTGCAGCTGTCGTTGCTGACCCCCTACGTTCAGCTTCTCGGCATTCCCCA
CAAGTGGGCTGCTTTTATCTGGCTCTGTGGTCCCATCTCCGGCATGATTGTGCAGCCGGTAGTTGGTTACCA
CAGCGACCGCTGCACATCCCGGTTTGGGCGTCGCCGCCCCTTCATCGCCGCCGGGGCTGTTCTCGTTGCCAT
CGCTGTGTTTCTCATCGGCTACGCAGCCGACATCGGAAGGGTTTCCGGCGACCCCCTCCATAATACTATCAA
AACCAGGGCGGTTGCGGTGTTCGTGGTTGGGTTTTGGATTCTGGATGTGGCTAATAATATGCTTCAAGGCCC
TTGCCGAGCCCTCCTAGCGGATCTCTCCGGCACCAGCGCTCGGCGGACTCGAACGGCGAACGCGCTGTATTC
```

GTTTTTCATGGCCGTCGGCAACGTCCTCGGCTACGCTGCCGGCTCCTTCAGCAAACTCCACAAGATGTTCCC
CTTCGCCAGAACCCAAGCCTGCGACCTCTATTGCGCCAATCTCAAAAGCTGCTTTTTCCTTTCTATCGCGCT
TCTTCTAATTCTGACAATCATCGCATTCGCCACCGTGCACGAAACCCCGCTCAACAGAGCCGACATCGCCGT
CGTCGAAGCCGGACAACCGTTCTATTCCCAGATGATGAATGCCTTCAGGCAGCTGAGAAGGCCCATGTGGGT
GCTTCTCCTTGTGACGTGTCTCAACTGGATTGGCTGGTTCCCTTTCCTTCTCTTCGACACCGATTGGATGGG
CAGAGAGGTGTACGGAGGCACCGTCGGAGAAGGCCCCAGAGGAAGGCTGTACGATCTGGGAGTCCGCGCGGG
TTCATTGGGGCTGATGCTGAACTCTGTGGTTCTGGGGTTGATGTCTCTCGGAGTTGAGTTCTTTGGCCGTGG
GGTTGGCGGCGTGAAGCGCCTCTGGGGTGGCGTCAATTTTCTGCTGGCGCTGTGCTTGGCACTGACGGTACT
TGTTAGCAAGTTGGCAGCGTCGTGGCGGCACAGCCTTGGCGGAGAGCTTCACCCACCGCCGATCGGCATCAA
GGCTGGAGCGTTATCTCTGTTCGCTGTTATGGGGGTACCTCTTGCGATCACCTACAGCATTCCATTTGCTCT
GGCTTCCATATTTTGCCACAGTTCTGGTGCAGGCCAAGGACTTTCTCTTGGAGTTCTAAATCTTGCAATTGT
TGTACCGCAGATGATGGTGTCGGTAGCGAGCGGGCCATGGGACGCGCGATTTGGGGGCGGCAACCTTCCCGC
GTTTGTAGTGGGTGCGTTTGCAGCCGCGCTGAACGGAGTGTTGGCGCTGACTATGCTCCCAGCTCCTCCTCC
TGATGTCCCCAACACCAAGGACGAGAGGACTCAGCCGTCGTCTTAATTTTGATTTAGGGTTGTTTAGAGTGA
CGTGTTTCCATTTGGAGCGTCGTCTGTAATGCCAGTCTCTCTTTCAAATGTACACATGCATAGGCTTAAGCT
TGCATGCAAGCTATATATATGGCCGTTTTCAGTTTTATTATTCTGTGCCCAGTTTTTTTAAACAAATTGTAT
TTTATCAGTCAATTAAGTGTCGTTCAAGTATGGCCAGAAAAAGGTCTTCCAAATGGGATGTGGCCTGTAGAG
CCCACGGTCATCTTTTAATATGACTATACCAAAATAAAAAAAATTCTTCCATA

Tomato genes

Alignment of callose synthase genes (*SlCAS2*: XM_004229311.1; *SlCAS3*: XM_004228545.1; *SlCAS7*: XM_004243161.1; *SlCAS8*: XM_004244335.1; *SlCAS9*: XM_004228544.1; *SlCAS10*: XM_004236267.1; *SlCAS11*: XM_004232827.1 ; *SlCAS12*: XM_004243304.1). Only the final regions of the transcript sequences have been reported. Primers used in Real Time PCRs are highlighted. Alignment was performed using the multiple sequence alignment program Clustal Omega (http://www.ebi.ac.uk/Tools/msa/clustalo/).

```
SlCAS10   GTTGTGTGGAGTTTGGGTCTGT-----------------GGGAATCTGTGAAGGAATTTG
SlCAS9    CTAATCAAGAAAATGGGGATGT-----------------GGAAGTCTTTCCGTTCAGTTG
SlCAS12   TTTTTGCAGAAGAGTATGATAT-----------------GGGGAACTGTTGTGTCTGTGG
SlCAS11   TTTTTGCAGTCTACTTTGGTTT-----------------GGGGCACTGTTGTGTCATTGG
SlCAS8    AAGATTGAAGGTACTGGATTGTGGCACTTCACTCG-------AGTGT----------TTG
SlCAS7    TGTTTTAAGGGACT-------------TGGAATTT----GGGATTCAGTGATGGAGTTGG
SlCAS5    GTAGTGAAAGGCATA-------------GGAATGT----GGGGATCTGTGAAGGCTCTAG
SlCAS3    GCATTGAAAC-CTGTTGTTCGGAGAGCTGGATTCT----GGGGATCAGTTCGAACTCTAG
SlCAS2    GTGTTGCAAAGGCCTTGTTTTACTCCCGGGAGCGTAAACCGGAGTGATTGGAAACTCCAA
              *  ..                                . : :           .

SlCAS10   CTAGAAT----GTATGATGCTGGGA------------------------TGGGTATCATT
SlCAS9    CTCGTCT----GTTTGACGCTGGTA------------------------TGGGTGTGCTC
SlCAS12   CGCGACT----ATATGAGATAATGT------------------------TTGGGATTATT
SlCAS11   CTCGGTT----ATATGACATGATGC------------------------TTGGGTTAATT
SlCAS8    CTCGAGC----TTATGACTATGGAATGGGTGTTGTTCTTTTC------------------
SlCAS7    CACGGGC----ATACGAATGCATCATGGGTCTGTTCATATTC------------------
SlCAS5    CTAGAGG----ATACGATTATTTAATGGGGCTTGTGATCTTC-----ACACCGGTTGCT-
SlCAS3    CTCGTGG----CTATGAGATTGTGATGGGATTGCTTCTGTTC-----ACTCCGGTTGCTT
SlCAS2    AACCTTTACAACTTCGATTTTCAGAAACCCCACCGTTTGAACAAACCCCGCCGGTTTTTT
          . .         *: **
```

```
SlCAS9    TATCACATTTAGGAGCCTTTA-GTAGAGTACTTT-ATGTTATTAGTAATTATTGTAAAAT
SlCAS12   ---------AAATATT--GTAGGAGCTTGTATTGTGAATTATACTGTGCACTTGGATTAC
SlCAS11   TCC-----TTAGTCTA--CCAAGTCGACGAGGTTTGCACCAGTTTAACTAAGCGGATGTA
SlCAS8    TACTAGACTATTGTGCATAGACGCTAATGAATAATACGCATTCTTAAAATCTCAAGGTTA
SlCAS7    ACA--TACTTGTAC---------TTCATTCAGATGATTAATATTTAATTCATTAA-TACT
SlCAS5    TAGTTTCAGAATAC------------------T----------ATAGCACAAGGT-GTAT
SlCAS3    TAG--------TGGT-------GATAGCAGCATTTTTGGGCAAATACCATATCAC-TTTT
SlCAS2    TCCTGGAACAGTGAT-------GTTGAGGAAGTGGAGAAGAGGTTAAGCCATGAC-TTGA
                                         :               .  .

SlCAS10   TAGCCCTATAATGCAGTATACATGAAGATGGGGTGACCAAATTTATTTTGGTTGTATTTA
SlCAS9    CTGG--TAATGTACAGTTTTCAGATATGTAAAATCA------TAATTTTGACTCTACATG
SlCAS12   CATTAGTTTGGTTGACGAGT------------TTTCATTCATCTTTTGTAATTGTTGTTG
SlCAS11   GAGCAGTTGGGGCTTCTCTT------------CTTAGTTCTAGTCT-----TAGTATGGA
SlCAS8    TCATCTTTCAGTAGAGTGTTGGTCAAA----ACTGAAAAATAAGTTCGTCCAAGTGTAAC
SlCAS7    CGTGGTTCTTGAAA-------------------------------------------------
SlCAS5    ACTCCTTTGTTGTAATTGCTC-----------GTGTAACC------A--GCTTGGACGCC
SlCAS3    TTTTTTTGGTGAAAATTCCT-------------------------T--AATGGAATCAT
SlCAS2    GCCGTTTTGAGATGATCTATG-----------ACCCAAGAAATGGTG--GCTTGGGTCGA
               *

SlCAS10   GGATCATGGCAATTTTGCTCCTTTTTTTGTATCTGT----CGTTTCTTCAT---------
SlCAS9    ------------------------------------A----TCCCTCATTAT---------
SlCAS12   TATTCATATGTTTTATTGTCATACTAGTGCACAGATGAGGAGCAT-----TATCTTA-TA
SlCAS11   TAGTAGTAGGTTCAGGAGT------CATGGTTAGATGGTACAACAATTCCAATTTTG-TA
SlCAS8    ACCAAATATGTTTTATATTAC----ATCGCGTATATCA--CAATTCTACATCAAGAG---
SlCAS7    -------------------------------------------------------------
SlCAS5    ACTCTATTTCTTTTGGCTCAG----TCAGATCCAACATTGTAGACAAAAAA---------
SlCAS3    TC-TCTTACATTTTTT-----------------------------------------------
SlCAS2    GATACGTATGATTTTGGTTAC----A--GAGTTGACGATGTGGAGGAACATATTGAGAGA


SlCAS10   -AGCTGTAAT-------GAGGGTTAATACTGCATTTTTGTCAC---ACTGCCTATTCAGG
SlCAS9    -TATTGCACT-------GAACATTATTGTTTGTATTAAATCAG---TTGGAAAAAAAA-G
SlCAS12   TTATTGTAGAACCCCC-ACAGTTCATTTTTGTACG------------------------
SlCAS11   GTAATGTATATATGGCCGCATGTAAATGGC-----------------------------
SlCAS8    -AGAAGTCTCAA-TACCGGAGCTGGCTGTGGAACTGTTGTCAACAGAAGGCGCTACAACT
SlCAS7    -------------------------------------------------------------
SlCAS5    -GGAATGAAGTAAATGCGAAAAATAAAGAGAAAAA------------------AAATGCA
SlCAS3    -------------------------------------------------------------
SlCAS2    TTGGAGGAGGAAAACATGGAGTTGAAGGAGAAAATGTATGTAAT-GGAGAGGGAATTGGA


SlCAS10   AAAGGTAAATTAATTTTGTAATCCTTTAGTAATT-------GTACTTCAGCTTTAT----
SlCAS9    AGAGGAAGAG--------------TTTAGATCTT-------ATTTTTA------------
SlCAS12   --------------GTTTTTGTAGTTTCTACTGGGGAGCCACGTTCAAGTATAGTAGCAA
SlCAS11   -----------------ATACTTGCTTCTGATAATAACACAACTATGCGTATTTTTTATG
SlCAS8    GGAGGTGAATCAA-CTGATGAAGGTTGAGACTCTGCATCAGAAATATCAGATTCCACAGA
SlCAS7    -------------------------------------------------------------
SlCAS5    CGA-TTGGAACAAAAGTCTCCTTGTGTATGATCATCACACAATTA---------------
SlCAS3    -------------------------------------------------------------
SlCAS2    GGAATTGCGGAAAAAGGTTCGGTATTTGGAAGGTGAAGATGATAATGGAGATGGAA----


SlCAS10   -----GGCTTT-----------------------------------------------------
SlCAS9    -------------------------------------------------------------
```

```
SlCAS12   T----TCCTTCTGGTATTAAATGATTTTAT-----------------------------
SlCAS11   -----GGCTAATGGACCACAGTGGACCTTTCACCAACT---------------------
SlCAS8    GCTCATTCTTTCGGTCTCTGATGATTCTACTTCCTCTTTAGATTTCCCTGATGACTTCCC
SlCAS7    ------------------------------------------------------------
SlCAS5    ------------------------------------------------------------
SlCAS3    ------------------------------------------------------------
SlCAS2    -----ACGAGTCGGATAATG---AAGCTGGTTCTGAGAAAAGTGTAGG------------


SlCAS10   ------------------------------------------------------------
SlCAS9    ------------------------------------------------------------
SlCAS12   ------------------------------------------------------------
SlCAS11   ------------------------------------------------------------
SlCAS8    AGACATCACTTCCTTTATGCCACCACCAACAGATTTGCCAGCATCTTTAAGGATTCTCTT
SlCAS7    ------------------------------------------------------------
SlCAS5    ------------------------------------------------------------
SlCAS3    ------------------------------------------------------------
SlCAS2    -------------------------------AGATTGA----------------------


SlCAS10   ------------------------------------------------------------
SlCAS9    ------------------------------------------------------------
SlCAS12   ------------------------------------------------------------
SlCAS11   ------------------------------------------------------------
SlCAS8    CGTCTTGCCCCATTTGTGAAACTTTTCCCATTTCCTGCACCGTTCTCTTTTCCATCTTCT
SlCAS7    ------------------------------------------------------------
SlCAS5    ------------------------------------------------------------
SlCAS3    ------------------------------------------------------------
SlCAS2    ------------------------------------------------------------


SlCAS10   ------------------------------------------------------------
SlCAS9    ------------------------------------------------------------
SlCAS12   ------------------------------------------------------------
SlCAS11   ------------------------------------------------------------
SlCAS8    GTAGGTGTTGTTGCTAATGATGAAGGCAAAATGGTGTCATCCACTATAATCTTCACTCTG
SlCAS7    ------------------------------------------------------------
SlCAS5    ------------------------------------------------------------
SlCAS3    ------------------------------------------------------------
SlCAS2    ------------------------------------------------------------


SlCAS10   ------------------------------------------------------------
SlCAS9    ------------------------------------------------------------
SlCAS12   ------------------------------------------------------------
SlCAS11   ------------------------------------------------------------
SlCAS8    ATATCCTTGGCATTAACTGCCCTAAGATTCACATGCAGAGATGAAATAGGCTCTCCAAGA
SlCAS7    ------------------------------------------------------------
SlCAS5    ------------------------------------------------------------
SlCAS3    ------------------------------------------------------------
SlCAS2    ------------------------------------------------------------


SlCAS10   ------------------------------------------------------------
SlCAS9    ------------------------------------------------------------
SlCAS12   ------------------------------------------------------------
```

```
SlCAS11   ------------------------------------------------------------
SlCAS8    TTGCTAGAACTTCTCCGGAGAACTGAGCTGATCTTATGTAAACCCCTGTGTAAACGACCT
SlCAS7    ------------------------------------------------------------
SlCAS5    ------------------------------------------------------------
SlCAS3    ------------------------------------------------------------
SlCAS2    ------------------------------------------------------------

SlCAS10   ------------------------------------------------------------
SlCAS9    ------------------------------------------------------------
SlCAS12   ------------------------------------------------------------
SlCAS11   ------------------------------------------------------------
SlCAS8    GGGGAATCCCCTAGGTAATTCAGGCTTAAACCAACATTTACAGTGAATAAGAAGATACCA
SlCAS7    ------------------------------------------------------------
SlCAS5    ------------------------------------------------------------
SlCAS3    ------------------------------------------------------------
SlCAS2    ------------------------------------------------------------

SlCAS10   ------------------------------------------------------------
SlCAS9    ------------------------------------------------------------
SlCAS12   ------------------------------------------------------------
SlCAS11   ------------------------------------------------------------
SlCAS8    AGGTCACCCACAGAACTGTAACGCAGAGCATACATGGTAAAAGTCAACGGACACACGGGG
SlCAS7    ------------------------------------------------------------
SlCAS5    ------------------------------------------------------------
SlCAS3    ------------------------------------------------------------
SlCAS2    ------------------------------------------------------------
```

Coding sequences of tomato genes analyzed using Real Time PCR and *in situ* hybridization technique. Primers used are highlighted in yellow.

>SlPp2 (NCBI accession no. XM_004233183.1)

```
ATGACTAATGATTAGGCCGTCCAGAATACATACACCAGCATCCACAAAGAGTTCTTCTCAGAGAAATGGGGT
CAGGGTTGTCACAAGATCAGGATTTACAACAAAATCAAGAACTAAGCAATGCTTCTCCTCAAGGCCACCATA
GTGATGCTGCCGTACTCAATGAAGAACCAAGAAAGATTATGCCACAGAGCATCAAGAGTACTAAGACTAACA
AGACAATGGAAGCCGCTAGAGTACTCAGATTTCCACATAATTATGAAGAAATCCTAAAAGAGGCAGATTCTT
CAGTTGACAGATCCTCCATGGACAAACTATATGACCAGCTATATACGGGAGTATTTCTGAACCAAAAGCGCA
AGAAATACTGGGTCGATAAGAAGTCATATGGCAACTGCTTCATGTTGTATGCAAGAGATCTCTTGATCACTT
GGGCAGAAAACAACCGTTTCTGGCACTGGCCCTTGGTACAAGAGTCAAGTGATGTCCTTCTTCCAGCAGCAG
AACTACTAGATGTTTGCTGGCTAGAAATCCATGGAAGATTCAATACAACTAAGCTGTCGCCAGGGCTCATTT
ATGAGGTTGTCTTCATTGTCATGTTAAAGGATCCTGCTTATGGATGGGAAAATCCAGTGAATCTACGACTCA
TACTCCCAGATGGTAGCAGACAAGGACATACCGAGAATATGGTGGAAAAACGACGAGAAAAATGGATAGAAA
TTCCAGCAGGAGAGTTCATGACTTCGGCAGATCAAAAGAATGGAGAAATAGAGTTCTCTCTATATGAATATG
AAGGTGGGAACTGGAAGAAGGGGCTTGTCATTAAATGTGCTGTCCTCCGTCCAAAAGCCTGAGTTCTATGGC
ATATGATACGAATTTAGCGTGCAACTGCAGTTTCTTTTTAGCTTTTTCACCCTAATGTTTACAATGATGAGC
ATTGAACTAGCAGCAAAAAGCATGAGATTGTGTTCTTTCTTTTGTATATGTAAATTAAGATGCATGTGCTAT
GCAGATATGTTCGATGCCTCAGAGATTTGGCGTTAAGCCCAGAA
```

>SlSEO (NCBI accession no. XM_004239105.1)

```
ACACACAACAATATTTAACTACACTTGCCTTTCTAAAAACCCTTTAGTGTTCTTTTTCCATCCATATAAATG
ACAAGTGTTAACCCATTGAATGAAAAGGTATCCATGAATAACCCAATGAATAATATGCCAAATGGATCTGCT
GCCAATATGATGCAACCAATGAGTAATCCAACTACAGGCCATCACATCAACCCTTTGAATGTCCAAATCAAT
```

CCTCATTCTGTTGTCAACCCAGTGAGTCGTGACATGATACCAGCTAGTGTTGTACCTGCTGCTCATCATACA
GCTCCGATCAATCCACGAACATCAAATCTAGCAGCTAGGCTTCCACACAGGAGAGGAGATCATCATATGTTT
TTGACATCTGATGATAATGCAATGATGAAGCACATTGAAGAAACTCATATCCCAGATGGCCGTGACTTTGAT
GTCAAGCCTCTTGTTCATATTATTGAGGATATTGTGCATCGCGCTACTCCCATTGCTGGACATGTTCATGAA
GCTAAAGTTCAAGCACATCTGGAAGCATTGGAAGAGAAGGCTCCCCACAATGAACTTATTGAAATACTCAAC
TATTTGGCATATCCTATACAAAGGATTAAAATGGAGTTGATAAGCAAATGTGCTAACAAAGAAGACGCTCAT
TCGACAACAATGTCACTGCTTCACTCACTCACAACCTATGCCTGGGACACGAAAGTAGCAATAACTTTCGCG
GCTTTTGCCCAGCTATATGGTGAATTTGGTCTGCTTACTCATCAATATACTACAAATCCTCTGGCTAAGTCT
GTTGCAATCATCATGGAACTTCCAGAAATAATGACACGTCAGGATATTCTCAAGCAGAAATTTGATGCAATC
CATGATCTGATCGACAAAATGCTGGATGTAACAAAGTGTATCATCGAGTTTAGAGACGTTCAATCGTCTCAA
AATCAACATGTTATCACACAAGAATTGGAAATGTTGATCAATACTGCCCATATTTCCACTGCTGCTTACTGG
ACTATGAGGGCTGCTGTCATGTGTGCTGCTATGATTTTGAATCTCATTGCCATTGGCCACGAGCAAATTTCT
TCAACATCTGAGGCTTGGGAGATATCTAGTTTGGCTCACAAGCTTGCAAACATATTGGATCATCTCAAAAAG
GTTCTTAACCTTTGTCACCAAAAGATTGAGGAGAAGAGGCAATATGATAAATTCGAAGCAATTCTACGACTT
CTCAGGACACCTCAACTTGATAACATGAAGATACTCTCCATGTTGATCCACTCCAGGGATGATCAGCTTCCA
CTTTTTGATGGAACTCATAAGAGAAGGGTAAGTCTTGATGTGCTAAGAAGGAAGCATGTTTTACTTTTGATC
TCCGACTTAGACATTGCACCCGAAGAGCTCTTTGTTCTCCACCACATGTACGAAGAATCCAAGGCACAACCA
AACAGGCCAGAGAGCAACTATGAGGTTGTATGGATCCCTGTGGTTGACAAGAGGCTAACACCATGGACTGAT
GCAAAACAAGTGAAATTTGAAGAAGTACAAGCTTCAATGCCATGGTATACAGTGGCACATCCATCGATGATC
GATCCAGCAGTGTTAAGGTGCATTAAAGAGGTGTGGGGATTCAAGAAGAAGCCTCAGCTTGTTGTTCTTGAT
CCACAAGGCAAAGAATCGAACAATAATGCTTACCATATATTATGGATTTGGGGAAGTTTGGCTTTTCCATTT
ACCAAAGCTAGGGAAACAGCTTTGTGGAAGGAACAAACTTGGAATGTTGAACTGTTAGCTGATTCCATTGAT
CAAAATGTTTTCACTTGGATAAGTGAAGGCAAATGCATATGCTTGTACGGAGGAGAAGATATTGAATGGATC
AGATCATTCACCTCATCAACGCGAGCTGTCGCAAATGCAGCTGGCGTTCCACTAGAGATGCTCTACGTGGGA
AAAAAGAACCCAAAAGAAAGAGTCCGGAAGAACAGCTCAATAATCCAAATGGAAAACTTGAGCCATGTGGTG
CAAGACCAAACTCTAATTTGGTTCTTTTGGGAAAGGCTAGAAAGCATGTGGCACTCTAGGACTCAACAAGAC
ATCCCCGGTGAAACTGACCCGATCCTTCAGGAGATTGTGACGATTTTGAGCTATGATGGAAGTGATCTTGGA
TGGGCTGTGTTCAGCCGCGGATTGGCTGAGATGACTAGAGGTAAAGGTGATCTGATAGTGCAAGTTATGAAG
GGATTTGATCGTTGGAGAAATGAAGTGAGTGATATAACTACATTTGTTCCTGCATTGGACCGTCAACTTCGT
GATCTTCATAGTCCACATCATTGTACTCGACTAATTCTACCGAGTACCTCTGGACATATTCCTGAGAGAGTG
GTTTGTGCTGAATGTAGTCGTCCCATGGAGAAGTTTATCATGTACCGCTGTTGCACTGATTGAGGAGTTATG
AGGAGTTGGGTCGCGTCTAGAGGACTACTATATATTTGAATAAAATGACCTCTCTTGTGAGTTTTTTTAAGT
ATTGGTTGTGCTTACTTTAATTAATGTTTAGAAAAAAAATGCCATGTATTGGCCTTTTCATATTTTCATGTA
CTTGTTTTTGAGATTTCAGTGTGTGATGTATTAATGAAGAATCAATAAACAGCTTTTCCAATTATATAAAGT
ATTTTTCTGTTTTAATTTT

>SlSWEET1 (NCBI accession no. XM_004237674.1)

AAATATATTCGACTTATTGTTCATTTTCCTCCTTTGGGTATTCAATTTTTTGAAATTCTTGGAGAGTTTGTT
AAGTTTCTTCACTTGGGTTTTCTTCAAAAAAACCAATCTTTTTCGTCTCTGAATCAAAGAAATTGCTACTCT
GTACTGCAAAAGTGAAGAAAGACATGGGTGTTGTTCATACTCTGCATTTTGTTTTTGGGATATTTGGAAATG
CCACTGCTCTGTTTCTGTTCTTGGCACCAATAATCACATTCAAGAGGGTTATACAAAATCGATCTACTGAAC
AATTCTCTGGCTTGCCTTACGTTATGACTTTACTCAACTGCCTTCTTTCTGCATGGTATGGTTTACCATTTG
TGTCACCAAATAATCTGTTGGTGTCTACAATCAATGGGACTGGAGCTGTAATTGAGACCATTTATGTGCTGA
TCTTCATTGCATTTGCACCAACTAAAGAGAAGAAGAAAATCTCAGCACTTTTTCTATTAGTCCTTACTGTTT
TTGCTGCTGTAGCCCTTGTTTCCATGCTTGGTTTACATGGAAGCAAAAGGAAGCTCTTTTGTGGTATCGCTG
CCACCATCTTCTCTATCATTATGTATGGATCTCCTCTATCCATCATAAGACTGGTGATCAAGACGAAGAGCG
TGGAGTTCATGCCATTTTTCTTGTCGTTGTTTGTGTTCTTATGTGGCGCTTCCTGGTTTGCATTTGGCCTTC
TTGGCAAGGACCCTTTTGTTGCTATTCCAAATGGTTTTGGTTTTGGTTTAGGAACAGTGCAACTTATCTTAT
ATGCAATCTACTGTGAGAAGAAGGGATTCACAAGGAAATCAAACCTTGATGAGTCAAATGGCAAGTCTCACC
AAGAGGAGAAGCAATCTAGCAAGTCAAGGCTTGAGCAAGTTTAGGACATGATTGCCTCTAATTCTTCTTGAA

TGATGATTGTGCATCTTCTTTTTGAGATGCTATAGTGATCTTTGACATATGTTTTAGTATTGGATTAGTTCA
TGTATTTGGAATTTCTTTCCCAATTATGTTGTTTTTTTTCATCATATTTTGCTGCCTGCTCAAATAAACCAT
AAGATCCTTCTTTTGTTT

In situ hybridization protocol

Samples mounted on slides underwent the following steps:

1. Slides rehydration:

10 minutes	Histoclear
15 minutes	Histoclear
1 minute	Ethanol 100%
30 seconds	Ethanol 100%
30 seconds	Ethanol 96%
30 seconds	Ethanol 85% - 0.425% NaCl solution
30 seconds	Ethanol 70% - 0.85% NaCl solution
30 seconds	Ethanol 50% - 0.85% NaCl solution
30 seconds	Ethanol 30% - 0.85% NaCl solution
2 minutes	0.85% NaCl solution

2. Treatment with Proteinase K:

2 minutes	1X Phosphate Saline Buffer (PBS)
10 minutes, shaking	Proteinase K (1 µg/mL Tris EDTA)
2 minutes	Glycine 0.2% in PBS
10 minutes, shaking	Acetic anhydride/Triethanol amine
2 minutes	1X PBS
30 seconds	0.85% NaCl solution
30 seconds	Ethanol 30% - 0.85% NaCl solution
30 seconds	Ethanol 50% - 0.85% NaCl solution
30 seconds	Ethanol 70% - 0.85% NaCl solution
30 seconds	Ethanol 85% - 0.425% NaCl solution
30 seconds	Ethanol 96%
30 seconds	Ethanol 100%
30 seconds	Ethanol 100%

3. Slides are incubated for one hour at -20° C.
4. Prehybridization step: slides are incubated at hybridization temperature for two hours in prehybridization buffer (Deionized formamide, 5X SSC 'Saline Sodium Citrate', 50 µg/mL heparin, 100 µg/mL tRNA, 0.1% Tween 20).
5. Hybridization step: slides are incubated at hybridization temperature overnight in hybridization buffer (50% Deionized formamide, 10% Dextran sulfate, 1 mg/mL tRNA, 7.5% Tween 20, 2.5X Denhardt's Solution, 1X NaCl Solution, 1X SSC) with 5 µL/mL of denatured probe.
6. Washing steps:

30 minutes, hybridization temperature	0.1X SSC+ 0.5% SDS
1 hour, hybridization temperature	2X SSC + 50% formamide
Rinse	1X NTE
15 minutes, 37° C	1X NTE + 20 µg/mL RNAse
Rinse	1X NTE
1 hour, hybridization temperature	2X SSC + 50% formamide
Rinse	0.1X SSC
Rinse	1X PBS

7. Detection steps:

Buffer 1: 100 mM pH 7.5 Tris HCl, 150 mM NaCl.

Buffer 2: Buffer 1, 0.5% Blocking Reagent.

Buffer 3: Buffer 1, 1% BSA (Bovin Serum Albumin), 0.3% Triton X100.

Buffer 4: 100 mM pH 9.5 Tris HCl, 100 mM NaCl, 50 mM $MgCl_2$.

1 hour, shaking platform	Buffer 2
1 hour, shaking platform	Buffer 3
1 hour	Antibody Anti-DIGoxygenin in Buffer 3
20 minutes (2 times)	Buffer 3
Rinse (3 times)	Buffer 1
15 minutes	Buffer 4

8. Revelation step: slides were incubated in Buffer 4 with NBT-BCIP (75 mg/mL NBT 'Nitro blue tetrazolium', 50 mg/mL BCIP '5-bromo-4-chloro-3-indolyl-phosphate') from some hours to some days.
9. Slides mounting: samples were covered with mounting and covered with coverglass.

Hybridization temperature was calculated with the following formula for each probe:

$Tm = 81,5 + 16,6 \log [Na^+] + 0,41 (G+C)\% - 0,61 \times \%\ Formamide - (500 / N) - 15.$

(N=probe length)

ACKNOWLEDGEMENTS

I would like to thank dr. Rita Musetti and dr. Simonetta Santi for their assistance and guidance during my PhD studies.
I would like to express my gratitude to my research group, especially to dr. Rachele Polizzotto, dr. Simone Grisan and Khaled Farhan. I would also like to thank Alberto Loschi for tomato plants breeding and grafting, dr. Paolo Ermacora for monitoring BN in the vineyard and dr. Marta Martini for primers used in stolbur 16rRNA detection experiments.

I am grateful to dr. Sabrina Palmano (CNR, Torino, Italy) for the review of the manuscript and the guidance on phytoplasma diagnosis and advice on the different protocols I had checked.
I express my appreciation to dr. Sylvie Dinant (Institut Jean-Pierre Bourgin, INRA, Centre of Versailles, France) for having accepted to revise my thesis and for her kindness and helpfulness during my staying at INRA centre. I would also thank all the members of PATS team at IJPB, especially dr. Rozenn Le Hir for her help with light and confocal microscopy and advice on experiments and Lawrence Bill for everyday assistance in the lab. I am also grateful to Halima Morin and Adeline Berger for the aid in ISH experiments.

This research was mostly funded by AGER project n◦ 2010-2106 “Grapevine Yellows: innovative technologies for the diagnosis and the study of plant/pathogen interactions.”

The completion of this manuscript was also due to my family, mia cugi Alessia, Steph, my Rich friend, Laura and the other lunchgirls, my special ‘Jeroen, Alessandra and Giorgiana’, my old friends and the new ones.

PUBLICATIONS

In this section there is the list of research papers and abstracts that include data obtained from investigations performed during my PhD studies.

Research papers:

- Santi S, De Marco F, Polizzotto R, Grisan S, Musetti R (2013). Recovery from stolbur disease in grapevine involves changes in sugar transport and metabolism. *Frontiers in Plant Science,* 4:171.
  In this paper my contribution was designing primers and performing Real Time PCRs for some of the investigated genes. I have also performed diagnosis on leaf samples.

- Santi S, Grisan S, Pierasco A, De Marco F, Musetti (2013). Laser microdissection of grapevine leaf phloem infected by stolbur reveals site-specific gene responses associated to sucrose transport and metabolism. *Plant, Cell & Environment,* 36:343-355.
  In this paper my contribution was designing primers and performing Real Time PCRs for some of the investigated genes.

- Musetti R, Buxa SV, De Marco F, Loschi A, Polizzotto R, Kogel KH, van Bel AJE (2013). Phytoplasma-triggered Ca^{2+} influx is involved in sieve-tube blockage. *Molecular Plant-Microbe Interactions,* 26:379-386.
  In this paper my contribution was to perform phytoplasma detection on *Vicia faba* plants.

- Musetti R, Farhan K, De Marco F, Polizzotto R, Paolacci A, Ciaffi M, Ermacora P, Grisan S, Santi S, Osler R (2013). Differentially-regulated defense genes in *Malus domestica* during phytoplasma infection and recovery. *European Journal of Plant Pathology,* 136:13-19.
  In this paper my contribution was designing primers and performing Real Time PCRs for some of the investigated genes.

- Buxa SV, Polizzotto R, De Marco F, Loschi A, Kogel KH, Van Bel AJE, Musetti R. Stolbur infection in tomato is associated with a re-organization of plasma membrane-ER network and actin filaments in sieve elements. *Article in preparation that will be submitted.*
  In this paper my contribution was to perform phytoplasma detection on tomato plants.

Abstracts:

- Buxa SV, Polizzotto R, De Marco F, Loschi A, Kogel KH, van Bel AJE, Musetti R. Re-arrangement of sieve element endomembrane network in tomato leaves infected by Stolbur phytoplasma. COST Action FA 0807 "Integrated Management of Phytoplasma Epidemics in Different Crop Systems". Lisbon, 30/09-01/10-2013.

- Musetti R, Farhan K, Grisan S, Polizzotto R, De Marco F, Ermacora P (2012). Fungal endophytes as innovative tools for phytoplasma disease control. Proceedings of COST Action FA1103 Meeting - Endophytes in Biotechnology and Agriculture: November 14-16th 2012, San Michele a/A (TN) Italy, p. 35.

- Farhan K, Grisan S, Polizzotto R, De Marco F, Ermacora P, Musetti R (2012) Induction of defense genes in apple leaf tissues by an endophytic strain of *Epicoccum nigrum* and its possible use in the control of the apple proliferation disease. Petria, Proceedings of 22nd 'International Conference on Virus and Other Graft Transmissible Diseases of Fruit Crops' (ICVF), 8th June 2012 Roma (Italy) p. 109.

frontiers in
PLANT SCIENCE

ORIGINAL RESEARCH ARTICLE
published: 04 June 2013
doi: 10.3389/fpls.2013.00171

Recovery from stolbur disease in grapevine involves changes in sugar transport and metabolism

Simonetta Santi, Federica De Marco, Rachele Polizzotto, Simone Grisan and Rita Musetti*

Department of Agricultural and Environmental Sciences, University of Udine, Udine, Italy

Edited by:
Aart Van Bel, Justus-Liebig-University Giessen, Germany

Reviewed by:
Biao Ding, The Ohio State University, USA
Gary A. Thompson, Pennsylvania State University, USA

***Correspondence:**
Rita Musetti, Department of Agricultural and Environmental Sciences, University of Udine, Via delle Scienze 206, I-33100 Udine, Italy
e-mail: rita.musetti@uniud.it

Grapevine can be severely affected by phytoplasmas, which are phytopathogenic *Mollicutes* invading the sieve elements of the host plant. The biochemical and molecular relationships between phytoplasmas and their hosts remain largely unexplored. Equally unknown is an interesting aspect of the pathogen–plant interaction called "recovery," which is a spontaneous remission of symptoms in previously symptomatic plants. Recovered plants develop resistance mechanisms correlated with ultrastructural and biochemical changes in the sieve elements. Callose as well as sugars are involved in several plant defense processes and signaling. In the present work we have examined the possible involvement of callose, as well as callose synthase, sugar transporter, and cell wall invertase genes, during the infection and after "recovery" of grapevine from bois noir (BN). Ultrastructural investigation of leaf tissue showed that callose accumulated in the sieve elements of diseased grapevine; moreover, two genes encoding for callose synthase were up-regulated in the infected leaves. Regarding sucrose, expression analysis showed that sucrose transport and cleavage were severely affected by BN phytoplasma, which induced the establishment of a carbohydrate sink in the source leaf, and was analogous to other obligate biotrophs that acquire most of their nutrients from the host plant. Interestingly, whereas in recovered plants the transcript level of sucrose synthase was similar to healthy plants, sucrose transporters as well as cell wall invertase were expressed to a greater degree in recovered leaves than in healthy ones. Recovered plants seem to acquire structural and molecular changes leading to increases in sucrose transport ability and defense signaling.

Keywords: callose, cell wall invertase, grapevine, recovery, stolbur, sucrose transporters, sucrose synthase

INTRODUCTION

Phytoplasmas have been associated with several hundred diseases affecting economically important crops, such as ornamentals, vegetables, fruit trees, and grapevines (Lee et al., 2000). Phytoplasmas are plant-pathogenic prokaryotes belonging to the class *Mollicutes*, a group of wall-less microorganisms phylogenetically related to low G+C, Gram-positive bacteria (Weisburg et al., 1989). In host plants, they are restricted to the sieve elements of phloem and are transmitted among plants by phloem sap feeding leafhoppers or psyllids in a persistent manner. Phytoplasmas remain as the most poorly characterized plant pathogens, primarily because efforts at *in vitro* culture, gene delivery and mutagenesis have been unsuccessful.

Bois noir (BN) is a grapevine disease associated with the presence of phytoplasmas of the stolbur group, 16SrXII, known as "*Candidatus* Phytoplasma solani" ("*Ca.* P. solani"), but still not described (Firrao et al., 2005). BN is often endemic, but, in some cases, can be associated with severe epidemics, as reported in several Italian regions in the past 15 years (Belli et al., 2010). BN causes symptoms such as abnormal lignification of canes, short internodes, flower abortion, and curling and discoloration of leaves with intervein yellowing or reddening, and these are accompanied by a dramatic reduction in yield (Osler et al., 1993). These symptoms have been related to stoma closure, reduced photosynthesis rate, and anomalous accumulation of carbohydrates in leaves (Bertamini et al., 2002; Musetti et al., 2007; Endeshaw et al., 2012).

Phytoplasmas are restricted mainly to sieve elements, where they move through the pores of sieve plates and accumulate especially in source leaves and to a lesser extent in petioles and stems (Christensen et al., 2004). Phytoplasmas induce characteristic symptoms in host plants, many of which point to impairment of sieve-tube function (such as low productivity, stunting, general decline, reduced vigor; Kartte and Seemüller, 1991). Cytological modifications such as sieve-element necrosis, abnormal callose deposition at the sieve plates, sieve-element wall thickening, and starch accumulation in the shoots of susceptible plants have been documented by electron microscopic observations (Braun and Sinclair, 1978; Kartte and Seemüller, 1991; Musetti et al., 1994; Musetti and Favali, 1999). During phytoplasma infection, assimilate translocation in the host plant is severely impaired, being responsible for massive changes in phloem physiology (Musetti et al., 2013). It was postulated that phytoplasmas secrete a variety of effector proteins that interfere with plant processes, leading to changes in plant development and physiology, but to date the biochemical and molecular relationships between phytoplasmas and their hosts remain largely unexplored. Global transcription profiles have been obtained from phytoplasma-infected grapevine leaves by hybridization of

microarrays (Albertazzi et al., 2009; Hren et al., 2009a) or protein profiling (Margaria and Palmano, 2011). These studies revealed that phytoplasma infection in grapevine altered the expression of more than one hundred genes and thirty proteins belonging to both primary and secondary metabolism. Inhibition of several Calvin-cycle enzyme genes was shown and explained by the accumulation of soluble carbohydrates and starch that had been observed in source leaves of plants infected by phytoplasmas (Lepka et al., 1999; Maust et al., 2003; André et al., 2005). On the other hand, genes encoding enzymes involved in hexose production from sucrose and starch, like vacuolar invertase, sucrose synthase (SUS), and alpha amylase, were shown to be up-regulated (Albertazzi et al., 2009; Hren et al., 2009a,b). A major effect on sucrose transport and metabolism has been confirmed thanks to gene expression analysis focused at the leaf phloem of stolbur-infected grapevine. Laser microdissection-assisted isolation of phloem transcripts and gene expression analysis showed inhibited sucrose loading and increased sucrose cleavage, suggesting the establishment of a phytoplasma-induced switch from a carbohydrate source to sink (Santi et al., 2013).

An interesting but still unclear aspect of the phytoplasma–plant interaction is "recovery," which is a spontaneous remission of symptoms in previously symptomatic plants, occurring also in BN-infected grapevines (Osler et al., 1993), where the remission of symptoms is associated with the disappearance of the phytoplasmas from the crown as also observed in apple trees recovered from Apple Proliferation disease (Osler et al., 2000; Carraro et al., 2004). Cytochemical analyses have revealed that recovery is accompanied by biochemical changes in the phloem, related to variation of the sieve-element oxidative status, leading to modifications in phloem protein (P-protein) conformation and in phloem occlusion expression patterns. In particular, in grapevines as well as in apple and apricot trees it has been demonstrated that recovery coincided with the accumulation of hydrogen peroxide in sieve elements (Musetti et al., 2004, 2005, 2007), which often signals increased resistance. Moreover, an anomalous accumulation of callose and protein associated with the up-regulation of callose synthase- and P-protein-coding genes has been observed in recovered apple trees (Musetti et al., 2010), supporting the hypothesis that recovered plants were able to develop resistance mechanisms dependent on Ca^{2+} signal activity (Musetti et al., 2010, 2013).

Callose is a structural component of the sieve elements (Ehlers et al., 2000; van Bel et al., 2002). Its activity in sieve-pore occlusion in the case of injuries (wounding, pathogen challenge, attack by phloem sap-sucking insects), is extensively reported (Knoblauch and van Bel, 1998; Furch et al., 2007) but roles in sieve element physiology are also recognized (Barratt et al., 2011; Xie et al., 2011). In intact phloem tissue, callose is involved in the correct functioning and development of the sieve elements and in flow regulation through the sieve pores (Barratt et al., 2011; Xie et al., 2011).

In this work we studied the responses (in term of morphological conformation and gene expression analyses) of callose during phytoplasma infection in grapevines affected by BN and their possible role in the establishment of "recovery." Moreover, the expression of sucrose metabolism-related genes such as sucrose transporters, SUS, and invertase genes were also investigated in leaves of recovered plants compared to infected and healthy plants.

MATERIALS AND METHODS

PLANT MATERIAL AND PHYTOPLASMA DETECTION

Grapevines (*Vitis vinifera* L. cv. Chardonnay) were grown in an experimental field located in Friuli Venezia Giulia (North-Eastern Italy). Plants were regularly treated with fungicides. Fully expanded, intact leaves were collected from five healthy (H), five symptomatic (D), and five recovered (R) plants in late summer (five leaves for each plant), when typical BN symptoms were evident. Leaves were collected from symptomatic canes of infected plants, and in similarly positioned canes of nearby recovered and healthy plants. For stolbur phytoplasma detection, RNA was extracted from frozen H, D, and R leaves enriched in midribs using RNeasy Plant Mini Kit (Qiagen GmbH, Hilden, Germany) with minor modifications (Santi et al., 2013). Total RNA quantity and purity were evaluated using a NanoDrop ND-1000 UV–Vis Spectrophotometer (Thermo Fisher Scientific, Inc., MA, USA).

RNAs were reverse-transcribed using a QuantiTect Reverse Transcription Kit (Qiagen GmbH, Hilden, Germany) with random hexamers following the manufacturer's instructions. Real-time PCR reactions were set up with SsoFast EvaGreen Supermix (Bio-Rad Laboratories Co., Hercules, CA, USA) using specific primers designed on the *16SrRNA* gene of "*Ca.* P. solani" (accession no. AF248959) 16Sstol(RT)F2 and 16Sstol(RT)R3 (Martini et al., unpublished results; Santi et al., 2013). Real-time PCR analyses were performed in a CFX96 Real Time PCR Detection System (Bio-Rad Laboratories Co., Hercules, CA, USA), imposing the following standard thermal profile: 98°C for 2 min, followed by 45 cycles for 5 s at 98°C and 5 s at 60°C. A melting curve analysis of the products was performed from 65 to 95°C to check primer specificity.

TRANSMISSION ELECTRON MICROSCOPY

To minimize the damage to sieve elements due to the electron microscopy preparation procedure, a gentle preparation of the samples has been performed according the method described by Ehlers et al. (2000). Segments (6–7 mm in length) of grapevine leaf tissues including the vein and 1–2 mm of blade on each side were excised, immersed in a buffered medium containing 10 mM NaOH-2-(*N*-morpholino) ethanesulfonic acid, 2 mM $CaC1_2$, 1 mM $MgC1_2$, 0.5 mM KC1, and 200 mM mannitol, pH 5.7 (van der Schoot and van Bel, 1989), and allowed to recover for 2 h at room temperature. Then, the buffer was replaced by a fixation solution of 3% paraformaldehyde and 4% glutaraldehyde in 50 mM sodium cacodylate buffer plus 2 mM $CaCI_2$, pH 7.2.

Samples were fixed for 6 h at room temperature, replacing the fixative every 30 min. Then they were washed for 1 h at 4°C in 50 mM sodium cacodylate buffer containing 2 mM $CaCl_2$ (pH 7.2) and postfixed overnight with 2% (w/v) OsO_4 in the above buffer at 4°C.

Dehydration was performed in a graded ethanol series and propylene oxide, and the samples were embedded in Epon/Araldite epoxy resin (Electron Microscopy Sciences, Fort Washington, PA, USA).

Several serial ultrathin sections of at least 100 samples from each of the three plant groups were collected on copper grids, stained in uranyl acetate and lead citrate and observed under a

PHILIPS CM 10 (FEI, Eindhoven, The Netherlands) transmission electron microscope (TEM) operating at 80 kV.

PLANT GENE EXPRESSION ANALYSES

For plant gene expression analyses, RNAs were extracted from frozen leaf midribs as described above. Nucleic acids were treated with Turbo DNase (Ambion, Life technologies Co., Carlsbad, CA, USA) and reverse-transcribed using a SuperScript III Platinum Two-Step qRT-PCR Kit (Invitrogen Life Technologies, Paisley, UK) in a total volume of 20 μL. Real-time RT-PCR analyses were performed on a CFX 96 instrument (Bio-Rad Laboratories Co., Hercules, CA, USA). SsoFast EvaGreen Supermix (Bio-Rad Laboratories Co., Hercules, CA, USA) was used for the analysis of callose synthases, while RealMasterMix SYBR ROX (5Prime Eppendorf, Hamburg, Germany) for all other genes. In both cases a melting curve analysis was performed from 65 to 95°C to check primer specificity. Primers were designed at 60°C Tm using Primer3 software[1], and then evaluated using the BLASTN (nucleotide basic local alignment search tool) algorithm (Altschul et al., 1997). Standard curves of different dilutions of pooled complementary DNA (cDNA) were used to calculate the PCR efficiency value (E) for each primer pair as described by Pfaffl (2001). Primers and E are indicated in **Table 1**.

Ubiquitin-60S ribosomal protein L40-like (*UBQ-L40*; accession no. XM_002273532.1) was used as a reference gene, as it was found to be stably expressed when compared with actin, *UBQCF* (Ubiquitin conjugating factor) or *60SRP* (60S ribosomal protein L18). The gene-stability measure (M) was calculated by the geNorm program (Vandesompele et al., 2002) using RNAs that were purified from midrib-enriched-samples of several D, R, and H plants. The M value for *UBQ-L40* was 0.45, thus confirming the validity of this gene as a reference. A mean normalized expression (MNE) for each target gene (Muller et al., 2002) was calculated by normalizing its mean expression level to the level of ubiquitin, with the transcript abundance of ubiquitin defined as 100 arbitrary units. Mean normalized gene expression values were graphed by assigning a value of zero to no expression. Each data point represents the mean of at least three biological replicates and three technical replicates. The sequences of the examined *V. vinifera* genes were identified *in silico* by Grape Genome browser[2] or retrieved from the National Center for Biotechnology Information (NCBI) database.

Statistical analyses of gene expression levels were performed with the InStat GraphPad software package (La Jolla, CA, USA) using an ANOVA Tukey–Kramer Multiple Comparisons Test.

RESULTS

PHYTOPLASMA DETECTION

Leaf samples were analyzed for the presence of BN phytoplasma by real-time RT-PCR. Starting from 10 ng of total RNA, stolbur

[1]http://frodo.wi.mit.edu/primer3/

[2]http://www.genoscope.cns.fr/externe/GenomeBrowser/Vitis/

Table 1 | Accession number of sequences and primers used for real-time RT-PCR.

Gene name	NCBI accession No.	Primer sequence (5′–3′)		nM	E	Grape Genome 12X Locus tag
VvUBQ-L40	XM_002273532.1	For: CCAAGATCCAGGACAAGGAA	Rev: GAAGCCTCAGAACCAGATGC	300	2.05	GSVIVT01038617001
VvSUC11	AF021808.1	For: ATGGAGAAGCTCTGCAGGAA	Rev: TCAGTGCAGCAATCACAACA	300	1.93	GSVIVT01009254001
VvSUC12	AF021809.1	For: CGGATTGGATGGGTAGAGAA	Rev: AGCAAACCAAATGCACCTTC	500	1.91	GSVIVT01020031001
VvSUC27	AF021810.1	For: CTCTTCGACACCGATTGGAT	Rev: CAACCCCAGAACCACAGAGT	300	1.97	GSVIVT01034886001
VvSUS4	XM_002275119.1	For: GCTGGCTCAATCAGTTCCTC	Rev: CCAAGCCTCAAACAATGACA	500	2.01	GSVIVT01015018001
VvSUS2	XM_002271860.1	For: GGCTGGGGTTTATGGTTTCT	Rev: ATTTTGCCAGATCACGGAAC	300	2.06	GSVIVT01028043001
VvSUS6	XM_002270825.1	For: TATGGCTTCTGGAGGCAGTT	Rev: CCTTCGCCAATTTTCTGAAT	500	2.02	GSVIVT01029388001
VvSUS5	XM_002266984.2	For: GCAGGGATGATTCAGACCAT	Rev: CTTGCTTGTGTTCCGTGTTC	300	2.07	GSVIVT01035210001
VvGIN2	XM_002272733.1	For: ACGAATTTTTGGGAGCACAG	Rev: GATGCATGTCCTTCCACCTT	500	2.05	GSVIVT01001272001
CWINV	AY538262.1	For: TATTGACGGTGAAGCCCACT	Rev: AAAGCCTGGCTCTTCACTCA	300	1.99	GSVIVT01016869001
VvGIN1	XM_002265498	For: CAATGCCACTGGAGTGAATG	Rev: GGGATTTCTCAGCAACCAAA	500	1.94	GSVIVT01018625001
VvCAS2	XM_002283262.2	For: TTCACCCCAGTTGCATTTCT	Rev: CCGATCCTTCCTATGACCAC	300	2.05	GSVIVT01025362001
VvCAS1	XM_002271612.2	For: GCCTTGCGCTTTTTCATCTA	Rev: CTTCGCCTTCCAACAGAGAG	300	2.01	GSVIVT01001361001
VvCAS7	XM_002279310.2	For: GCTGGGAAGGGCTTATGAGT	Rev: GGCCTCTACTGAATGCCTGA	300	2.01	GSVIVT01020854001
VvCAS11	XM_002263721.2	For: GCTGAACAGAGCTGGGAAAC	Rev: CGCCGTACTGGAAAAAGAAG	300	1.97	GSVIVT01005204001
VvCAS5	XM_002274301.1	For: GCATGGTTCCCATTTGTCTC	Rev: TCATCACAGCCTCACTCTGC	300	1.96	GSVIVT01026489001
VvCAS10	XM_002275082.2	For: GATGCTGGGATGGGTATGAT	Rev: CCTGCAAGGATGATGGAGAT	300	2.03	GSVIVT01007560001

16SrRNA transcripts were detected in symptomatic samples (D) at an average quantification cycle (Cq) value (±SE) of 24.0 ± 0.5, while no amplicons of the *16SrRNA* gene were obtained in healthy (H) and recovered (R) samples. Molecular diagnosis confirmed the presence of stolbur in 98% of leaf samples collected from plants classified as symptomatic in the field.

TRANSMISSION ELECTRON MICROSCOPY

Transmission electron microscopy investigations showed different ultrastructural traits in the phloem of the grapevines, depending on their status (H, D, or R). The leaf tissues from H plants were well preserved. As expected, in the sieve elements of these plants phytoplasmas were not detected. P-protein was uniformly dispersed in the lumen of most sieve elements (**Figures 1A,B**, pp) and sieve pores were surrounded by a very thin stratum of callose (**Figure 1C**, arrows) or had callose collars that did not occlude their lumen (**Figure 1D**, arrows).

In D leaf tissues phytoplasmas were detected in the lumen of sieve tubes (**Figure 2A**, arrows). Their presence is associated with severe ultrastructural modifications of the phloem (**Figures 2B** through F). Many companion and phloem parenchyma cells showed plasmolysis and consequent cytoplasm condensation (**Figure 2B**, arrows), others were necrotized (**Figure 2B**, n). Increased thickness of the sieve-element walls (**Figure 2C**, arrows) and a large accumulation of callose at the sieve plates, plugging the sieve pores (**Figures 2D,E**, c), were also visible. Sieve elements were often collapsed (**Figure 2F**, arrows). Given the serious ultrastructural disorganization of D grapevine leaf tissues, in many cases it was not possible to discern P-proteins in the sieve-element lumen. When detectable, P-protein filaments were organized in electron-dense clumps (**Figure 2C**, pp).

In R plants the leaf tissue was, in general, well preserved and phytoplasmas were not observed in the sieve elements (**Figure 3**). P-protein was observed in the sieve-element lumen as condensed plugs (**Figures 3A,B**, pp) or as filaments (**Figures 3C,D**, pp) likely passing through the sieve pores (**Figures 3C,D**, arrows). Callose was also found in sieve tubes of R plants, forming collars around the sieve pores (**Figures 3C,D**, c), and in some cases occluding them (**Figures 3A,B**, c).

CALLOSE SYNTHASE GENE EXPRESSION ANALYSIS

Callose synthases synthesize the β-1,3-glucan (callose) that accumulates at the sieve plates. Callose is usually deposited at plasmodesmata and at sieve plates as a response to developmental cues and pathogen attack, with the aim of limiting spread of the infection or reinforcing the cell wall (Nakashima et al.,

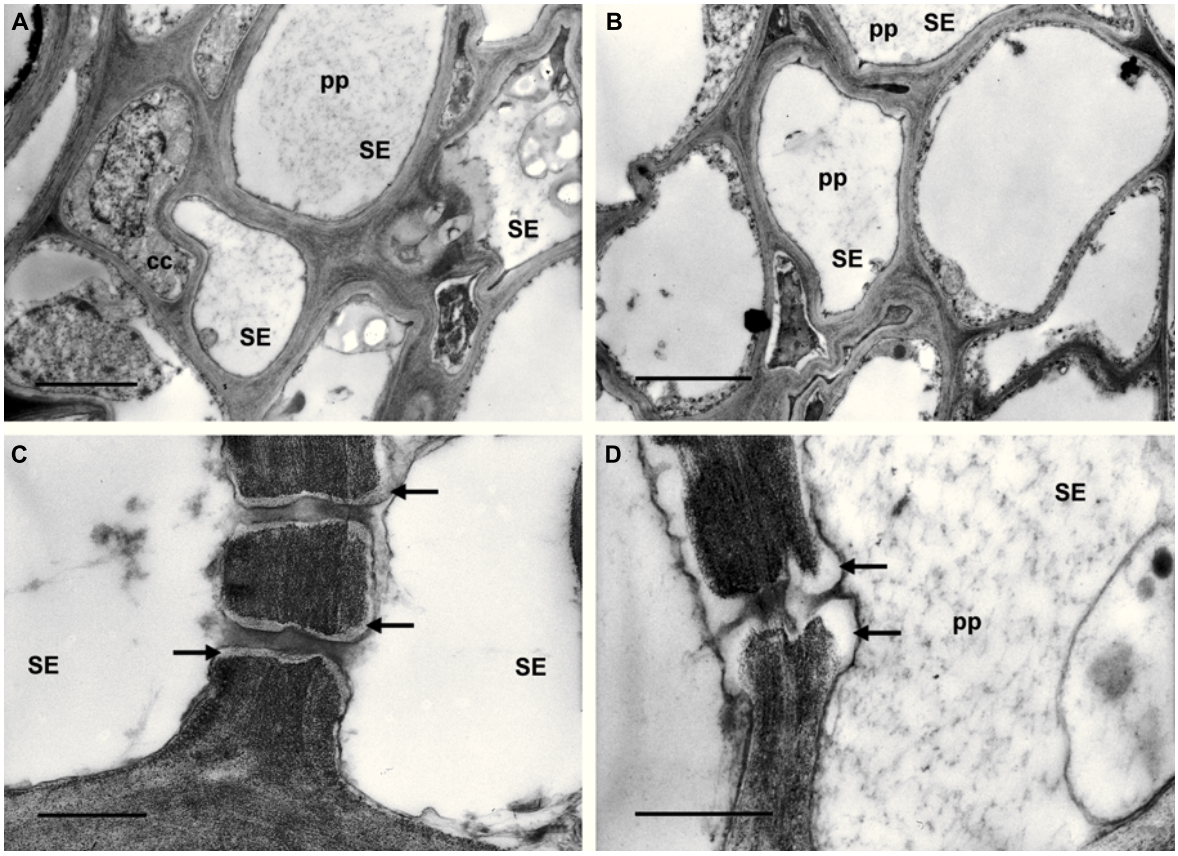

FIGURE 1 | Transmission electron micrographs of leaf tissues from healthy grapevines. (A,B) P-protein (pp) is uniformly dispersed in the lumen of most sieve elements (SE). **(C,D)** Sieve pores are surrounded by a thin callose layer (**C**, arrows) or show callose collars that do not occlude their lumen (**D**, arrows). In **(A)** and **(B)** bars correspond to 2 μm; in **(C)** and **(D)** bars correspond to 0.5 μm.

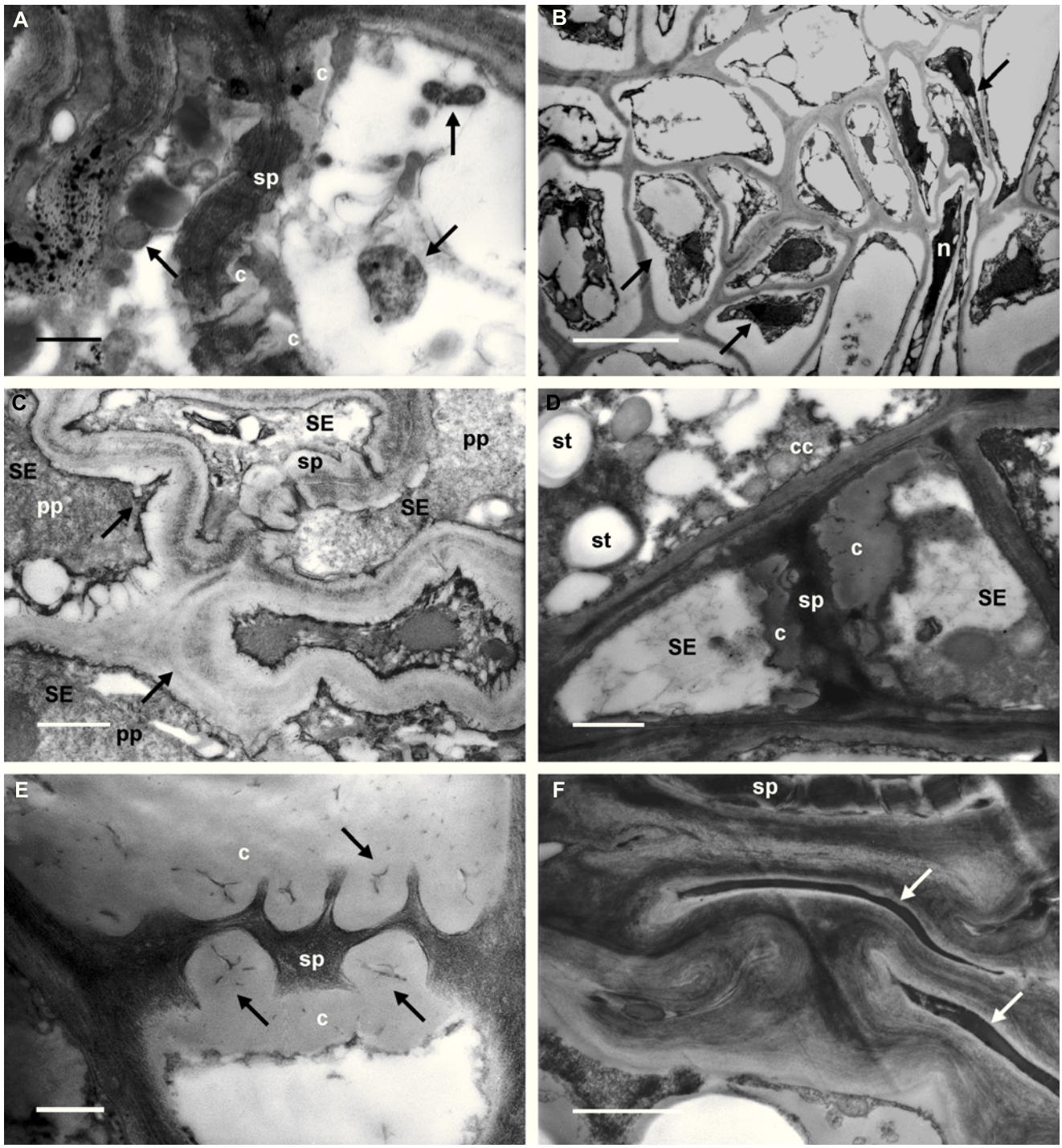

FIGURE 2 | Transmission electron micrographs of leaf tissues from diseased grapevines. (A) Phytoplasmas are visible in the lumen of sieve elements (arrows). Callose (c) is accumulated at the sieve plate (sp). **(B)** Phloem parenchyma and companion cells show plasmalemma detachment from the cell wall and condensed cytoplasm (arrows). Some cells are necrotized (n). **(C)** Sieve-element (SE) walls appear increased in thickness (arrows) and P-protein filaments (pp) are organized in dense plugs (sp: sieve plate). **(D,E)** A big accumulation of callose (c) at the sieve plates (sp), and occluding the sieve pores (**E**, arrows), is visible in infected samples. Starch granules (**D**, st) are detectable in the companion cell (cc; SE, sieve elements). **(F)** Groups of collapsed cells are present in the phloem of infected grapevine leaves (arrows); at the top, a sieve plate (sp) is still recognizable. In **(A)** and **(E)** bars correspond to 0.5 μm; in **(B)** bar corresponds to 5 μm. In **(C)**, **(D)**, and **(F)** bars correspond to 1 μm.

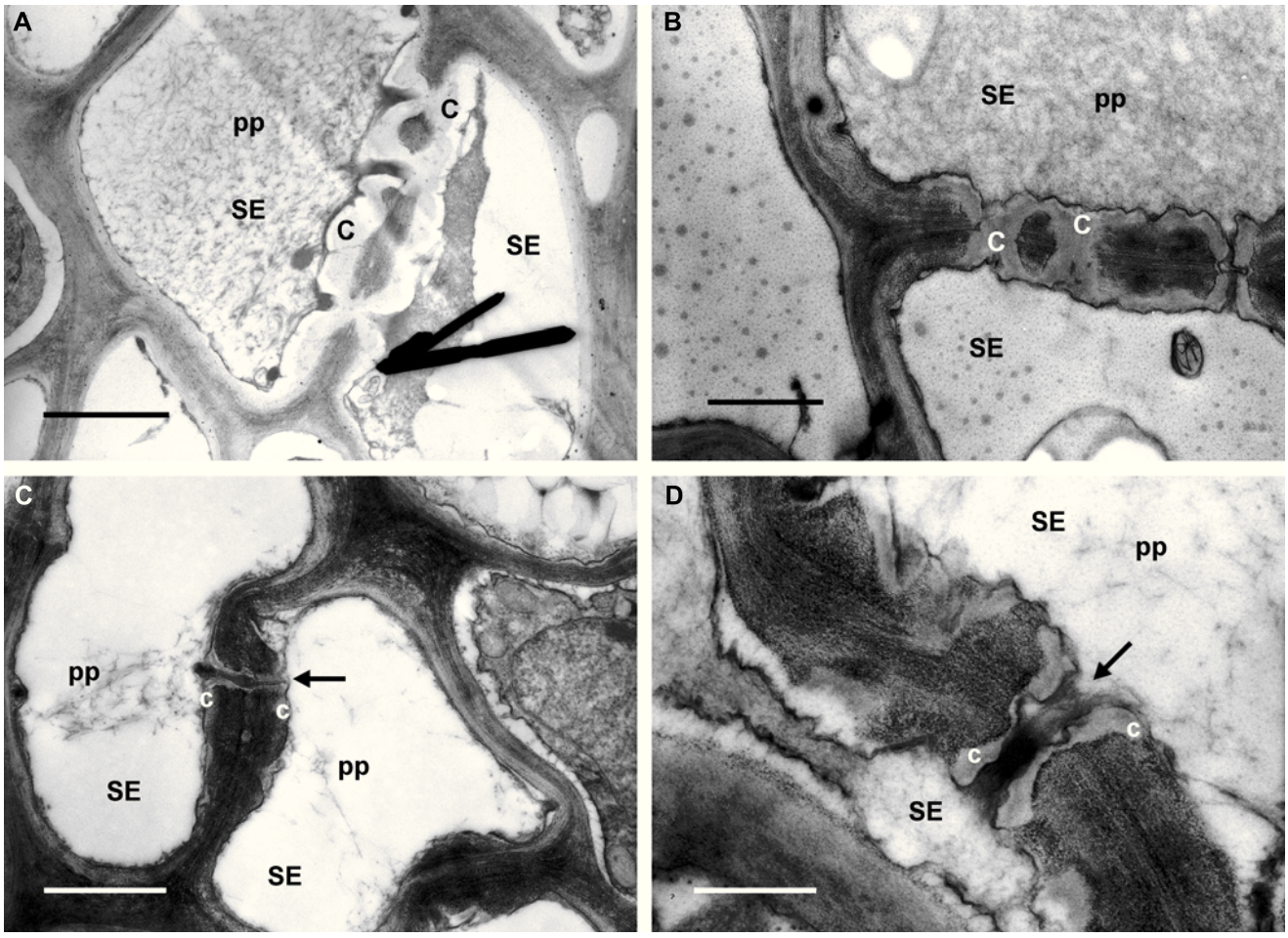

FIGURE 3 | Micrographs of leaf tissue from recovered grapevines. **(A,B)** P-protein (pp) in condensed form is present in the sieve-element (SE) lumen and also in association with callose collars around the sieve pores (c). **(C,D)** P-protein filaments (pp) are localized in the proximity of the sieve plate, and were likely passing through the sieve pores (arrows). Note the thin callose layers (c) surrounding the sieve pores (arrows). In **(A)**, **(B)**, and **(C)** bars correspond to 1 μm; in **(D)** bar corresponds to 0.5 μm.

2003). The *Arabidopsis* genome contains 12 callose synthases (CalS), also known as glucan synthase-like genes (GLS), which are each expressed in a tissue- and developmental stage-specific manner, as well as in response to different physiological and environmental inducers (Verma and Hong, 2001). Among seven genes encoding for callose synthases (called *CAS* in this work) that were identified from the Grape Genome browser[3] in the Grape 12X genome Database, six were expressed in leaves of D, R, and H plants, and only two were up-regulated in D leaves; *VvCAS2* (accession no. XM_002283262.2) and *VvCAS7* (accession no. XM_002279310.2; **Figure 4**). The expression levels of *VvCAS2* and *VvCAS7* were 9.9 and 5.5 MNE units, respectively, in D leaves, whereas the levels were 3.8 and 1.2, respectively, in H leaves. H and R samples did not show significant differences in *VvCAS2* and *VvCAS7* transcript levels (**Figure 4**). *VvCAS1* (accession no. XM_002271612.2) was the most highly expressed in leaves, and was not even differentially modulated in response to infection or after recovery, similar to the other expressed CAS isogenes (accession numbers and primers are reported in **Table 1**).

The CAS member of the family called *CAS8-like* (accession no. XM_002267920.2) showed a transcript level lower than 0.5% compared to the reference gene in all samples and is not shown.

EXPRESSION ANALYSIS OF GENES FOR SUCROSE TRANSPORT AND METABOLISM

Expression analysis of genes related to sucrose transport and metabolism was performed in midrib-enriched, fully expanded intact leaves of infected, recovered and healthy grapevines by real-time RT-PCR (**Figures 5** and **6**). In grapevines, as in most plants, sucrose is the carbohydrate for long distance transport, and glucose and fructose are the major soluble sugars that accumulate in sink organs like berries (Coombe, 1992). Accumulation of glucose and fructose is mainly attributed to three families of proteins: the sucrose transporters (Sauer, 2007), the acid (vacuolar or cell

[3]http://www.genoscope.cns.fr/externe/GenomeBrowser/Vitis/

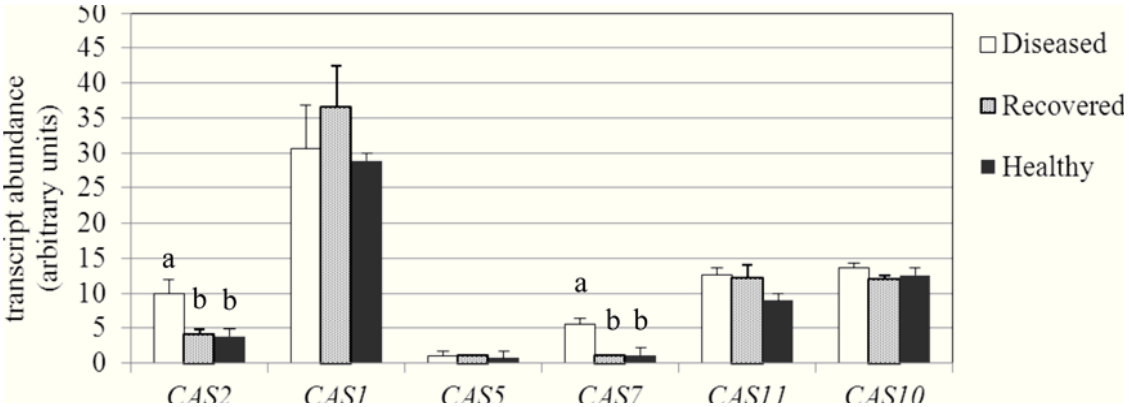

FIGURE 4 | Gene expression analysis of *Vitis vinifera* callose synthase (CAS) genes. Mean expression (MNE) values from at least three individuals for each plant group (H, D, R) plus standard errors are shown. Expression levels of the genes of interest are normalized to ubiquitin (*UBQ-L40* expression level = 100). Statistical comparisons were made using an ANOVA Tukey–Kramer Multiple Comparisons Test to evaluate significant differences. When indicated, different letters denote significant differences ($P < 0.05$).

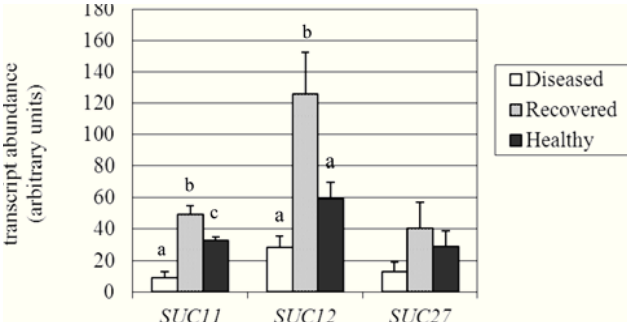

FIGURE 5 | Gene expression analysis of *Vitis vinifera* sucrose transporter (SUC) genes. Mean expression (MNE) values from at least three individuals for each plant group (H, D, R) plus standard errors are shown. Expression levels of the genes of interest are normalized to ubiquitin (*UBQ-L40* expression level = 100). When indicated, different letters denote significant differences ($P < 0.05$).

wall-associated) and neutral (cytosolic) invertases, and the SUSs (Koch, 2004).

The expression of the three sucrose transporter genes (*SUC27*, *SUC11*, and *SUC12*; Davies et al., 1999) investigated in the present work (accession numbers and primers are reported in **Table 1**) was confirmed as being decreased in D leaves, as already observed by Santi et al. (2013). *SUC12* was the most highly expressed transporter in the H leaves, but was down-regulated more than twofold in D samples, although the high variability among individuals negatively affected the significance of the difference (**Figure 5**). Our analysis was extended to the recovered plant leaves, where *SUC12* was more than fourfold (125.9 vs 28.4 MNE units) and twofold (125.9 vs 59.2 MNE units) higher than in D and H samples, respectively, due to it being highly affected during recovery from the pathogen. The *SUC12* gene belongs to the type IIA cluster of sucrose transporters (Reinders et al., 2012), which include the *Arabidopsis SUT2/SUC3* gene. A role for *SUC12* in sucrose unloading into grapevine berry tissues was proposed by Afoufa-Bastien et al. (2010). In accordance with this role, *SUC12* was almost undetectable in phloem cells (including sieve elements, companion cells, and surrounding parenchyma cells) that had been captured by laser microdissection from source leaves of grapevine (Santi et al., 2013). Similarly, *SUC11* expression was shown to be 3.5-fold inhibited in D leaves (8.9 vs 32.9 MNE units) compared to H leaves, while it was up-regulated in R leaves, where the transcript level (49.3 MNE units) was more than fivefold higher than in D leaves (**Figure 5**). The grapevine *SUC11* belongs to the type III group of low affinity sucrose transporters and its *Arabidopsis* ortholog is *ATSUC4* (Reinders et al., 2012). *ATSUC4* is localized at the tonoplast of *Arabidopsis* mesophyll cells (Endler et al., 2006). *SUC11* transcripts were found to be expressed at a very low level in the phloem tissue of source leaves (Santi et al., 2013). When analyzed in R leaves, the *SUC27* gene also seemed to be more induced (threefold) than in D leaves, although the difference between R leaves, and D and H leaves was not significant (**Figure 5**). The *SUC27* gene belongs to the type I cluster of sucrose transporters, including transporters necessary for loading sucrose into the phloem, among which the *Arabidopsis ATSUC2* is also grouped (Reinders et al., 2012). *SUC27* is the only sucrose transporter that is expressed in the phloem tissue of source leaves of grapevine and was seen to be dramatically down-regulated in the presence of stolbur (Santi et al., 2013). The phloem specificity of *SUC27* gene expression and thus the dilution of its transcripts by functionally different tissues could explain why the differences observed in the leaf samples were not significant. In conclusion, the examined *SUC* genes confirmed an overall expression decrease in stolbur-infected leaves, even if to a different extent, while they were up-regulated during the recovery from BN compared to H leaves.

Sucrose synthase has a dual role in directing carbon to polysaccharide biosynthesis and in conserving energy throughout the production of adenylated-glucose (Winter and Huber, 2000; Koch, 2004). Its cleavage activity produces fructose and both uridine diphoshate-glucose (UDPG) and adenosine diphosphate-glucose (ADPG); ADPG is necessary for starch biosynthesis, while UDPG

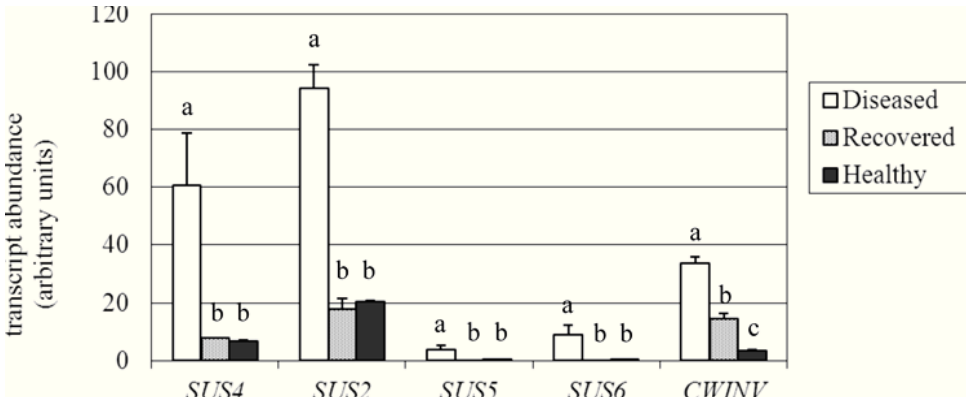

FIGURE 6 | Gene expression analysis of *Vitis vinifera* sucrose synthase (SUS) and cell wall invertase (cwINV) genes. Mean expression (MNE) values from at least three individuals for each plant group (H, D, R) plus standard errors are shown. Expression levels of the genes of interest are normalized to ubiquitin (*UBQ-L40* expression level = 100). When indicated, different letters denote significant differences ($P < 0.05$).

is necessary for cell wall and glycoprotein biosynthesis (Baroja-Fernández et al., 2012). UDPG is also used by callose synthase (CAS) as a glucose donor to the growing polymer chain (Amor et al., 1995). Among *SUS* isoforms (at least five in grapevine), four were found to be expressed in leaves and thus were investigated by real-time RT-PCR (accession numbers and primers are reported in **Table 1**). Transcripts of a fifth *SUS* (accession no. XM_002271494) were almost undetectable in leaves and are thus not shown. Although expressed at different levels in H leaves (**Figure 6**), all the examined SUS genes were significantly up-regulated in the presence of the pathogen, as previously observed just for the *VvSUS4* gene (named *VvSUS2-like* in Santi et al., 2013). The analysis of leaves from plants recovered from infection showed the expression of all the investigated *SUS* genes at the level of healthy leaves. The most expressed SUS in H and R leaves was *VvSUS2* (about 19 MNE units), which was 4.7-fold induced in D leaves. This gene of the family (annotated as *SUS2* with the accession no. XM_002271860.1 in the NCBI database) shares 82 and 79% identity (at the amino acid level) with *ATSUS3* (AT4G02280.1) and *ATSUS2* (AT5G49190.1), respectively. In addition, *VvSUS4* was investigated by real-time RT-PCR in leaves where it had increased approximately ninefold in response to stolbur infection (60.8 vs 6.6 and 7.9 MNE units in H and R leaves). This gene shares 82 and 81% identity at the level of amino acidic sequence with *Arabidopsis SUS4* (AT3G43190.1) and *SUS3*, respectively (Bieniawska et al., 2007), and was found to be highly affected by stolbur alongside the *SUC27* transporter in phloem cells (Santi et al., 2013). Two other *SUS* genes were examined, *VvSUS5* and *VvSUS6*; although barely expressed in H and R leaves, they were both significantly up-regulated in D leaves like the other SUS genes.

Accumulation of glucose and fructose in grapevine is mainly attributed to the cleavage activity of invertases (Davies and Robinson, 1996). The acid soluble vacuolar invertases *GIN1* and *GIN2* (Davies and Robinson, 1996) were investigated. In our experiment *GIN1* and *GIN2* were expressed at a very low level (on average around 0.3 MNE units) both in H and R leaves, and only for *GIN2* was it possible to detect an up-regulation of the gene in D conditions (data not shown). Low expression of *GIN* genes depends on the fact that their transcripts decline during leaf development (Davies and Robinson, 1996) and in our experiments could reflect the use of mature leaves. Therefore, our attention was focused on the expression of the acid cell wall invertase *VvcwINV* (accession no. AY538262.1). We found that the expression of *VvcwINV* was more than ninefold and fourfold induced in stolbur-infected leaves and recovered leaves, respectively, in comparison with healthy leaves (**Figure 6**).

DISCUSSION

The phloem is the transmission route for photoassimilates in plants, but it is also a preferred destination for plant pathogens because it is a pathway for their movement and spread inside the host.

Phytoplasmas are phloem-restricted pathogens: knowledge about their ability to interact with sieve elements is essential for understanding the relationships with the whole host plant during both the symptomatic and the following "recovery" phases. Given that "recovery" is a natural, spontaneous event, and not reproducible artificially, an explanation of the phenomenon is not simple. However, this phenomenon is pivotal to counteracting phytoplasmas because there are no effective treatments available. This study confirmed that recovered plants are not colonized by phytoplasmas in the canopy, as already reported in literature (Carraro et al., 2004; Musetti et al., 2007), therefore, regarding the epidemiological and practical aspects, recovered individuals exhibit a performance similar to healthy, never infected plants (Osler et al., 2000).

For the first time we have investigated and reported modifications occurring in the sieve elements of grapevine during BN infection and "recovery." An integrated approach has been adopted through the combined use of ultrastructural and gene expression analyses of leaf tissues.

Ultrastructural observation of phloem tissues is problematic, because the excision of the samples for electron microscope preparation provokes artifacts due to the immediate wounding response in the sieve elements. To minimize this risk, a gentle method for

sample preparation was used, as described by Ehlers et al. (2000). The method allowed us to compare the ultrastructure of the sieve elements and the sieve plates in H, D, and R grapevine leaf tissues and observing differences that are mostly related to callose deposition.

Interestingly, the ultrastructural characteristics found in the sieve elements of R plants were not different from those observed in the H plants, apart from callose.

Callose accumulation is one of the major ultrastructural characteristics of sieve elements of D grapevines. Also, in the case of BN-infected grapevines, phytoplasma-induced callose could be responsible for sieve-tube occlusion and mass flow impairment (linked to the expression of typical BN disease symptoms) as recently demonstrated in a different plant/phytoplasma interaction (Musetti et al., 2013).

Callose depositions in sieve elements of R plants appeared thicker than those observed in H grapevines and, only in some sporadic cases, they occluded the pores of the sieve plates. It seems that these ultrastructural characteristics are compatible with the correct physiology of R plants that are asymptomatic and look identical to H plants. It has been demonstrated that callose deposition in the phloem is not only associated with responses to wounding or to pathogen spread but also that it takes part in the normal processes of phloem maturation in intact plants, influencing the length of the sieve-plate pores and determining the flow characteristics (Barratt et al., 2011; Xie et al., 2011).

Ultrastructural observations about callose deposition in grapevine are in accordance with the results obtained from the gene expression analyses, demonstrating that at least two different isoforms of callose synthase genes are triggered in grapevine during phytoplasma infection and that they return to a lower level (not different from the H plants) during the "recovery" phase.

Most genes encoding CAS, identified in several plant species, are members of multigene families (Verma and Hong, 2001). Multiple *CAS* genes may have evolved in higher plants for callose synthesis at different locations and in response to different physiological and developmental signals (Chen and Kim, 2009). Six *CAS* genes were expressed in the leaves of H, D, and R grapevines. One of these, *VvCAS7*, which is an ortholog of the *Arabidopsis CalS7* that is responsible for callose deposition in the phloem (Xie et al., 2011), was significantly up-regulated in D leaf tissues compared to H and R plants, in accordance with observations by TEM. The second up-regulated gene in D grapevines was *VvCAS2*, which is induced when its expression is examined in the whole leaf (as previously reported by Hren et al., 2009a) but not affected by stolbur in the phloem (Santi et al., 2013).

Our results suggested that at least two CAS genes could be coordinately expressed with SUS genes, which were up-regulated in D leaves but showed a similar expression level in R and H leaves. As the synthesis of callose requires several steps, and hence a single peptide may not be able to perform all the necessary functions, the existence of a callose synthase complex has been suggested (Verma and Hong, 2001). It has been demonstrated that the callose synthase complex has a transmembrane domain and hydrophilic loop interacting with different proteins, related to sucrose synthesis and metabolism, among which SUS is included (Verma and Hong, 2001). The function of some of these proteins may be involved in controlling CAS activity, particularly in response to biotic/abiotic signals (Verma and Hong, 2001). At confirmation of the link between CAS and SUS, Barratt et al. (2009) reported that callose at the sieve plates is reduced significantly in *Arabidopsis* double mutants for the phloem-specific *SUS5* and *SUS6*.

CASs are membrane-associated enzymes (Chen and Kim, 2009). Like several plant membrane-associated polysaccharide synthases (among which cellulose synthase, callose synthase, xyloglucan glucan synthase and multiple related glycan synthases) the CASs have the topological requirements to couple synthesis with the transport of callose into the extracellular matrix and thus are included in the group of dual-function cell wall glycan synthases (Davis, 2012).

The anomalous deposition of callose in the infected phloem tissue and the altered modulation of two callose synthase genes were only a part of the large modifications at the transcriptional level observed for sucrose transport and metabolism of the leaf. Accumulations of soluble carbohydrates and starch in source leaves, complemented by a decrease of sugar levels in sink organs, have been reported for periwinkle, tobacco, and coconut palm infected by phytoplasmas (Lepka et al., 1999; Maust et al., 2003). We previously demonstrated that, analogously to other obligate biotrophs that need to acquire most nutrients from the host plant, the stolbur phytoplasma induces the establishment of a carbohydrate sink in the phloem of the leaf, thus altering the normal pattern of sugar partitioning of a source leaf (Santi et al., 2013). In fact, in laser-microdissected phloem tissue of stolbur-infected leaves, we observed a dramatic decrease of expression of *SUC27*, the grapevine transporter mediating sucrose apoplasmic loading into the phloem, and a huge up-regulation of a SUS gene (*VvSUS4*, Santi et al., 2013). A co-regulation of both sucrose transport and cleavage would be advantageous for the pathogen as both responses are crucial to access hexoses, which could be the only usable carbon source (Christensen et al., 2005). In the present work we analyzed the expression of the *SUC* genes together with four *SUS* genes and the cell wall invertase gene, *cwINV*, in midrib-enriched leaves of D and H plants, extending our investigation to leaves of plants recovered from the disease. Even though they changed to a different extent, all the *SUC* genes were down-regulated in D leaves as expected, confirming that the stolbur-induced establishment of a carbohydrate sink in the phloem alters sucrose partitioning in tissues distal to the infection site. A role for *SUC11* and *SUC12* in sucrose accumulation in the vacuole and in sucrose unloading into sink tissues (berry), respectively, has been suggested by Afoufa-Bastien et al. (2010). In accordance the above finding, all the examined *SUS* genes together with *cwINV* were up-regulated in D leaves.

Sucrose synthase utilizes sucrose to produce fructose and nucleoside diphosphate-glucose (mainly UDPG and ADPG; Winter and Huber, 2000) and thus has a role in producing metabolic substrates, in conserving energy in the form of adenylated-glucose, and in initiating sugar signaling (Koch, 2004). SUS is encoded by a small family of genes that are divergent and differently

expressed. The *Arabidopsis* genome contains six SUS genes whose exact function remains unknown because most mutants show few observable effects (Bieniawska et al., 2007). Four grapevine genes were found expressed in leaves, although at a different level, and all were up-regulated in the presence of the phytoplasma confirming the pivotal role of this gene family in both carbohydrate partitioning and plant–pathogen interactions. SUS is also believed to play a major role in both starch and cellulose biosynthesis (Baroja-Fernández et al., 2012). The UDPG produced by a membrane-associated form of SUS is thought to be used directly as a substrate for cellulose synthase in the rosette complex where SUS is an integral component (Amor et al., 1995; Fujii et al., 2010). As discussed above, UDPG is also used as a glucose donor to the growing polymer chain by callose synthases, similar to cellulose synthases.

Cell wall invertase (cwINV), a sucrose-splitting enzyme that produces hexoses, is a sink-specific enzyme, normally found in various kinds of carbohydrate consuming tissues, and its activity is usually low in source leaves. Extracellular invertases are important for apoplastic phloem unloading and are key enzymes in determining sink strength (Roitsch and Gonzàlez, 2004). The inhibition of phloem loading and the induction of SUS genes that were observed in stolbur-infected leaves were expected to be accompanied by elevated cwINV activity, as already observed in *Arabidopsis* (Fotopoulos et al., 2003; Chandran et al., 2010), wheat (Sutton et al., 2007), and grapevine leaves (Hayes et al., 2010) when infected by biotrophic fungi. In the case of grapevine, *VvcwINV* was highly induced in coordination with the hexose transporter, *VvHT5*, by powdery and downy mildew infection. Interestingly, this response, which was also observed with abiotic stress (such as wounding), mirrored the response observed when leaves were treated with ABA (abscisic acid), suggesting the concept that the transition from source to sink following the induction of *cwINV* and *HT* genes is part of a general ABA-mediated stress response (Hayes et al., 2010). It is well established that cwINVs are transcriptionally regulated by hexoses (Roitsch and Gonzàlez, 2004), but interestingly, both ABA-responsive (ABRE) and hexose-responsive (SURE) elements were identified in the promoter of *VvcwINV* (Hayes et al., 2010). It is likely that a coordinated interaction of sugar and hormonal pathways in plants leads to effective immune responses (Bolouri-Moghaddam and Van den Ende, 2012).

It is known that plant cell wall invertases have a pivotal role in plant defense (Roitsch and Gonzàlez, 2004; Berger et al., 2007). Genes encoding cwINV are induced by elicitors in different plant species (Roitsch et al., 2003). Several lines of evidence suggest that plants establish high hexose levels in response to invading pathogens, which in turn support defense responses of the host. Indeed, RNA interference knockdown of cwINV in tobacco leaves inhibited defense responses such as callose deposition, induction of pathogenesis-related proteins, and hydrogen peroxide-mediated cell death against the biotrophic oomycete *Phytophthora nicotianae* (Essmann et al., 2008). Within sugar pools, the cellular sucrose:hexose ratio is emerging as an important parameter determining cellular responses (Bolouri-Moghaddam and Van den Ende, 2012).

Regarding the "recovery" phenomenon, we analyzed the expression of the *SUC* genes together with four *SUS* genes and the cell wall invertase gene, *cwINV*, in leaves of plants recovered from the disease. When analyzed in R leaves, the expression of *SUC* transporters was higher than in leaves of D plants. Similarly, the gene encoding for the cell wall invertase was up-regulated both in D and R samples. On the other hand, the expression of all the SUS genes was found to be at the same level as leaves from H plants. This finding seems to suggest a direct relationship between phytoplasma and, in particular, SUSs that restore the level of expression of H plants when the pathogen disappears.

Recovered plants seem to fully establish the carbohydrate source function of leaves; moreover, recovered plants seem to acquire increased transport ability and defense signaling. This finding seems to be confirmed by the performance of field growing plants that become resistant to new attaches when recovered from phytoplasma diseases (Osler et al., 2000). Sugars such as glucose, fructose, and sucrose are recognized as signaling molecules in plants, in addition to their roles as carbon and energy sources (Koch, 2004; Rolland et al., 2006). Sucrose specifically stimulates the accumulation of anthocyanins (Solfanelli et al., 2006), which can act as antimicrobial agents in the plant defense system against pathogen invasion (Winkel-Shirley, 2001). Sugar signals, in particular a high sucrose:hexose ratio, may contribute to immune responses and probably function as priming molecules for more rapid and robust activation of defense to biotic or abiotic stress (Bolouri-Moghaddam and Van den Ende, 2012).

Stolbur is not detected in leaves of recovered grapevines, which is similar to observations in the crown of apple trees recovered from the phytoplasma-associated-Apple Proliferation disease (Osler et al., 2000; Carraro et al., 2004). For this reason, the signal triggering the up-regulation of sucrose transport and apoplastic cleavage must originate from organs distal from the leaves. Whereas the pathogen has been detected in roots of recovered apple trees (Carraro et al., 2004), to date no data are available for grapevine roots, probably because the stolbur titer is very low and diagnostic tools are still not sensitive enough. Concerning the features of the signal molecule, it is noteworthy that sugar production and use can be controlled in part at the transcriptional level by sugars themselves.

CONCLUSION

Phytoplasmas interfere with plant processes, leading to severe changes in plant development and physiology, but to date the biochemical and molecular interactions between phytoplasmas and their hosts remain largely unexplored. "Recovery" from the disease is often observed, but the molecular basis is almost completely unknown as well.

The present work has unveiled structural and physiological modifications occurring in the grapevine leaf phloem, which is the site where phytoplasmas live, multiply and spread. Our findings have demonstrated that phloem is severely affected by phytoplasma infection. Callose accumulates anomalously in the infected sieve elements, but its deposition is only a part of the large

number of modifications at the transcriptional level observed for sucrose transport and metabolism in the whole leaf. The decreased sucrose transport observed at the transcriptional level, as well as the increased sucrose cleavage mediated by cell wall invertase and SUS, confirm the establishment of a stolbur-induced carbohydrate sink in the leaves. Plants that have recovered from the disease seem to fully restore the carbohydrate source function of leaves and acquire increased transport ability and defense signaling.

ACKNOWLEDGMENTS

We would like to thank Paolo Ermacora (DISA, University of Udine, Italy) for the excellent work of monitoring BN in the vineyard and Marta Martini (DISA, University of Udine, Italy) for primers used in stolbur 16rRNA detection experiments. We thank Dr. Laurence Cantrill (Out of site English, Sydney) for English revision. This research was funded by AGER project n° 2010-2106 "Grapevine Yellows: innovative technologies for the diagnosis and the study of plant/pathogen interactions."

REFERENCES

Afoufa-Bastien, D., Medici, A., Jeauffre, J., Coutos-Thévenot, P., Lemoine, R., Atanassova, R., et al. (2010). The *Vitis vinifera* sugar transporter gene family: phylogenetic overview and macroarray expression profiling. *BMC Plant Biol.* 10:245. doi: 10.1186/1471-2229-10-245

André, A., Maucourt, M., Moing, A., Rolin, D., and Renaudin, J. (2005). Sugar import and phytopathogenicity of *Spiroplasma citri*: glucose and fructose play distinct roles. *Mol. Plant Microbe Interact.* 18, 33–42. doi: 10.1094/MPMI-18-0033

Albertazzi, G., Milc, J., Caffagni, A., Francia, E., Roncaglia, E., Ferrari, F., et al. (2009). Gene expression in grapevine cultivars in response to Bois Noir phytoplasma infection. *Plant Sci.* 176, 792–804. doi: 10.1016/j.plantsci.2009.03.001

Altschul, S. F., Madden, T. L., Schaffer, A. A., Zhang, J., Zhang, Z., Miller, W., et al. (1997). Gapped BLAST and PSIBLAST: a new generation of protein database search programs. *Nucleic Acids Res.* 25, 3389–3402. doi: 10.1093/nar/25.17.3389

Amor, Y., Haigler, C. H., Johnson, S., Wainscott, M., and Delmer, D. P. (1995). A membrane-associated form of sucrose synthase and its potential role in synthesis of cellulose and callose in plants. *Proc. Natl. Acad. Sci. U.S.A.* 92, 9353–9357. doi: 10.1073/pnas.92.20.9353

Baroja-Fernández, E., Muñoza, F. G., Lia, J., Bahajia, A., Almagroa, G., Monteroa, M., et al. (2012). Sucrose synthase activity in the sus1/sus2/sus3/sus4 *Arabidopsis* mutant is sufficient to support normal cellulose and starch production. *Proc. Natl. Acad. Sci. U.S.A.* 109, 321–326. doi: 10.1073/pnas.1117099109

Barratt, D. H. P., Derbyshire, P., Findlay, K., Pike, M., Wellner, N., Lunn, J., et al. (2009). Normal growth of *Arabidopsis* requires cytosolic invertase but not sucrose synthase. *Proc. Natl. Acad. Sci. U.S.A.* 106, 13124–13129. doi: 10.1073/pnas.0900689106

Barratt, D. H. P., Kolling, K., Graf, A., Pike, M., Calder, G., Findlay, K., et al. (2011). Callose synthase GLS7 is necessary for normal phloem transport and inflorescence growth in *Arabidopsis*. *Plant Physiol.* 155, 328–341. doi: 10.1104/pp.110.166330

Belli, G., Bianco, P. A., and Conti, M. (2010). Grapevine yellows in Italy: past, present and future. *J. Plant Pathol.* 92, 303–326.

Berger, S., Sinha, A. K., and Roitsch, T. (2007). Plant physiology meets phytopathology: plant primary metabolism and plant–pathogen interactions. *J. Exp. Bot.* 58, 4019–4026. doi: 10.1093/jxb/erm298

Bertamini, M., Nedunchezhian, N., Tomasi, F., and Grando, M. S. (2002). Phytoplasma [Stolbur-subgroup (Bois Noir-BN)] infection inhibits photosynthetic pigments, ribulose-1,5-bisphosphate carboxylase and photosynthetic activities in field grown grapevine (*Vitis vinifera* L. cv. Chardonnay) leaves. *Physiol. Mol. Plant Pathol.* 61, 357–366. doi: 10.1006/pmpp.2003.0449

Bieniawska, Z., Barratt, D. H. P., Garlick, A. P., Thole, V., Kruger, N. J., Martin, C., et al. (2007). Analysis of the sucrose synthase gene family in *Arabidopsis*. *Plant J.* 49, 810–828. doi: 10.1111/j.1365-313X.2006.03011.x

Bolouri-Moghaddam, M. R., and Van den Ende, W. (2012). Sugars and plant innate immunity. *J. Exp. Bot.* 63, 3989–3998. doi: 10.1093/jxb/ers129

Braun, E. J., and Sinclair, W. A. (1978). Translocation in phloem necrosis-diseased American elm seedlings. *Phytopathology* 68, 1733–1737. doi: 10.1094/Phyto-68-1733

Carraro, L., Ermacora, P., Loi, N., and Osler, R. (2004). The recovery phenomenon in apple proliferation infected apple trees. *J. Plant Pathol.* 86, 141–146.

Chandran, D., Inada, N., Hather, G., Kleindt, C. K., and Wildermuth, M. C. (2010). Laser microdissection of *Arabidopsis* cells at the powdery mildew infection site reveals site-specific processes and regulators. *Proc. Natl. Acad. Sci. U.S.A.* 107, 460–465. doi: 10.1073/pnas.0912492107

Chen, X.-Y., and Kim, J.-Y. (2009). Callose synthesis in higher plants. *Plant Signal. Behav.* 4, 489–492. doi: 10.4161/psb.4.6.8359

Christensen, N. M., Axelsen, K. B., Nicolaisen, M., and Schulz, A. (2005). Phytoplasmas and their interactions with hosts. *Trends Plant Sci.* 10, 526–535. doi: 10.1016/j.tplants.2005.09.008

Christensen, N. M., Nicolaisen, M., Hansen, M., and Schulz, A. (2004). Distribution of phytoplasmas in infected plants as revealed by real-time PCR and bioimaging. *Mol. Plant Microbe Interact.* 17, 1175–1184. doi: 10.1094/MPMI.2004.17.11.1175

Coombe, B. C. (1992). Research on development and ripening of the grapeberry. *Am. J. Enol. Vitic.* 43, 101–110.

Davies, C., and Robinson, S. P. (1996). Sugar accumulation in grape berries: cloning of two putative vacuolar invertase cDNAs and their expression in grapevine tissues. *Plant Physiol.* 111, 275–283. doi: 10.1104/pp.111.1.275

Davies, C., Wolf, T., and Robinson, S. P. (1999). Three putative sucrose transporters are differentially expressed in grapevine tissues. *Plant Sci.* 147, 93–100. doi: 10.1016/S0168-9452(99)00059-X

Davis, J. K. (2012). Combining polysaccharide biosynthesis and transport in a single enzyme: dual-function cell wall glycan synthases. *Front. Plant Sci.* 3:138. doi: 10.3389/fpls.2012.00138 doi: 10.3389/fpls.2012.00138

Ehlers, K., Knoblauch, M., and van Bel, A. J. E. (2000). Ultrastructural features of well-preserved and injured sieve elements: minute clamps keep the phloem transport conduits free for mass flow. *Protoplasma* 214, 80–92. doi: 10.1007/BF02524265

Endeshaw, S. T., Murolo, S., Romanazzi, G., and Neri, D. (2012). Effects of Bois Noir on carbon assimilation, transpiration, stomatal conductance of leaves and yield of grapevine (*Vitis vinifera*) cv. Chardonnay. *Physiol. Plant.* 145, 286–295. doi: 10.1111/j.1399-3054.2012.01576.x

Endler, A., Meyer, S., Schelbert, S., Schneider, T., Weschke, W., Peters, S. W., et al. (2006). Identification of a vacuolar sucrose transporter in barley and *Arabidopsis* mesophyll cells by a tonoplast proteomic approach. *Plant Physiol.* 141, 196–207. doi: 10.1104/pp.106.079533

Essmann, J., Schmitz-Thom, I., Schon, H., Sonnewald, S., Weis, E., and Scharte, J. (2008). RNA interference-mediated repression of cell wall invertase impairs defense in source leaves of tobacco. *Plant Physiol.* 147, 1288–1299. doi: 10.1104/pp.108.121418

Firrao, G., Gibb, K., and Stereten, C. (2005). Short taxonomic guide to the genus '*Candidatus phytoplasma*'. *J. Plant Pathol.* 87, 249–263. doi: 10.4454/jpp.v87i4.926

Fotopoulos, V., Gilbert, M. J., Pittman, J. K., Marvier, A. C., Buchanan, A. J., Sauer, N., et al. (2003). The monosaccharide transporter gene, AtSTP4 and the cell-wall invertase, at beta fruct1, are induced in *Arabidopsis* during infection with the fungal biotroph *Erysiphe cichoracearum*. *Plant Physiol.* 132, 821–829. doi: 10.1104/pp.103.021428

Fujii, S., Hayashi, T., and Mizuno, K. (2010). Sucrose synthase is an integral component of the cellulose synthesis machinery. *Plant Cell Physiol.* 51, 294–301. doi: 10.1093/pcp/pcp190

Furch, A. C. U., Hafke, J. B., Schulz, A., and van Bel, A. J. E. (2007). $Ca2^{+}$-mediated remote control of reversible sieve tube occlusion in *Vicia faba*. *J. Exp. Bot.* 58, 2827–2838. doi: 10.1093/jxb/erm143

Hayes, A., Feechan, A., and Dry, I. B. (2010). Involvement of abscisic acid in the coordinated regulation of a stress-inducible hexose transporter (VvHT5) and a cell wall invertase in grapevine in response to biotrophic fungal infection. *Plant Physiol.* 153, 211–221. doi: 10.1104/pp.110.154765

Hren, M., Nikolic, P., Rotter, A., Blejec, A., Terrier, N., Ravnikar, M., et al. (2009a). Bois noir phytoplasma induces significant reprogramming of the leaf transcriptome in the field grown grapevine. *BMC Genomics*

10:460. doi: 10.1186/1471-2164-10-460

Hren, M., Ravnikar, M., Brzin, J., Ermacora, P., Carraro, L., Bianco, P. A., et al. (2009b). Induced expression of sucrose synthase and alcohol dehydrogenase I genes in phytoplasma-infected grapevine plants grown in the field. *Plant Pathol.* 58, 170–180. doi: 10.1111/j.1365-3059.2008.01904.x

Kartte, S., and Seemüller, E. (1991). Histopathology of apple proliferation in *Malus taxa* and hybrids of different susceptibility. *J. Phytopathol.* 131, 149–160. doi: 10.1111/j.1439-0434.1991.tb04740.x

Knoblauch, M., and van Bel, A. J. E. (1998). Sieve tubes in action. *Plant Cell* 10, 35–50.

Koch, K. (2004). Sucrose metabolism: regulatory mechanisms and pivotal roles in sugar sensing and plant development. *Curr. Opin. Plant Biol.* 7, 235–246. doi: 10.1016/j.pbi.2004.03.014

Lee, I. M., Davis, R. E., and Gundersen-Rindal, D. E. (2000). Phytoplasma: phytopathogenic mollicutes. *Annu. Rev. Microbiol.* 54, 221–255. doi: 10.1146/annurev.micro.54.1.221

Lepka, P., Stitt, M., Moll, E., and Seemüller, E. (1999). Effect of phytoplasmal infection on concentration and translocation of carbohydrates and amino acids in periwinkle and tobacco. *Physiol. Mol. Plant Pathol.* 55, 59–68. doi: 10.1006/pmpp.1999.0202

Margaria, P., and Palmano, S. (2011). Response of the *Vitis vinifera* L. cv. 'Nebbiolo' proteome to Flavescence dorée phytoplasma infection. *Proteomics* 11, 212–224. doi: 10.1002/pmic.201000409

Maust, B. E., Espadas, F., Talavera, C., Aguilar, M., Santamaría, J. M., and Oropeza, C. (2003). Changes in carbohydrate metabolism in coconut palms infected with the lethal yellowing phytoplasma. *Phytopathology* 93, 976–981. doi: 10.1094/PHYTO.2003.93.8.976

Muller, P. Y., Janovjak, H., Miserez, A. R., and Dobbie, Z. (2002). Processing of gene expression data generated by quantitative realtime RT-PCR. *Biotechniques* 32, 1372–1379.

Musetti, R., Buxa, S. V., De Marco, F., Loschi, A., Polizzotto, R., Kogel, K.-H., et al. (2013). Phytoplasma-triggered $Ca2^{+}$ influx is involved in sieve-tube blockage. *Mol. Plant Microbe Interact.* 26, 379–386. doi: 10.1094/MPMI-08-12-0207-R

Musetti, R., and Favali, M. A. (1999). Histological and ultrastructural comparative study between *Prunus* varieties of different susceptibility to plum leptonecrosis. *Cytobios* 99, 73–82.

Musetti, R., Favali, M. A., Carraro, L., and Osler, R. (1994). Histological detection of Mycoplasma-like organisms causing leptonecrosis in plum trees. *Cytobios* 78, 81–90.

Musetti, R., Marabottini, R., Badiani, M., Martini, M., Sanità di Toppi, L., Borselli, S., et al. (2007). On the role of H2O2 in the recovery of grapevine (*Vitis vinifera* cv. Prosecco) from Flavescence dorée disease. *Funct. Plant Biol.* 34, 750–758. doi: 10.1071/FP06308

Musetti, R., Paolacci, A., Ciaffi, M., Tanzarella, O. A., Polizzotto, R., Tubaro, F., et al. (2010). Phloem cytochemical modification and gene expression following the recovery of apple plants from apple proliferation disease. *Phytopathology* 100, 390–399. doi: 10.1094/PHYTO-100-4-0390

Musetti, R., Sanità di Toppi, L., Ermacora, P., and Favali, M. A. (2004). Recovery in apple trees infected with the apple proliferation phytoplasma: An ultrastructural and biochemical study. *Phytopathology* 94, 203–208. doi: 10.1094/PHYTO.2004.94.2.203

Musetti, R., Sanità di Toppi, L., Martini, M., Ferrini, F., Loschi, A., Favali, M. A., et al. (2005). Hydrogen peroxide localization and antioxidant status in the recovery of apricot plants from European Stone Fruit Yellows. *Eur. J. Plant Pathol.* 112, 53–61. doi: 10.1007/s10658-004-8233-z

Nakashima, J., Laosinchai, W., Cui, X., and Brown, R. M. (2003). New insight into the mechanism of cellulose and callose biosynthesis: proteases may regulate callose biosynthesis upon wounding. *Cellulose* 10, 369–386. doi: 10.1023/A:1027336605479

Osler, R., Carraro, L., Loi, N., and Refatti, E. (1993). Symptom expression and disease occurrence of a yellows disease of grapevine in north-eastern Italy. *Plant Dis.* 77, 496–498. doi: 10.1094/PD-77-0496

Osler, R., Loi, N., Carraro, L., Ermacora, P., and Refatti, E. (2000). "Recovery in plants affected by phytoplasmas", in *Proceedings 5th Congress of the European Foundation for Plant Pathology*, ed. Società Italiana di Patologia Vegetale, Taormina, 589–592.

Pfaffl, M. W. (2001). A new mathematical model for relative quantification in real-time RT-PCR. *Nucleic Acid Res.* 29, e45.

Reinders, A., Sivitz, A. B., and Ward, J. M. (2012). Evolution of plant sucrose uptake transporters (SUTs). *Front. Plant Sci.* 3:22. doi: 10.3389/fpls.2012.00022

Roitsch, T., Balibrea, M. E., Hofmann, M., Proels, R., and Sinha, A. K. (2003). Extracellular invertase: key metabolic enzyme and PR protein. *J. Exp. Bot.* 54, 513–524.

Roitsch, T., and Gonzàlez, M.-C. (2004). Function and regulation of plant invertases: sweet sensations. *Trends Plant Sci.* 9, 606–613. doi: 10.1016/j.tplants.2004.10.009

Rolland, F., Baena-Gonzalez, E., and Sheen, J. (2006). Sugar sensing and signaling in plants: conserved and novel mechanisms. *Annu. Rev. Plant Biol.* 57,675–709. doi: 10.1146/annurev.arplant.57.032905.105441

Santi, S., Grisan, S., Pierasco, A., De Marco, F., and Musetti, R. (2013). Laser microdissection of grapevine leaf phloem infected by stolbur reveals site-specific gene responses associated to sucrose transport and metabolism. *Plant Cell. Environ.* 36, 343–355. doi: 10.1111/j.1365-3040.2012.02577.x

Sauer, N. (2007). Molecular physiology of higher plant sucrose transporters. *FEBS Lett.* 581, 2309–2317. doi: 10.1016/j.febslet.2007.03.048

Solfanelli, C., Poggi, A., Loreti, E., Alpi, A., and Perata G. (2006). Sucrose-specific induction of the anthocyanin biosynthetic pathway in Arabidopsis. *Plant Physiol.* 140, 637–646. doi: 10.1104/pp.105.072579

Sutton, P. N., Gilbert, M. J., Williams, L. E., and Hall, J. L. (2007). Powdery mildew infection of wheat leaves changes host solute transport and invertase activity. *Physiol. Plant.* 129, 787–795. doi: 10.1111/j.1399-3054.2007.00863.x

van Bel, A. J. E., Ehlers, K., and Knoblauch, M. (2002). Sieve elements caught in the act. *Trends Plant Sci.* 7, 126–132. doi: 10.1016/S1360-1385(01)02225-7

van der Schoot, C., and van Bel, A. J. E. (1989). Glass microelectrode measurements of sieve tube membrane potentials in internode discs and petiole strips of tomato (*Solanum lycopersicon* L.). *Protoplasma* 149, 144–154. doi: 10.1007/BF01322986

Vandesompele, J., De Preter, K., Pattyn, F., Poppe, B., Van Roy, N., De Paepe, A., et al. (2002). Accurate normalization of real-time quantitative RT-PCR data by geometric averaging of multiple internal control genes. *Genome Biol.* 3, research 0034. doi: 10.1186/gb-2002-3-7-research0034

Verma, D. P. S., and Hong, Z. (2001). Plant callose synthase complexes. *Plant Mol. Biol.* 47, 693–701. doi: 10.1023/A:1013679111111

Weisburg, W. G., Tully, J. G., Rose, D. L., Petzel, J. P., Oyaizu, H., Yang, D., et al. (1989). A phylogenetic analysis of the mycoplasmas: basis for their classification. *J. Bacteriol.* 171, 6455–6467.

Winkel-Shirley, B. (2001). Flavonoid biosynthesis: a colorful model for genetics, biochemistry, cell biology, and biotechnology. *Plant Physiol.* 126, 485–493. doi: 10.1104/pp.126.2.485

Winter, H., and Huber, S. (2000). Regulation of sucrose metabolism in higher plants: localisation and regulation of activity of key enzymes. *Crit. Rev. Plant Sci.* 19, 31–67. doi: 10.1016/S0735-2689(01)80002-2

Xie, B., Wang, X., Zhu, M., Zhang, Z., and Hong, Z. (2011). CalS7 encodes a callose synthase responsible for callose deposition in the phloem. *Plant J.* 65, 1–14. doi: 10.1111/j.1365-313X.2010.04399.x

Conflict of Interest Statement: The authors declare that the research was conducted in the absence of any commercial or financial relationships that could be construed as a potential conflict of interest.

Received: 15 March 2013; accepted: 14 May 2013; published online: 04 June 2013.

Citation: Santi S, De Marco F, Polizzotto R, Grisan S and Musetti R (2013) Recovery from stolbur disease in grapevine involves changes in sugar transport and metabolism. Front. Plant Sci. ***4****:171. doi: 10.3389/fpls.2013.00171*

This article was submitted to Frontiers in Plant Physiology, a specialty of Frontiers in Plant Science.

Plant, Cell & Environment

Plant, Cell and Environment (2013) **36**, 343–355 doi: 10.1111/j.1365-3040.2012.02577.x

Laser microdissection of grapevine leaf phloem infected by stolbur reveals site-specific gene responses associated to sucrose transport and metabolism

SIMONETTA SANTI, SIMONE GRISAN, ALESSANDRO PIERASCO, FEDERICA DE MARCO & RITA MUSETTI

Dipartimento di Scienze Agrarie e Ambientali, University of Udine, Via delle Scienze 208, I-33100 Udine, Italy

ABSTRACT

Bois Noir is an emergent disease of grapevine that has been associated to a phytoplasma belonging to the XII-A stolbur group. In plants, phytoplasmas have been found mainly in phloem sieve elements, from where they spread moving through the pores of plates, accumulating especially in source leaves. To examine the expression of grapevine genes involved in sucrose transport and metabolism, phloem tissue, including sieve element/companion cell complexes and some parenchyma cells, was isolated from healthy and infected leaves by means of laser microdissection pressure catapulting (LMPC). Site-specific expression analysis dramatically increased sensitivity, allowing us to identify specific process components almost completely masked in whole-leaf analysis. Our findings showed decreased phloem loading through inhibition of sucrose transport and increased sucrose cleavage activity, which are metabolic changes strongly suggesting the establishment of a phytoplasma-induced switch from carbohydrate source to sink. The analysis focused at the infection site also showed a differential regulation and specificity of two pathogenesis-related thaumatin-like genes (*TL4* and *TL5*) of the PR-5 family.

Key-words: Bois Noir phytoplasma; gene expression; phloem cells; sucrose metabolism.

INTRODUCTION

Grapevine (*Vitis vinifera* L.) is seriously affected by phytoplasma diseases in several regions of the Mediterranean area. Bois Noir (BN), similar to Flavescence dorée (FD), causes symptoms such as abnormal lignification of canes, short internodes, flower abortion, curling and discoloration of leaves with inter-vein yellowing or reddening, which are accompanied by a dramatic reduction in yield (Osler *et al.* 1993). These symptoms have been related to stoma closure, reduced photosynthesis rate and anomalous accumulation of carbohydrates in leaves of grapevine, tobacco, periwinkle and coconut palm (Lepka *et al.* 1999; Bertamini *et al.* 2002; Maust *et al.* 2003). BN is often endemic, but, in some cases, can be associated with severe epidemics, as reported in several Italian regions in the past 15 years (Belli, Bianco & Conti 2010).

The BN disease has been associated to the presence of phytoplasmas of the stolbur group 16SrXII. On the basis of *16S rRNA* gene sequence analysis, the agent has been identified as a phytoplasma belonging to the stolbur subgroup 16SrXII-A and is called '*Candidatus* Phytoplasma solani' (*Ca*. P. solani), but still not described (Firrao, Gibb & Stereten 2005). Phytoplasmas remain as the most poorly characterized plant pathogens, primarily because efforts at *in vitro* culture, gene delivery and mutagenesis have been unsuccessful. They are cell-wall-less pleomorphic bacteria belonging to the class *Mollicutes* and are obligate parasites replicating intracellularly in their insect (belonging to the order Hemiptera) and plant hosts (Hogenhout *et al.* 2008). Sequencing of the genome of two '*Ca.* Phytoplasma asteris' strains (Oshima *et al.* 2004), '*Ca*. P. australiense' (Tran-Nguyen *et al.* 2008) and '*Ca*. P. mali' (Kube *et al.* 2008), has highlighted how these microorganisms must assimilate a wide range of molecules from the host cells as they come from a reductive evolution resulting in the lack of most of the common metabolic pathways. In particular, phytoplasmas lack the pentose phosphate cycle and ATP-synthase subunits; thus, ATP synthesis is thought to be strongly dependent on glycolysis (Oshima *et al.* 2004). On the basis of the known phytoplasma genomes, the pathogen could depend on the uptake of phosphorylated hexoses for its carbon sources (Christensen *et al.* 2005). Recently, their ability to interfere with the host plant metabolism through the secretion of small effector proteins has been discovered (Bai *et al.* 2009; Hoshi *et al.* 2009).

In plants, phytoplasmas have been found mainly in phloem elements, including both mature (without nuclei) and immature (with nuclei) sieve elements. Phytoplasmas spread throughout the plant phloem, moving through the pores of sieve plates and accumulate especially in source leaves, and, to a lesser extent, in petioles and stems, whereas a few or non-detectable amounts have been revealed in sink organs such as roots and young leaves (Christensen *et al.* 2004).

Despite its severe affection of grapevine, the molecular aspects of BN are still poorly understood. Molecular methods are currently used for diagnostics or phylogenetic

Correspondence: S. Santi. E-mail: simonetta.santi@uniud.it

analysis; however, molecular interactions between the pathogen and the plant host are still largely unclear. Global transcription profiles have recently been obtained from grapevine leaves infected with BN by hybridization of microarrays (Albertazzi *et al*. 2009; Hren *et al*. 2009). Moreover, interaction of FD phytoplasma with grapevine has been studied by monitoring the effects of infection on the protein profile (Margaria & Palmano 2011). These studies revealed that phytoplasma infection in grapevine can alter the expression of more than 100 genes and 30 proteins belonging to both primary and secondary metabolism. An overall decrease in transcript abundance was observed, together with a shift from housekeeping to defence metabolism genes. Photosynthesis I system and the whole photosynthetic chain were found to be inhibited at the transcriptional level, as well as Calvin cycle, carbohydrate and lipid metabolism. Inhibition of several Calvin-cycle enzymes was explained by the accumulation of soluble carbohydrates and starch observed in source leaves of plants infected by phytoplasmas (Lepka *et al*. 1999; Maust *et al*. 2003; André *et al*. 2005). On the other hand, genes encoding enzymes involved in hexoses production from sucrose and starch, such as vacuolar invertase, sucrose synthase and alpha amylase, were up-regulated, suggesting some affection of sucrose metabolism (Albertazzi *et al*. 2009; Hren *et al*. 2009). Transcript level of a significant number of genes related to wall metabolism, stress response and defence was also shown to be changed in infected grapevine (Albertazzi *et al*. 2009; Hren *et al*. 2009). Plant active defence systems include the expression of pathogenesis-related (PR) proteins. Several PR-protein genes are up-regulated in infected leaves. In particular, genes encoding for thaumatin-like proteins belonging to the PR-5 group were found to be significantly induced in BN- and FD-infected leaves (Albertazzi *et al*. 2009; Hren *et al*. 2009; Margaria & Palmano 2011).

Despite the fact that phytoplasmas have been seen as almost exclusively restricted to the network of sieve tubes of infected leaves, all the work done to date to elucidate the interaction between plant and pathogen has been carried out on whole leaf or on midrib-enriched tissue. Information about a co-ordinated expression of the genes specifically involved in plant–pathogen interaction in phloem cells is lacking, while a single-cell approach could enhance sensitivity in detecting responses localized at the infection site and reduce complexity associated with the expression of distal tissues. The aim of the present work was to optimize a tissue-specific approach to analyse gene expression in the leaf phloem of infected and healthy grapevine plants. In particular, our analysis focused on some genes of sucrose transport and metabolism. Functional analysis was permitted by the isolation of phloem parenchyma cells and companion cell-sieve element complexes from paraffin-embedded leaf sections by laser microdissection (LM). This technique allows cell-specific resolution of gene expression, which is critical for the analysis of responses that are restricted to a particular tissue or cell. LM has mainly been applied in combination with RT-PCR and microarray technologies (for a review, see Kerk *et al*. 2003; Nelson *et al*. 2006; Day, McNoe & Macknight 2007), and rarely with protein and metabolite profiling (Shad *et al*. 2005a,b). LM has already been chosen to isolate cells from complex tissue samples such as phloem (Nakazono *et al*. 2003; Deeken *et al*. 2008). It has also been used to characterize the response of plants grown in different environmental conditions (Santi & Schmidt 2008) or under a pathogen attack. In this last case, transcriptomic events were investigated in nematode-induced giant cells of soybean, tomato or *Arabidopsis* (Klink *et al*. 2007; Fosu-Nyarko, Jones & Wang 2009; Barcala *et al*. 2010), in maize stalk infected by the fungus *Colletotrichum graminicola* (Tang *et al*. 2006) and in powdery mildew-infected epidermal cells of *Arabidopsis* (Chandran *et al*. 2010). In all cases, particular attention was paid to optimize the protocol of preparation of the tissue to be studied. We optimized methods of tissue preparation, RNA isolation and RNA amplification from grapevine leaf phloem. Nanogram quantities of total RNA extracted from laser-microdissected tissues were amplified and reverse-transcribed into cDNA and used in RT-PCR expression analyses. This allowed us to explore how host gene expression is altered at the site of infection, particularly focusing on sucrose transporters, vacuolar invertase and sucrose synthase, and defence genes encoding callose synthase (CAS) and thaumatin-like proteins of the PR-5 group.

MATERIALS AND METHODS

Plant material

Plants of *Vitis vinifera* L. Chardonnay grafted on SO4 rootstock were examined. Field-grown plants were located in a vineyard near Gorizia, in north-eastern Italy. Plants were regularly treated with fungicides. BN symptoms were monitored during summer 2008, 2009, 2010 and 2011, allowing several healthy (never symptomatic), diseased (symptomatic) and recovered plants (i.e. previously diseased plants that were symptom-free and negative to molecular diagnosis) to be identified. About five fully expanded, not damaged, leaves were collected from at least five healthy and diseased plants at the end of August in 2010, when symptoms were particularly evident. Leaves were collected from symptomatic canes of infected plants and in similarly positioned canes of nearby healthy plants.

RNA isolation

About 1 g of leaf tissue enriched in rids was homogenized by mortar and liquid nitrogen and RNA extracted with the RNeasy Plant Mini Kit (Qiagen GmbH, Hilden, Germany), with minor modifications to the manufacturer's instructions (MacKenzie *et al*. 1997). Briefly, 90–100 mg of powder was homogenized with 1 mL of lysis buffer (RLT buffer of the Kit, containing guanidine isothiocyanate) added with 2.5% (w/v) polyvinylpyrrolidone-40 (PVP-40) and 1% (v/v) β-mercaptoethanol (β-ME). After vortexing for 30 s, the homogenate was mixed with 1/10 vol of 20% (v/v) *N*-lauroylsarcosine (Sigma-Aldrich Co., St. Louis, MO,

USA) and then incubated at 70 °C for 10 min. After a centrifugation at 3000 *g* for 5 min, approximately 600 μL of the supernatant was transferred to a QIAshredder column (supplied with the Qiagen Kit), and then extraction was performed according to the instructions. Nucleic acid quantity and integrity were evaluated by using a NanoDrop ND-1000 UV-visible spectrophotometer (Thermo Fisher Scientific, Inc., Waltham, MA, USA).

Bois Noir phytoplasma detection

A rapid protocol for detecting the BN phytoplasma was optimized using one-step real-time RT-PCR. About 10 ng of total RNA purified from leaf tissue was added to a final volume reaction of 10 μL provided by the EXPRESS One-Step SYBR GreenER™ Kit (Life Technologies Ltd, Paisley, UK). Primers were designed on the *16S rRNA* gene of *Ca.* P. solani (accession no. AF248959) and were 16Sstol(RT)F2 (5′-AGGGTAGCTAAAGCGTAAGC-3′) and 16Sstol(RT)R3 (5′-CATCAACCCTACCTTAGACG-3′) (Martini *et al.*, unpublished results). PCR was performed in a CFX96 real-time PCR detection system (Bio-Rad Laboratories Co., Hercules, CA, USA). The following standard thermal profile was used: 55 °C for 5 min, 95 °C for 2 min, 45 cycles at 95 °C for 15 s and 60 °C for 1 min, followed by a melting curve analysis 60–95 °C. The presence of contaminating genomic DNA was checked in reaction without reverse transcriptase. Moreover, one-step real-time RT-PCR was carried out to detect transcripts of the *DNAK* gene of *Ca.* P. solani (accession no. AJ970678.1); primers were DNAKF (5′-AGACAAATGGCGATGCAA-3′) and DNAKR1 (5′-TGGTACTAAACAACGGTCAACTAAA-3′). Primers were designed by the Primer3 program (Rozen & Skaletsky 2000). Specificity of primers was ensured through sequence alignment by the BLASTN algorithm (Altschul *et al.* 1997) and experimentally by analysis of the melting curves of the products.

Molecular diagnosis by one-step RT-PCR was also performed on 1 μL of RNA extracted both from scraped whole tissue sections and from laser-microdissected cells.

Laser microdissection

Material was collected from healthy and infected plants. Five symptomatic leaves from each plant were cut in 4- to 5-mm-wide and 2- to 3-mm-long pieces, including vein and part of the blade. Specimens were cut in ice-cold 100% acetone and then fixed in fresh acetone overnight at 4 °C. Before fixing, vacuum was applied three times for 1 min and then released. Fixative was exchanged for a mixture of acetone : xylene (1:1) at room temperature (RT) for 60 min, and then replaced with acetone : xylene (1:3) for 60 min and 60 min twice with 100% (v/v) xylene. Specimens were then transferred into plastic cassettes and infiltrated with xylene : Paraplast Plus [1:1 (v/v)] (Mc Cormick Scientific, St. Louis, MO, USA) at 59 °C for 60 min. The xylene : Paraplast mixture was replaced with pure Paraplast three times at intervals of 60 min. Fixed specimens were embedded in Paraplast Plus. Blocks were first cooled to RT and then placed at 4 °C for easy unmoulding. The blocks were kept in plastic bags at 4 °C. Twelve-micrometre-thick slices were sectioned on a rotary microtome (Leica, Bensheim, Germany). Sections were stretched at 42 °C for a few seconds on a drop of diethylpyrocarbonate (DEPC)-water directly delivered on the polyethylene naphthalate (PEN)-covered glass slides (PALM Carl Zeiss GmbH, Munchen, Germany) and then dried at 42 °C for not more than 30 min. Slides were stored under vacuum in a desiccator at RT. Sections were de-paraffinized twice for 5 min each in xylene and then air-dried just before microdissection.

In order to verify the amount and integrity of RNA prior to LMPC, and also to check for the presence of stolbur (by one-step RT-PCR, as described above), whole tissue sections were scraped off the microscope slide into a tube for RNA extraction. Laser microdissection pressure catapulting (LMPC) was used for the isolation of phloem. The de-paraffinized sections were microdissected with a PALM Laser-Microbeam System (PALM Microlaser Technologies, Carl Zeiss MicroImaging GmbH). Phloem areas from leaves were cut and catapulted in 0.2 mL tubes with adhesive cap (PALM Carl Zeiss). Phloem areas of about 2×10^6 μm^2 from sections of each plant sample were collected in four tubes.

RNA extraction and amplification from LMPC-captured cells

RNA was extracted from cells using the Absolutely RNA Nanoprep Kit (Stratagene, Agilent Technologies, Inc., Santa Clara, CA, USA) with minor changes to the manufacturer's instructions. Briefly, 30 μL of lysis buffer supplemented with 2.5% (w/v) PVP-40 and 0.7% (v/v) β-ME was applied to laser-captured cells collected on the adhesive cap of a microcentrifuge tube. After inverting and vortexing, the tube was stored at –80 °C. Cells were subsequently pooled and lysis buffer adjusted to 150 μL, then added with 1/10 vol of 20% (v/v) *N*-lauroylsarcosine and incubated at 70 °C for 5 min. After vortexing and centrifuging at 6000 *g* for 5 min, an equal volume of 80% (v/v) sulfolane (Sigma-Aldrich Co.) was added to the supernatant. This mixture was transferred to the RNA-binding column, and then filter washing was performed. RNA was eluted in 14 μL of RNase-free water heated to 60 °C. For the sections scraped from slides, 200 mL of lysis buffer was used, and subsequent steps were carried out as described for laser-microdissected cells.

RNA amplification was performed using the MessageAmp II aRNA Amplification Kit (Ambion, Life Technologies Co., Carlsbad, CA, USA) according to the manufacturer's instructions. Briefly, first-strand cDNA synthesis was performed with an oligo(dT) primer containing a T7 promoter sequence. One microlitre of T7 oligo(dT) primer was added to a maximum of 10 μL of RNA in a 12 μL total volume and heated to 70 °C for 5 min. After cooling on ice, 8 μL of the complete first-strand synthesis mix was added, and a 120 min incubation period at

Table 1. Primer characteristics for real-time RT-PCR

Gene name	Accession No.	Primer sequence (5′–3′)	nM	*E*
VvUBQ1	XM_002273532.1	For: CCAAGATCCAGGACAAGGAA Rev: GAAGCCTCAGAACCAGATGC	300	2.05
VvUBQCF	CF203557.1	For: CTATATGCTCGCTGCTGACG Rev: AAGCCAGGCAGAGACAACTC	300	2.05
VvSUC11	AF021808.1	For: ATGGAGAAGCTCTGCAGGAA Rev: TCAGTGCAGCAATCACAACA	300	1.93
VvSUC12	AF021809.1	For: CGGATTGGATGGGTAGAGAA Rev: AGCAAACCAAATGCACCTTC	500	1.91
VvSUC27	AF021810.1	For: CTCTTCGACACCGATTGGAT Rev: CAACCCCAGAACCACAGAGT	300	1.97
VvGIN2	XM_002272733.1	For: ACGAATTTTTGGGAGCACAG Rev: GATGCATGTCCTTCCACCTT	500	2.05
VvCAS2	CBI16456.3	For: TTCACCCCAGTTGCATTTCT Rev: CCGATCCTTCCTATGACCAC	300	2.05
VvTLP5	XM_002283046.1	For: CTAGGGTGCTTTTGAGTCCA Rev: CGTAGAAAAGTTGTTGCATGAG	300	2.04
VvTLP4	XM_002282957.1	For: CACTGTTTTCAGGACCGATG Rev: GGGCATGTAAAGGTGCTTGT	300	1.99
VvSUS2-like	XM_002275119.1	For: GCTGGCTCAATCAGTTCCTC Rev: CCAAGCCTCAAACAATGACA	500	1.97

42 °C and subsequent cooling to 4 °C was carried out. Second-strand synthesis was started with the addition of 80 μL of second-strand mix containing both DNA polymerase and RNase H. The reaction was performed at 16 °C for 120 min. The cDNA was purified according to the manufacturer's instructions and eluted with 20 μL of DNA elution buffer. For *in vitro* transcription, 16 μL of double-stranded cDNA was used in a 40 μL total volume reaction containing the T7 RNA polymerase, incubated at 37 °C for 14 h. The amplified RNA (aRNA) was purified with the RNeasy Micro Kit (Qiagen; http://www.qiagen.com/) according to the manufacturer's instructions and eluted with 14 μL of RNase-free water. A maximum amount of 24 ng of aRNA was obtained from the amplification of 8 μL of eluted total RNA. Nucleic acid quantity and integrity were evaluated using an RNA 6000 Pico Assay kit on the Agilent 2100 Bioanalyzer (Agilent Technologies).

Real-time RT-PCR

For gene expression analyses in grapevine leaves, about 0.5 μg of total DNase-treated RNA was reverse-transcribed using Superscript® III Reverse Transcriptase (Invitrogen, Life Technologies Co., Carlsbad, CA, USA) and random hexamers in a total volume of 20 μL. For the expression analysis by real-time RT-PCR, the cDNA synthesis reaction mixture was diluted and about 10 ng of the initial RNA was used for PCR. Real-time RT-PCR was performed using the RealMasterMix SYBR ROX (5Prime, Eppendorf, Hamburg, Germany) in a 25 μL total volume. A CFX96 real-time PCR system (Bio-Rad Laboratories Co.) was used, imposing the following standard thermal profile: 5 min at 95 °C, followed by 40 cycles of 15 s at 94 °C, 20 s at 56–60 °C and 30 s at 68 °C. In addition, a melting curve analysis at 65–95 °C was performed, which resulted in single product-specific melting temperatures. To enable detection of contaminating genomic DNA, PCR was performed with RNA as template. Gene-specific primer couples had previously been evaluated using the BLASTN algorithm (Altschul *et al*. 1997) and in standard calibration curves. Five-point standard curves of different dilutions of pooled cDNA were used for PCR efficiency calculation of each primer pair. The efficiency (*E*) was calculated as described by Pfaffl (2001). Primers and *E* are indicated in Table 1. A mean normalized expression (MNE) for each target gene (Muller *et al*. 2002) was calculated, normalizing the mean expression level to the level of ubiquitin, and imposing transcript abundance of ubiquitin (*UBQ1*) = 100 arbitrary units. Mean normalized gene expression values were graphed, assigning a value of zero to no expression. Each data point represents the mean of at least three biological replicates and three technical replicates.

For gene expression analysis in LMPC-collected cells, 8 μL of aRNA was reverse-transcribed using random hexamers and the Superscript III Reverse Transcriptase (Invitrogen, Life Technologies Co.) in a total volume of 20 μL. Real-time RT-PCR was performed using the conditions described above, after diluting the cDNA to 1:10.

RESULTS

Phytoplasma detection

Leaf samples were analysed for the presence of BN phytoplasma by one-step real-time RT-PCR. Starting from 10 ng of total RNA, stolbur *16SrRNA* transcripts were detected in symptomatic samples at an average Cq value (±SE) of 18.6 ± 0.9, while no amplicon of the *16SrRNA* gene but unspecific products, as deduced by their melting curve and gel electrophoresis analysis, were obtained in healthy samples. The presence of phytoplasma was further confirmed by analysing transcripts of the stolbur *DNAK* gene,

which encodes for a chaperonin and has been shown to be constitutively expressed in *Ca*. P. asteris (Bai *et al*. 2009). *DNAK* gene was detected in the positive samples at an average Cq value of 28.0 ± 0.9. Molecular diagnosis confirmed the presence of stolbur in 98% of leaf samples collected from plants classified as symptomatic in the field, while unspecific amplification products were found in healthy plant samples by using both *16SrRNA* and *DNAK* gene primers.

LM of phloem from grapevine leaves

The LMPC technique was applied to grapevine leaf phloem to allow for a tissue-specific expression analysis of the host genes associated to stolbur infection. The presence of stolbur was checked further in the same LMPC cells. To prepare tissue for LMPC, cold acetone was used to fix grapevine leaf tissues, followed by paraffin embedding. Other fixatives containing ethanol and acetic acid (Kerk *et al*. 2003; Deeken *et al*. 2008) yielded less total RNA, which was poorer in quality than acetone-fixed samples (not shown). Groups of cells including companion cell-sieve element complexes and parenchyma cells were collected from 12 μm sections of infected and healthy leaves (Fig. 1a–f). The auto-fluorescence of lignin deposits displayed the vascular system and xylematic vessels in particular, therefore helping in the identification of the adjacent phloem areas (Fig. 1a). In order to avoid a stochastic behaviour for low abundance messages, areas of about 2×10^6 μm^2 were collected from each plant sample. The maximum total RNA yield was about 3.5 ng. Cells were separately collected from at least three individuals from each of the two groups (namely infected and healthy plants).

Diagnosis in LMPC-collected phloem cells

One-step real-time RT-PCR of stolbur *16SrRNA* from a small aliquot of total RNA (1 μL) isolated from LMPC cells allowed us to definitively confirm the presence of the phytoplasma in the phloem of each infected leaf sample before expression analysis. The amplification products for *16SrRNA* (234 bp in size) were found in the phloem of infected leaves, while no amplicon of the expected size was seen either in the epidermis of the same sample or in phloem cells isolated from healthy leaves. A plant conjugating factor of ubiquitin gene (*UBQCF*) was amplified (154 bp in size) as control by one-step RT-PCR in parallel (Fig. 1, bottom panel).

Plant gene expression analysis in LMPC-collected phloem cells

LMPC-collected phloem was analysed for single cell type-specific expression of host genes associated to stolbur infection. Groups of cells including sieve elements, companion cells and parenchyma cells were collected separately from infected and healthy leaves by LMPC (Fig. 1a–f). The amount of RNA purified from LM-collected cells depends on tissue and fixation/processing protocol (Nelson *et al*. 2006); in most cases, the yield is too low for expression analysis of several genes or more complex global profiling, thus an amplification step is required. We used a T7 RNA polymerase-based linear amplification procedure of poly(A)-RNAs in a one-round reaction, which yielded about 23 ng of aRNA from a maximum amount of 2.5 ng of total RNA purified from LMPC cells. All the aRNA samples showed smears ranging from 0.2 to 2 kb, with a peak at approximately 0.5 kb (Fig. 2). The linearity of amplification was checked using real-time RT-PCR by comparing the expression level of *UBQ1* and *SUC27* transcripts before and after RNA amplification (data not shown). The comparison confirmed the manufacturer's quality test. All the aRNA samples yielded real-time RT-PCR products having the melting temperature expected in the absence of genomic DNA contamination. Ubiquitin (*UBQ1*) was used as reference gene, as found to be the most stably expressed after the pairwise comparison with actin or *UBQCF* by the ΔCt method (Silver *et al*. 2006). Moreover, the gene-stability measure (*M*) was calculated by the geNorm program (Vandesompele *et al*. 2002) using several infected and healthy RNAs that were purified from scraped midrib-enriched sections. The *M*-value for *UBQ1* was <1.0, thus confirming the validity of this gene as reference. Expression of the ubiquitin gene was shown to be non-cell-specific in several experiments of LM (Kerk *et al*. 2003; Inada & Wildermuth 2005; Chandran *et al*. 2010).

Expression analysis of genes referred to sucrose transport and metabolism, together with PR genes, was examined in phloem cells of grapevine leaves by real-time RT-PCR (Fig. 3a,b).

Accumulation of glucose and fructose in grapevine is mainly referred to three families of proteins: the acid (vacuolar or cell wall associated) and neutral (cytosolic) invertases, sucrose synthases and sucrose transporters. Among the three sucrose transporter genes (*SUC* genes; Davies, Wolf & Robinson 1999) that were investigated in the present work (accession numbers and primers are reported in Table 1), *SUC12* transcripts were not detected in phloem cells, while *SUC11* showed low and comparable expression levels (3.4 and 3.8 MNE units, imposing a MNE value for *UBQ1* = 100) in healthy and infected samples (Fig. 3a). *SUC11* transporter falls into the family of the tonoplast transporters with *AtSUT4* (Sauer 2007), and its low expression level could be explained by the scarce vacuolization of sieve elements/companion cells complexes. On the contrary, high message levels for *SUC27* (130.4 MNE units) were observed in phloem cells, suggesting preferential expression of this gene in this specific cell type. SUC27 protein shares the highest similarity (59%) with the high-affinity *Arabidopsis* transporter SUC2, which was proposed as marker of leaf phloem (Imlau, Truernit & Sauer 1999; Deeken *et al*. 2008). When comparing its expression in phloem of infected and healthy leaves, *SUC27* gene resulted as more than sixfold down-regulated in infected samples.

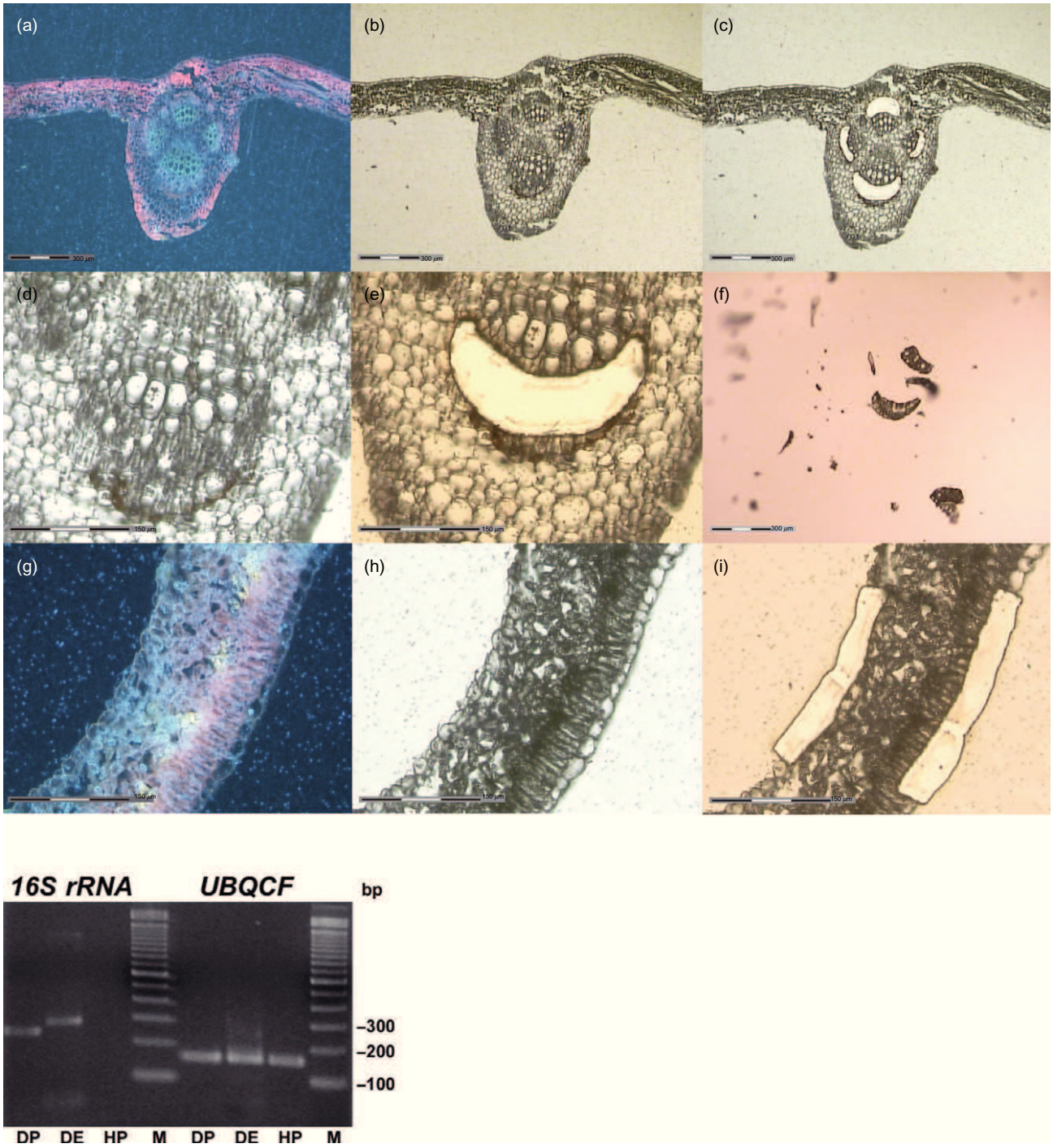

Figure 1. Laser microdissection pressure catapulting (LMPC) of grapevine leaf phloem and epidermal cells and localization of stolbur. Representative cross section (12 μm) of leaf under UV (a,g) and bright field (b–f,h,i). Section before (a,b) and after (c) cutting and catapulting phloem. Bars = 300 μm. Magnification of the targeted site before and after cutting (d,e). Bars = 150 μm. Captured areas (f). LMPC of epidermal cells before (g,h) and after cutting (i). Bars = 150 μm. Bottom panel: RT-PCR products for stolbur *16S rRNA* and grapevine *UBQCF* from phloem and epidermal cells. Phloem of infected leaves (lanes DP); epidermal cells of infected leaves (lanes DE); phloem of healthy leaves (lanes HP); Marker, TrackIt 100 bp DNA Ladder (Invitrogen) (M).

Among the acid invertase genes in grapevine, only the vacuolar acid invertase *GIN2* (Davies & Robinson 1996) (Table 1) was shown by global transcripts profiling to be significantly up-regulated in midribs of leaves infected by stolbur phytoplasma (Albertazzi *et al.* 2009; Hren *et al.* 2009). We examined its gene expression in phloem cells (Fig. 3a) and found a 15-fold up-regulation in infected samples, although at a very low expression level

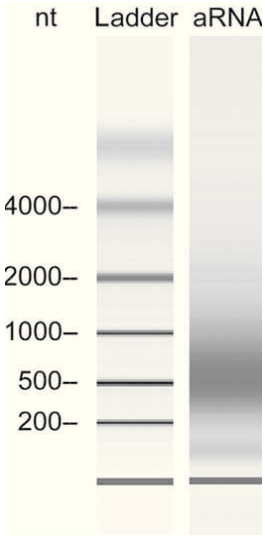

Figure 2. Electropherogram of amplified RNA of a representative laser microdissection pressure catapulting (LMPC) sample. Total RNA purified from leaf phloem was amplified by T7-polymerase in a one-round reaction (aRNA). The ladder size is indicated on the left.

(MNE = 1.5 versus MNE = 0.1). Similar to *SUC11*, low expression of *GIN2* probably reflects the scarce vacuolization of phloem cells.

Sucrose synthase (SUS) has a dual role in producing both UDP-glucose (UDPG, necessary for cell wall and glycoprotein biosynthesis) and ADP-glucose (ADPG, necessary for starch biosynthesis) (Baroja-Fernández *et al*. 2012). Among the *SUS* gene isoforms (at least five in grapevine), one was shown by Hren *et al*. (2009) to be 2.5-fold induced in stolbur-infected leaves. This gene of the family (*VvSUS2-like*; Table 1) shares 82 and 81% identity at the level of amino acidic sequence with *Arabidopsis* SUS4 and SUS3, respectively (Bieniawska *et al*. 2007), and 84% with *Populus trichocarpa* SUS2 (Zhang *et al*. 2011).

Expression of *VvSUS2-like* was investigated by real-time RT-PCR in LMPC-collected phloem cells, where it was shown to be increased by approximately 35-fold in response to stolbur infection (262.5 versus 7.2 MNE units) (Fig. 3a). *SUS* appeared to be the most affected gene among those examined in infected phloem cells.

SUS hydrolyses sucrose into UDPG, a molecule used by CAS as glucose donor to the growing polymer chain. Callose is usually deposited at plasmodesmata and at sieve plates as a response to developmental cues and pathogen attack, with the aim of limiting spread of the infection or reinforcing the cell wall (Nakashima *et al*., 2003). We examined the expression of *CAS2* (Table 1), belonging to a gene family of at least seven members, which was seen to be induced in stolbur-infected grapevine leaves (Hren *et al*. 2009). Focusing on phloem cells (Fig. 3a), transcript level of *CAS2* was not significantly different in infected and healthy samples (50.3 versus 57.8 MNE units).

Besides genes referred to sucrose metabolism, gene expression of two plant PR proteins of group 5 (PR-5) was examined by focusing analysis on LMPC-collected phloem cells (Fig. 3b). We examined two thaumatin-like genes (*TLP*) already shown to be induced in stolbur-infected grapevine (Hren *et al*. 2009), in this work called *TLP4* and *TLP5* (Table 1). TLP4 and TLP5 proteins share 78% identity. TLP4 shows 79% identity with a *Sultanina* grape protein (previously called OSM1 by Loulakakis 1997), closely related to grapevine berry VvTL2 (Davies & Robinson 2000). TLP5 protein shares 84 and 83% identity with VvTL2 and VvTL3 (Davies & Robinson 2000), respectively. In phloem cells of healthy control leaves, *TLP5* gene was found to be highly expressed (381.9 MNE units), almost two orders of magnitude more expressed than *TLP4* (5.0 MNE units). Moreover, in phloem cells of diseased leaves, the expression of both genes was significantly induced, although 20-fold for *TLP4*, whereas only threefold for *TLP5*. Transcripts amount of *TLP5* appeared highly variable among the infected individuals (1258.6 ± 468.0 MNE units).

Gene expression analysis in whole leaves infected by stolbur

Expression analysis of the genes referred to sucrose transport and metabolism, together with the two PR-5 genes already characterized in phloem cells (Fig. 3a,b), was performed in parallel in fully expanded, not damaged, leaves of infected and healthy grapevines by real-time RT-PCR (Fig. 4a,b). Leaf samples enriched in midribs were collected for RNA extraction.

Different from phloem cells, not only *SUC27* but all *SUC* genes were expressed when analysis was extended to the whole leaf, although midrib-enriched (Fig. 4a). Moreover, in healthy leaves, transcript level was of the same order of magnitude for each gene, reflecting the different contribution of tissues functionally different from phloem. *SUC12*, which was not detected in phloem cells, was the more expressed transporter in whole leaf (59.2 MNE units), where, similarly, *SUC11* also appeared almost 10-fold more expressed (32.9 MNE units). On the contrary, *SUC27* transcripts amount was found to be almost fivefold lower than in phloem, indicating some dilution and thus confirming its preferential localization in phloem cells. As regards the effect of stolbur infection, all the examined *SUC* genes appeared significantly down-regulated (two to four times) in whole leaves.

Expression of the vacuolar invertase *GIN2* was barely detectable in whole leaf (Fig. 4a). Low expression of *GIN2* depends on the fact that *GIN* transcripts decline during leaf development (Davies & Robinson 1996) and in our experiments could reflect the use of mature leaves.

Expression level of *SUS2-like* gene was of the same order of magnitude in healthy whole leaves (Fig. 4a) and healthy phloem cells (Fig. 3a), suggesting an almost ubiquitous distribution of its transcripts in the leaf. Its level in the infected leaves was just fivefold higher than in healthy ones; thus, the extent of its up-regulation in infected phloem cells was 22-fold higher than in the whole leaf. Together with *SUC27*,

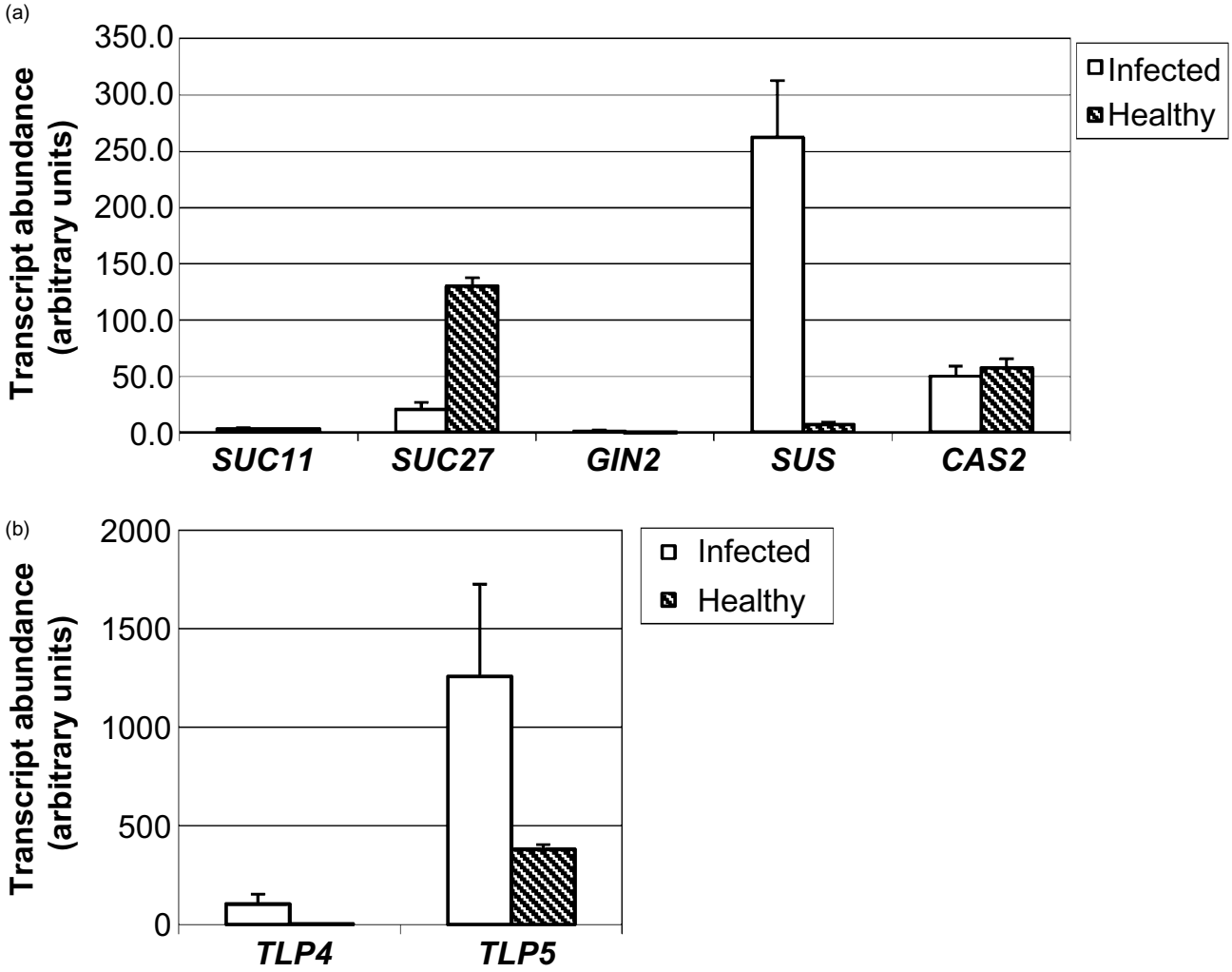

Figure 3. Gene expression analysis in laser microdissection pressure catapulting (LMPC)-collected phloem cells. Real-time RT-PCR of sucrose metabolism (a) and pathogenesis-related genes of the PR-5 group (b). Mean normalized expression (MNE) was calculated in arbitrary units, imposing MNE of *UBQ1* = 100. Note the different scales in (a) and (b).

this gene appeared to be the most affected one when its expression was focused at the infection site, and probably what was observed at the whole leaf level simply reflects their specific regulation in phloem cells.

As regards the examined *CAS* gene, whereas no difference in its regulation was seen in phloem following infection, a 2.2-fold up-regulation was shown in whole infected leaf. The expression level of this gene was about 25-fold higher in phloem cells (57.8 MNE units; Fig. 3a) compared with the whole leaf (2.3 MNE units; Fig. 4a) in healthy conditions.

Expression of the PR-5 gene *TLP4* was similar in healthy phloem (Fig. 3b) and whole leaf (Fig. 4b), suggesting an almost ubiquitous distribution of its transcripts, analogous to what was observed for sucrose *SUS2-like*. The dramatic up-regulation of *TLP4* observed when focusing its analysis on infected phloem (Fig. 3b) was not shown in whole leaves, where its expression was not affected by stolbur (Fig. 4b). Instead, the extent of *TLP5* up-regulation due to infection was greater (25-fold) when analysed on the whole leaf, although its expression level resulted as higher in phloem cells in both healthy and infected conditions.

DISCUSSION

In this study, we investigated the tissue-specific expression of genes involved in the response to stolbur infection in the phloem of grapevine leaves. Cells of the phloem, which included sieve elements together with companion cells and surrounding parenchyma cells, were captured by LMPC from leaves of infected and healthy plants. The expression profile obtained with LMPC-captured cells was validated in parallel in whole leaf samples. Moreover, molecular diagnosis was directly and rapidly carried out on both whole leaf and phloem cells by means of one-step real-time RT-PCR. The single cell type-specific approach eliminates the transcriptional noise due to the mixture of different tissues and avoids the dilution of transcripts with low abundance. This

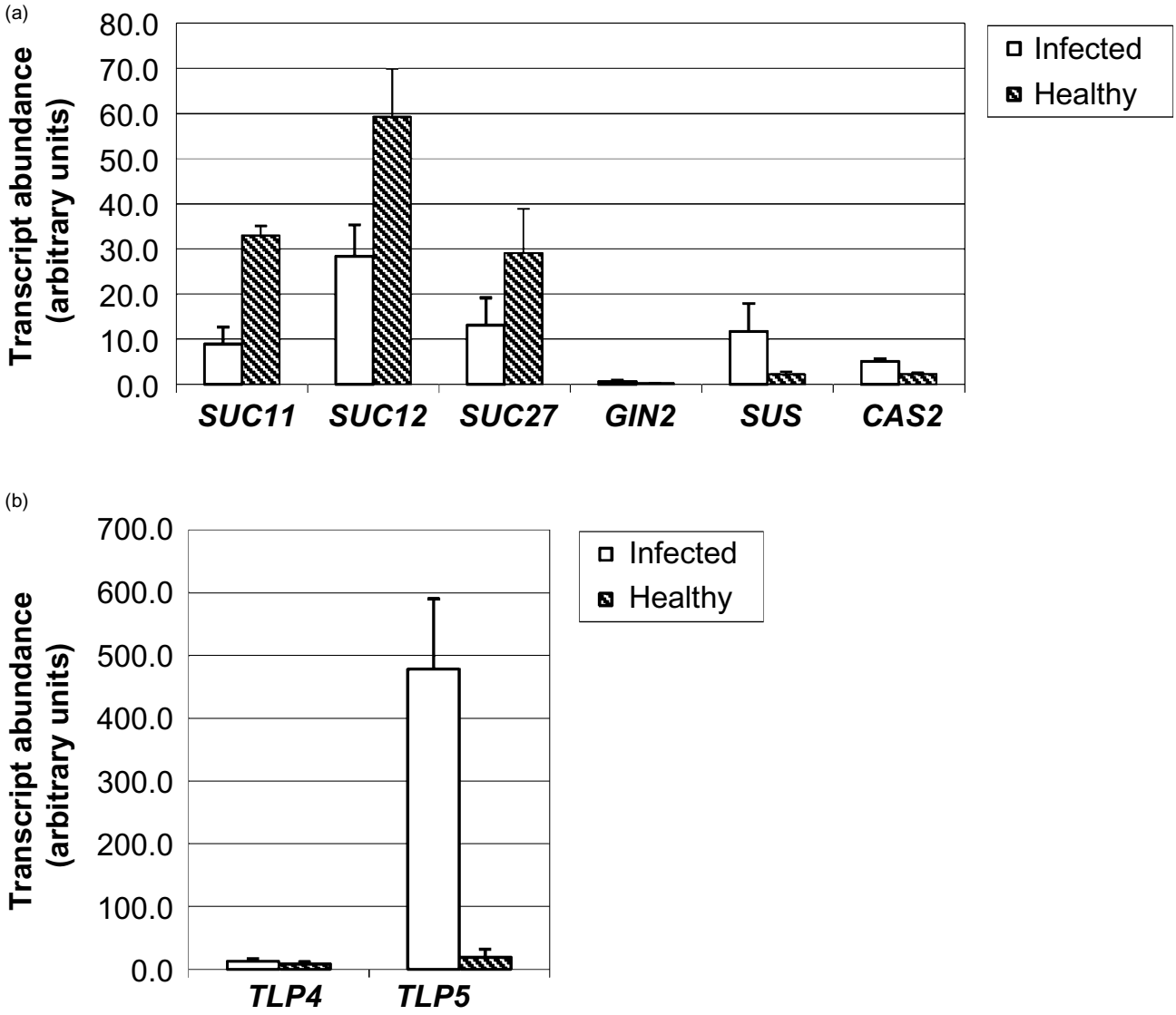

Figure 4. Gene expression analysis in whole leaves. Real-time RT-PCR of sucrose metabolism (a) and pathogenesis-related genes of the PR-5 group (b). Mean normalized expression (MNE) was calculated in arbitrary units, imposing MNE of *UBQ1* = 100. Note the different scales in (a) and (b).

was clearly evidenced by the strikingly different expression level of the investigated genes in both approaches. In addition, the transcriptional regulation of different genes can be compared within the cell type in which they are preferentially expressed, which may gain insights into the relative importance of particular components for a given stress response and their potential roles. Understanding the gene expression pattern of the resistance reaction locally may lead to an understanding of the genetic programme underlying the response. In the present study, the advantage of using phloem cells was evident for all the examined genes, particularly in the case of sucrose transporters. Among the examined *SUC* genes, only *SUC27* was significantly expressed in phloem cells; in this specific tissue, its expression level resulted as being much higher compared with the whole leaf, suggesting preferential expression of this gene in phloem. In addition, it appeared dramatically down-regulated in the response to stolbur in the infection site, a performance that was not evidenced by global transcript profiling of grapevine leaves (Albertazzi *et al*. 2009; Hren *et al*. 2009). SUC27 protein shares the highest similarity (59%) with the high-affinity *Arabidopsis* transporter SUC2, which was proposed as a marker of companion cells of the phloem (Imlau *et al*. 1999; Ivashikina *et al*. 2003; Deeken *et al*. 2008). As regards its function in sucrose partitioning, *SUC27* was found to be highly expressed in grapevine vegetative organs and lowly in berries by Afoufa-Bastien *et al*. (2010), so it was indicated as being potentially responsible for phloem loading and sugar retrieval during long-distance transport. In our experiments, the dramatic *SUC27* down-regulation observed in phytoplasma-infected phloem strongly suggests reduced phloem loading in the leaf, which

would also be mirrored by the inhibition of all *SUC* transporters in leaf cells distal to phloem. Reduced phloem loading, increased phloem unloading, increase in soluble carbohydrate concentrations and elevated invertase activity are metabolic changes suggesting the establishment of a pathogen-induced carbohydrate sink, which has often been observed during infection by biotrophic pathogens (Hayes, Feechan & Dry 2010). Accumulations of soluble carbohydrates and starch in source leaves, complemented by a decrease of sugar levels in sink organs, were reported for periwinkle, tobacco and coconut palm infected by phytoplasmas (Lepka *et al*. 1999; Maust *et al*. 2003). In *Spiroplasma citri*-infected *Catharanthus roseus*, reduction of sucrose loading with subsequent impairment of carbohydrate partitioning was supposed to be part of pathogenicity together with a preferential use of fructose, leading to increased invertase activity, glucose accumulation and inhibition of photosynthesis (Gaurivaud *et al*. 2000). Indeed, in our work, there seems to be impairment of sucrose loading due to decreased sucrose transport associated with increased activity of sucrose synthase and invertase at the site of infection. In particular, sucrose synthase, more than invertase, was shown to be dramatically and specifically up-regulated in infected phloem cells. An abundant availability of nucleoside diphosphate-glucose (UDPG and ADPG) caused by high SUS activity in the cleavage direction could explain the callose and starch accumulation often observed in phytoplasma-infected phloem tissue (Musetti 2010). Nevertheless, fructose utilization has not been demonstrated for the phytoplasma (Oshima *et al*. 2007), and comparison among phytoplasma genomes revealed that phytoplasmas lack phosphotransferases and could depend on host phosphorylated hexoses (Christensen *et al*. 2005). Indeed, in the genome of *Ca.* P. asteris (Oshima *et al*. 2004), among a group of five genes that are retained in the full-ORF in different strains, a 6-phosphofructokinase gene, known as a rate-limiting enzyme of glycolysis, has been identified (Oshima *et al*. 2007).

From our results, reduced sucrose transport and elevated sucrose synthase and invertase expression at the infection site strongly suggest the occurrence of a pathogen-induced switch from carbohydrate source to sink. It is noteworthy that stolbur spread in the phloem also had a significant impact on sucrose partitioning in tissues distal to the infection site, because all *SUC* genes were shown to be down-regulated in the whole leaf, including *SUC11* and *SUC12*, which were barely or not expressed at all in phloem cells. Our results seem to exclude a role in phloem loading for these two transporters in source leaves. A role for *SUC11* and *SUC12* in sucrose accumulation in the vacuole and in sucrose unloading into berry tissues, respectively, was suggested by Afoufa-Bastien *et al*. (2010).

The gene of sucrose hydrolyzing vacuolar invertase *GIN2* was found to be barely expressed both in whole leaf and in phloem, where, anyway, it resulted as significantly induced in response to stolbur infection. In the case of grapevine infected by different biotrophic fungal pathogens, the response of the vacuolar invertases *GIN1* and *GIN2* was found to be extremely variable (Hayes *et al*. 2010). On the contrary, a decrease in vacuolar invertase transcription was observed in *Vicia faba* leaves in response to infection by the biotrophic rust fungus *Uromyces fabae* (Voegele *et al*. 2006), and this was associated with a decrease in sucrose available for vacuolar storage. Interestingly, a significant increase in apoplastic cell wall invertase expression was observed in grapevine leaves in response to infection by biotrophic fungal pathogens, which was linked to a reduced phloem loading and thus to leaves switching from source organs to carbohydrate sinks (Hayes *et al*. 2010). The transcriptional regulation of cell wall invertase, much more than vacuolar invertase, in response to phytoplasma infection deserves attention in the future.

Together with impaired sucrose loading and increased invertase expression, analysis focused on phloem revealed a specific dramatic up-regulation of *SUS* in the response to stolbur, thus suggesting high rates of sucrose metabolism in the infection site. Co-regulation of both sucrose transport and cleavage would be advantageous for the pathogen, as both responses are crucial to access hexoses. SUS is often regarded as being more energy conservative than invertase reaction, as it produces fructose and nucleoside diphosphate-glucose (mainly UDPG and ADPG), the latter being used as phosphorylated sugar in biosynthetic processes (Winter & Huber 2000). SUS is encoded by a small family of genes, divergent and differentially expressed. Recently, immunolocalization and Western blot analysis showed a several-fold induction of a low oxygen inducible SUS isoform in companion cells of phytoplasma-inhabited phloem of maize leaf sheaths and stems (Brzin *et al*. 2011), suggesting a pivotal role of this enzyme both in sucrose partitioning and in responding to the pathogen. SUS is also believed to play a major role in both starch and cellulose biosynthesis (Baroja-Fernández *et al*. 2012). The UDPG produced by a membrane-associated form of SUS is thought to be used directly as a substrate for cellulose synthase in the rosette complex where the SUS is an integral component (Amor *et al*. 1995; Fujii, Hayashi & Mizuno 2010). UDPG is also used as a glucose donor to the growing polymer chain similar to cellulose synthases by CASs. Callose is usually deposited at plasmodesmata and at sieve plates as a response to developmental cues and pathogen attack. Together with restriction of phytoplasmas to the sieve elements, callose deposits on the sieve plates, often followed by collapse of the sieve elements, has been observed (Musetti 2010). Nevertheless, the *CAS2* gene examined in our work was not affected by stolbur in phloem, although induced when its expression was analysed in the whole leaf, thus confirming what was observed by Hren *et al*. (2009) in leaves. This, of course, does not mean that *CAS* genes cannot be co-ordinately expressed with SUS in the phloem; probably different genes of the *CAS* family have to be considered for the analysis of phloem cells.

The transcript levels of a significant number of genes related to wall metabolism, stress response and defence were shown to be changed in infected grapevine

(Albertazzi *et al*. 2009; Hren *et al*. 2009). Among these, genes belonging to the PR group 5 (PR-5) such as osmotin and thaumatin-like were found to be significantly induced in BN- and FD-infected leaves (Albertazzi *et al*. 2009; Hren *et al*. 2009; Margaria & Palmano 2011), as well as in other plant/phytoplasma interactions (Zhong & Shen 2004). Most TLPs, which belong to the superfamily of glycoside hydrolases, possess antifungal or glycan-lytic activity, and could hinder the growth of plant invading microbes by affecting pathogen membrane permeability (van Loon, Rep & Pieterse 2006). These properties are likely associated with the presence of a conserved acid cleft in their three-dimensional (3D) structure (Petre *et al*. 2011). We examined gene expression of two TLPs, *TLP4* and *TLP5*, which resulted as differentially responsive to stolbur infection. The *TLP4* gene, which was barely detectable in healthy but several fold (20-fold) induced in infected phloem cells, appeared directly involved in the plant response to stolbur at the site of infection. Differently, the expression of *TLP5* was more induced in the whole leaf than in phloem cells, where, in any case, it resulted as being the most expressed among the examined genes in both healthy and infected samples. The high expression of this latter defence gene could be related to the reported ability of some members of this gene family to respond to different environmental stresses, such as pathogen/pest attack, drought, salt stress and cold (van Loon *et al*. 2006).

In conclusion, our findings demonstrated that phytoplasma infection in grapevine is correlated with important changes in sugar metabolism and transport in the phloem, suggesting the establishment of a phytoplasma-induced switch from carbohydrate source to sink. Moreover, the expression analysis focused on the phloem showed a differential regulation of two PR thaumatin-like genes (*TLP4* and *TLP5*) of the PR-5 family, with a similar function but supposedly different characteristics. These findings were permitted by the tissue-specific approach, which dramatically increased sensitivity, thus highlighting specific host processes otherwise almost completely masked in the whole-leaf analysis. Global expression analysis associated with the LM technique, which has been optimized for grapevine leaf in this work, can be a very powerful approach to identify host genes and processes directly involved in the interaction with the phytoplasma.

ACKNOWLEDGMENTS

We would like to thank Stefano Gustincich (SISSA, International School for Advanced Studies, Trieste, Italy) for the use of the LMPC system. We also thank Paolo Ermacora (DISA, University of Udine, Italy) for the excellent work of monitoring BN in vineyard, Marta Martini (DISA, University of Udine, Italy) for primers used in experiments of stolbur *16S rRNA* detection and helpful suggestions, and Giannina Vizzotto (DISA, University of Udine, Italy) for critical comments on the manuscript. Text has been revised by 'WS traduzioni', Udine, Italy.

This research was funded by AGER, Project No. 2010–2106 'Grapevine yellows: innovative technologies for the diagnosis and the study of plant/pathogen interactions'. The authors have no conflict of interest to declare.

AUTHORS CONTRIBUTIONS

S.S. established the protocol for LMPC, collected cells and performed real-time RT-PCR with the contribution of S.G and A.P. S.S. established and carried out one-step RT-PCR analyses. F.D.M and A.P. performed real-time RT-PCR on leaves. S.S and R.M. conceived and supervised the study. S.S. wrote the manuscript with input from R.M.

REFERENCES

Afoufa-Bastien D., Medici A., Jeauffre J., Coutos-Thévenot P., Lemoine R., Atanassova R. & Laloi M. (2010) The *Vitis vinifera* sugar transporter gene family: phylogenetic overview and macroarray expression profiling. *BMC Plant Biology* **10,** 245.

Albertazzi G., Milc J., Caffagni A., *et al.* (2009) Gene expression in grapevine cultivars in response to Bois Noir phytoplasma infection. *Plant Science* **176,** 792–804.

Altschul S.F., Madden T.L., Schaffer A.A., Zhang J., Zhang Z., Miller W. & Lipman D.J. (1997) Gapped BLAST and PSI-BLAST: a new generation of protein database search programs. *Nucleic Acids Research* **25,** 3389–3402.

Amor Y., Haigler C.H., Johnson S., Wainscott M. & Delmer D.P. (1995) A membrane-associated form of sucrose synthase and its potential role in synthesis of cellulose and callose in plants. *Proceedings of the National Academy of Sciences of the United States of America* **92,** 9353–9357.

André A., Maucourt M., Moing A., Rolin D. & Joël Renaudin J. (2005) Sugar import and phytopathogenicity of *Spiroplasma citri*: glucose and fructose play distinct roles. *Molecular Plant-Microbe Interactions* **18,** 33–42.

Bai X., Correa V.R., Toruño T.Y., Ammar E.-D., Kamoun S. & Hogenhout S.A. (2009) AY-WB phytoplasma secretes a protein that targets plant cell nuclei. *Molecular Plant-Microbe Interactions* **22,** 18–30.

Barcala M., Garcia A., Cabrera J., Casson S., Lindsey K., Favery B., Garcia- Casado G., Solano R., Fenoll C. & Escobar C. (2010) Early transcriptomic events in microdissected Arabidopsis nematode-induced giant cells. *The Plant Journal* **61,** 698–712.

Baroja-Fernández E., Muñoza F.G., Lia J., Bahajia A., Almagroa G., Monteroa M., Etxeberriac E., Hidalgoa M., Sesmaa M.T. & Pozueta-Romeroa J. (2012) Sucrose synthase activity in the sus1/sus2/sus3/sus4 *Arabidopsis* mutant is sufficient to support normal cellulose and starch production. *Proceedings of the National Academy of Sciences of the United States of America* **109,** 321–326.

Belli G., Bianco P.A. & Conti M. (2010) Grapevine yellows in Italy: past, present and future. *Journal of Plant Pathology* **92,** 303–326.

Bertamini M., Nedunchezhian N., Tomasi F. & Grando M.S. (2002) Phytoplasma [stolbur-subgroup (Bois Noir-BN)] infection inhibits photosynthetic pigments, ribulose-1,5-bisphosphate carboxylase and photosynthetic activities in field grown grapevine (*Vitis vinifera* L. cv. *Chardonnay*) leaves. *Physiological and Molecular Plant Pathology* **61,** 357–366.

Bieniawska Z., Barratt D.H.P., Garlick A.P., Thole V., Kruger N.J., Martin C., Zrenner R. & Smith A.M. (2007) Analysis of the sucrose synthase gene family in Arabidopsis. *The Plant Journal* **49,** 810–828.

Brzin J., Petrovic N., Ravnikar M. & Kovac M. (2011) Induction of sucrose synthase in the phloem of phytoplasma infected maize. *Biologia Plantarum* **55,** 711–715.

Chandran D., Inada N., Hather G., Kleindt C.K. & Wildermuth M.C. (2010) Laser microdissection of *Arabidopsis* cells at the powdery mildew infection site reveals site-specific processes and regulators. *Proceedings of the National Academy of Sciences of the United States of America* **107,** 460–465.

Christensen N.M., Nicolaisen M., Hansen M. & Schulz A. (2004) Distribution of phytoplasmas in infected plants as revealed by real-time PCR and bioimaging. *Molecular Plant-Microbe Interactions* **17,** 1175–1184.

Christensen N.M., Axelsen K.B., Nicolaisen M. & Schulz A. (2005) Phytoplasmas and their interactions with hosts. *Trends in Plant Science* **10,** 526–535.

Davies C. & Robinson P. (2000) Differential screening indicates a dramatic change in mRNA profiles during grape berry ripening. Cloning and characterization of cDNAs encoding putative cell wall and stress response proteins. *Plant Physiology* **122,** 803–812.

Davies C. & Robinson S.P. (1996) Sugar accumulation in grape berries: cloning of two putative vacuolar invertase cDNAs and their expression in grapevine tissues. *Plant Physiology* **111,** 275–283.

Davies C., Wolf T. & Robinson S.P. (1999) Three putative sucrose transporters are differentially expressed in grapevine tissues. *Plant Science* **147,** 93–100.

Day R.C., McNoe L.E. & Macknight R.C. (2007) Transcript analysis of laser microdissected plant cells. *Physiologia Plantarum* **129,** 267–282.

Deeken R., Ache P., Kajahn I., Klinkenberg J., Bringmann G. & Hedrich R. (2008) Identification of *Arabidopsis thaliana* phloem RNAs provides a search criterion for phloem-based transcripts hidden in complex datasets of microarray experiments. *The Plant Journal* **55,** 746–759.

Firrao G., Gibb K. & Stereten C. (2005) Short taxonomic guide to the genus '*Candidatus* phytoplasma'. *Journal of Plant Pathology* **87,** 249–263.

Fosu-Nyarko J., Jones M.G.K. & Wang Z.H. (2009) Functional characterization of transcripts expressed in early-stage *Meloidogyne javanica*-induced giant cells isolated by laser microdissection. *Molecular Plant Pathology* **10,** 237–248.

Fujii S., Hayashi T. & Mizuno K. (2010) Sucrose synthase is an integral component of the cellulose synthesis machinery. *Plant & Cell Physiology* **51,** 294–301.

Gaurivaud P., Danet J.L., Laigret F., Garnier M. & Bové J.M. (2000) Fructose utilization and phytopathogenicity of *Spiroplasma citri*. *Molecular Plant-Microbe Interactions* **13,** 1145–1155.

Hayes A., Feechan A. & Dry I.B. (2010) Involvement of abscisic acid in the coordinated regulation of a stress-inducible hexose transporter (VvHT5) and a cell wall invertase in grapevine in response to biotrophic fungal infection. *Plant Physiology* **153,** 211–221.

Hogenhout S.A., Oshima K., Ammar E., Kakizawa S., Kingdom H.N. & Namba S. (2008) Phytoplasmas: bacteria that manipulate plants and insects. *Molecular Plant Pathology* **9,** 403–423.

Hoshi A., Oshima K., Kakizawa S., Ishii Y., Ozeki J., Hashimoto M., Komatsu K., Kagiwada S., Yamaji Y. & Namba S. (2009) A unique virulence factor for proliferation and dwarfism in plants identified from a phytopathogenic bacterium. *Proceedings of the National Academy of Sciences of the United States of America* **106,** 6416–6421.

Hren M., Nikolic P., Rotter A., Blejec A., Terrier N., Ravnikar M., Dermastia M. & Gruden K. (2009) Bois noir phytoplasma induces significant reprogramming of the leaf transcriptome in the field grown grapevine. *BMC Genomics* **10,** 460.

Imlau A., Truernit E. & Sauer N. (1999) Cell-to-cell and long-distance trafficking of the green fluorescent protein in the phloem and symplastic unloading of the protein into sink tissues. *The Plant Cell* **11,** 309–322.

Inada N. & Wildermuth M.C. (2005) Novel tissue preparation method and cell-specific marker for laser microdissection of mature leaf. *Planta* **221,** 9–16.

Ivashikina N., Deeken R., Ache P., Kranz E., Pommerrenig B., Sauer N. & Hedrich R. (2003) Isolation of AtSUC2 promoter-GFP-marked companion cells for patch-clamp studies and expression profiling. *The Plant Journal* **36,** 931–945.

Kerk N.M., Ceserani T., Tausta S.L., Sussex I.M. & Nelson T.M. (2003) Laser capture microdissection of cells from plant tissues. *Plant Physiology* **132,** 27–35.

Klink V.P., Overall C.C., Alkharouf N.W., MacDonald M.H. & Matthews B.F. (2007) Laser capture microdissection (LCM) and comparative microarray expression analysis of syncytial cells isolated from incompatible and compatible soybean (*Glycine max*) roots infected by the soybean cyst nematode (*Heterodera glycines*). *Planta* **226,** 1389–1409.

Kube M., Schneider B., Kuhl H., Dandekar T., Heitmann K., Migdoll A.M., Reinhardt R. & Seemüller E. (2008) The linear chromosome of the plant pathogenic mycoplasma '*Candidatus* Phytoplasma mali'. *BMC Genomics* **9,** 306.

Lepka P., Stitt M., Moll E. & Seemuller E. (1999) Effect of phytoplasmal infection on concentration and translocation of carbohydrates and amino acids in periwinkle and tobacco. *Physiological and Molecular Plant Pathology* **55,** 59–68.

van Loon L.C., Rep M. & Pieterse C.M.J. (2006) Significance of inducible defense-related proteins in infected plants. *Annual Review of Phytopathology* **44,** 135–162.

Loulakakis K.A. (1997) Nucleotide sequence of a *Vitis vinifera* L. cDNA (accession no. Y10992) encoding for osmotin-like protein (PGR 97-064). *Plant Physiology* **113,** 1464.

MacKenzie D.J., McLean M.A., Mukerji S. & Green M. (1997) Improved RNA extraction from woody plants for the detection of viral pathogens by reverse transcription-polymerase chain reaction. *Plant Disease* **81,** 222–226.

Margaria P. & Palmano S. (2011) Response of the *Vitis vinifera* L. cv. 'Nebbiolo' proteome to Flavescence dorée phytoplasma infection. *Proteomics* **11,** 212–224.

Maust B.E., Espadas F., Talavera C., Aguilar M., Santamaría J.M. & Oropeza C. (2003) Changes in carbohydrate metabolism in coconut palms infected with the lethal yellowing phytoplasma. *Phytopathology* **93,** 976–981.

Muller P.Y., Janovjak H., Miserez A.R. & Dobbie Z. (2002) Processing of gene expression data generated by quantitative real-time RT-PCR. *Biotechniques* **32,** 1372–1379.

Musetti R. (2010) Biochemical changes in plant infected by phytoplasmas. In *Phytoplasmas: Genomes, Plant Hosts and Vectors* (eds P. Jones & P. Weintraub), pp. 132–146. CABI Publishing, Wallingford.

Nakashima J., Laosinchai W., Cui X. & Brown R.M. Jr (2003) New insight into the mechanism of cellulose and callose biosynthesis: protease may regulate callose biosynthesis upon wounding. *Cellulose* **10,** 369–386.

Nakazono M., Qiu F., Borsuk L.A. & Schnable P.S. (2003) Laser-capture microdissection, a tool for the global analysis of gene expression in specific plant cell types: identification of genes expressed differentially in epidermal cells or vascular tissues of maize. *The Plant Cell* **15,** 583–596.

Nelson T., Tausta S.L., Gandotra N. & Liu T. (2006) Laser microdissection of plant tissue: what you see is what you get. *Annual Review of Plant Biology* **57,** 181–201.

Oshima K., Kakizawa S., Nishigawa H., *et al.* (2004) Reductive evolution suggested from the complete genome sequence

of a plant-pathogenic phytoplasma. *Nature Genetics* **36,** 27–29.

Oshima K., Kakizawa S., Arashida R., Ishii Y., Hoshi A., Hayashi Y., Kagiwada S. & Namba S. (2007) Presence of two glycolytic gene clusters in a severe pathogenic line of *Candidatus* Phytoplasma asteris. *Molecular Plant Pathology* **8,** 481–489.

Osler R., Carraro L., Loi N. & Refatti E. (1993) Symptom expression and disease occurrence of a yellows disease of grapevine in northeastern Italy. *Plant Disease* **77,** 496–498.

Petre B., Major I., Rouhier N. & Duplessis S. (2011) Genome-wide analysis of eukaryote thaumatin-like proteins (TLPs) with an emphasis on poplar. *BMC Plant Biology* **11,** 33.

Pfaffl M.W. (2001) A new mathematical model for relative quantification in real-time RT-PCR. *Nucleic Acid Research* **29,** e45.

Rozen S. & Skaletsky H. (2000) Primer3 on the WWW for general users and for biologist programmers. *Methods in Molecular Biology* **132,** 365–386.

Santi S. & Schmidt W. (2008) Laser microdissection-assisted analysis of the functional fate of iron deficiency-induced root hairs in cucumber. *Journal of Experimental Botany* **59,** 697–704.

Sauer N. (2007) Molecular physiology of higher plant sucrose transporters. *Federation of European Biochemical Societies Letters* **581,** 2309–2317.

Shad M., Lipton M.S., Giavalisco P., Smith R.D. & Kehr J. (2005a) Evaluation of2-DE and LC-MS/MS for tissue-specific protein profiling of laser microdissected plant samples. *Electrophoresis* **26,** 2729–2738.

Shad M., Mungur R., Fiehn O. & Kehr J. (2005b) Metabolic profile of laser microdissected vascular bundles of *Arabidopsis thaliana*. *Plant Methods* **1,** 1–10.

Silver N., Best S., Jiang J. & Thein S.L. (2006) Selection of housekeeping genes for gene expression studies in human reticulocytes using real-time PCR. *BMC Molecular Biology* **7,** 33.

Tang W., Coughlan S., Crane E., Beatty M. & Duvick J. (2006) The application of laser microdissection to in planta gene expression profiling of the maize anthracnose stalk rot fungus *Colletotrichum graminicola*. *Molecular Plant-Microbe Interactions* **11,** 1240–1250.

Tran-Nguyen L.T.T., Kube M., Schneider B., Reinhardt R. & Gibb K.S. (2008) Comparative genome analysis of '*Candidatus* Phytoplasma australiense' (subgroup *tuf*-Australia I; *rp*-A) and '*Ca*. Phytoplasma asteris' strains OY-M and AY-WB. *Journal of Bacteriology* **190,** 3979–3991.

Vandesompele J., De Preter K., Pattyn F., Poppe B., Van Roy N., De Paepe A. & Speleman F. (2002) Accurate normalization of real-time quantitative RT-PCR data by geometric averaging of multiple internal control genes. *Genome Biology* **3,** research0034.

Voegele R.T., Wirsel S., Möll U., Lechner M. & Mendgen K. (2006) Cloning and characterization of a novel invertase from the obligate biotroph *Uromyces fabae* and analysis of expression patterns of host and pathogen invertases in the course of infection. *Molecular Plant-Microbe Interactions* **19,** 625–634.

Winter H. & Huber S. (2000) Regulation of sucrose metabolism in higher plants: localisation and regulation of activity of key enzymes. *Critical Reviews in Plant Sciences* **19,** 31–67.

Zhang D., Xu B., Yang X., Zhang Z. & Li B. (2011) The sucrose synthase gene family in Populus: structure, expression, and evolution. *Tree Genetics & Genomes* **7,** 443–456.

Zhong B.X. & Shen Y.W. (2004) Accumulation of pathogenesis related type-5 like proteins in phytoplasma-infected garland chrysanthemum *Chrysanthemum coronarium*. *Acta Biochimica et Biophysica Sinica* **36,** 773–779.

Received 31 May 2012; received in revised form 5 July 2012; accepted for publication 8 July 2012

MPMI Vol. 26, No. 4, 2013, pp. 379–386. http://dx.doi.org/10.1094/MPMI-08-12-0207-R.

e-Xtra*

Phytoplasma-Triggered Ca^{2+} Influx Is Involved in Sieve-Tube Blockage

Rita Musetti,[1] Stefanie V. Buxa,[2] Federica De Marco,[1] Alberto Loschi,[1] Rachele Polizzotto,[1] Karl-Heinz Kogel,[1] and Aart J. E. van Bel[2]

[1]Department of Agricultural and Environmental Sciences, University of Udine, via delle Scienze, 208, I-33100 Udine, Italy; [2]Department of Phytopathology and Applied Zoology, Justus Liebig University, Heinrich-Buff-Ring 26-32, D-35392 Giessen, Germany

Submitted 31 August 2012. Accepted 30 November 2012.

Phytoplasmas are obligate, phloem-restricted phytopathogens that are disseminated by phloem-sap-sucking insects. Phytoplasma infection severely impairs assimilate translocation in host plants and might be responsible for massive changes in phloem physiology. Methods to study phytoplasma-induced changes thus far provoked massive, native occlusion artifacts in sieve tubes. Hence, phytoplasma-phloem relationships were investigated here in intact *Vicia faba* host plants using a set of vital fluorescent probes and confocal laser-scanning microscopy. We focused on the effects of phytoplasma infection on phloem mass-flow performance and evaluated whether phytoplasmas induce sieve-plate occlusion. Apparently, phytoplasma infection brings about Ca^{2+} influx into sieve tubes, leading to sieve-plate occlusion by callose deposition or protein plugging. In addition, Ca^{2+} influx may confer cell wall thickening of conducting elements. In conclusion, phytoplasma effectors may cause gating of sieve-element Ca^{2+} channels leading to sieve-tube occlusion with presumptive dramatic effects on phytoplasma spread and photoassimilate distribution.

Phytoplasmas are prokaryotic microorganisms that bring about several hundred diseases affecting economically important crops such as ornamentals, vegetables, fruit trees, and grapevines. Phytoplasmas mostly colonize the sieve tubes and manipulate the host to ensure an efficient distribution and multiplication (Hogenhout et al. 2008). To date, the physiological relationship between phytoplasmas and their hosts has remained largely unexplored (Hogenhout et al. 2008). Phytoplasmas have a very small genome (530 to 1,350 kb) and lack many genes otherwise considered to be essential for cell metabolism (Marcone et al. 1999).

Several studies demonstrated that phytoplasma infection induces important cytological and physiological modifications in the phloem of host plants, in several cases severely affecting phloem transport (Braun and Sinclair 1978; Kartte and Seemüller 1991; Lepka et al. 1999; Maust et al. 2003). It has been speculated that mechanisms involved in phloem impairment could differ between pathosystems and vary with the plant susceptibility to infection (Kartte and Seemüller 1991; Musetti and Favali 1999).

Histological studies on several plant species infected by phytoplasmas showed that the first detectable anatomical aberration is an abnormal deposition of callose in the sieve-plate regions which is followed by a collapse of sieve elements and companion cells (Kartte and Seemüller 1991). Sieve-plate occlusion has been regarded as a defense mechanism leading to the formation of physical barriers aimed to achieve pathogen containment (Musetti et al. 2008). In phytoplasma-infected tobacco plants treated with fungal elicitors (Lherminier et al. 2003) as well as in other pathosystems (Elad and Evensen 1995; Koh et al. 2012), concomitant callose accumulation and P protein agglutination have been reported to occur in sieve tubes in response to infection.

Expression of genes responsible for callose deposition in sieve tubes is finely tuned. This is exemplified by the role of callose synthase (CLS7) in normal sieve-element maturation in *Arabidopsis* as well as in the response to wounding (Barratt et al. 2011; Xie et al. 2011), showing that callose production is a balancing act for plants. An analogous trade-off event must occur in infected plants: massive callose deposition restricts host colonization by phytoplasmas but, at the same time, impedes photo-assimilate transport. Moreover, recovery—a spontaneous reduction of the disease symptoms of phytoplasma-infected plants—is accompanied by an appreciable upregulation of two callose synthase and three phloem protein (PP2) genes (Musetti et al. 2010).

It has been demonstrated that sieve plates are plugged by proteins in response to mechanical injuries prior to callose deposition (Furch et al. 2007, 2010). Structural proteins in sieve tubes have been observed for a long time (Cronshaw and Sabnis 1990). Some of these proteins (later named sieve-element occlusion [SEO] proteins) (Pelissier et al. 2008) are involved in sieve-tube plugging. In members of the family Fabaceae, SEO are aggregated in giant protein bodies called forisomes (Knoblauch et al. 2001). In response to different stresses (wounding, burning, and cold), forisomes undergo a conformational change from a condensed to a dispersed state which plugs the sieve plates and prevents loss of photoassimilates (Furch et al. 2007; Knoblauch et al. 2001; Thorpe et al. 2010). Genes encoding SEO protein components do not occur only in Fabaceae species (Pelissier et al. 2008; Tuteja et al. 2010) but appear to be widespread among dicotyledonous plants such as apple, grapevine, and *Arabidopsis* (Rüping et al. 2010). Preliminary gene expression analyses for SEO protein components revealed an upregulation in phytoplasma-infected apple trees compared with healthy ones (Musetti et

Corresponding author: R. Musetti; Telephone: +(39) 0432 558521; Fax: +(39) 0432 558501; E-mail: Rita.Musetti@uniud.it

*The *e*-Xtra logo stands for "electronic extra" and indicates that a supplementary table is published online.

al. 2011), indicating potential involvement in response to phytoplasma infection.

Callose synthesis as well as P protein aggregation are Ca^{2+}-dependent phenomena (Knoblauch et al. 2001; Köhle et al. 1985) triggered by Ca^{2+} influx into sieve elements (Furch et al. 2007, 2009, 2010). Thus, occlusion events suggest that phytoplasma infection induces gating of Ca^{2+} channels and consequent influx of Ca^{2+} into sieve elements (Musetti et al. 2008). This would confer a quick and straightforward defense response in plants undergoing phytoplasma attack.

Because unequivocal in vivo evidence for phytoplasma-mediated sieve-tube occlusion is lacking thus far, the aim of this work was to design and optimize a method to perform in vivo observation of the phloem in phytoplasma-infected intact plants. Deposition of callose and changes in forisome conformation were examined in relation to mass flow and compared between healthy and phytoplasma-infected broadbean (*Vicia faba* L.) plants (used as hosts of '*Candidatus* Phytoplasma vitis', associated with grapevine Flavescence Dorée [FD]) by using confocal laser-scanning microscopy (CLSM). In particular, we evaluated whether phytoplasmas induce Ca^{2+} influx leading to occlusion by callose deposition or protein plugging and inherent impairment of mass flow.

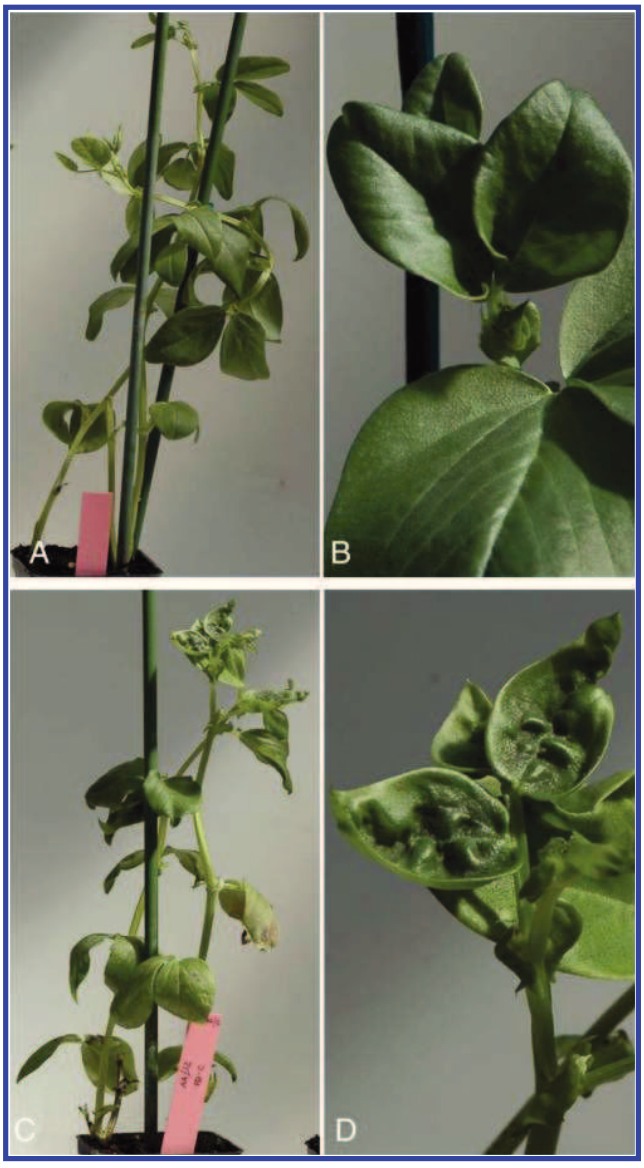

Fig. 1. Images of healthy (left half of the panel) and Flavescence Dorée (FD)-infected (right half) *Vicia faba* plants. **A** through **D,** Whole plants and leaf details. **A** and **B,** Healthy *V. faba* plants show regular growth and do not develop disease symptoms. **C** and **D,** In FD-infected plants (C and D) typical symptoms are visible, such as general decline, beginning leaf decoloration, and leaf deformation.

RESULTS

Plant materials and phytoplasma detection by polymerase chain reaction.

Control *V. faba* plants, not exposed to leafhoppers, showed regular growth without disease symptoms (Fig. 1A and B). In infected plants, typical FD symptoms such as leaf-size reduction, leaf yellowing, and curling (Fig. 1C and D) emerged approximately 1 month after inoculation by the insect vectors.

Real-time polymerase chain reaction (RT-PCR) of '*Ca.* P. vitis' 16SrRNA confirmed the presence of phytoplasmas in infected *V. faba* leaf samples before CLSM examination. Starting from 40 ng of total DNA, FD-phytoplasma 16SrDNA was detected in symptomatic samples, whereas no amplification of the 16SrRNA gene was obtained in healthy ones. DNAs isolated from FD-diseased *Catharanthus roseus* and FD-infected *Vitis vinifera* were also amplified as positive parallel controls (Supplementary Table S1).

Optical phytoplasma detection and mass flow.

In vivo observation of *Vicia faba* phloem by CLSM enabled us to observe sieve elements in intact plants. Under transmission light, healthy sieve elements were characterized by the presence of condensed forisomes (Fig. 2A), while the sieve plates were free of visible occluding substances (Fig. 2A).

After (5)6 carboxyfluorescein diacetate (CFDA) application to healthy *V. faba* plants, phloem-mobile (5)6 carboxyfluorescein (CF) was translocated through the sieve tubes and accumulated in the companion cells, which indicates a regular mass flow and a high degree of metabolic activity in companion cells (Fig. 2B). As reported previously for other cell types (Goodwin et al. 1990), CF accumulated in the vacuoles of phloem parenchyma cells. In stained sieve elements, several parietal plastids were visible (Fig. 2B), probably anchored to the plasma membrane (Ehlers et al. 2000). Nuclei were recognizable in both companion and phloem parenchyma cells (Fig. 2B), probably after CFDA movement through plasmodesmata. It was more difficult to focus and discern sieve tubes in FD-diseased plants due to the presence of thicker cell walls and sediments onto the sieve plates (Fig. 2C). In such plants, only a few sieve elements were weakly fluorescent after CFDA application, indicating that mass flow was blocked or strongly reduced (Fig. 2D). Even when mass flow in sieve tubes appeared to be reduced or eliminated, CFDA was observed to accumulate in the vacuoles of companion cells (Fig. 2D), which may indicate the maintenance of some metabolic ability.

After 4′,6-diamidino-2-phenylindole (DAPI) application to enable phytoplasma detection, no DAPI fluorescence showed up in sieve elements of healthy plants; only the nuclei of companion cells and phloem parenchyma cells were stained (Fig. 2E). Under transmission light, the sieve elements were well preserved and unstained in healthy plants (Fig. 2F). In FD-diseased plants, dotted fluorescent aggregates were accumulated predominantly at the sieve plates (Fig. 2G, arrows). In FD-diseased sieve elements, cell walls and sediments on the sieve plates were thicker than in control plants (Fig. 2H), as described above.

Successive local DAPI and distant CFDA staining demonstrated that absence of DAPI staining is related to intense CFDA translocation in the phloem of healthy plants (Fig. 2I and J). By contrast, DAPI fluorescence (Fig. 2K) coincides with

impaired sieve-tube translocation in infected plants (Fig. 2L). In both healthy and infected plants, the reverse CFDA/DAPI double-staining procedure produced results similar to those for DAPI/CFDA staining (Fig. 2M through P).

Occlusion events and Ca^{2+} concentration.

Combined 5-chloromethyl-fluoresceindiacetate and 5-chloromethyl-eosin-diacetate (CMFDA/CMFDA) staining provided unequivocal information on the forisome conformation and protein distribution inside the sieve elements of healthy and FD-diseased plants in CLSM images. In healthy plants, forisomes were always in the condensed, spindle-shaped form (Fig. 3A and B) and were mostly located near the sieve plates at the downstream end of the sieve elements. In FD-diseased plants, discrete forisomes were not detectable (Fig. 3C and D), which is indicative of their dispersion (Knoblauch et al. 2001). Unidentified protein structures—dispersed forisomes or clogged P proteins—occurred in FD-diseased sieve elements (Fig. 3C).

Aniline blue at nonlethal concentrations (Furch et al. 2007) was administered to bare-lying phloem tissue to acquire a qualitative in vivo estimate of callose deposition in sieve elements. In healthy plants, callose was not detectable (Fig. 3E) or occurred in minor amounts at the margins of the sieve plates (Fig. 3I) and the sieve elements were well preserved, containing condensed forisomes (Fig. 3F and J).

By contrast, aniline blue signals were much stronger in FD-diseased *V. faba* plants, indicating massive callose depositions at the sieve plates and along the sieve elements, probably at the pore-plasmodesmata-unit orifices (Fig. 3G) (Furch et al. 2009) to the point of plug formation (Fig. 3K, arrows). Increased thickness of the sieve-element walls and accumulation of dark material at the sieve plates were also visible under transmission light (Fig. 3H and L).

Oregon Green 1,2-bis(o-aminophenoxy)ethane-N,N,-N′,N′-tetraacetic acid (OGB-1) was used as a qualitative indicator of Ca^{2+} concentration inside the sieve elements. No fluorescent signals were detected in intact sieve elements of uninfected

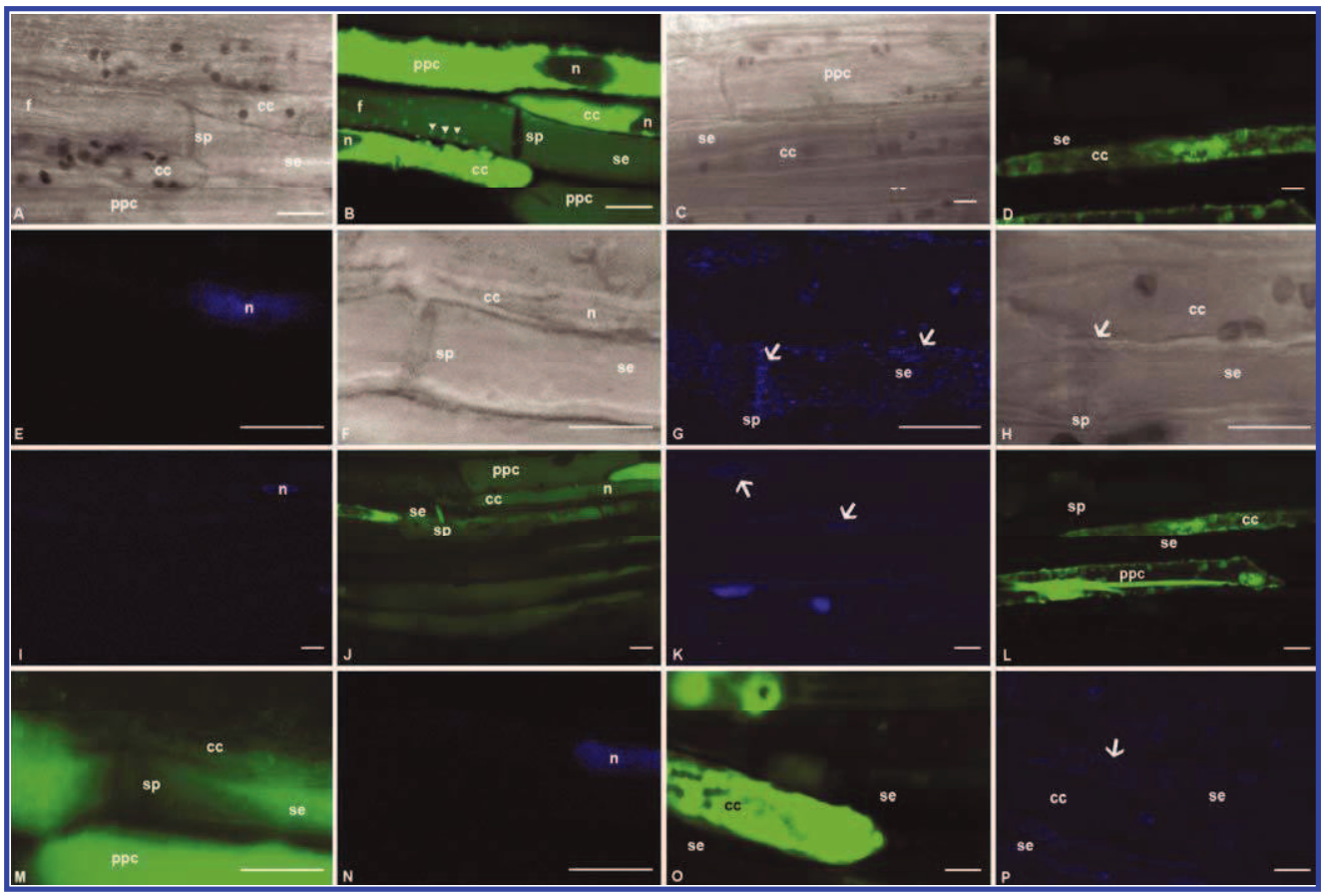

Fig. 2. Confocal laser-scanning microscopy (CLSM) images of phloem tissue in intact healthy (left half of the panel) and Flavescence Dorée (FD)-infected (right half) *Vicia faba* plants. **A** and **B,** Healthy and **C** and **D,** FD-infected phloem under **A** and **C,** transmission light and **B** and **D,** after distant (5)6 carboxyfluorescein diacetate (CFDA) application, observed at 488 nm. In healthy *V.* faba plants, sieve elements (se) are characterized by the presence of forisomes (A, f) and plastids (B, arrowheads). FD-infected *V. faba* plants do not show remarkable content in transmission light (C). Following sieve-tube translocation of CFDA in healthy plants (B), CFDA is accumulated in the vacuoles of companion (cc) and phloem parenchyma cells (ppc). With the exception of the vacuoles of companion cell (cc), fluorescence is absent in sieve elements of FD-infected plants (D), indicative of mass-flow inhibition. **E** and **F,** Healthy and **G** and **H,** FD-infected phloem after 4′,6-diamidino-2-phenylindole (DAPI) staining, observed at **E** and **G,** 405 nm and **F** and **H,** under transmission light. In sieve elements of FD-infected plants, blue fluorescent dots (arrows) mainly aggregate on both sides of the sieve plate (G, sp). Phloem in healthy plants remains unlabeled apart from the stained nuclei (E, n). Under transmission light, in healthy plants (F), cell walls and sieve plate thickening seem inconspicuous. Note the distorted thickened cell walls and sieve plate thickenings (arrow) visible in FD-infected plants (H). **I** through **L,** Subsequent local DAPI staining and distant CFDA application demonstrate that absence of DAPI staining (I) (apart from the stained nuclei) concurs with regular CFDA translocation (J) in the phloem of healthy plants. By contrast, DAPI fluorescence, indicating phytoplasma presence (K, arrows), seems to coincide with impaired sieve-tube translocation in infected plants (L). **M** through **P,** Reverse CFDA/DAPI double-staining procedure renders results similar to those obtained with DAPI/CFDA treatment in both healthy (M and N) and infected (O and P) plants. cc = companion cell, f = forisome, n = nucleus, ppc = phloem parenchyma cell, se = sieve element, sp = sieve plate. Arrowheads in B indicate sieve-element plastids; in G, K, and P, arrows indicate phytoplasma/DAPI fluorescence. Bars correspond to 10 µm.

V. faba plants (Fig. 4A). The identical optical section observed under transmission light showed unstressed sieve elements as inferred by the presence of condensed forisomes (Fig. 4B). In the phloem of diseased plants, OGB-1 fluorescence was often intense, with strong signals at the sieve plates (Fig. 4C and G). Under transmission light, condensed forisomes did not occur (Fig. 4D and H). Weak OGB-1 signals were sometimes found in healthy sieve elements (Fig. 4E, arrow) that were mechanically stressed as a result of the preparation procedure, as indicated by forisome dispersion (Fig. 4F).

Fluorescence was not detected in unstained healthy (Fig. 4I and J) or FD-infected (Fig. 4K and L) samples, with the exception of the chloroplasts. Neither of the excitation wavelengths used for the respective fluorochromes (405 nm [Fig. 4I and K] or 488 nm [Fig. 4J and L]) elicited fluorescent signals.

DISCUSSION

Because phytoplasmas are obligate parasites transmitted to host plants by insect vectors in a persistent manner (Hogenhout et al. 2008) and insect inoculation requires several days, it is difficult to pinpoint the exact moment at which phytoplasmas initiate the infective processes in host plants. Therefore, we were urged to use systemically infected plants to study occlusion events; however, it is obvious that the initial occlusion stages have not been caught here.

In vivo phytoplasma detection.

In contrast to the progress made in detection and taxonomic classification of phytoplasmas, very little is known about plant–phytoplasma interactions. Phytoplasmas induce characteristic symptoms in host plants, many of which (such as low productivity, stunting, general decline, and reduced vigor) point to impairment of sieve-tube function (Kartte and Seemüller 1991). Because phytoplasmas (mainly in the case of woody plants) are not evenly distributed over the sieve tubes (Faoro 2005), despite the systemic spread via the phloem, phloem impairment and the subsequent development of the disease symptoms cannot be explained solely by the presence of phytoplasmas plugging the sieve elements, but also must involve the impact of phytoplasma-secreted effector proteins on plant cells (Hogenhout et al. 2008).

Knowledge about the phytoplasma capability to spread through sieve elements is essential for understanding the relationships with the host. Previous attempts to describe the colonization behavior of phytoplasmas via sieve tubes have been made using conventional microscopic, serological, or molecular methods (Lherminier et al. 1994; Marcone 2010). Cytological modifications such as sieve-element necrosis, abnormal callose deposition at the sieve plates, sieve-element wall thickening, and starch accumulation in the shoots of susceptible plants have been documented by electron microscopic observations (Braun and Sinclair 1978; Kartte and Seemüller 1991; Musetti and Favali 1999; Musetti et al. 1994).

Moreover, one should bear in mind that studies of ultrathin sections are laborious and time-consuming and only small portions of fixed and embedded tissue of interest can be examined. Both electron-microscopic techniques and molecular methods, based on extraction of different cell components (i.e., DNA, RNA, and proteins), are destructive. The necessity to kill plant tissues causes instantaneous, irreversible, and massive reactions of sieve elements to wounding (van Bel 2003), which may lead to pieces of misleading information and erroneous interpretations. To intercept this drawback, Christensen

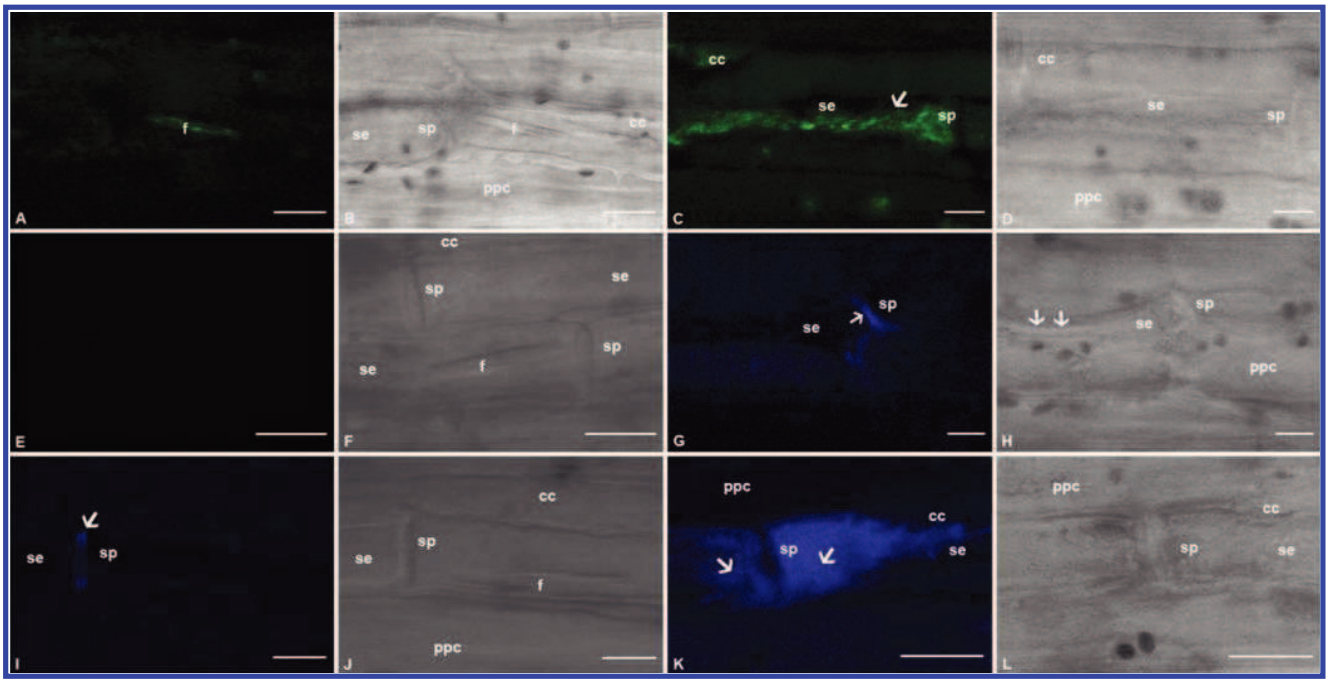

Fig. 3. Confocal laser-scanning microscopy (CLSM) and transmission microscopic images of phloem tissue in intact healthy (left half of the panel) and Flavescence Dorée (FD)-infected (right half) *Vicia faba* plants. Phloem tissue observed **A** and **C,** at 488 nm and **B** and **D,** under transmission light after combined 5-chloromethyl-fluoresceindiacetate and 5-chloromethyl-eosin-diacetate (CMFDA/CMEDA) staining. **A** and **B,** In healthy sieve elements, forisomes occur in the condensed conformation. **C** and **D,** In FD-infected phloem, forisomes bodies are not visible and nonidentified proteinaceous dispersed material is present along the sieve elements (C, arrow). **E** through **L,** Phloem tissue after aniline blue treatment, specific for callose detection in intact sieve tubes, observed **E, G, I,** and **K,** at 405 nm; and **F, H, J,** and **L,** under transmission light. In healthy sieve elements, callose is not detectable (E) or deposited in small amounts at the sieve-plate margins (I, arrow). In infected plants, aniline blue staining indicates large callose depositions along the sieve elements; in particular, in the vicinity of the sieve plates (G) through to plug formation (K, arrows). Note that forisomes are invisible in sieve elements of infected plants. f = forisome, cc = companion cell, se = sieve element, ppc = phloem parenchyma cell, sp = sieve plate. In H, arrows indicate thickened sieve-element walls. Bars correspond to 10 µm.

and co-workers (2004) used CLSM to detect phytoplasmas in freshly sectioned stems and petioles of *Euphorbia pulcherrima* and *C. roseus*. Using two different DNA dyes (SYTO 13 and $DiOC_7(3)$), phytoplasmas appeared as dense fluorescent masses in sieve elements.

All in all, however, involvement of callose as well as proteinaceous substances in plant defense reactions has not been conclusively proven thus far, given the native occlusion reactions in response to sectioning (Knoblauch and van Bel 1998). Computerized image processing and analysis by CLSM using an array of vital fluorescent probes appears to be the appropriate tool for in vivo investigation of phloem-specific phytoplasmas and their interactions with the plant host (Reichel and Beachy 1998). Therefore, we used CLSM techniques for observation of phtytoplasmas in the phloem of intact plants (Knoblauch and van Bel 1998).

Diverse fluorochromes enabled us to stain and distinguish in vivo structural components of intact sieve elements in both intact healthy and FD-diseased *V. faba* plants. The images provided real-time information on structural and biochemical modifications in sieve elements following phytoplasma infection. The DNA-specific dye DAPI was used to detect phytoplasmas in diseased plants (Loi et al. 2002), and identified phytoplasmas inside sieve elements in vivo. Use of DAPI in living cells, as well as the fact that it does not affect cell viability, is well documented in literature for both animal and plant cells (Cai et al. 2008; Ocarino et al. 2008; Subramaniam et al. 2001). Phytoplasmas were found to be distributed along the sieve elements, particularly in the vicinity of the sieve plates. In the enucleate sieve elements (van Bel 2003), no interference with nuclear staining can occur. Theoretically, sieve-element plastids which are of the same size as phytoplasmas may have become stained as well but there is no overlap between the location of the plastids and the DAPI-stained dots.

Phytoplasmas trigger Ca^{2+} influx leading to sieve-element occlusion.

The membrane-permeant, colorless CFDA enters sieve elements via the plasma membrane and, following de-esterification, the membrane-impermeant carboxyfluorescein is translocated by mass flow through the sieve tubes (Oparka et al. 1994). Most of it is retrieved by companion cells and phloem parenchyma cells along the pathway and sequestered in the vacuoles (Knoblauch and van Bel 1998). Its phloem-mobility is indicative of mass flow. In diseased plants, mass flow was significantly reduced compared with the healthy ones and, in most cases, had fully ceased. DAPI/CFDA double staining demonstrated that stoppage of mass flow and phytoplasma accumulation coincide.

Although phytoplasma aggregates may be able to plug the sieve pores, it is more likely that phytoplasma-induced sealants are responsible for sieve-tube occlusion. It is important to underline that CFDA has been detected in the companion cell vacuoles of the diseased plants, indicating that the companion cell activity is not totally impaired by infection, which could be important for phytoplasma survival. After having lost nuclei and most of their organelles during their ontogeny, sieve-elements rely on the metabolic activities of companion cells (van Bel et al. 2002) and may fail to fully nourish phytoplasmas. Companion cells are metabolically active and provide all the compounds essential for sieve-element maintenance. Because phytoplasmas lack many genes indispensable for cell metabolism (Christensen et al. 2005), compounds provided by companion cells might be an important source of nutrition for these pathogens.

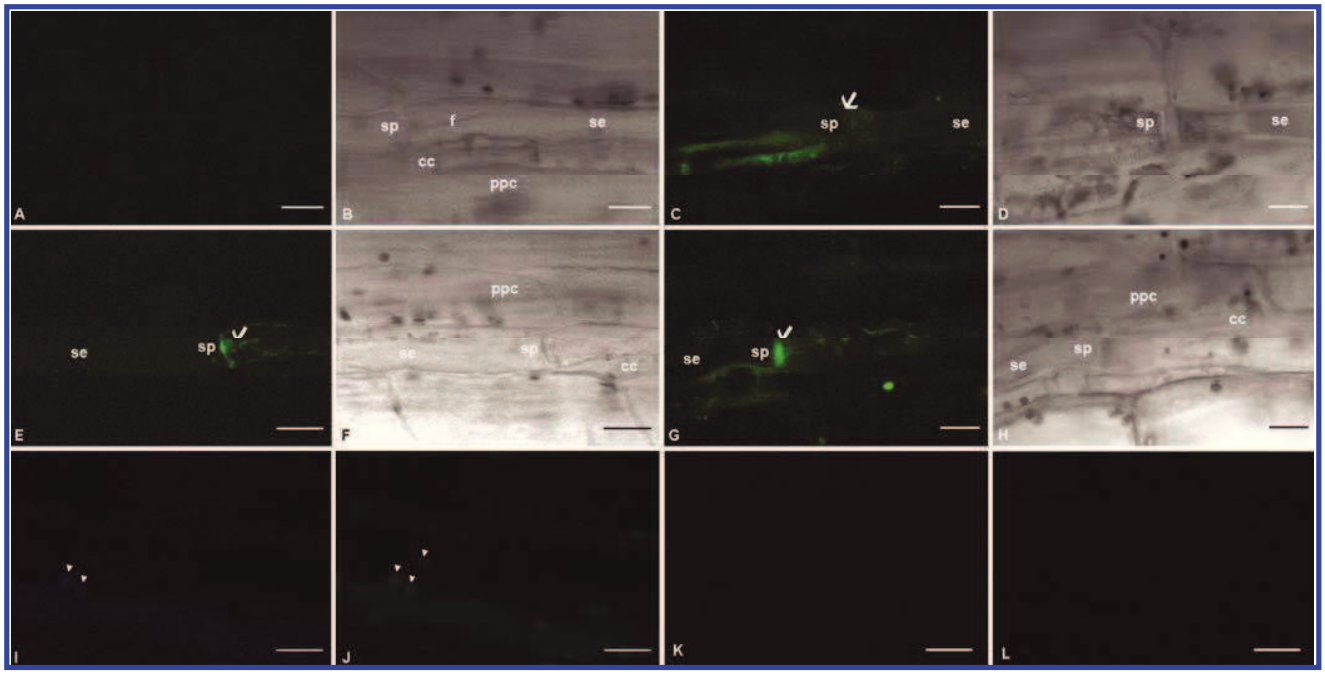

Fig. 4. A through **H,** Confocal laser-scanning microscopy (CLSM) and transmission microscopic images of healthy (left half of the panel) and Flavescence Dorée (FD)-infected (right half) *Vicia faba* phloem after Oregon Green 1,2-bis(o-aminophenoxy)ethane-N,N,-N′,N′-tetraacetic acid (OGB-1) staining, observed **A, C, E,** and **G,** at 488 nm; and **B, D, F,** and **H,** under transmission light. In healthy sieve elements, OGB-1 fluorescence is absent (A) or weakly present in the sieve plate region (E, arrow). In infected plants, the fluorescence signal is very strong along the sieve-element plasma membrane (C), particularly at the sieve plates (G). Note the dark undefined substances in sieve elements of FD-infected plants (D and H) and the transparent sieve elements of healthy plants (B and F). **I** through **L,** CLSM of unstained *Vicia faba* phloem, observed at 405 and 488 nm. Sieve elements of healthy plants using **I,** 405 nm or **J,** 488 nm do not exhibit strong signals. Arrowheads indicate autofluorescence of chloroplasts in the parenchyma cell above the sieve element. Similar results were obtained for FD-infected sieve elements both at **K,** 405-nm and **L,** 488-nm wavelengths. f = forisome, cc = companion cell, se = sieve element, ppc =: phloem parenchyma cell, sp = sieve plate. Bars correspond to 10 µm.

Severe phytoplasma infection is inextricably bound up with forisome dispersion and callose deposition. In FD-diseased plants, spindle-shaped forisomes are dispersed and, hence, become invisible under the light microscope, while high amounts of callose occur in the vicinity of the sieve plates and sometimes in the adjacent zones. Forisome dispersion and callose deposition are Ca^{2+} dependent (Knoblauch et al. 2001; Thonat et al. 1993) and are likely triggered by release of Ca^{2+} into the sieve element lumen (Furch et al. 2009; Hafke et al. 2009). pH-induced modifications in functional (mass flow blockage) and structural (forisome dispersion) properties in FD-infected sieve elements can be excluded. It has been reported that the pH of phloem exudates from phytoplasma-infected plants is not different from that of exudates from control plants (7.5 to 8.0) (Kollar and Seemüller 1990). In addition, forisomes only disperse at nonphysiological pH values under 4 and above 11 (Knoblauch et al. 2003) and, hence, the pH induction of changes in the forisome conformation is more than unlikely.

Application of OGB-1 verified the correlation between phloem occlusion—induced by phytoplasmas—and the rise of Ca^{2+} concentration inside FD-diseased sieve elements (Furch et al. 2007). In diseased plants, the Ca^{2+} concentration in the sieve elements was markedly elevated compared with the healthy ones. The presence of other unidentified protein structures indicates that phloem proteins other than forisomes are involved in sieve-pore plugging in FD-diseased plants, as already shown for cucurbits in response to abiotic stresses and stimuli (Furch et al. 2010).

It appears that phytoplasma infection—possibly by secretion of phytoplasma effectors (Sugio et al. 2011)—induces Ca^{2+} influx into the sieve elements. The scattered distribution of Ca^{2+} ions inside the sieve elements and callose deposition along the longitudinal walls indicates that the phytoplasma effectors activate Ca^{2+} channels not only near the sieve plates but also at other Ca^{2+} hotspots such as the pore-plasmodesma units between sieve elements and companion cells (Furch et al. 2009; Hafke et al. 2009). Recovery of the occlusion phenomena some time after the passage of electrical potential waves demonstrated that occlusion can be reversed following Ca^{2+} extrusion (Furch et al. 2007, 2010). However, it seems that, in FD-diseased broadbean, phytoplasmas impose continuous gating of the Ca^{2+} channels, given the permanent occlusion of infected sieve elements. On the other hand, in some plant–phytoplasma interactions (i.e., apple, alder, and aspen), and in only a few highly susceptible individuals, sealing mechanisms may be considerably affected, leading to sieve-tube sap exudation from cut, infected trunks (Kollar and Seemüller 1990; Kollar et al. 1989).

In addition to sieve-plate occlusion, the sieve-element path may also be narrowed in diseased plants by thickening of the walls, as revealed by CLSM observations. Increased sieve element wall thickness and enhanced total phenolics have been reported for phytoplasma-diseased plants (Choi et al. 2004; Musetti et al. 2000). This would be consistent with apposition of phenolic materials—probably by companion cells, because a Golgi system is absent in sieve elements—against the sieve-element walls for most of those facing the companion cells. It has been demonstrated that a Ca^{2+} signal is required to induce phenylalanine ammonia-lyase (PAL) activity (Messiaen et al. 1993), a key enzyme of the phenol synthesis pathway, as well as PAL gene expression (Long and Jenkins 1998). This would add an interesting side-effect of Ca^{2+} influx on phytoplasma restriction.

In conclusion, we demonstrated that phytoplasma infection leads to sieve-tube occlusion, impairing phloem functions in *V. faba* plants. In systemically infected plants, phytoplasmas—probably by secretion of effector proteins—trigger Ca^{2+} influx into the sieve elements, conferring forisome dispersion, callose deposition, and probably cell wall thickening. The discovery of phytoplasma effector proteins (Sugio et al. 2011) could give a boost to studies of the initial mechanisms involved in phloem–phytoplasma interactions. Application of phytoplasma effectors to intact plants might help to establish the time course of the events involved in phloem reactions to infection.

MATERIALS AND METHODS

Plant material and phytoplasma inoculation.

V. faba plants ('Aguadulce supersimonia') were infected with the phytoplasma related to FD, '*Ca*. P. vitis', strain C (16SrV-C) (Lee et al. 2004). FD-infective leafhoppers (*Euscelidius variegatus*) were caged to inoculate 15-day-old broadbean seedlings in a controlled environment insectarium (22°C, 16-h photoperiod) for a week. Test plants were sprayed with an insecticide solution after the inoculation period and kept in a greenhouse for further growth. The greenhouse conditions were 22 to 25°C (day) and 12 to 16°C (night), 40 to 80% relative humidity, and a 16-h photoperiod. Control plants were not exposed to leafhoppers. FD symptoms (leaf-size reduction along with yellowing and curling) emerged approximately 1 month after inoculation by the vectors.

Phytoplasma presence was assessed by RT-PCR analyses. Total DNA was extracted from 1 g of frozen leaf midribs according to Doyle and Doyle (1990). RT-PCR analyses were performed using the 16S rDNA-based phytoplasma universal primer pair 16S (RT) F1 and 16S (RT) R1, in a DNA Engine Opticon2 System using 40 ng of DNA, 10× PCR buffer, 2.5 mM dNTPs, 25 mM $MgCl_2$, primers at 300 nM each, 0.15 µl of AmpliTaq Gold DNA Polymerase at 5 U/µl (Applied Biosystems, Foster City, CA, U.S.A.) and 10× SYBR Green I in dimethyl sulfoxide (Molecular Probes, Invitrogen, Eugene, OR, U.S.A.) in a total volume of 25 µl. Thermocycling was performed using the following conditions: 11 min at 95°C; 40 cycles of 15 s at 94°C, 15 s at 57°C, and 20 s at 72°C; and 8 min at 72°C. The melting curve was performed with a ramp from 65 to 95°C at 0.2°C/s.

Preparation of intact plants for microscopy.

For in vivo observation of sieve tubes, cortical cell layers were removed from the lower side of the main vein of a fully expanded leaf, still attached to an intact plant, to provide a CLSM observation window (Knoblauch and van Bel 1998). In translocation experiments, phloem-mobile dyes were administered to the cut midrib after having removed the leaf tip at a distance of approximately 3 cm from the observation window. In the other tests, fluorochromes were administered directly on the bare-lying phloem tissues at the observation window. Observations were performed using four healthy and four diseased 6-week-old plants, as soon as symptoms appeared on the infected ones. The experiments were repeated on at least two different leaves per plant.

Fluorescent probes and CLSM imaging.

An apoplasmic physiological buffer containing 1 mM $CaCl_2 \cdot 2H_2O$, 2 mM KCl, 50 mM mannitol, 2.5 mM MES $\cdot H_2O$, and 1 mM $MgCl_2 \cdot 6H_2O$, pH 5.7, was used to solve the dyes (Knoblauch and van Bel 1998). The fluorochromes were imaged by CLSM using a Leica TCS SP2 (Leica Microsystems, Rijswijk, The Netherlands) equipped with a 75-mW argon/krypton laser (Omnichrome, Chino, CA, U.S.A.). Aniline blue and DAPI (Sigma, Milano, Italy) fluorescence was recorded by a Leica TCS SP2 CLSM equipped with a UV laser (Leica Microsystems). The phloem tissue was observed at the observa-

tion window using a ×63 water immersion objective (HCX APO L40x0.80 W U-V-I objective; Leica Microsystems) in the dipping mode.

The phloem-mobile dye CFDA (Invitrogen, Karlsruhe, Germany) was used to investigate phloem flow in healthy and FD-infected plants. After application of drops of a freshly prepared 1 µM CFDA solution followed by an incubation period of 2 h at room temperature, the phloem tissue was examined at 488 nm.

Local staining by DAPI enabled detection of phytoplasmas inside intact sieve elements. A drop of DAPI (1 µg/ml) was applied to the observation window. After incubation for 15 to 20 min at room temperature in darkness, DAPI was removed and replaced by the apoplasmic buffer and the tissue was observed at 405 nm. In the majority of experiments, DAPI and CFDA were applied in succession (or in the reverse order) and the phloem tissue was observed at 405 as well as at 488 nm.

CMEDA/CMFDA mixtures (Molecular Probes), both membrane-permeant fluorochromes, were used for forisome and protein observations in intact sieve tubes, according to Furch and co-workers (2007). Drops of a freshly prepared mixture (1:1, vol/vol) were applied to the observation window and incubated for 1 h at room temperature. Tissues were observed at 488 nm.

In order to visualize callose depositions, a drop of aniline blue, (Merck, Darmstadt, Germany) at the non-lethal concentration of 0.005% (Furch et al. 2007), was applied to the observation window and incubated for 30 min at room temperature. Aniline blue fluorescence was detected at 405 nm.

To reach a qualitative indication of Ca^{2+} concentrations in sieve elements, the membrane-permeant Ca^{2+} marker OGB-1 (Molecular Probes) was applied at a concentration of 5 µM and incubated for 30 min. After removal of dye by rinsing with apoplasmic buffer for 30 min, observations were performed at 488 nm.

To eliminate misinterpretations due to autofluorescence, in vivo unstained *V. faba* sieve elements were observed by CLSM at the same excitation wavelengths used for the above-mentioned fluorochromes (i.e., 488 or 405 nm) as controls.

ACKNOWLEDGMENTS

This work was supported by the Deutscher Akademischer Austauschdienst (DAAD), (grant number A/11/04104 for R. Musetti). R. Musetti and S. V. Buxa contributed equally to this publication. R. Musetti conceived the project under the supervision of A. J. E. van Bel and K.-H. Kogel. S. V. Buxa established the protocols for CLSM. A. Loschi prepared *Vicia faba* infected plants. F. De Marco and R. Polizzotto performed phytoplasma detection by real-time RT-PCR on *V. faba* leaves. R. Musetti and A. J. E. van Bel wrote the manuscript. We thank D. Bosco, Dipartimento di Valorizzazione e Protezione delle Risorse Agroforestali, University of Torino (Italy), for kindly providing infected *Vicia faba* plants; A. Holz and A. Dorresteijn, University of Giessen, for providing a CLSM equipped with a UV laser; and S. Grisan, University of Udine, for expert assistance in preparing the figures.

LITERATURE CITED

Barratt, D. H. P., Kolling, K., Graf, A., Pike, M., Calder, G., Findlay, K., Zeeman, S. C., and Smith, A. M. 2011. Callose synthase GLS7 is necessary for normal phloem transport and inflorescence growth in *Arabidopsis*. Plant Physiol. 155:328-341.

Braun, E. J., and Sinclair, W. A. 1978. Translocation in phloem necrosis-diseased American elm seedlings. Phytopathology 68:1733-1737.

Cai, J., Zhang, X., Wang, X., Li, C., Liu, G. 2008. In vivo MR imaging of magnetically labeled mesenchymal stem cells transplanted into rat liver through hepatic arterial injection. Contrast Media Mol. Imag. 3:72-77.

Choi, Y. H., Casas Tapias, E., Kim, H. K., Lefeber, A. W. M., Erkelens, C., Verhoeven, J. Th. J., Brzin, J., Zel, J., and Verpoorte, R. 2004. Metabolic discrimination of *Catharanthus roseus* leaves infected by phytoplasma using 1H-NMR spectroscopy and multivariate data analysis. Plant Physiol. 135:2398-2410.

Christensen, N. M., Nicolaisen, M., Hansen, M., and Schulz, A. 2004. Distribution of phytoplasmas in infected plants as revealed by real-time PCR and bioimaging. Mol. Plant-Microbe Interact. 17:1175-1184.

Christensen, N. M., Axelsen, K. B., Nicolaisen, M., and Schulz, A. 2005. Phytoplasmas and their interactions with hosts. Trends Plant Sci. 10:526-535.

Cronshaw, J., and Sabnis, D. D. 1990. Phloem proteins. Pages 255-383 in: Sieve Elements. Comparative Structure, Induction and Development. H.-D. Behnke and R. D. Sjolund, eds. Springer-Verlag, Berlin.

Doyle, J. J., and Doyle, J. L. 1990. Isolation of plant DNA from fresh tissue. Focus 12:13-15.

Ehlers, K., Knoblauch, M., and van Bel, A. J. E. 2000. Ultrastructural features of well-preserved and injured sieve elements: Minute clamps keep the phloem transport conduits free for mass flow. Protoplasma 214:80-92.

Elad, Y., and Evensen, K. 1995. Physiological aspects of resistance to *Botrytis cinerea*. Phytopathology 85:637-643.

Faoro, F. 2005. Perché è così difficile osservare al microscopio elettronico i fitoplasmi della vite? Petria 15:99-101.

Furch, A. C. U., Hafke, J. B., Schulz, A., and van Bel, A. J. E. 2007. Ca^{2+}-mediated remote control of reversible sieve tube occlusion in *Vicia faba*. J. Exp. Bot. 58:2827-2838.

Furch, A. C. U., van Bel, A. J. E., Fricker, M. D., Felle, H. H., Fuchs, M., and Hafke, J. B. 2009. Sieve element Ca^{2+} channels as relay stations between remote stimuli and sieve tube occlusion in *Vicia faba*. Plant Cell 21:2118-2132.

Furch, A. C. U., Zimmermann, M. R., Will, T., Hafke, J. B., and van Bel, A. J. E. 2010. Remote-controlled stop of phloem mass flow by biphasic occlusion in *Cucurbita maxima*. J. Exp. Bot. 61:3697-3708.

Goodwin, P. B., Shepherd, V., and Erwee, M. G. 1990. Compartmentation of fluorescent tracers injected into the epidermal cells of *Egeria densa* leaves. Planta 181:129-136.

Hafke, J. B., Furch, A. C. U., Fricker, M. D., and van Bel, A. J. E. 2009. Forisome dispersion in *Vicia faba* is triggered by Ca^{2+} hotspots created by concerted action of diverse Ca^{2+} channels in sieve elements. Plant Signal. Behav. 4:968-972.

Hogenhout, S. A., Oshima, K., Ammar, E., Kakizawa, S., Kingdom, H. N., and Namba, S. 2008. Phytoplasmas: Bacteria that manipulate plants and insects. Mol. Plant Pathol. 9:403-423.

Kartte, S., and Seemüller, E. 1991. Histopathology of apple proliferation in *Malus* taxa and hybrids of different susceptibility. J. Phytopathol. 131:149-160.

Knoblauch, M., and van Bel, A. J. E. 1998. Sieve tubes in action. Plant Cell 10:35-50.

Knoblauch, M., Peters, W. S., Ehlers, K., and van Bel, A. J. E. 2001. Reversible calcium-regulated stopcocks in legume sieve tubes. Plant Cell 13:1221-1230.

Knoblauch, M., Noll, G. A., Müller, T., Prüfer, D., Schneider-Hüther, I., Scharner, D., van Bel, A. J. E., and Peters, W. S. 2003. ATP-independent contractile proteins from plants. Nat. Mater. 2:600-603.

Koh, E.-J., Zhou, L., Williams, D. S., Park, J., Ding, N., Duan, Y.-P., and Kang, B.-H. 2012. Callose deposition in the phloem plasmodesmata and inhibition of phloem transport in citrus leaves infected with '*Candidatus* Liberibacter asiaticus'. Protoplasma 249:687-697.

Köhle, H., Jeblick, W., Poten, F., Blascheck, W., and Kauss, H. 1985. Chitosan-elicited callose synthesis in soybean cells as a Ca^{2+}-dependent process. Plant Physiol. 77:544-551.

Kollar, A., and Seemüller, E. 1990. Chemical composition of phloem exudate of mycoplasma-infected apple trees. J. Phytopathol. 128:99-111.

Kollar, A., Seemüller, E., and Krczal, G. 1989. Impairment of the sieve tube sealing mechanism of trees infected by Mycoplasma-like organisms. J. Phytopathol. 124:7-12.

Lee, I. M., Martini, M., Marcone, C., and Zhu, S. F. 2004. Classification of phytoplasma strains in the elm yellows group (16SrV) and proposal of '*Candidatus* Phytoplasma ulmi' for the phytoplasma associated with elm yellows. Intern. J. Syst. Evol. Microbiol. 54:337-347.

Lepka, P., Stitt, M., Moll, E., and Seemüller, E. 1999. Effect of phytoplasmal infection on concentration and translocation of carbohydrates and amino acids in periwinkle and tobacco. Physiol. Mol. Plant Pathol. 55:59-68.

Lherminier, J., Courtois, M., and Caudwell, A. 1994. Determination of the distribution and multiplication sites of Flavescence Dorée mycoplasma-like organisms in the host plant *Vicia faba* by ELISA and immunocytochemistry. Physiol. Mol. Plant Pathol. 45:125-138.

Lherminier, J., Benhamou, N., Larrue, J., Milet, M. L., Boudon-Padieau, E., Nicole, M., and Blein, J. P. 2003. Cytological characterization of elicitin induced protection in tobacco plants infected by *Phytophthora parasitica* or phytoplasma. Phytopathology 93:1308-1319.

Loi, N., Ermacora, P., Carraro, L., Osler, R., and Chen, T. A. 2002. Production of monoclonal antibodies against apple proliferation phytoplasma and their use in serological detection. Eur. J. Plant Pathol. 108:81-86.

Long, J. C., and Jenkins, G. I. 1998. Involvement of plasma membrane redox activity and calcium homeostasis in the UV-B and UV-A/blue light induction of gene expression in *Arabidopsis*. Plant Cell 10:2077-2086.

Marcone, C. 2010. Movement of phytoplasmas and the development of disease in the plant. Pages 114-131 in: Phytoplasmas: Genomes, Plant Hosts and Vectors. P. Jones and P. Weintraub, eds. CABI Publishing, Wallingford, U.K.

Marcone, C., Neimark, H., Ragozzino, A., Lauer, U., and Seemüller, E. 1999. Chromosome sizes of phytoplasmas composing major phylogenetic groups and subgroups. Phytopathology 89:805-810.

Maust, B. E., Espadas, F., Talavera, C., Aguilar, M., Santamaria, J. M., and Oropeza, C. 2003. Changes in carbohydrate metabolism in coconut palms infected with the lethal yellowing phytoplasma. Phytopathology 93:976-981.

Messiaen, J., Read, N. D., van Cutsem, P., and Trewavas, A. J. 1993. Cell wall oligogalacturonides increase cytosolic free calcium in carrot protoplasts. J. Cell Sci. 104:365-371.

Musetti, R., and Favali, M. A. 1999. Histological and ultrastructural comparative study between *Prunus* varieties of different susceptibility to plum leptonecrosis. Cytobios 99:73-82.

Musetti, R., Favali, M. A., Carraro, L., and Osler, R. 1994. Histological detection of Mycoplasma like organisms causing leptonecrosis in plum trees. Cytobios 78:81-90.

Musetti, R., Favali, M. A., and Pressacco, L. 2000. Histopathology and polyphenol content in plants infected by phytoplasmas. Cytobios 102:133-147.

Musetti, R., Tubaro, F., Polizzotto, R., Ermacora, P., and Osler, R. 2008. Il "Recovery" da Apple Proliferation in melo è associato all' aumento della concentrazione dello ione calcio nel floema. Petria 18:380-383.

Musetti, R., Paolacci, A., Ciaffi, M., Tanzarella, O. A., Polizzotto, R., Tubaro, F., Mizzau, M., Ermacora, P., Badiani, M., and Osler, R. 2010. Phloem cytochemical modification and gene expression following the recovery of apple plants from apple proliferation disease. Phytopathology 100:390-399.

Musetti, R., De Marco, F., Farhan, K., Polizzotto, R., Santi, S., Ermacora, P., and Osler, R. 2011. Phloem-specific protein expression patterns in apple and grapevine during phytoplasma infection and recovery. Bull. Insectol. 64 (Suppl.):211-212.

Ocarino, N. M., Bozzi, A., Pereira, R. D. O., Breyner, N. M., Silva, V. L., Castanheira, P., Goes, A. M., and Serakides, R. 2008. Behavior of mesenchymal stem cells stained with 4′,6-diamidino-2-phenylindole dihydrochloride (DAPI) in osteogenic and non osteogenic cultures. Biocell 32:175-183.

Oparka, K. J., Duckett, C. M., Prior, D. A. M., and Fisher, D. B. 1994. Real-time imaging of the phloem unloading in the root tip of *Arabidopsis*. Plant J. 6:759-766.

Pelissier, H. C., Peters, W. S., Collier, R., van Bel, A. J. E., and Knoblauch, M. 2008. GFP tagging of sieve element occlusion (SEO) proteins results in green fluorescent forisomes. Plant Cell Physiol. 49:1699-1710.

Reichel, C., and Beachy, R. N. 1998 Tobacco mosaic virus infection induces severe morphological changes of the endoplasmic reticulum. Proc. Natl. Acad. Sci. U.S.A. 95:11169-11174.

Rüping, B., Ernst, A.M., Jekat, S. B., Nordzieke, S., Reineke, A. R., Müller, B., Bornberg-Bauer, E., Prüfer, D., and Noll, G. A. 2010. Molecular and phylogenetic characterization of the sieve element occlusion gene family in Fabaceae and non-Fabaceae plants. BMC Plant Biol. 10:219.

Subramaniam, R., Desveaux, D., Spickler, C., Michnick, S. W., and Brisson, N. 2001. Direct visualization of protein interactions in plant cells. Nat. Biotechnol. 19:769-772.

Sugio, A., Kingdom, H. N., MacLean, A. M., Grieve, V. M., and Hogenhout, S. A. 2011. Phytoplasma protein effector SAP11 enhances insect vector reproduction by manipulating plant development and defense hormone biosynthesis. Proc. Natl. Acad. Sci. U.S.A. 108:E1254-E1263.

Thonat, C., Boyer, N., Penel, C., Courduroux, J. C., and Gaspar, T. 1993. Cytological indication of the involvement of calcium and calcium-related proteins in the early responses of *Bryonia dioica* to mechanical stimulus. Protoplasma 176:133-137.

Thorpe, M. R., Furch, A. C. U., Minchin, P. E. H., Föller, J., van Bel, A. J. E., and Hafke, J. B. 2010. Rapid cooling triggers forisome dispersion just before phloem transport stops. Plant Cell Environ. 33:259-271.

Tuteja, N., Umate, P., and van Bel, A. J. E. 2010. Forisomes: Calcium-powered protein complexes with potential as 'smart' biomaterials. Trends Biotechnol. 28:102-110.

Van Bel, A. J. E. 2003. The phloem, a miracle of ingenuity. Plant Cell Environ. 26:125-149.

Van Bel, A. J. E., Ehlers, K., and Knoblauch, M. 2002. Sieve elements caught in the act. Trends Plant Sci. 7:126-132.

Xie, B., Wang, X., Zhu, M., Zhang, Z., and Hong, Z. 2011. *CalS7* encodes a callose synthase responsible for callose deposition in the phloem. Plant J. 65:1-14.

Eur J Plant Pathol
DOI 10.1007/s10658-012-0147-6

Differentially-regulated defence genes in *Malus domestica* during phytoplasma infection and recovery

Rita Musetti · Khaled Farhan · Federica De Marco · Rachele Polizzotto · Annarita Paolacci · Mario Ciaffi · Paolo Ermacora · Simone Grisan · Simonetta Santi · Ruggero Osler

Accepted: 29 November 2012

Abstract To improve knowledge about plant/phytoplasma interactions and, in particular, about the 'recovery' phenomenon in previously-infected plants, we investigated and compared expression levels of several defence-related genes (four pathogenesis-related proteins and three jasmonate-pathway marker enzymes) in apple plants showing different states of health: vigorous (healthy), phytoplasma-infected, and recovered. Real Time-PCR analyses demonstrated that genes are differentially expressed in apple leaf tissue according to the plants' state of health. *Malus domestica* Pathogenesis-Related protein (*MdPR) 1*, *MdPR 2* and *MdPR 5* were significantly induced in leaves of diseased and symptomatic plants compared to leaves of those plants that were healthy or recovered. On the other hand, levels of all the jasmonate (JA)-pathway marker genes that we selected for this study, were up-regulated in the leaves of recovered plants compared to the diseased ones. In conclusion, our study demonstrated that two different sets of defence genes are involved in the interactions between apple plants and '*Candidatus* Phytoplasma mali' ('*Ca*. P. mali') and that these genes are differentially expressed during phytoplasma infection or recovery.

Keywords Apple proliferation · Jasmonic acid · Pathogenesis-related proteins · Real-Time PCR

Phytoplasmas are prokaryotic micro-organisms which are responsible for several hundred diseases affecting economically important crops including ornamental plants, vegetables, fruit trees and grapevines. Phytoplasmas mostly colonize sieve tubes and manipulate the host to ensure efficient distribution and multiplication (Hogenhout et al. 2008). Notwithstanding extensive research over recent years, several aspects of physiological and molecular interactions between phytoplasmas and host plants, (nominally apples and grapes), are still little understood.

An interesting spontaneous phenomenon, called 'recovery' (Osler et al. 2000), has been observed in economically important crops such as apple trees, grapevines and apricot trees affected by phytoplasmas. Recovery manifests via a complete remission of symptoms in grapevine plants and apple trees, with the disappearance of the phytoplasmas from the crown (Osler et al. 1993, 2000; Carraro et al. 2004). Recovery can also occur in

Electronic supplementary material The online version of this article (doi:10.1007/s10658-012-0147-6) contains supplementary material, which is available to authorized users.

R. Musetti (✉) · K. Farhan · F. De Marco · R. Polizzotto · P. Ermacora · S. Grisan · S. Santi · R. Osler
Dipartimento di Scienze Agrarie e Ambientali,
Università di Udine,
via delle Scienze, 208,
33100 Udine, Italy
e-mail: Rita.Musetti@uniud.it

A. Paolacci · M. Ciaffi
Dipartimento di Agrobiologia e Agrochimica,
Università della Tuscia,
Via S. Camillo de Lellis snc,
01100 Viterbo, Italy

Published online: 15 December 2012

individual plants which have severe symptoms over several years. When these recovered plants are exposed to significant levels of disease in the field, the probability of developing symptoms is four times lower than trees which have never been infected (Osler et al. 2000), which suggests the establishment of a type of induced resistance in the formerly infected plants.

Nevertheless, the basis for this phenomenon is not yet completely understood. Recovery in apple plants is associated with the disappearance of phytoplasmas in the canopy, despite the fact that the roots of the plants remain fully infected (Carraro et al. 2004). It is possible that heavy deposition of callose may be responsible for sequestering phytoplasmas in the root sieve tubes and, furthermore that the newly-developing sieve tubes in the upper part of the plant may have developed increased resistance (Musetti et al. 2010). In apple, apricot and grapevine plants, recovery from phytoplasma-associated diseases coincided with the accumulation of hydrogen peroxide in sieve elements (Musetti et al. 2004, 2005, 2007), which often signals increased resistance. Moreover, Musetti et al. (2010, 2011) reported an anomalous accumulation of callose and protein in the phloem of recovered apple plants associated with the up-regulation of callose synthase- and phloem protein-coding genes, supporting the hypothesis that recovered apple plants were able to develop resistance mechanisms depending on Ca^{2+} signal activity (Musetti et al. 2010). Induced defence mechanisms in plants are modulated by a complex signal network in which different signal molecules are involved. Salicylic acid (SA) induces the accumulation of Pathogenesis-Related (PR) proteins in a variety of plants as downstream components of systemic acquired resistance (SAR) (Durrant and Dong 2004), so they are usually used for the evaluation of defence activation. Furthermore, jasmonic acid (JA), its volatile ester methyl jasmonate (MJ) and other derivatives, collectively known as jasmonates (JAs), are ubiquitous signalling molecules which also mediate plant responses to environmental stress such as wounding, and attack by insect and pathogen (Wasternack 2007). The different methods of signalling mediated by SA and JA are balanced in the plant and the two pathways can cross talk (van Wees et al. 2000). In apple plants, it has been reported that PR 1, PR 2, PR 5, PR 8 are produced in response to inoculation of pathogens, such as *Venturia inaequalis* and *Erwinia amylovora* (Gau et al. 2004; Bonasera et al. 2006; Malnoy et al. 2007) but, to the best of our knowledge, there are no specific reports about the activation of defence-related pathways in apple plants in response to Apple proliferation (AP) disease, associated to '*Candidatus* Phytoplasma mali' ('*Ca*. P. mali') nor at onset of recovery.

In this work, we investigated the expression of apple genes coding for four PR proteins, PR 1, PR 2, PR 5, PR 8, and for three JA-pathway marker enzymes, allene oxide synthase 2 (AOS 2); 12-oxyphytodienoate reductase 3 (12-OPR 3); JA-inducible proteinase inhibitor II (PI II), and we compared their relative expression levels in apple plants showing different phytosanitary status (i.e. healthy, symptomatic and recovered). Our aim was to add new insights to the apple/'*Ca*. P. mali' interaction.

An experimental organic apple orchard (cv. Florina, virus-free clone) was established in 1988 in an area of the Friuli Venezia Giulia region, North East Italy, where serious epidemics of AP have occurred. The orchard had been checked at least three times per year for the presence of AP symptoms.

Three groups of plants, AP-symptomatic (diseased, D), healthy (H) and recovered (R), were selected in the orchard. Plants, which all had M26 as rootstock, were 20 years old. Recovered plants were asymptomatic during the previous four consecutive years and healthy plants had been asymptomatic since planting.

Detection of phytoplasma in randomly sampled leaves was carried out by means of polymerase chain reaction (PCR), as described by Lorenz et al. (1995). To perform analyses of gene expression, total RNA was extracted from frozen tissues using a cetyl-methyl ammonium bromide based method, as described by Gasic et al. (2004). The extracted RNA was treated with RNase-free DNase I (Promega Italia, Milano, Italy) according to the manufacturer's protocol. Following digestion, nucleotides were removed from RNA using a G50 Sepharose buffer exchange column (GE Healthcare Europe, Milano, Italy). RNA concentration and purity were checked with a Lambda 3B spectrophotometer (Perkin Elmer Italy, Cologno Monzese, Italy) before and after DNase I digestion. Only RNA samples with a 260/280 ratio between 1.9 and 2.1 and a 260/230 ratio greater than 2.0 before and after DNase I digestion were used for cDNA synthesis. The quality of RNA samples, as well as the efficiency of the DNase treatment, were assessed by electrophoresis on 1 % formaldehyde agarose gels (Musetti et al. 2010). The transcripts of the identified genes were amplified by qRT-PCR using RNAs extracted from

D, H, and R plants as described above. First-strand cDNA was synthesized from 3 μg of total RNA by Expand Reverse Transcriptase (Roche Diagnostics, Milano, Italy) according to the manufacturer's protocol. Gene expression was analyzed by quantitative real-time reverse transcription-PCR (qRT-PCR) in leaves from three individual trees for each of the D, H, and R groups, sampled in September, when typical AP symptoms are visible. cDNA was diluted ten-fold for qRT-PCR analyses.

Specific primers for apple *PR 1, PR 2, PR 5* genes were employed in real-time RT-PCR experiments according to Bonasera et al. (2006). Primers for *PR 8* were re-designed according to the gene sequences cited by Bonasera et al. (2006).

Sequences of three *Malus x domestica* genes of the Jasmonic acid (JA) signalling pathway, namely: allene oxide synthase (*AOS2*); oxophytodienoate reductase (*12-OPR 3*); and finally JA-inducible proteinase inhibitor II (*PI-II*), were retrieved from the TIGR Apple Gene Index database by BLASTN or TBLASTN with homologous sequences of *Medicago truncatula*. The accession numbers are TC59991, TC87763 and TC65477, respectively. Primer 3 software was used for primer picking. Efficiency and specificity of the primer pairs were determined in real-time RT-PCR experiments as described in the Additional file 1. The melting curves shown a single peak indicating the primer amplification specificity. The sequences of each primer pair is given in Table 1.

qRT-PCR analyses were performed in a Bio-Rad CFX96 Real Time PCR System using Sso Fast EvaGreen SuperMix (Bio-Rad Laboratories, Inc., USA). The thermal profile comprised three segments: (i) 95 °C for 3 min; (ii) 40 cycles of 5 s of denaturation at 95 °C, 10 s of annealing and extension at 60 °C (amplification data collected at the end of each extension step); and (iii) a dissociation curve from 65 °C to 95 °C, with 0.5 °C increment intervals followed by plate reading. Three technical replicates were analyzed for each biological replicate.

Five-point standard curves of different dilutions from pooled cDNA (corresponding to 10, 5, 2, 1, and 0.5 ng of the initial RNA used for cDNA synthesis) were employed to calculate the efficiency of each primer pair. Efficiency (E) was calculated according to the protocol described by Pfaffl (2001). Pairs of primers with a PCR efficiency in the range of 96–104 % were chosen. Raw Ct values were transformed to relative quantities using the formula: $MNE=2^{Ct,\ reference\ mean} / 2^{Ct,\ target\ mean}$, where MNE=Mean Normalized Expression (Muller et al. 2002). The expression level of each target gene was normalized to the expression level of the reference gene GAPDH, after that the expression stability of some candidate reference genes had been evaluated by the software program NormFinder (Musetti et al. 2010).

Pairwise comparisons between the mean levels of the three groups (H, D, and R) were analyzed with "In Stat GraphPad" software package (La Jolla, CA, USA) using the Kruskal-Wallis non-parametric method (Dunn's multiple comparison test) to evaluate significant differences. The mean square error was computed as mean of the variances of the three groups. Different letters in the figures denote significant differences at $P \leq 0.01$.

PCR analysis, performed using group-specific primers for AP, confirmed the presence of phytoplasmas in all the leaves of D apple trees, but never in those of H or R plants (data not shown), confirming the association of remission of AP symptoms and disappearance of phytoplasma from plant leaves as previously observed (Carraro et al. 2004).

Expression levels of *MdPR 1*, *MdPR 2*, *MdPR 5*, *MdPR 8* and of the three genes encoding for JA-pathway enzymes are reported in Figs. 1 and 2, respectively. qRT-PCR analyses demonstrated that the diverse genes are differentially expressed in apple leaves according to the phytosanitary status of the plants. In particular, *MdPR 1* and *MdPR 2* were 2.5 times higher in D plants than in H plants and more than two times higher than in R plants. *MdPR 5* was 6-fold induced in D plants compared to H plants and 2.5-fold to R plants (Fig. 1). It is interesting to note that the level of expression of PR1 and PR5 genes in R leaves sits in between the levels in H and D plants. The transcription level of *MdPR 8* was similar in the D and R plants being on average, about two times that of H plants (Fig. 1).

Plant-pathogen interactions can result in the activation of numerous mechanisms of local and systemic defences. PR proteins are generally considered to be defence proteins whose function is to prevent or limit of the invasion or spreading of the pathogens in plants. However, the modus operandi of such proteins and their contribution to resistance have not been elucidated in many cases (van Loon et al. 2006). In plants belonging to the genus *Malus*, *MdPR* 1, *MdPR* 2, *MdPR* 5, *MdPR* 8 were proposed as candidate genes involved in plant response to attacks by pathogens *E. amylovora* and *V. inaequalis* (Bonasera et al. 2006; Malnoy et al. 2007). In

Table 1 Primer sequences used for the quantitative real time-polymerase chain reaction (qRT-PCR)

Primer name	Oligonucleotide sequence (5′– 3′)	References	Sequence accession number	Primer specificity
Md PR1a for Md PR1a rev	GCTCAGCCCTAATACAATCCTCTC TACCCCCACTACTGCACCTCACT	(Bonasera et al. 2006) (Bonasera et al. 2006)	CV524932.1	Pathogenesis-related protein 1a coding gene
Md PR2 for Md PR2 rev	CTTCACAGTCACCATCTTCAACA GGTGCACCAGCTTTTTCAA	(Bonasera et al. 2006) (Bonasera et al. 2006)	AY548364.1	Pathogenesis-related protein 2 coding gene
Md PR5 for Md PR5 rev	GGCAGGCGCAGTTCCACCAG GACATGTCTCCGGCATATCA	(Bonasera et al. 2006) (Bonasera et al. 2006)	DQ318213.1	Pathogenesis-related protein 5 coding gene
Md PR8 for2 Md PR8 rev2	CGTTCCCGGATACTCACCTA ACCGTCTGCATACTGGCATT	present work present work	DQ318214.1	Pathogenesis-related protein 8 coding gene
Md AOS2 for Md AOS2 rev	GGGAGAAGCTGTTGAAGCAC TCCAGCACACTGTTTGTTCC	present work present work	TC59991	Allene oxide synthase 2 coding gene
Md OPR12 for Md OPR12 rev	GACAGGGAAGATGGGAACAA CTTCGGCAAGTCTGGGTTAG	present work present work	TC87763	Oxophytodienoate reductase 12 coding gene
Md PI II for Md PI II rev	TGGTGGAGAAAACAATTCGTC AGTGCCTGGTTAGCGAAAAA	present work present work	TC65477	Proteinase inhibitor II coding gene
GAPDH for GAPDH rev	TGACAGGTTCGGAATTGTTGAG CCAGTGCTGCTAGGAATGATG	(Musetti et al. 2010) (Musetti et al. 2010)	CN929227	Glyceraldehyde-3-phosphate dehydrogenase coding gene
fO1 rO1	CGGAAACTTTTAGTTTCAGT AAGTGCCCAACTAAATGAT	(Lorenz et al. 1995) (Lorenz et al. 1995)	JN555598.1	*Candidatus* Phytoplasma mali 16S ribosomal RNA gene

this work we demonstrate that the above mentioned genes are involved in the response of apple plants to AP infection which also results in the over-expression of the genes in infected apple trees, thus confirming that these proteins are not pathogen-specific, but are determined by the reaction of the host plants.

As regarding R apple plants, results revealed an increased transcript abundance of PR 1, PR 5 and PR 8 in comparison to H individuals. This finding gives reason for the activation of plant defences and could explain the fact that R plants are more resistant than H plants to new phytoplasma infections (Osler et al. 2000).

PR 1 proteins are those which are most abundantly produced after pathogen infection and following the accumulation of the transcript occurring during pathogen attack. As previously reported, these proteins are strongly induced by SA (Durrant and Dong 2004). Patui et al. (2012) reported data about a significant increase of SA content in D apple leaf tissues compared to H or R tissues, while JA content was higher in R plants than H

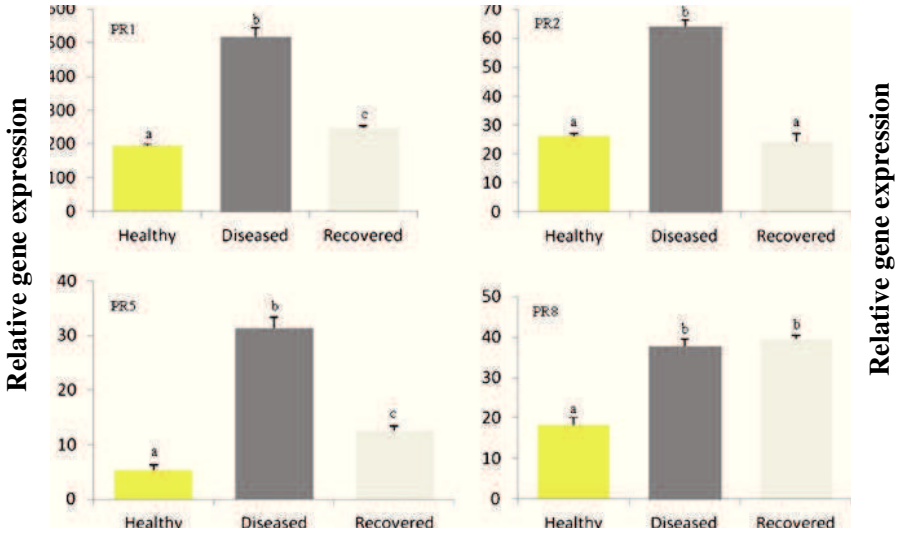

Fig. 1 Expression level of PR genes in healthy, diseased and recovered plants. Relative expression levels by quantitative real-time reverse transcription-polymerase chain reaction of four genes encoding PR 1, PR 2, PR 5 and PR 8 based on the average of three plants for each of the three experimental groups (healthy, diseased and recovered). Normalized values of relative expressions of the four genes are given as means ± SE. Different *letters* denote significant differences at $P \leq 0.01$

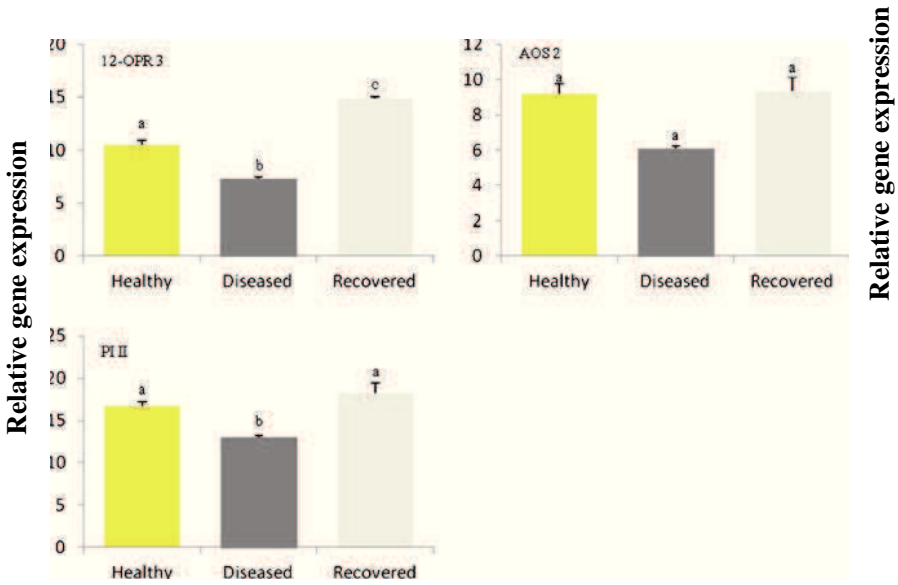

Fig. 2 Expression level of JA genes in healthy, diseased and recovered plants. Relative expression levels by quantitative real-time reverse transcription-polymerase chain reaction of three genes from the JA signaling pathway, allene oxide synthase 2 (AOS2), oxophytodienoate reductase (12-OPR 3), and JA-inducible proteinase inhibitor II (PI-II) based on the average of three plants for each of the three experimental groups (healthy, diseased and recovered). Normalized values of relative expressions of the four genes are given as means ± SE. Different *letters* denote significant differences at $P \leq 0.01$

plants. The fact that *MdPR 1* was found over-expressed in D plants confirms this latter finding.

Increased expression levels of PR 2 and/or PR 8 genes were also found in other plant-phytoplasma interactions, such as in grapevines infected by Bois Noir phytoplasma (both PR 2 and PR 8) (Landi and Romanazzi 2011) and in tomatoes infected by Stolbur (PR 2) (Ahmad and Eveillard 2011). PR 2 and PR 8 proteins are respectively a β-1,3-glucanase and a class III chitinase, exhibiting direct anti-pathogen activities (van Loon et al. 2006). In particular, β-1,3-glucanase has an important role in regulating callose metabolism. Iglesias and Meins (2000) reported that host β-1,3-glucanase affects trafficking through plasmodesmata in virus-infected plants and suggested that viruses might shift the dynamic equilibrium between callose synthesis and degradation by locally promoting host β-1,3-glucanase expression. An induction of this gene could decrease deposition of callose associated with plasmodesmata and phloem sieve pores and could facilitate the spread of viruses. The possibility of analogous action via a similar mechanism cannot be excluded in phytoplasma infections.

Among PR proteins, those belonging to group 5 exhibit similarities in the structure of amino acid, as well as structural similarities to thaumatin and osmotin and also show strong antimicrobic properties. In fact, these proteins affect membrane permeability, disrupting the lipid bilayer and impeding the growth of invading microbes (van Loon et al. 2006).

Increased expression level of PR 5, associated to a PR 5 protein accumulation, has been found in grapevine infected by Flavescence dorée and in *Chrysanthemum carinatum* infected by Onion Yellows (Margaria and Palmano 2011; Zhong and Shen 2004). El-kereamy et al. (2011) suggested that in addition to known direct antifungal/antibacterial activity for the PR 5 proteins, the same proteins may have additional function in plant cells, correlated to the synthesis and accumulations of phytoalexins. In this regard, Landi and Romanazzi (2011) hypothesized that recovery could be connected with metabolic processes linked to phytoalexin production and accumulation.

Regarding the JA-marker genes, we evaluated the expression level of three genes encoding key enzymes of the JA pathway, namely AOS 2, 12-OPR 3 and PI II. AOS catalyzes the first step in the biosynthesis of JA from lipoxygenase-derived hydroperoxides of free fatty acids, while OPR enzymes convert the precursor 12-oxophytodienoic acid (OPDA) to JA (Schaller et al. 2005). The expression of PI II has been extensively characterized as a final event in the JA-induced signal transduction cascade, especially in tomato plants (Sivasankar et al. 2000).

12-OPR 3 and PI II were significantly repressed in the leaves of D apple plants compared to the leaves of H plants (Fig. 2). On the other hand, these genes tended to have higher expression levels in R plants compared to the D ones.

The occurrence of JA-related defence response in plant/phytoplasma/vector relationships was recently illustrated by Sugio et al. (2011) in *Arabidopsis thaliana*. These authors reported that JA synthesis is down-regulated in Aster Yellows-infected *Arabidopsis* compared to the healthy plants and that phytoplasma effectors are able to target JA-mediated plant response. In particular, these authors demonstrated that SAP 11, an AY phytoplasma effector, targets JA synthesis via interaction with a plant transcription factor and modulates plant defence responses by reducing JA production to the advantage of the AY insect vector. The observed repression of the JA- pathway marker genes in apples affected by AP would confirm Sugio et al. (2011).

In conclusion, the different transcription profiles found for the examined genes in AP diseased and recovered apple plants allow us to hypothesize that plant defence could take place in at least two subsequent phases, regulated by two different pathways.

According to our results, it seems that during the spread of pathogens in the host tissues and the development of disease and symptoms, SA is involved in the prompt response to disease (Patui et al. 2012) inducing PR gene up-regulation, thereby antagonizing JA-dependent defences; in fact, in the diseased apple trees, two of the tested JA-pathway genes are significantly repressed compared to healthy ones, with the consequence that JA production is impaired in plants during the development of symptoms. On the other hand, inhibition of the PR-genes and activation of the JA-related defence mechanism via JA gene up-regulation occur in recovered compared to diseased plants. This fact would explain the accumulation of JA observed in apple leaves by Patui et al. (2012).

Given that recovery is a natural, spontaneous event not reproducible artificially, explanation of the phenomenon is not simple. It has been hypothesized that different defence signals are finely tuned in plants (Beckers and Spoel 2006) and that SA and JA pathways could be simultaneously activated, resulting in an enhanced resistance for the host, compared to either defence response alone (van Wees et al. 2000).

Our work demonstrates for the first time that two diverse sets of defence genes are involved in the interaction between apple plants and '*Ca*. P. mali' and that they are differentially expressed during phytoplasma infection or recovery.

Acknowledgments Authors are grateful to Dr Eleanor Callanan, University of Udine, for critical reading of the manuscript and for English revision.

References

Ahmad, J. N., & Eveillard, S. (2011). Study of the expression of defense related protein genes in stolbur C and stolbur PO phytoplasma-infected tomato. *Bulletin of Insectology, 64* (Supplementum), S159–S160.

Beckers, G. J. M., & Spoel, S. H. (2006). Fine-tuning plant defence signaling: salicilate vs jasmonate. *Plant Biology, 8*, 1–10.

Bonasera, J. M., Kimand, J. F., & Beer, S. V. (2006). PR genes of apple: identification and expression in response to elicitors and inoculation with *Erwinia amylovora*. *BMC Plant Biology, 6*, 23.

Carraro, L., Ermacora, P., Loi, N., & Osler, R. (2004). The recovery phenomenon in apple proliferation infected apple trees. *Journal of Plant Pathology, 86*, 141–146.

Durrant, W. E., & Dong, X. (2004). Systemic acquired resistance. *Annual Review of Phytopathology, 42*, 185–209.

El-kereamy, A., El-sharkawy, I., Ramamoorthy, R., Taheri, A., Errampalli, D., Kuare, P., & Jayasankar, S. (2011). *Prunus domestica* pathogenesis-related protein-5 activated the defense pathway and enhances the resistance to fungal infection. *PloS One, 6*, e17973.

Gasic, K., Hernandez, A., & Korban, S. S. (2004). RNA extraction from different apple tissues rich in polyphenols and polysaccharides for cDNA.library construction. *Plant Molecular Biology Reports, 22*, 437a–437g.

Gau, A. E., Koutb, M., Piotrowski, M., & Kloppstech, K. (2004). Accumulation of pathogenesis-related proteins in the apoplast of a susceptible cultivar of apple (*Malus domestica cv.* Elstar) after Infection by *Venturia inaequalis* and constitutive expression of PR genes in the resistant cultivar remo. *European Journal of Plant Pathology, 110*, 703–711.

Hogenhout, S. A., Oshima, K., Ammar, E., Kakizawa, S., Kingdom, H. N., & Namba, S. (2008). Phytoplasmas: bacteria that manipulate plants and insects. *Molecular Plant Pathology, 9*, 403–423.

Iglesias, V. A., & Meins, F. (2000). Movement of plant viruses is delayed in a β-1,3-glucanase deficient mutant showing a reduced plasmodesmatal size exclusion limit and enhanced callose deposition. *The Plant Journal, 21*, 157–166.

Landi, L., & Romanazzi, G. (2011). Seasonal variation of defense-related gene expression in leaves from bois noir affected and recovered grapevines. *Journal of Agricultural and Food Chemistry, 59*, 6628–6637.

Lorenz, K.-H., Schneider, B., Ahrens, U., & Seemüller, E. (1995). Detection of the apple proliferation and pear decline phytoplasmas by PCR amplification of ribosomal and nonribosomal DNA. *Phytopathology, 85*, 771–776.

Malnoy, M., Jin, Q., Borejsza-Wysocka, E. E., He, S. Y., & Aldwinckle, H. S. (2007). Overexpression of the apple MpNPR1 gene confers increased disease resistance in malus × domestica. *Molecular Plant-Microbe Interaction, 20*, 1568–1580.

Margaria, P., & Palmano, S. (2011). Response of the *Vitis vinifera* L. cv. 'Nebbiolo' proteome to Flavescence dorèe phytoplasma infection. *Proteomics, 11*, 212–224.

Muller, P. Y., Janovjak, H., Miserez, A. R., & Dobbie, Z. (2002). Processing of gene expression data generated by quantitative real-time RT-PCR. *Biotechniques, 32*, 1372–1379.

Musetti, R., Sanità di Toppi, L., Ermacora, P., & Favali, M. A. (2004). Recovery in apple trees infected with the apple proliferation phytoplasma: an ultrastructural and biochemical study. *Phytopathology, 94*, 203–208.

Musetti, R., Sanità di Toppi, L., Martini, M., Ferrini, F., Loschi, A., Favali, M. A., & Osler, R. (2005). Hydrogen peroxide localisation and antioxidant status in the recovery of apricot plants from European stone fruit yellows. *European Journal of Plant Pathology, 112*, 53–61.

Musetti, R., Marabottini, R., Badiani, M., Martini, M., Sanità di Toppi, L., Borselli, S., Borgo, M., & Osler, R. (2007). On the role of H_2O_2 in the recovery of grapevine (*Vitis vinifera* cv. Prosecco) from Flavescence Dorée disease. *Functional Plant Biology, 34*, 750–758.

Musetti, R., Paolacci, A., Ciaffi, M., Tanzarella, O. A., Polizzotto, R., Tubaro, F., Mizzau, M., Ermacora, P., Badiani, M., & Osler, R. (2010). Phloem cytochemical modification and gene expression following the recovery of apple plants from apple proliferation disease. *Phytopathology, 100*, 390–399.

Musetti, R., De Marco, F., Farhan, K., Polizzotto, R., Santi, S., Ermacora, P., & Osler, R. (2011). Phloem-specific protein expression patterns in apple and grapevine during phytoplasma infection and recovery. *Bulletin of Insectology, 64*, 211–212.

Osler, R., Carraro, L., Loi, N., & Refatti, E. (1993). Symptom expression and disease occurrence of a yellows disease of grapevine in northeastern Italy. *Plant Disease, 77*, 496–498.

Osler, R., Loi, N., Carraro, L., Ermacora, P., & Refatti, E. (2000). Recovery in plants affected by phytoplasmas. *Proceedings of the 5th Congress of the European Foundation for Plant Pathology*, Taormina, Italy, September 18–22 2000, pp. 589–592.

Patui, S., Bertolini, A., Clincon, L., Ermacora, P., Braidot, E., Vianello, A., & Zancani, M. (2012). Involvement of plasma membrane peroxidases and oxylipin pathway in the recovery from phytoplasma disease in apple (*Malus domestica*). *Physiologia Plantarum*. doi:10.1111/j1399-3054.2012.01708.x.

Pfaffl, M. W. (2001). A new mathematical model for relative quantification in real-time RT-PCR. *Nucleic Acid Research, 29*, e45.

Schaller, F., Schaller, A., & Stintzi, A. (2005). Biosynthesis and metabolism of Jasmonates. *Journal of Plant Growth Regulation, 23*, 179–199.

Sivasankar, S., Sheldrick, B., & Rothstein, S. J. (2000). Expression of allene oxide synthase determines defense gene activation in tomato. *Plant Physiology, 122*, 1335–1342.

Sugio, A., Kingdom, H. N., MacLean, A. M., Grieve, V. M., & Hogenhout, S. A. (2011). Phytoplasma protein effector SAP11 enhances insect vector reproduction by manipulating plant development and defense hormone biosynthesis. *Proceedings of the National Academy of Science of USA, 108*, E1254–E1263.

van Loon, L. C., Rep, M., & Pieterse, C. M. J. (2006). Significance of inducible defense-related proteins in infected plants. *Annual Review of Phytopathology, 44*, 135–162.

van Wees, S. C. M., De Swart, E. A., van Pelt, J. A., van Loon, L. C., & Pieterse, C. M. J. (2000). Enhancement of disease induced resistance by simultaneous activation of salicylate- and jasmonate-dependent defense pathways in *Arabidopsis thaliana*. *Proceedings of the National Academy of Science of USA, 97*, 8711–8716.

Wasternack, C. (2007). Jasmonates, an update on biosynthesis, signal transduction and action in plant stress response, growth and development. *Annals of Botany, 100*, 681–697.

Zhong, B. X., & Shen, Y. W. (2004). Accumulation of pathogenesis related type-5 like proteins in phytoplasma-infected garland chrysanthemum *Chrysanthemum coronarium*. *Acta Biochemica Biophysica Sinica, 36*, 773–779.